DISTRIBUTIONS AND STABLE ISOTOPE CHARACTERISTICS OF MALEIMIDES (1-*H*-PYRROLE-2,5-DIONES)

By

Simon Lee Magness

April 2001

This thesis is submitted to the Faculty of Science of the University of Bristol, U.K.

In fulfillment of the requirements for the degree of Doctor of Philosophy

Word Count: 42,066

ABSTRACT

Alkyl maleimides (1-*H*-pyrrole-2,5-diones), degradation products of photosynthetic tetrapyrrole pigments, occur either as natural diagenetic products in sedimentary organic matter or can be generated by laboratory oxidation of chlorins or porphyrins. The distributions are characteristically dominated by methyl ethyl (Me,Et) maleimide, mainly derived from chlorophyll *a* (Chl *a*). The detection of methyl *n*-propyl (Me,*n*-Pr) and methyl *iso*-butyl (Me,*i*-Bu) maleimdes denotes on structural grounds an origin from the bacteriochlorophylls *c*, *d* or *e* of the Chlorobiaceae (green sulfur bacteria). The Chlorobiaceae are obligate anaerobes and exist in water columns where anoxic conditions have penetrated the photic zone.

Investigations of two Recent sediments (Priest Pot, England and Lake Pollen, Norway) have confirmed that maleimides are genuine water column degradation products of tetrapyrroles and are not simply artefacts of oxidation of tetrapyrroles during sample storage. Both Me,H and Me,Et maleimides were detected in Priest Pot sediment, whereas Me,Et and Et,Et maleimides were discovered in Lake Pollen sediment.

The distributions of maleimides in 10 sub-samples of marl IV and 3 sub-samples of marl VIII of the Vena del Gesso (Italy) Messinian evaporitic sequence have been obtained. Both Me,*n*-Pr and Me,*i*-Bu maleimides occurred in certain marl IV (IV-1 to IV-8) and marl VIII (VIII-a and VIII-b) samples; $\delta^{13}C$ values of Me,Et, Me,*n*-Pr and Me,*i*-Bu maleimides for sub-samples IV-1 and IV-3 show Me,*i*-Bu maleimide (reversed TCA pathway for carbon fixation) to be enriched in ^{13}C relative to Me,Et maleimide (C_3 pathway) and confirm earlier work that Me,*n*-Pr maleimide may not necessarily be of Chlorobiaceae origin, since it is not always enriched in ^{13}C. Additionally, the free base alkyl porphyrins in sub-samples IV-1 and IV-5 were photo-oxidised to reveal the presence of Me,*i*-Bu maleimide in both cases. Overall, the results strongly indicate that the Chlorobiaceae once existed in the water column and that photic zone anoxia was indeed recurrent throughout the deposition of these marls. The $\delta^{13}C$ values for Me,Et maleimide were monitored over the 10 sub-samples from marl IV in an attempt to assess the utility of Me,Et maleimide as an isotopic productivity indicator.

Maleimide distributions were also determined for Italian black shale sequences from Moria (M) and Monte Petrano (MP), which were deposited during the Cenomanian/Turonian (C/T) oceanic anoxic event (OAE). Previous distributions of MP samples revealed the presence of Me,*i*-Bu maleimide, indicating that an intensified and expanded oxygen minimum zone (OMZ) had encroached into the zone of light penetration during sediment deposition. However, Me,*n*-Pr and Me,*i*-Bu maleimides were not detected in samples (M3, M5, M7, M9, M12 and M13) suggesting that PZA did not occur during the deposition of the sediments at the Moria site. Maleimide distributions obtained from the photo-oxidation of nickel porphyrin fractions from samples M3, M5, M7 and M9 also failed to produce maleimides characteristic of the Chlorobiaceae. Me,Et maleimide was used as an isotopic biomarker and a $\delta^{13}C$ positive excursion of *ca.* 3.2 $^{0}/_{00}$ was observed over the MP sequence. This shift is in accordance with that observed previously for bulk $\delta^{13}C_{org}$ measurements.

Finally, attempts were made to develop a method for the determination of $\delta^{15}N$ values for maleimides using GC-C-IRMS in view of the fact that if the $\delta^{15}N$ values for each of the pyrroline rings of Chl *a* could be obtained and it was found that all four have the same $\delta^{15}N$ values (as the biosynthetic pathway predicts), then Me,Et maleimide could be used as a nitrogen isotopic proxy for photoautotrophs.

Dedicated to my Parents
and Samantha

ACKNOWLEDGEMENTS

First, I would like to thank Professor James Maxwell FRS for his overall supervision and valuable hours of discussion and advice throughout the project.

Dr. Neil Crawford is thanked for his initial laboratory supervision and for the time spent discussing a few of the essential theories of this work.

Drs. Brendan Keely (University of York) and Paul Farrimond (University of Newcastle) are thanked for the provision of some samples.

Jim Carter is particularly thanked for his invaluable advice, ideas, optimism and help regarding GC-MS, HPLC-MS and $\delta^{15}N$ analyses.

Special thanks to Andy Gledhill for advice and help with GC-MS and $\delta^{13}C$ analyses.

Dr. Helen Talbot is thanked for her assistance regarding the analysis of chlorins.

The EPSRC is thanked for the provision of a studentship.

Also thanked is Dr. David Roberts for his many jokes, advice and friendship.

Many thanks to Sue Trott and to all the members of the Organic and Biological section, past and present for their friendship, help and support.

Finally, I would like to thank my entire family, especially Mum, Dad and Samantha for their love, support and encouragement throughout the last three years.

Declaration

I hereby certify that the work described herein is my own, except where otherwise stated and has not been submitted for a degree at this or any other university

S. L. Magness

Simon Lee Magness

CONTENTS

CHAPTER 2: PRIEST POT/LAKE POLLEN

LIST OF FIGURES

LIST OF TABLES

ABBREVIATIONS

AKA	α-ketoglutaric acid
ALA	δ-aminolevulinic acid
APCI	atmospheric pressure chemical ionisation
ASP	aspartic acid
Bchl	bacteriochlorophyll
BenzoCAP	benzocycloalkanoporphyrin
BiCAP	bicycycloalkanoporphyrin
Bu	butyl
CAP	cycloalkanoporphyrin
Chl	chlorophyll
C/T	Cenomanian/Turonian
DCM	dichloromethane
DPEP	desoxophylloerythroaetioporphyrin
DSDP	deep sea drilling project
EA	elemental analyser
Et	ethyl
eV	electron volts
GC	gas chromatography
GC-C-IRMS	gas chromatography-combustion-isotope ratio mass spectrometry
GC-MS	gas chromatography-mass spectrometry
GLU	glutamic acid
GPC	gel permeation chromatography
h	hours
HMW	high molecular weight
HPLC	high performance liquid chromatography
HPLC-MS	high performance liquid chromatography-mass spectrometry
i	iso
i.d.	internal diameter
LC	liquid chromatography
M	Moria
Ma	million annums
Me	methyl
MeOH	methanol
Min	minutes
MP	Monte Petrano
MS	mass spectrometry
m/z	mass to charge ratio
NADPH	nicotinamide adenine dinucleotide phosphate
NMR	nuclear magnetic resonance
OAE	oceanic anoxic event
o.d.	outer diameter
OM	organic matter
OMZ	oxygen minimum zone
PBG	porphobilinogen

Pr	propyl
PZA	photic zone anoxia
SAM	S-adenosyl-methionine
sec	secondary
TBDMS	tertiary-butyldimethylsilyl
TCA	tricarboxylic acid
TFA	trifluoroacetic acid
TLC	thin layer chromatography
TOC	total organic carbon
TOE	total organic extract
TS	total sulfur
UV	ultraviolet
UV/vis	ultraviolet/visible (spectrophotometry)
vanadyl	oxovanadium (IV)
VdG	Vena del Gesso
Yr	years

NOMENCLATURE

The I.U.P.A.C. system of numbering for chlorophylls and porphyrins, shown below, has been used throughout. In addition, trivial names with abbreviations have been used for pyrrole-2,5-diones. Hence, 4-methyl-3-ethyl-1-*H*-pyrrole-2,5-dione becomes methyl ethyl maleimide or Me,Et maleimide.

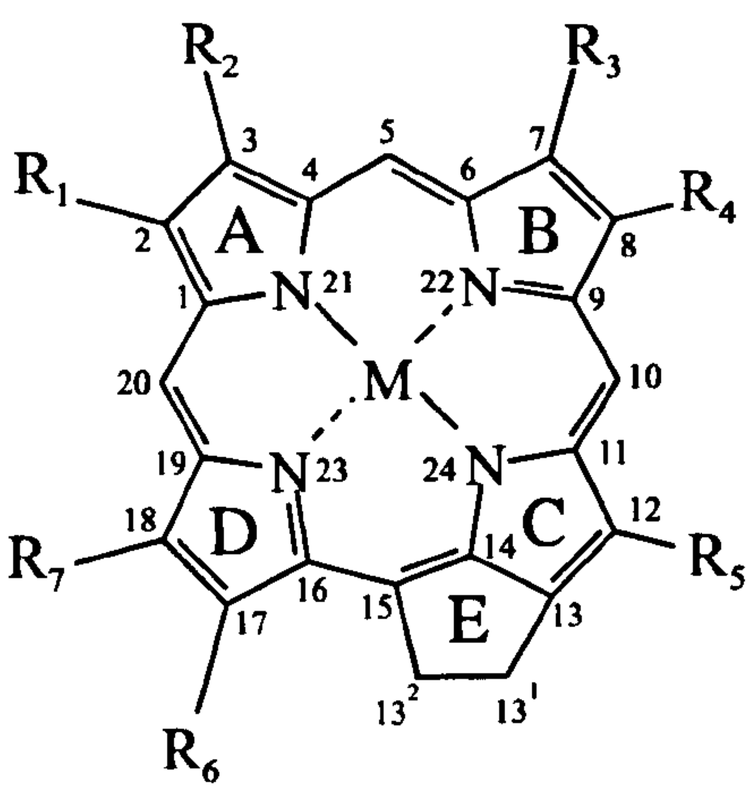

Cycloalkanoporphyrin (CAP)

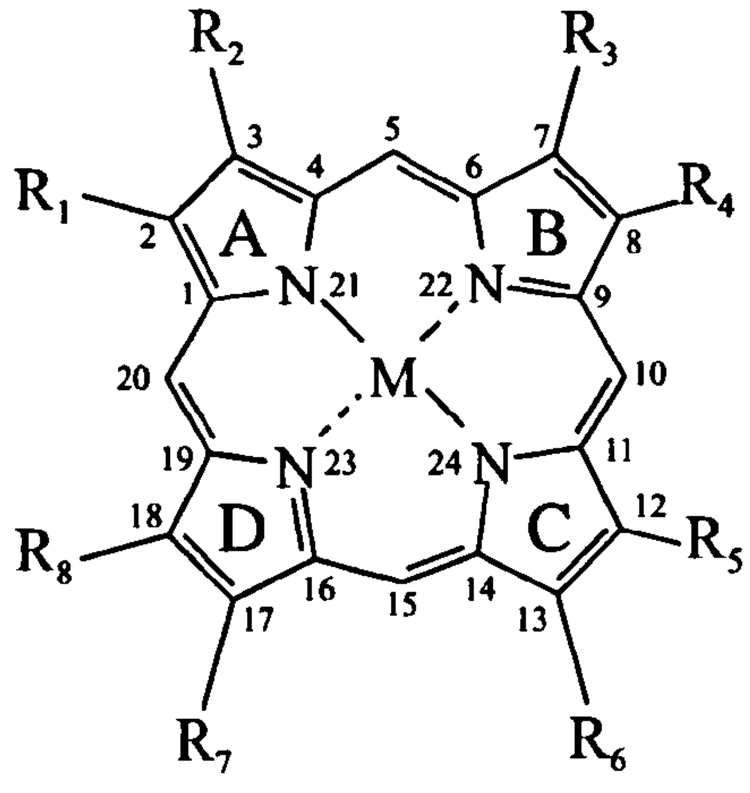

Aetioporphyrin

CHAPTER 1:

INTRODUCTION

INTRODUCTION

CHLOROPHYLLS

General

Chlorophylls (Chls, *e.g.* Chl *a* **1**) are green tetrapyrrole pigments that convert solar energy into chemical energy during photosynthesis. The former is absorbed by antenna pigments that are comprised of Chl-protein complexes in oxygenic organisms, *e.g.* cyanobacteria, algae and higher plants, or bacteriochlorophyll (Bchl)-protein complexes in anoxygenic photosynthetic bacteria. The antenna pigments are often accompanied by so-called accessory pigments (*e.g.* Chl *b* **2**), which also include carotenoids (*e.g.* chlorobactene **3**). The combination of these pigments enhances the overall light absorption range of the photosynthetic organism and, to some extent it is possible to distinguish among certain organisms based solely on the composition of their photosynthetic pigments (Table 1.1). Furthermore, there is a wide structural diversity in the Chl macrocycle and around twenty-five Chls have been identified in Nature so far. The majority of eukaryotes, both terrestrial and aquatic, contain Chl *a* (**1**) as the major pigment in addition to Chl *b* (**2**) as accessory pigment. However, prokaryotic cyanobacteria contain only Chl *a* (**1**). The most prevalent esterifying alcohol in eukaryotes is phytol (*e.g.* in Chl *a* **1**), with the exception of the Chls *c* (**4**, **5** and **6**), which lack an esterifying alcohol and are thus carboxylic acids. Other Chls that are thought to be important include Chl *d* (**7**) found in red algae (Rhodophyta; Manning and Strain, 1943; Sagromsky, 1960) and [8-vinyl]-chl *a* (divinyl Chl *a* **8**) originally found in the greening tissues of higher plants, *e.g.* cucumber seedlings (Rebeiz *et al.*, 1980; Scheer, 1991), but which has since been discovered in certain marine microalgae, *e.g.* the oxygenic photosynthetic prokaryote *Prochlorococcus marinus* (Partensky *et al.*, 1993; Moore *et al.*, 1995; Bricaud *et al.*, 1999).

Table 1.1 Typical Chlorophylls of Photosynthetic Organisms
(Updated from Crawford, 1998)

Photosynthetic Organism	Principal Chlorophyll	Accessory Pigment	
Higher Plants	*a*	*b*	
Green Algae	*a*	*b*	
Prochlorophytes	[8-vinyl]-Chl *a*	[8-vinyl]-Chl *b* + *b*	
Red Algae	*a*	*d*	OXYGENIC PHOTOTROPHS
Brown Algae	*a*	c_1	
Diatoms	*a*	c_1	
Dinoflagellates	*a*	c_2	
Cyanobacteria (blue-green algae)	*a*	-	
Purple sulfur bacteria	Bchls *a* and *b*	-	FACULTATIVE PHOTOTROPHS
Filamentous green bacteria	Bchls *a*, *c* and *d*	-	
Green sulfur bacteria (green species)	Bchls *c* and *d*	Bchl *a*	ANOXYGENIC PHOTOTROPHS
Green sulfur bacteria (brown species)	Bchl *e*	Bchl *a*	

Bacteriochlorophylls

These prokaryotic Chls have a greater structural variation than those of the eukaryotes (*e.g.* Keely and Maxwell, 1993 and references therein). For example, alcohols such as geranylgeraniol (Bchl *a* **9**) and farnesol (*e.g.* Bchl *d* **10**) may replace the more widespread phytol of eukaryotes. The majority of photosynthetic bacteria utilise Bchl *a* (**9**) as the primary photosynthetic pigment and contain Bchl *b* (**11**) as the dominant accessory pigment. However, some species (*e.g.* certain non-sulfur bacteria) use Bchl *b* (**11**) as the major antenna pigment instead (Resnick and Madigan, 1989). A further three homologous series of Chls exist and these are known as the Bchls *c* (**12**), *d* (**10**)

and *e* (**13**). When compared with the Bchls *a* (**9**) and *b* (**11**), it can be seen that the *c*, *d* and *e* series have an α-hydroxyethyl group at C-3, lack the 13^2 carbomethoxy substituent and have farnesol as the main esterifying alcohol, although perhaps the most significant structural difference is the additional alkylation that may occur at specific positions: in the Bchls *d* (**10**) at C-8 and C-12 and in the Bchls *c* (**12**) and *e* (**13**) at C-8, C-12 and C-20. The alkylation takes place *via* a stepwise S-adenosyl methionine methylation (Smith and Bobe, 1987). In essence, the organism is able to adapt in response to lowered light availability, since the aggregation characteristics of the pigment are altered, allowing the organism to utilise light of longer wavelengths (Smith and Bobe, 1987). For example, a 20nm bathochromic shift is observed after methylation at C-20 in the Bchl *d* (**10**) series, which is thought, incidentally, to give rise to the Bchl *c* (**12**) series (Keely, 1989 and references therein). However, the Bchl *e* (**13**) series, unlike the *c* (**12**) and *d* (**10**) series, bears a formyl group at C-7, as does Chl *b* (**2**). The Bchls *a* (**9**) and *b* (**11**) are the major pigments of the anoxygenic purple sulfur bacteria (*i.e.* Chromatiaceae), whereas the Bchls *c* (**12**), *d* (**10**) and *e* (**13**) are the primary pigments of the photosynthetic green sulfur bacteria (*i.e.* Chlorobiaceae).

PHOTOSYNTHETIC SULFUR BACTERIA AND THEIR HABITAT

The transport of oxygen in aquatic environments is normally achieved by mixing. In certain environments, however, water circulation may be inhibited due to stratification and the transport of oxygen is inhibited. There are two basic causes for stratification and these are either due to temperature or salinity-induced density gradients. The former may occur in lakes during the summer, where surface waters are heated by solar radiation (Demaison and Moore, 1980). This forms a warmer layer, known as the epilimnion, that floats over a colder deeper hypolimnion. The region between these layers is known as the thermocline. In the autumn, the solar radiation becomes less intense, the thermocline ceases to exist and mixing occurs. On the other hand, salinity-induced stratification usually takes place when an influx of freshwater enters a restricted marine basin (*e.g.* the Black Sea). The less saline freshwater forms a layer over the more saline marine water. The zone between the two layers is often referred to as the halocline (Demaison and Moore, 1980). The only time that salinity-induced stratification is likely to break down is when a change in sea level occurs. In the oxic

upper parts of a stratified water column, the level of productivity is usually restricted by a low concentration of nutrients, which may be replenished during periods of terrestrial run-off. As detritus sinks through the water column it is biodegraded, utilising oxygen in the process. Eventually, at the bottom of the water column the oxygen becomes depleted, leading to anoxic conditions. Sulfate-reducing bacteria are known to thrive in anaerobic regions of stratified lakes and restricted marine basins. When sulfate concentrations are high, the activity level of the sulfate-reducing bacteria increases, resulting in the accumulation of free hydrogen sulfide (H_2S). However, in stratified freshwater lakes that have a low sulfate concentration, the activity of sulfate-reducing bacteria and concentration of free H_2S are generally low. As long as the water body remains stratified, the anoxic, H_2S-liberating conditions will slowly ascend the water column until they eventually penetrate the photic zone. Anoxic water within the photic zone describes the condition often referred to as "photic zone anoxia" (PZA; Fig. 1.1). The occurrence of PZA is significant since it is thought to play an important role in oil exploration, in that many important source rocks were deposited under such conditions (*e.g.* Kimmeridge Clay, van Kaam-Peters *et al.*, 1997a; van Kaam-Peters *et al.*, 1999) and also in helping us to understand the history of the oceans and seas (Sinninghe Damsté *et al.*, 1998). Furthermore, towards the surface of the stratified water body, the concentration of sulfide ions gradually decreases until they eventually coincide with the lower limit of dissolved oxygen (Fig. 1.1). This region is known as the chemocline and although light intensities are normally low, photosynthetic sulfur bacteria can exist within or just below it. Algae and cyanobacteria usually flourish near the surface whilst the Chromaticeae grow beneath them in the chemocline. The Chromaticeae are facultative anaerobes and are able to tolerate low levels of oxygen. However, in such oxygenic conditions photosynthetic pigment synthesis is almost completely inhibited (de Wit, 1992 and references therein). The Chromaticeae use H_2S during anaerobic photosynthesis and have the ability to store sulfur within their cells, giving them a greater level of independence when H_2S concentrations are low. On the other hand, the Chlorobiaceae are strict anaerobes and are unable to survive in the presence of oxygen. So, these organisms live below the Chromaticeae and also require less light (de Wit, 1992 and references therein). Moreover, light utilised by the Chlorobiaceae, is not absorbed by the Chromaticeae (Montesinos *et al.*, 1983). In addition, the Chlorobiaceae only use free H_2S as a proton donor, instead of water. There are two strains of Chlorobiaceae,

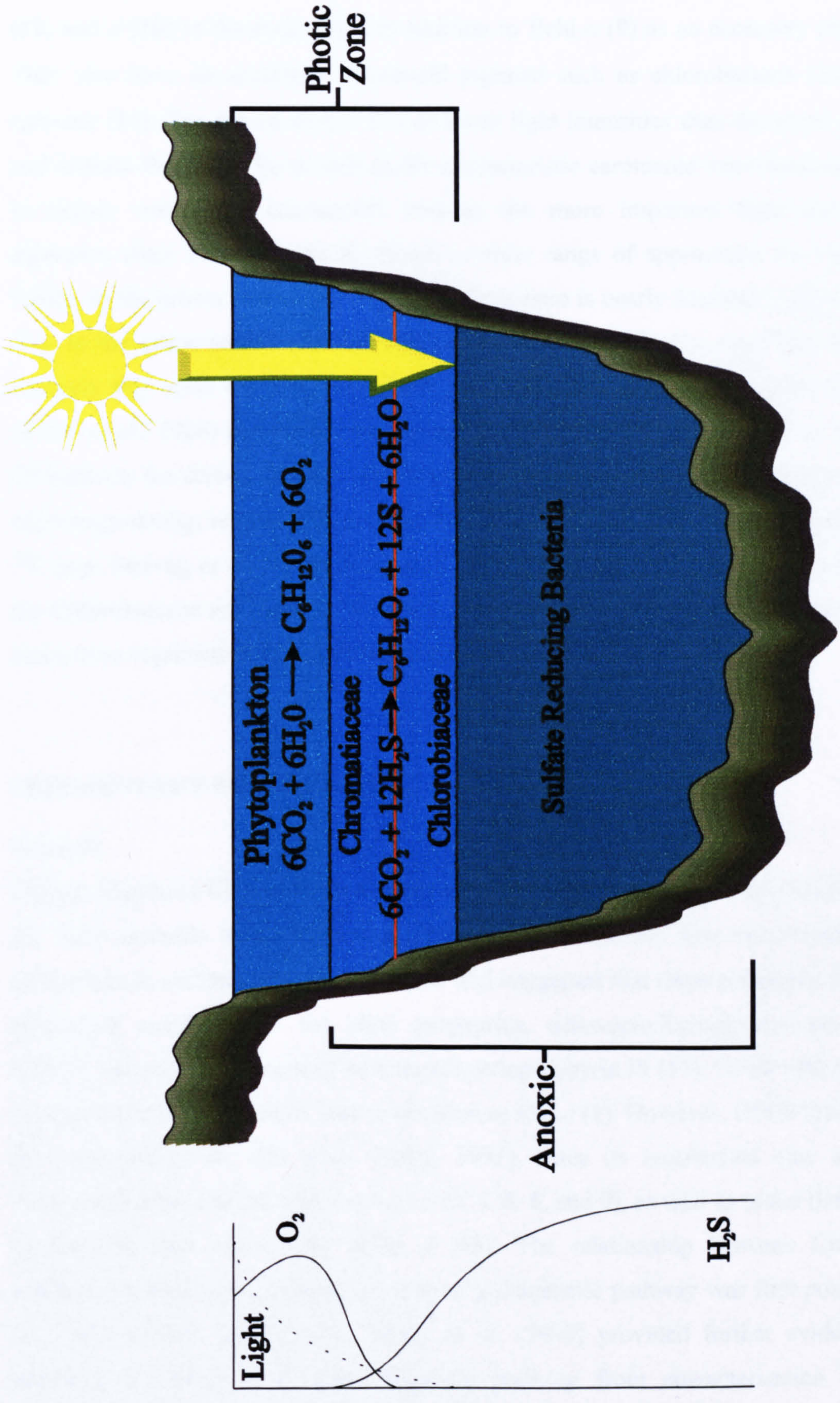

Fig. 1.1 Organism distributions within a stratified basin (after de Wit, 1992)

the green-coloured and the brown-coloured strains. The green strains contain Bchls *c* (**12**) and *d* (**10**) as the main Chls, in addition to Bchl *a* (**9**) as an accessory pigment. They also have an accessory carotenoid pigment such as chlorobactene (**3**), or γ-carotene (**14**). The brown strains live at lower light intensities than the green strains and contain Bchls *e* (**13**), as well as the characteristic carotenoid isorenieratene (**15**). In deeper waters the carotenoids become the more important light harvesting pigments, since they are able to absorb a wider range of appropriate wavelengths. Hence, in the brown strains, the carotenoid:Bchl ratio is nearly four times greater than it is in the green strains (de Wit and Caumette, 1995). Finally, the Chlorobiaceae uniquely rely upon the reversed tricarboxylic acid (TCA) cycle for carbon fixation (Evans *et al.*, 1966) and the Chromaticeae, like photosynthetic phytoplankton, use the C3 pathway for carbon fixation. The major difference between these pathways is that the energy-saving, reversed TCA cycle discriminates less against the incorporation of ^{13}C (*e.g.* Sirevag *et al.*, 1977; Summons and Powell, 1986). Thus, compounds from the Chlorobiaceae are likely to be less depleted in ^{13}C relative to carbon source than those from organisms utilising the C3 pathway.

SEDIMENTARY PORPHYRINS

General

During diagenesis Chls undergo a series of transformations that yield porphyrins with the fully aromatic tetrapyrrole ring structure. Treibs (1934) first discovered these biomarkers in sedimentary organic matter and suggested that these red pigments were metallated complexes of the alkyl porphyrins, desoxophylloerythroaetioporphyrin (DPEP; **16**) and its ring opened counterpart aetioporphyrin III (**17**). DPEP (**16**) is a C_{32} component and has the same carbon skeleton as Chl *a* (**1**). However, DPEP (**16**) is not the only marker for Chl *a* (**1**; Callot, 1991), since its macrocycle may also be structurally related to the Chls *b*, *c* and *d* (**2**, **4**, **5**, **6**, and **7**), as well as to the Bchls *a*, *b* (**9** and **11**) and one of the Bchls *d* (**10**). The relationship between Chls and sedimentary porphyrin pigments by way of a diagenetic pathway was first postulated by Treibs (1936). Additionally, Keely *et al.* (1990) provided further evidence to reinforce the initial postulated diagenetic pathway from characterisation of the minimum number of intermediates on it. Most of the intermediary steps include 1)

demetallation, *i.e.* loss of Mg^{2+}, 2) ester hydrolysis, 3) decarbomethoxylation, 4) vinyl reduction, 5) chlorin ring aromatisation, 6) keto group reduction, 7) decarboxylation and 8) metal ion insertion. The diagenetic stage at which metal ion insertion occurs is uncertain, but the process of metallation is thought to increase the stability of porphyrins (Quirke, 1987; Callot, 1991). Porphyrins are mainly preserved in ancient sediments and oils as nickel (Ni^{2+}) and vanadium (VO^{2+}) complexes. Other complexes such as Mn^{2+}, Ga^{3+}, Fe^{3+} (Bonnett and Czechowski, 1980; Bonnett and Czechowski, 1981; Bonnett *et al.*, 1983), and Cu^{2+} (Palmer and Baker, 1978) have also been discovered, in addition to the free base alkyl porphyrins usually associated with immature lake/marine sediments (Keely *et al.*, 1994; Keely *et al.*, 1995).

Alkyl Porphyrins - Structural Types

Cycloalkanoporphyrins (CAPs)

The alkyl porphyrin group may be sub-divided into two further groups, cycloalkanoporhyrins (CAPs) and aetioporphyrins. CAPs typically contain an exocyclic ring, whereas aetioporphyrins do not. The most predominant CAPs in the geosphere are those that contain a five membered exocyclic ring, as in the case of DPEP (**16**). Furthermore, certain CAPs may possess a rearranged exocyclic ring that is 5, 6 or 7 membered (*e.g.* **18a-b**, **19a-b** and **20a-b** respectively). It is believed that the rearranged five membered ring is derived from the Chls *c* (**4**, **5** and **6**; Dougherty *et al.*, 1970).

Bicycloalkanoporphyrins (BiCAPs)

A further type of CAP, known as the bicycloalkanoporphyrins (BiCAPs) exists and these nominally contain two exocyclic rings. The BiCAPs occur either as species with a six membered ring at the C-7 and C-8 position (*e.g.* **21a-b**, **22**), as was found in the Maastrichtian Timhadit oil shale (Verne-Mismer *et al.*, 1987) or with two fused (5+7) exocyclic rings (**23a-b**). This latter component (**23a-b**) has been identified in the sulfur-rich Messinian marls of Sicily (Schaeffer *et al.*, 1993) and also in the immature Late Pliocene Willershausen lake sediment (**23b**; Keely *et al.*, 1994) and was originally thought to be mainly of diatom Chl *a* (**1**) origin (Watanabe *et al.*, 1993 and

references therein), although more recent studies indicate that it can arise from other plankton species (Talbot *et al.*, 1999 and references therein).

Benzocycloalkanoporphyrins (BenzoCAPs)

These often used to be referred to as "rhodoporphyrins" in geochemical literature due to the similarity of their visible spectra with those of the true rhodoporphyrins (Smith, 1975). Although such components were observed relatively early in sediments (Baker *et al.*, 1967), it wasn't until much later that two benzoCAPs (**24a-b**) were isolated from Boscan crude oil and their structures fully elucidated (Chicarelli *et al.*, 1987; Kaur *et al.*, 1986). Despite this, it is still unclear as to how and at what stage formation of the benzene ring occurs (Callot, 1991). During diagenesis it is perceived that benzoCAPs (*e.g.* **24a-b**) arise from tetrahydrobenzoporphyrins (*e.g.* BiCAPs **21a-b**) (Verne-Mismer *et al.*, 1987) and thus are attributed the same origin.

Aetioporphyrins

The origin of these porphyrins (*e.g.* aetioporphyrin III **17**) remains unclear since on structural grounds they lack specific precursor Chls, although there is recent evidence to suggest that they may be derived from Chls, since oxidised products of Chl *a* (**1**), such as purpurin-18 (**25**) and purpurin-7 phytyl ester (**26**) (Naylor, 1997; Naylor and Keely, 1997) containing an open ring E have been found in immature lake sediments. This implies that Chl defunctionalisation may lead to the formation of aetioporphyrins. However, an alternative source is that they originate from haeme or cytochromes. For example, aetioporhyrin III (**17**) samples from the Albian Julia Creek and Tertiary Condor oil shales were depleted in ^{13}C by approximately $4^{o}/_{oo}$ relative to C_{32} DPEP (**16**) (Boreham *et al.*, 1989; Ocampo *et al.*, 1989). Hence, these results indicate a possible origin from the cytochromes of microorganisms.

Acidic Porphyrins

Carboxylated porphyrins are necessary intermediates in the Treibs scheme of transformation of Chls into alkyl porphyrins. They have been discovered mostly in immature sediments such as the Eocene Messel oil shale (Ocampo *et al.*, 1985a;

Ocampo *et al.*, 1992) and are attributed an origin from Chl when they contain a cyclopentane ring (*e.g.* **27a-b**). Likewise, a C_{33} porphyrin acid related to DPEP has also been identified in the immature lacustrine Willershausen (Pliocene) sediment (Keely *et al.*, 1994). However, specific high molecular weight (HMW) acidic porphyrins (see below) have also been detected and are thought to originate from the Bchl *d* (**10**) series (Ocampo *et al.*, 1985b).

Bound Porphyrins

Previous studies indicate that bound components within a kerogen matrix are better preserved than their solvent extractable counterparts (*e.g.* Adam *et al.*, 1993; Kohnen *et al.*, 1991a), therefore providing more information with regard to organic source inputs and ultimately a greater appreciation of palaeoenvironmental conditions. Furthermore, bound porphyrins have a different distribution to, and are more widespread than, the free porphyrins. The porphyrins may be bound either by sulfide (*e.g.* Schaeffer *et al.*, 1993) or ester bonds (Huseby and Ocampo, 1995). Such ester-bound species may be released by acid or base hydrolysis and component distributions released from the Eocene Messel oil shale include both mono- and di-carboxylic acids. It is likely that these acidic porphyrins derive from Chls and bacterial cytochromes respectively.

Porphyrins as Indicators of PZA

It is assumed that the Bchls of the Chlorobiaceae follow an analogous diagenetic pathway as that suggested for the conversion of Chl *a* (**1**) to DPEP (**16**) (Keely *et al.*, 1990 and references therein). Therefore, it should not be surprising to find Bchl-derived carbon skeletons, with extended alkylation at C-8, C-12 and C-20, in sedimentary organic matter. As mentioned previously, Ocampo *et al.* (1985b) were the first to fully elucidate the structures of a minor homologous series of acidic porphyrins (C_{34}-C_{36}) (*e.g.* **28a-c**) discovered in the Eocene Messel oil shale. Moreover, the carbon skeletons of these components exactly matched members of one of the two Bchl *d* (**10**) series (*i.e.* an Et substituent at C-12 and an Et, *n*-Pr or *i*-Bu substituent at C-8). Later, evidence to further substantiate these early findings came from the evaporitic Mulhouse Basin (Alsace, France). Using high performance liquid chromatography

(HPLC), Keely and Maxwell (1993) co-injected a synthesised C_{34} standard which co-eluted with a HMW C_{34} CAP in the porphyrins of the Oligocene marls. The component was therefore tentatively attributed an origin from the second Bchl *d* (**10**) series (*i.e.* a Me substituent at C-12). More recently, Gibbison *et al.* (1995; 1996) isolated porphyrin fractions of the Permian Kupferschiefer from the Lower Rhine Basin and used nuclear magnetic resonance (^{1}H-NMR) to fully elucidate the structures of a series of three HMW CAPs (**29, 30** and **31**). Extended alkylation (Et, *n*-Pr and *i*-Bu) at C-8 in conjunction with an Et at C-12 indicates that the precursor was a different member of the Bchl *d* (**10**) series in each case. Consequently, these molecular fossils indicate that the green strains of the Chlorobiaceae had once existed in the ancient water column. However, other HMW CAPs (*i.e.* $>C_{32}$), such as a C_{34} CAP with an Et-substituted 5-membered exocyclic ring (**32**) and a C_{33} CAP with a Me-substituted 7-membered exocyclic ring (**33**) were also partially elucidated by ^{1}H-NMR. Significantly, no structural correlation exists between these porphyrins and the Bchls. Hence, the presence of $>C_{32}$ CAPs alone does not necessarily indicate the past existence of the Chlorobiaceae. Further evidence to highlight the danger of this assumption stems from the full characterisation of a C_{33} CAP obtained from Boscan crude oil (Verne-Mismer *et al.*, 1986). It would appear that this particular structure, although related to Chl *a* (**1**), has undergone ester hydrolysis, followed by diagenetic reduction to yield a Pr substituent instead of the more expected Et substituent which usually arises as a result of decarboxylation.

Aryl Isoprenoids as Indicators of PZA

The diaromatic carotenoid isorenieratene (**15**) originates from the brown strains of the Chlorobiaceae and has been found in both Holocene Black Sea sediments and in certain relatively immature sediments (Repeta, 1993; Brassell *et al.*, 1983; Sinninghe Damsté *et al.*, 1993; Keely *et al.*, 1995). Its reduced counter-part isorenieratane (**34**) was initially detected in the Toarcian Paris Basin (Schaeflé *et al.*, 1977), but has since been discovered in many other samples, including Paleozoic source rocks and oils (*e.g.* Requejo *et al.*, 1992; Sinninghe Damsté and Köster, 1998). It has also been released from sulfur-rich geomacromolecules (*e.g.* Kenig *et al.*, 1995; Schaeffer *et al.*, 1995; Sinninghe Damsté *et al.*, 1995). The green strains of the Chlorobiaceae contain chlorobactene (**3**) as an accessory pigment instead of isorenieratene (**15**). During

diagenesis both of these carotenoids may give rise to a series of low molecular weight (LMW) monoaromatic aryl isoprenoids, *i.e.* 1-alkyl-2,3,6-trimethylbenzenes (*e.g.* **35**). However, Koopmans *et al.* (1996) found for a North Sea oil that $\delta^{13}C$ measurements are required for these components since certain LMW monoaromatic aryl isoprenoids with a 2,3,6-trimethyl substitution pattern for the aromatic ring were intermediate between those of β-isorenieratane (from the β-carotene of algae) and isorenieratane (from the isorenieratene of Chlorobiaceae), suggesting a mixed source. The results show that the presence of LMW monoaromatic aryl isoprenoids in sedimentary organic matter on its own does not necessarily indicate the past existence of the Chlorobiaceae and the presence of PZA, unless they are significantly enriched in ^{13}C compared to phytoplanktonic components.

MALEIMIDES

General

Maleimides (1-*H*-pyrrole-2,5-diones) are oxidative degradation products of tetrapyrrolic pigments that occur in sedimentary organic matter or can be generated by laboratory (chemical or photo-) oxidation of chlorins or porphyrins. In addition, the alkyl substituents at the C-3 and C-4 positions can give information about the precursor biomolecules.

Previous Work

Initially, maleimides were obtained from Chl *a* (**1**) by oxidation with a strong oxidising agent, such as chromic acid (Ellsworth and Aronoff, 1968; Ellsworth, 1970). The products were analysed by gas chromatography - mass spectrometry (GC-MS) and were subsequently identified as methyl ethyl (Me,Et) maleimide (**36a**), Me,vinyl maleimide (**37**) and Me,H maleimide (**36b**) when the oxidation was carried out after degradation (pyrolysis) of pheophorbide *a* (**38**) to pyrroporphyrin (**39**), and dihydrohematinic acid (**40**). Later, Hodgson *et al.* (1971) also used chromic acid oxidation to obtain the maleimide distributions of alkyl porphyrin fractions isolated from three different locations: a Gilsonite bitumen (USA) and Lloydminster (Canada) and Boscan (Venezuela) crude oils. Using GC-MS, they found that the latter most

likely contained Me,H (**36b**), Et,H (**41a**), Me,Et (**36a**), Me,*n*-Pr (**36c**) and Et,*n*-Pr (**41b**) maleimides, whereas the Gilsonite and Lloydminster samples were thought to contain Me,H (**36b**), Et,H (**41a**), Me,Et (**36a**) and Me,*n*-Pr (**36c**) maleimides. Not surprisingly, Me,Et maleimide (**36a**) was found to be the most abundant in all three samples due to the overwhelming occurrence of DPEP (**16**) and other sedimentary alkyl porphyrins containing Me,Et substitution. A later study involving oxidation of vanadyl porphyrins from Boscan crude (Quirke *et al.*, 1980) revealed a homologous series of 3-methyl components with 4-*n*-alkyl side chains extending to C_{11}. A number of maleimide standards were synthesised and co-injected to ensure the identity of the components that were only tentatively assigned by Hodgson *et al.* (1971). Indeed, it was found that the previously assigned Et,H maleimide (**41a**) was actually Me,Me maleimide (**36d**). Other maleimides previously not found included the H,H (**42**), Et,Et (**41c**), Me,*sec*-Bu (**36e**), Me,*i*-Bu (**36f**), Me,*n*-Bu (**36g**), and Me,*n*-Hex (**36h**) components. It was suggested that the long *n*-alkyl chains were formed as a result of thermal cracking of the porphyrins from kerogen and that Me,*i*-Bu maleimide (**36f**) originated from the Chlorobiaceae.

Chemical oxidation is not the only method for the production of maleimides. Chls are normally protected from photo-oxidation by the presence of carotenoids. However, after the death of an organism the level of protection afforded by the carotenoids slowly diminishes. Consequently, the photosynthetic pigments of phytoplankton are at risk of photo-oxidation within the euphotic zone (Jen and MacKinney, 1970b; Brown *et al.*, 1980) where they probably degrade to form maleimides. It is likely that the mechanism for photo-oxidation of tetrapyrrolic compounds involves degradation of the methine bridges. This was reported by Jen and MacKinney (1970b) who isolated pink or red coloured intermediates from a solution of Chl *a* (**1**) after solar irradiation. The NMR spectra of these intermediates showed a lack of proton signals at the methine bridges. It has also since been reported that Me,Et maleimide (**36a**) may be obtained from a solution of Chl *a* (**1**) in synthetic seawater after exposure to sunlight (Rontani *et al.*, 1991). Such work provides evidence to suggest that maleimides are formed naturally in the palaeo water column and are not simply artefacts that occur during storage (see also Chapter 2). More recently, maleimides have been located in sulfur-rich immature kerogens from the Nordlinger Ries in southern Germany (Barakat and Rullkotter, 1998) after treatment with sodium dichromate in glacial acetic acid. As expected, Me,Et maleimide (**36a**) was found to be the most dominant,

but also found was a lesser quantity of Me,Me maleimide (**36d**). It is suspected that the maleimides originated from trapped tetrapyrroles (*e.g.* aetioporphyrins) in the kerogen matrix. Very recently, Suzuki *et al.* (1999) also employed chromic acid oxidation and developed a HPLC technique with UV_{280} detection to analyse the oxidation products, especially maleimide derivatives of Chl, which emerge during Chl breakdown in biological systems.

Maleimides as Biomarkers

The work outlined above mostly concentrated on distributions obtained from chemically oxidised porphyrin fractions and did not attempt to determine their ultimate origin in the natural environment. However, Grice *et al.* (1996) found free maleimides [analysed as tertiary-butyldimethylsilyl (TBDMS) derivatives] for the first time in sediments from two restricted marine basins: Kupferschiefer from the Lower Rhine Basin (Permian) and Serpiano shale (Mid-Triassic). Me,Et maleimide (**43a**) was again the most dominant, but Me,*n*-Pr (**43b**) and Me,*i*-Bu (**43c**) maleimides were also detected. The significance of these latter components is that on structural grounds they fit with Bchl *c* (**12**), *d* (**10**) or *e* (**13**) origin. Indeed, the only known precursors from which Me,*i*-Bu maleimide (**43c**) can originate are the Bchls, with an *i*-Bu side chain at C-8. Unfortunately, Me,*n*-Pr (**43b**) maleimide has two possible sources on structural grounds, one from the Bchls *c*, *d* and *e* (**12, 10** or **13**) containing a *n*-Pr side chain at C-8 and the other from, for example, Chl *a* (**1**) if it undergoes hydrolysis of the C-17 ester, followed by reduction of the resulting C-3 acid substituent (Fig. 1.2). However, it is unlikely that the latter contributed much to the source input of Me,*n*-Pr (**43b**) maleimide in these sediments, since both Me,*n*-Pr (**43b**) and Me,*i*-Bu (**43c**) maleimides were enriched in ^{13}C relative to Me,Et maleimide (**43a**) which is thought to be mainly of phytoplanktonic origin. Therefore, Grice *et al.* (1996) concluded that Chlorobiaceae had existed in the palaeo water column during periods of PZA. To further substantiate this, Grice *et al.* (1997) analysed more Kupferschiefer extracts from the Lower Rhine Basin and obtained similarly high $\delta^{13}C$ values for isorenieratane (**34**), which originates from the characteristic carotenoid isorenieratene (**15**) used only by the brown strains of the Chlorobiaceae. Later, Crawford (1998) extended these studies by investigating the maleimide (free and laboratory oxidised products) and porphyrin distributions of Kupferschiefer samples from the main

Fig. 1.2 Dual Origin of Me,*n*Pr Maleimide

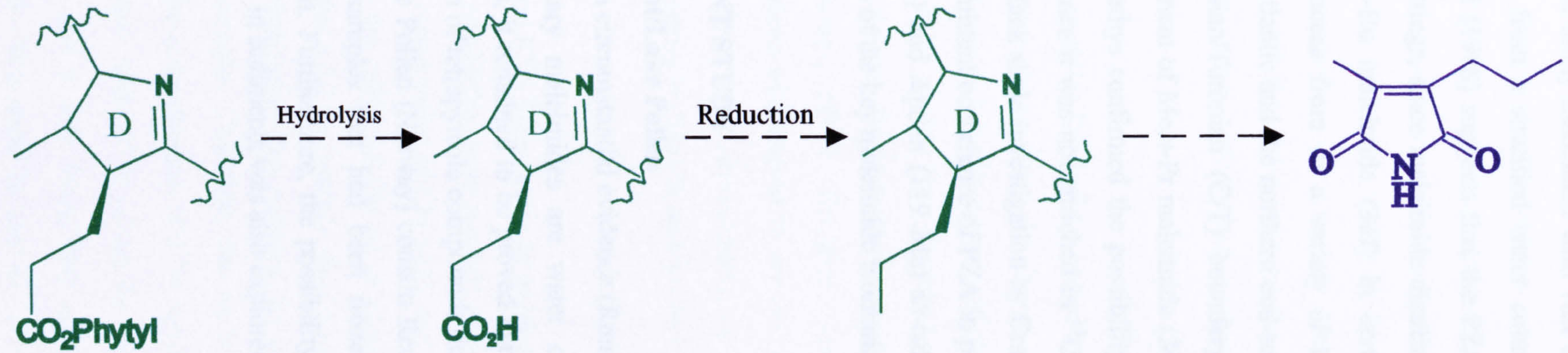

Southern and Northern Permian Basins. The results indicate that episodes of PZA were most likely associated with vast areas of the Zechstein Sea in the late Permian, resulting from a stratified water column. Moreover, another study carried out by Crawford (1998) suggests that the PZA phenomenon may also occur in more open ocean settings, since maleimide distributions, in conjunction with heavy $\delta^{13}C$ values for Me,*i*-Bu maleimide (**36f**) in certain samples, indicate the past presence of Chlorobiaceae from of a variety of black shales, deposited at different locations (North Atlantic and the northern and southern regions of the Tethys, Italy) around the Cenomanian/Turonian (C/T) boundary (91.5 – 90.5 Ma). Interestingly, the $\delta^{13}C$ measurement of Me,*n*-Pr maleimide (**36c**) in three samples from the northern regions of the Tethys confirmed the possibility that it may not always be of Chlorobiaceae origin, since it was not enriched in ^{13}C relative to Me,Et maleimide (**36a**). Finally, a further black shale investigation by Crawford (1998) provided additional evidence for the intermittent occurrence of PZA in pelagic sediments deposited during the Toarcian (194 Ma) and Aptian (119 Ma) so-called Oceanic Anoxic Events (OAEs) with the detection of the key maleimide biomarker, Me,*i*-Bu maleimide (**36f**).

PRESENT STUDY

Priest Pot/Lake Pollen

Although circumstantial evidence (Rontani *et al.*, 1991; Crawford, 1998) suggests that sedimentary maleimides are water column degradation products of tetrapyrrole pigments, it remained to be proved that they are not simply artefacts formed from the oxidation of tetrapyrrole compounds during sample storage. Both Priest Pot (England) and Lake Pollen (Norway) contain Recent sediments and investigations were carried out on samples that had been frozen and stored in the dark immediately after collection. Furthermore, the possibility of finding acidic maleimides (*e.g.* hematinic acid, **44**) in sediments was also explored using the same samples.

Vena del Gesso

Previous studies (*e.g.* Keely *et al.*, 1995; Schaeffer *et al.*, 1995; Sinninghe Damsté *et al.*, 1995; Kenig *et al.*, 1995) of samples from this restricted marine basin mainly concentrated on obtaining the distributions and concentrations of diaromatic isoprenoid compounds with the specific 2,3,6-trimethyl substitution as biomarkers indicative of the brown strains of the Chlorobiaceae. The aim of this study was to further substantiate the work of the above authors by investigating the possible occurrence of PZA and to demonstrate the relative ease with which maleimides can be used as indicators of PZA compared with the isoprenoid compounds.

The Cenomanian/Turonian Oceanic Anoxic Event

The above study on Vena del Gesso involved the possibility of PZA occurring in a restricted marine basin as a result of salinity-induced stratification. However, previous work on black shales from the Northern Tethys (Italy) of the Cretaceous C/T OAE suggests the possible occurrence of PZA in a more open ocean setting (Crawford, 1998; Turner, 1998). Therefore, the aim of this study was to further these investigations with respect to solvent-extractable maleimide distributions, maleimides obtained from the photo-oxidation of porphyrin fractions and $\delta^{13}C$ measurements of Me,Et maleimide (**36a**) in certain black shale samples of C/T age.

Attempted $\delta^{15}N$ Measurement of Maleimides

Sachs *et al.* (1999a) have recently explored the relationship between the nitrogen and carbon isotopic ratios of Chl *a* (**1**), and total biomass in cultured marine phytoplankton to assess the utility of Chl as an isotopic proxy for photoautotrophs. Their findings suggest that a 5.1 ‰ isotopic depletion of Chl *a* (**1**) relative to total algal nitrogen is a robust relationship that justifies the use of Chl as a nitrogen isotopic surrogate for photoautotrophs. Therefore, the main aim of this study was to develop a suitable method for determination of $\delta^{15}N$ values in maleimides using GC-C-IRMS, in view of the fact that, if the $\delta^{15}N$ values for each of the pyrroline rings of Chl *a* (**1**) could be obtained and it was found that all four have the same $\delta^{15}N$ values, then Me,Et maleimide (**36a**) could be used as a nitrogen isotopic proxy for photoautotrophs.

CHAPTER 2:

PRIEST POT/LAKE POLLEN

INTRODUCTION

BACKGROUND

General

Predominantly, there are two sides to the argument as to when maleimides are formed: the precursor Chls (and/or their early stage diagenetic transformation products, *i.e.* chlorins) of an organism after death may be either enzymatically or photo-oxidatively degraded to maleimides in the water column. Rontani *et al.* (1991) provided some circumstantial evidence, since they reported that Me,Et maleimide (**36a**) may be obtained from a solution of Chl *a* (**1**) in synthetic seawater after photo-oxidative degradation. On the other hand, maleimides may be merely artefacts formed from the oxidation of tetrapyrrole compounds during sample storage or in ancient sediments even during the weathering of outcrops. Indeed, circumstantial evidence here stems from the ready oxidation of thioethers to sulfoxides on storage (Kohnen *et al.*, 1990; Schouten *et al.*, 1995). Some evidence against an artefactual origin was provided by Crawford (1998). Analysis (within a few weeks) of a black shale of C/T age collected from an outcrop thought to be unweathered (approx. 0.75m from the surface and immediately wrapped in foil to exclude light) revealed a simple distribution of maleimides. Moreover, if maleimides did indeed arise from the oxidation of porphyrins in weathered outcrops or durlng sample storage then one would expect the distribution of the free maleimides to match exactly that obtained from the photo-oxidised porphyrin fractions. Previous studies by Crawford (1998) and later work (see Chapter 3) indicate that this is clearly not the case, since maleimides from the photo-oxidised porphyrin fractions often have subtly and sometimes widely differing distributions to those of the free maleimides. Despite such evidence against an artefactual origin it is still possible that maleimides could form within a few weeks or even days if samples are left exposed to both air and light at room temperature. In the present study it was decided to use Recent sediments (*e.g.* Priest Pot and Lake Pollen) with cores that had preferably been immediately sealed and frozen. The main objective of this investigation was to prove that maleimides are formed in the water column and/or sediment by natural processes.

Priest Pot, England

Priest Pot is a small highly productive lake in the English Lake District, Cumbria (Fig. 2.1). It is very shallow and only reaches a maximum depth of 4 m. During summer, solar energy heats the upper layer of water, the epilimnion which overlies the cold, more dense and lower lying meta- and hypolimnion (Innes *et al.*, 1997). The bottom waters and sediments are anoxic during these times (Robinson *et al.*, 1984) and it is known that the surface sediment contains abundant lipids of terrestrial origin, in addition to large contributions from organisms in the aquatic food web, such as phytoplankton and bacterial sources (Robinson *et al.*, 1984; Cranwell *et al.*, 1987).

Lake Pollen, Norway

Pollen is a small lake *ca.* 20 km south of Oslo (Fig. 2.1). During summer (May to September) it becomes thermally stratified and throughout this period the anoxic zone often extends from the bottom sediment (*ca.* 18 m maximum depth) to the chemocline typically at 7m. However, in November as heating by the sun is reduced, the water column overturns and mixing occurs to a depth of approximately 10m, but beneath this the water column and bottom sediments remain perpetually anoxic (Ficken, 1994; Innes *et al.*, 1998). Such mixing is occasionally referred to as autumn turnover (Demaison and Moore, 1980). Lake Pollen was once connected to the sea as part of the Oslo fjord system, but in the late 18th century became isolated due to isostatic uplift after the removal of glacial ice sheets (Ficken, 1994; Innes *et al.*, 1998). The environmental change from fjord (marine) to an isolated (lacustrine) lake is recorded in the organic geochemical record (see later).

Fig. 2.1 Approximate Location of: (a) Priest Pot and (b) Lake Pollen

(a)

(b)

PREVIOUS STUDIES

Priest Pot

The total organic carbon (TOC) values for the sediment range from 16-25% and appear to reflect the levels of high productivity and excellent conditions for preservation, since the water column is very shallow and the bottom waters are oxygen deficient (Innes *et al.*, 1997). Furthermore, there is a small but progressive decrease in TOC values downcore, which indicates a general diagenetic trend and fairly constant deposition of organic matter. Innes *et al.* (1997) examined the distribution and obtained the concentrations of both bio- and geohopanoids (up to 3000 μg/g dry sed. and 1700 μg/g dry sed. respectively) in the sediments. Hopanoids are pentacyclic triterpenes and are widely used as biomarkers in ancient sediments and oils due to their widespread occurrence. The biohopanoids are synthesised as membrane lipids by oxygenic bacteria of many different taxonomic groups (Rohmer *et al.*, 1984), and the geohopanoids are formed through diagenesis of biohopanoids. Innes *et al.* (1997) concluded that the high relative abundance of both bio- and geohopanoids in Priest Pot sediments is due to a high level of bacterial productivity combined with favourable conditions of preservation. Furthermore, the lack of evidence for the conversion of free bio- to geohopanoids with depth indicated to the authors that in this sediment incorporation into kerogen may be occurring very early in diagenesis. Additionally, an earlier study by Spooner *et al.* (1994) revealed that the $\delta^{13}C$ values of sedimentary hopenes (*e.g.* hop-22(29)-ene, -55.2 ‰) were markedly depleted in ^{13}C compared with those determined for phytoplanktonic hop-22(29)-ene (-32.7 ‰), attributed an origin from cyanobacteria. They concluded that the highly depleted ^{13}C source provides a significant contribution and that the sedimentary hopenes are partly derived from methanotrophic bacteria existing in the water column. More recently, a study of Priest Pot sediment by Harradine and Maxwell (1998) proved that Chls c_1 (**4**) and c_2 (**5**) undergo enzymatic removal of the C-13^2 carbomethoxy substituent in the water column, as a result of zooplankton herbivory, which is an essential prerequisite for the diagenetic transformation pathway of the Chls *c* to several sedimentary alkyl porphyrins. Finally, an earlier attempt (Crawford, personal communication) to detect maleimides in Priest Pot sediment was unsuccessful due to the overwhelming presence of chlorins with a similar polarity, which are thought to have masked the detection of maleimides by GC-MS.

Lake Pollen

The sediment TOC values are in the range of 1.9% (± 0.04%) to 8.3% (± 0.17%) and reflect both high productivity and favourable conditions for preservation within the water column (Innes *et al.*, 1998). Furthermore, total sulfur (TS) values are in the range of 1.1% (± 0.01%) to 2.6% (± 0.03%). Interestingly, the downcore plots of TOC and TS reveal a greater variation in samples deposited under marine conditions *i.e.* below 25 to 30cm. Such data indicated that redox conditions within the water column might have stabilised after isolation of the lake (Innes *et al.*, 1998). Analysis of the sedimentary alkenones revealed a distribution typical of a cool marine environment, since the high relative abundance of C_{39} and C_{40} alkenones and the presence of the $C_{37:4}$ methyl ketone, usually associated with lacustrine conditions, were not found (Cranwell, 1985; Brassell, 1993; Li *et al.*, 1996; Thiel *et al.*, 1997). The long chain unsaturated ketones are thought to originate mostly from marine prymnesiophytes (*e.g.* Brassell *et al.*, 1980; Volkman *et al.*, 1980) and the depth profile of the total alkenone abundance shows the absence of such compounds between 25 and 30cm depth; interestingly, this corresponds to the boundary during which the change between marine and lacustrine conditions occurred (Ficken, 1994). In a more recent study, Innes *et al.* (1998) discovered that both bio- and geohopanoids were present in high concentrations in the sediments (up to 321 μg/g dry sed. and 307 μg/g dry sed. respectively) and that the downcore profiles are comparable, with the largest amounts detected at the base of the core. Interestingly, there is a noticeable decrease in the abundance of both bio- and geohopanoids above 25 to 30cm depth, which coincides with a definite change in environment from fjord to lacustrine conditions, previously evidenced by a lack of alkenones at the same depth.

THIS STUDY

General

The major aim was to prove that maleimides are formed naturally in the water column and/or sediment from the degradation of tetrapyrrole pigments, since it has been suggested (*e.g.* Sinninghe Damsté, personal communication) that maleimides are merely artefacts formed from the oxidation of tetrapyrrole compounds during sample storage.

Priest Pot

The sediment (upper 24 cm) was removed from a core of Priest Pot (Lake District; 54° 22'N, 3°00'W) in September 1995 with a Jenkin corer (Innes *et al.*, 1997). The core was taken from the lake bottom (< 1 mg O_2/l; 4 m depth). It was stored in a cool room (4°C; 24 h), then sectioned under nitrogen into slices (1 cm depth; 7 cm diameter). Without delay, the sub-samples were frozen at -20°C, before being transported in an ice packed cool box (2-4°C; *ca.* 5 h) to the University of Bristol where they were immediately stored at -20°C. Prior to analyses they were freeze-dried and crushed to a fine powder. For the purposes of this study the sub-samples were combined to form one bulk sample before extraction.

Lake Pollen

With the use of a simple gravity corer, a core of anoxic sediment (46 cm long, 4.4 cm diameter) was collected in June 1992 from a water depth of 18m (Ficken, 1994). It was quickly sealed and frozen (-20°C), before being transported in an ice packed cool box (2-4°C; *ca.* 5 h) to the University of Bristol where it was immediately stored at -20°C. Whilst frozen, the core was cut with a mechanical hacksaw into two sections; the first (0-27 cm, top to bottom) represents the lacustrine period after the lake became isolated and the second (27-46 cm, top to bottom) denotes the fjord stage during which the sediment was deposited in a marine environment. Finally, prior to analysis, the samples were freeze-dried and pulverised to a fine powder.

RESULTS

PRIEST POT

Extractable (Free) Maleimides

Bulk Sample

GC-MS revealed the presence of Me,H (**36b**) and Me,Et (**36a**) maleimides (Fig. 2.2). Me,Et maleimide (**36a**) was the more abundant and its presence was confirmed by comparison with the relative retention time and mass spectrum of the standard obtained by the oxidation of aetioporphyrin III (**17**). The other component's spectrum and relative retention time agreed with those observed by Quirke *et al.* (1980). The two may be differentiated by a few distinctive ions, primarily the molecular ion (Fig. 2.3). For Me,Et (**36a**) maleimide there is an additional ion at *m/z* 124 arising from the loss of a methyl radical due to β cleavage of the ethyl group. The concentration of both Me,H (**36b**) and Me,Et (**36a**) maleimides (29 and 555 ng/g dry sed. respectively) was also obtained, since phthalimide (**45**) was added as an internal standard to the bulk sample at the total organic extract (TOE) stage.

Acidic Maleimides

Bulk Sample

Hematinic acid (analysed as the Me ester, **46**) was detected by GC-MS in the acidic fraction (F4.3) of the bulk sample (Fig. 2.2). Its presence was confirmed by comparison with the relative retention time and mass spectrum of the standard obtained by the oxidation of bilirubin (**47**). Furthermore, the relative abundance of the molecular ion in the spectrum is very low compared to that typically found for the alkyl maleimides. Instead, the ions at *m/z* 137 and 165 (base peak) are the most characteristic (Fig. 2.3).

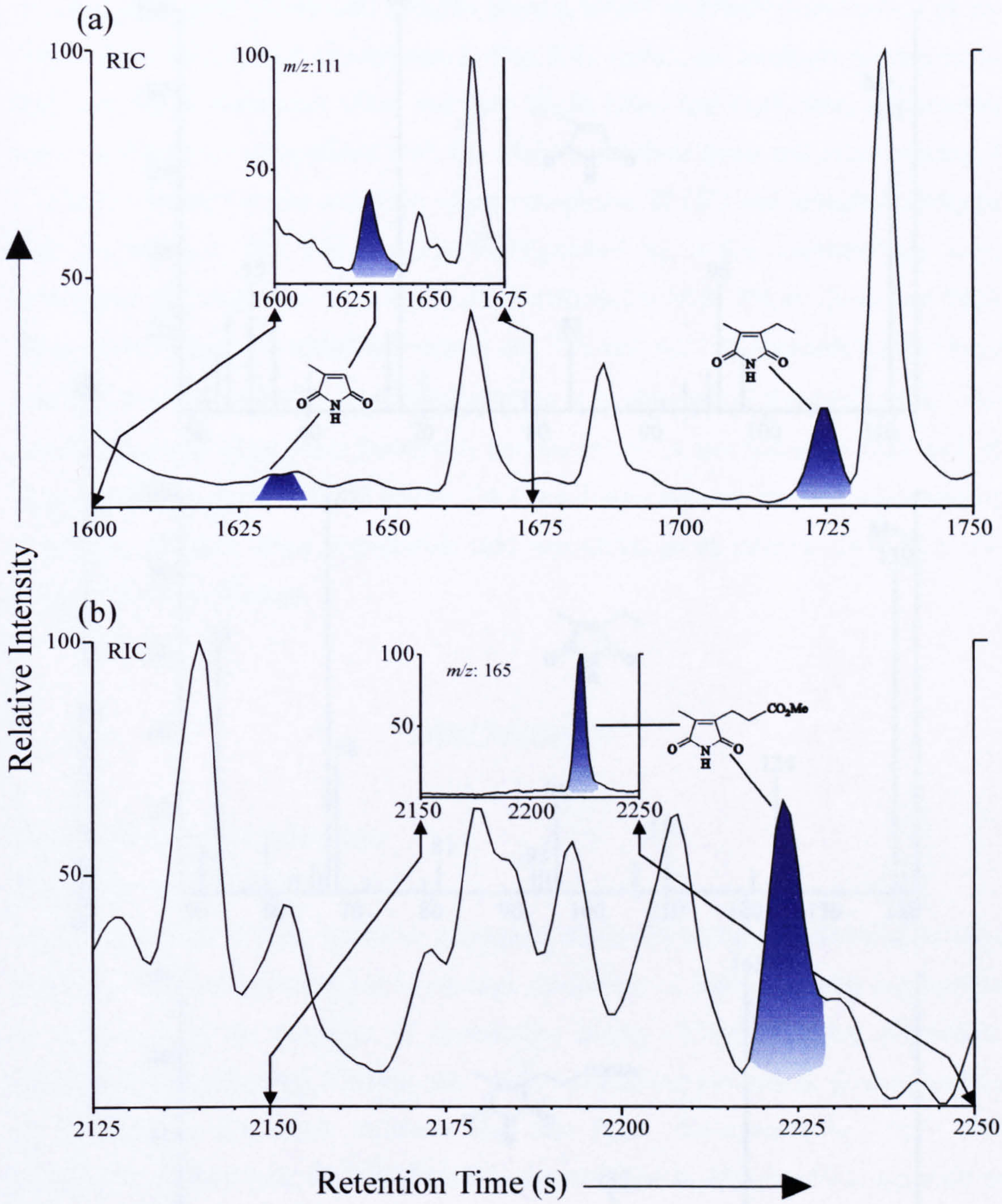

Fig. 2.2 Partial RIC and Mass Chromatograms of Priest Pot:
(a) maleimides and (b) hematinic acid using
CP-WAX 52 CB Stationary Phase

Fig. 2.3 Mass Spectra of Free Maleimides Obtained from Priest Pot

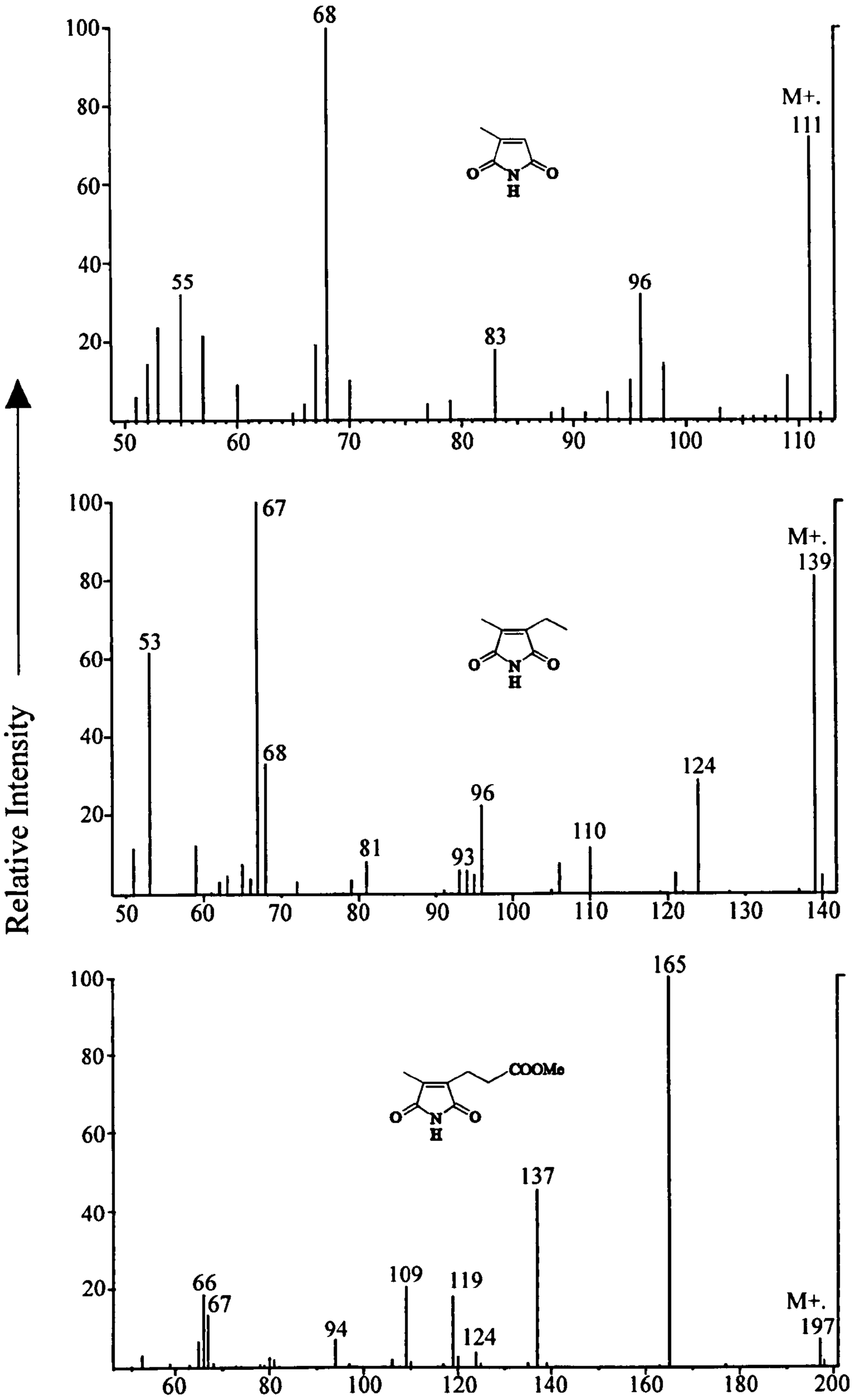

LAKE POLLEN

Extractable (Free) Maleimides

Maleimides detected by GC-MS in the polar fraction (F4.2) of both the lacustrine (0-27 cm) and marine (27-46 cm) samples show a simple distribution comprised of the Me,Et (**36a**) and Et,Et (**41c**) components (Fig. 2.4). Again, the dominant component in both was Me,Et maleimide (**36a**) and both Me,Et (**36a**) and Et,Et (**41c**) components were confirmed by comparison with the relative retention times and mass spectra of standards obtained by the oxidation of aetioporphyrin III (**17**) and octaethylporphyrin (**48**) respectively. The two may be distinguished by a few characteristic ions, principally the molecular ion (Fig. 2.5). Furthermore, both Me,Et (**36a**) and Et,Et (**41c**) maleimides have additional ions at *m/z* 124 and *m/z* 138 respectively that have resulted from the loss of a methyl radical due to β cleavage of the ethyl group. The Me,Et (**36a**) and Et,Et (**41c**) maleimide concentrations in the lacustrine (324 and 96 ng/g dry sed. respectively) and marine (182 and 3 ng/g dry sed. respectively) samples were also obtained, since phthalimide (**45**) was added as an internal standard to the samples at the TOE stage.

DISCUSSION

Extractable (Free) Maleimides

Priest Pot and Lake Pollen

As mentioned previously, an earlier attempt to obtain the maleimide distribution from Priest Pot was unsuccessful due to the high abundance of chlorins, which are thought to have masked the presence of maleimides during GC-MS analysis (Crawford, personal communication). Clearly, the "usual" extraction and purification procedure for maleimides (*i.e.* flash columns and thin layer chromatography, TLC) was insufficient to deal with the high chlorin content found in Recent sediments such as Priest Pot. To overcome this problem, a gel permeation chromatography (GPC) method utilising the principle of size exclusion was developed (see Chapter 7 for details) which enabled separation of maleimides from the vast majority of the chlorins. The maleimide fraction was further purified using TLC as the final step, before analysis by GC-MS.

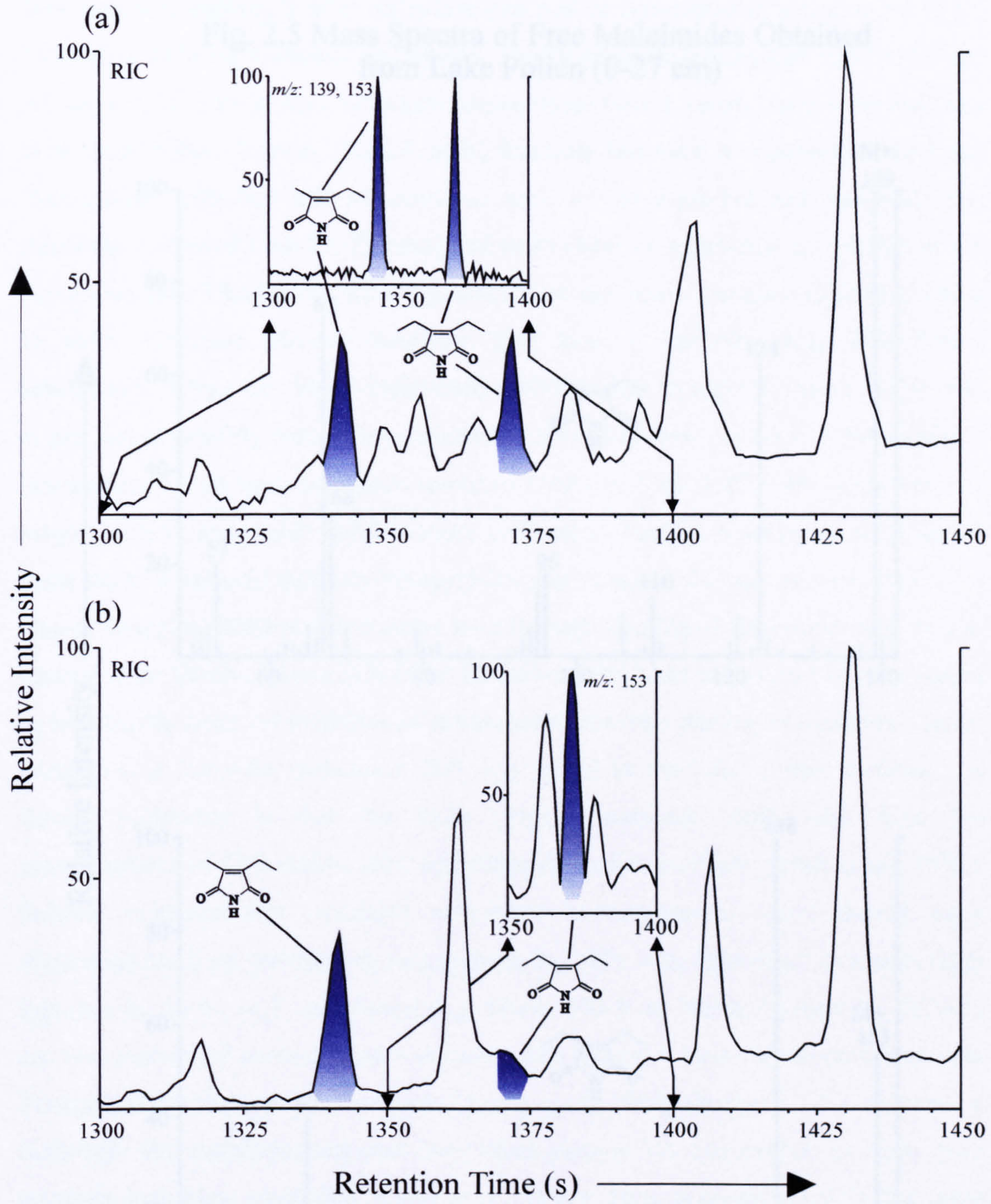

Fig. 2.4 Partial RIC and Mass Chromatograms of Solvent Extractable Maleimides from Lake Pollen (a) 0-27 cm and (b) 27-46 cm using CP-WAX 52 CB Stationary Phase

Fig. 2.5 Mass Spectra of Free Maleimides Obtained from Lake Pollen (0-27 cm)

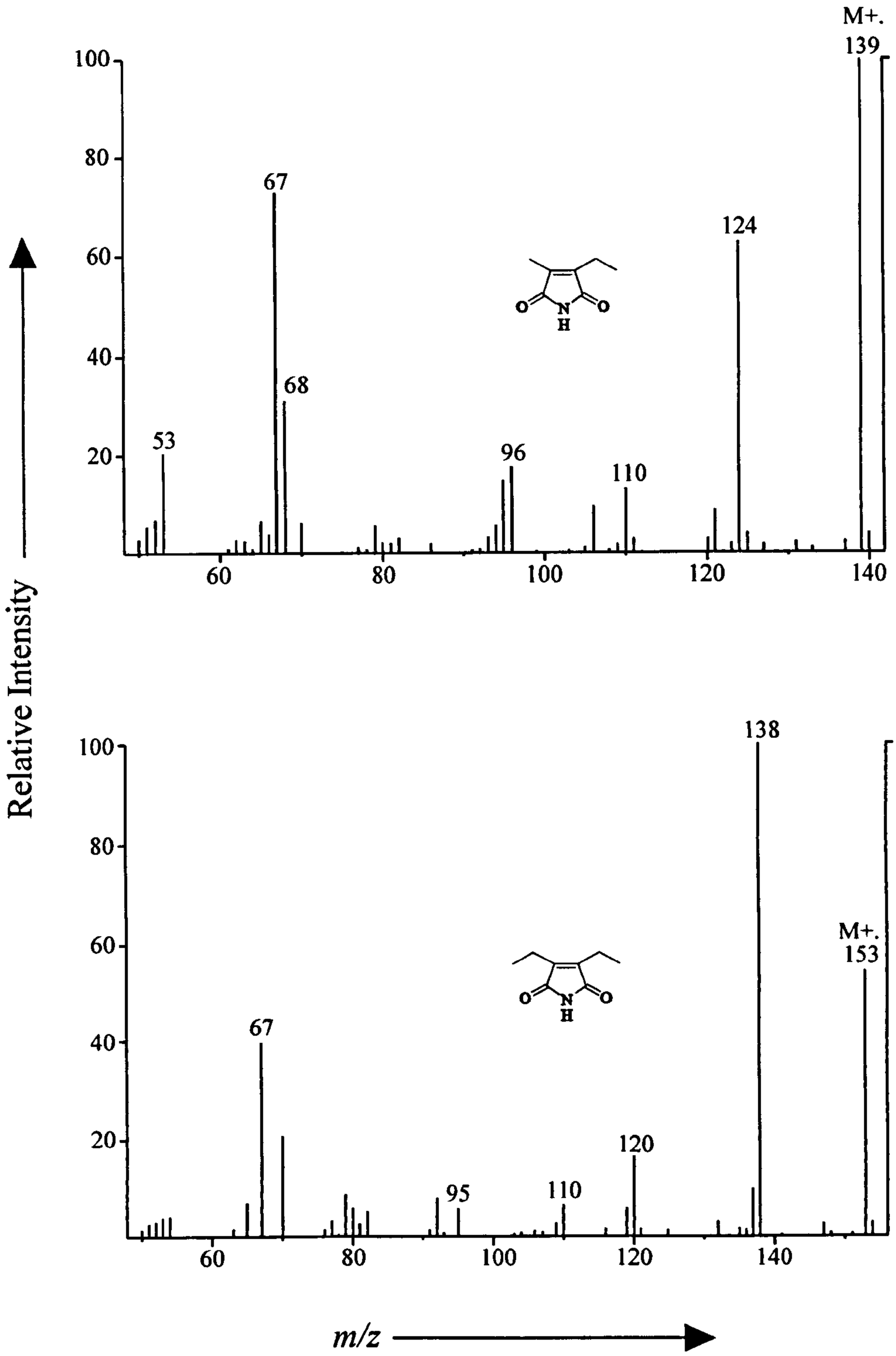

The Priest Pot sediment distribution shows both Me,H (**36b**) and Me,Et (**36a**) maleimides along with the presence of hematinic acid (**44**); however, the core had not been frozen immediately after collection and was in fact stored in a cold room (4°C; 24 h) prior to being sectioned and frozen. Therefore, to be certain that maleimides are not derived from an artefactual origin two samples from a second core were analysed from Lake Pollen, Norway. Significantly, this core had been immediately sealed and frozen after collection and remained so until it was extracted and analysed. The distribution showed both Me,Et (**36a**) and Et,Et (**41c**) maleimides with the former the more abundant. This is not surprising, since there are many precursor Chls (*e.g.* Chl *a* **1**) and/or chlorins derived therefrom that have a pyrroline ring with Me,Et substituents. Likewise, Me,H maleimide (**36b**) is also thought to be of planktonic origin and is possibly formed by a similar process that removes the C-3 functionality that eventually, on later diagenesis produces CAPs (*e.g.* C_{30} DPEP **49**). However, the origin of Et,Et maleimide (**41c**) is more difficult to explain, although it must derive from early diagenetic product tetrapyrroles that contain the appropriate alkyl side chains. One possibility is that it could arise through opening of the exocyclic E ring of certain of the Bchls *c*, *d* or *e* (**12**, **10** or **13**; Grice, 1995), but in this case this is thought to be unlikely since no evidence of components from the photosynthetic green sulfur bacteria (*e.g.* Me,*i*-Bu maleimide **36f**) was found in the Lake Pollen sediment. A further possibility is that the Et,Et (**41c**) component could arise from the rearrangement of Chls and/or their early transformation products (Grice *et al.*, 1996). Indirect evidence that extensive enzymatic rearrangements occur during early diagenesis has been provided by ring systems in CAPs with rearranged exocyclic rings that may be 5-, 6-, or 7- membered (*e.g.* **18a-b, 19a-b or 20a-b**; Chapter 1). BiCAPs are also rearranged products and component **23b** has been found in the immature Late Pliocene Willershausen lake sediment (Keely *et al.*, 1994; Chapter 1). Furthermore, it is thought that rearrangement must have taken place at low temperature and may have involved biological mediation (Keely *et al.*, 1994). Thus, it seems possible that other such transformations could yield maleimides whose structural origins are not obvious (Grice *et al.*, 1996). However, the primary aim of this study was to firmly establish that maleimides are indeed formed in the water column and/or sediment by natural processes; and this has been shown to be the case.

Acidic Maleimides

Priest Pot

The additional GPC method employed to purify the alkyl maleimides was not required for the detection of hematinic acid (**44**) because the acidic maleimide fraction (F4.3) was sufficiently purified with an aminopropyl cartridge followed by methylation with boron trifluoride in methanol (BF_3/MeOH), before finally being purified with TLC prior to analysis by GC-MS.

The origin of hematinic acid (**44**) is difficult to explain, but it probably originates from Chls and/or other tetrapyrroles that contain an appropriate acidic substituent. One possibility is that it may be derived from Chl *a* (**1**) after very early diagenetic hydrolysis of the C-17 ester, indicating that oxidative degradation of the Chl tetrapyrrole macrocycle occurs after hydrolysis of the C-17 ester in the diagenetic pathway. As indicated in Chapter 1, Verne-Mismer *et al.* (1986) discovered the presence of a C_{33} member of the DPEP series in Boscan crude oil, which is thought to have resulted from hydrolysis of the C-17 ester of Chl *a* (**1**), followed by reduction of the resulting C_3 acid substituent. By analogy, reduction of hematinic acid (**44**) would produce Me,*n*-Pr maleimide (**36c**) of planktonic origin as an alternative to a green sulfur bacterial origin from a Bchl with a propyl substituent at C-8 (see Chapter 3).

CONCLUSIONS

- Maleimides are formed from tetrapyrrolic compounds by natural processes that occur in the water column and/or sediment.

- Me,*n*-Pr maleimide (**36c**) of planktonic origin may arise either from reduction of free hematinic acid (**44**) or from oxidative degradation of certain C_{33} CAPs (Verne-Mismer *et al.*, 1986). Alternatively, Me,*n*-Pr maleimide (**36c**) may have a green sulfur bacterial origin from a Bchl with a propyl substituent at C-8.

CHAPTER 3:

VENA DEL GESSO

INTRODUCTION

GEOLOGICAL BACKGROUND OF VENA DEL GESSO

The Vena del Gesso (VdG) basin is located in the northern part of the Periadriatic trough, northern Italy (Fig. 3.1). The sediments of which were deposited during the Messinian (*ca.* 5.1 Ma), which was the final age in the Miocene (Harland *et al.*, 1982). The combination of a tectonically-induced basin collapse and a worldwide fall in sea level meant that the flow of marine waters between the Atlantic Ocean and the Mediterranean Sea was restricted by the presence of a connective sill (*i.e.* the Straits of Gibraltar, which are thought to have been closed *ca.* 6.5-5.1 Ma). These conditions led to an event entitled the "Messinian Salinity Crisis" (Hsü *et al.*, 1973), which affected the entire Mediterranean region and reduced it to a series of evaporitic basins (Vai and Ricci Lucchi, 1977). During transgressive phases marine waters from the Atlantic Ocean flowed over the Straits of Gibraltar and into the Mediterranean Sea. Evaporation of water on its way to the VdG basin meant that marine waters with enhanced salinity flowed from the Mediterranean Sea into the VdG basin (max. water depth of the order of some tens of m; Vai and Ricci Lucchi, 1977). Thus, stratification occurred as a result of a salinity-induced mechanism. Examination of the VdG marls revealed the presence of fine-scale laminations and an almost complete absence of benthic organisms and bioturbation (Vai and Ricci Lucchi, 1977). These findings indicate that anoxic bottom waters, during the filling of the basin, led to a period of increased organic matter preservation in the sediments and the formation of organic-rich marls (up to 2.5% TOC; Sinninghe Damsté *et al.*, 1995). Subsequent evaporation resulted in the formation of stromatolites (algal mats) and eventual precipitation and deposition of gypsum. Thus, the sediments of the VdG (Gessoso-solfifera Formation) appear to have been formed by a cycle of repeated transgressive and regressive phases. The sediment was largely deposited on the perimeter of the northern Apennines and also on the southern Po Plain and is composed of an immense gypsum body 150-170m thick, the outcrop of which forms a well developed ridge which runs parallel to the northern Apennines for approximately 30 km. Between each gypsum bed (*ca.* 25 m) lies a thin marl (*ca.* 1.5 m) and carbonate layer (*ca.* 20 cm; Vai and Ricci Lucchi, 1977). There are 16 depositional cycles in total (Fig. 3.2). The first two

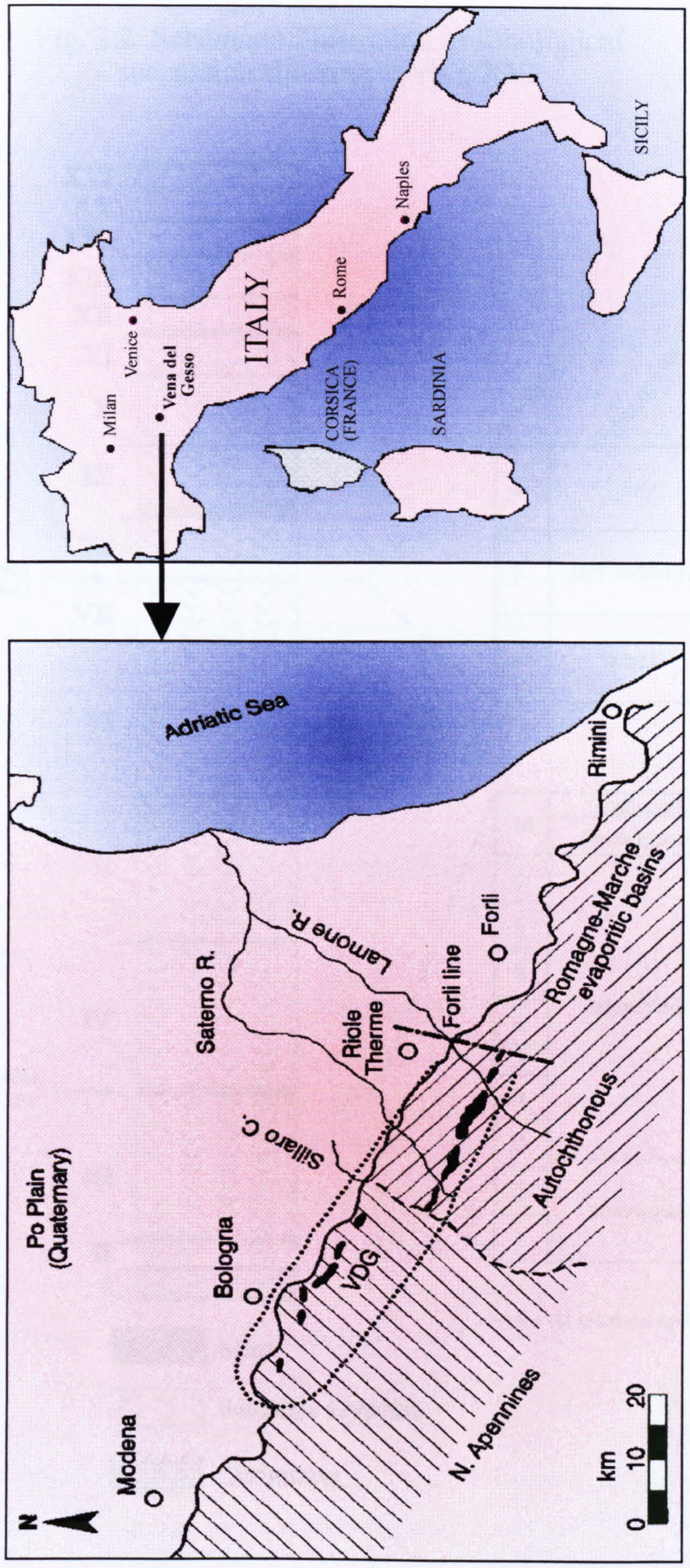

Fig 3.1 Vena del Gesso outcrops (black) and inferred original extent of the Basin (VdG) delimited by dotted lines (modified from Sinninghe Damsté *et al.*, 1995). The Forli line denotes a structural high which separates VdG from the Romagna-Marche evaporite basins to the southeast.

Fig. 3.2 Schematic illustration of lithological succession showing marls I-XVI

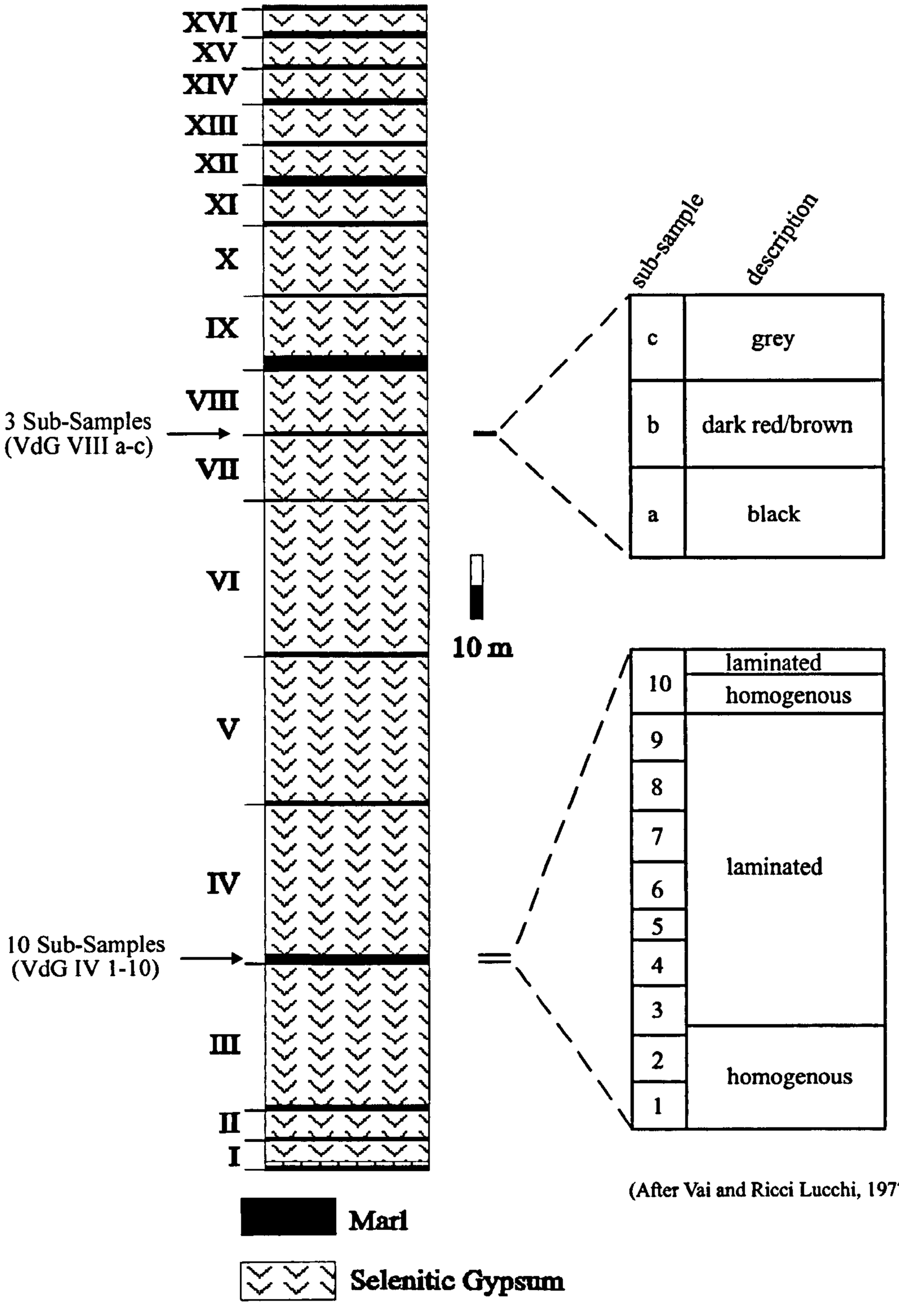

(After Vai and Ricci Lucchi, 1977)

(cycles I and II) are comprised of stromatolites and gypsum. The remaining 14 depositional cycles (III - XVI) are composed of a marl-gypsum couplet.

PREVIOUS WORK ON VENA DEL GESSO

General

Earlier work by Vai and Ricci Lucchi (1977) indicates that the bottom waters of the VdG basin were once anoxic (see above). However, later investigations attempted to reconstruct the particular types of palaeoenvironmental and biological diversity represented by the concentrations and isotopic signals of certain biomarkers; for example, Sinninghe Damsté *et al.* (1995) examined the sulfur-bound fractions from 10 of 14 evaporite cycles and attempted to reconstruct the depth of the chemocline throughout, using the concentration depth profiles of isorenieratane (**34**, derived from the brown strains of the Chlorobiaceae, which indicates the occurrence of PZA) and gammacerane (**50**, inferred to derive from anaerobic bacterivorous ciliates residing at or below the chemocline). They concluded that PZA often occurred during marl deposition and that there were only short periods during the development of the basin in which the chemocline was found in the sediment or in the water column but not in the photic zone. In addition, they found evidence of a large diversity of species that had once existed in the palaeo water column, as well as evidence to suggest an influx from the continent. Similarly, Kenig *et al.* (1995) carried out an in-depth study of ten sub-samples of marl IV and recovered the sulfur-bound lipids *via* desulfurisation from both polar and asphaltene fractions. After determining the isotopic composition of the free and sulfur-bound hydrocarbons, they examined the relationships between those carbon skeletons, precursor biolipids and the organisms producing them. They too concluded that the lagoonal basin was stratified and that PZA occurred during the early and middle stages of marl deposition. They also provided evidence to suggest that the chemocline was highest during the deposition of IV-2. Furthermore, Keely *et al.* (1995) found variations in abundance and composition of porphyrins and carotenoids throughout the entire evaporitic sequence (see below), whilst Schaeffer *et al.* (1995) found that the aliphatic hydrocarbon distributions and concentrations released from sulfur-rich kerogens matched those recovered from the desulfurisation of polar fractions from solvent extracts. Although most biomarkers were dominated by components of an algal origin, they too found diaromatic isoprenoids derived from

Chlorobiaceae which again indicates the occurrence of PZA during sediment deposition.

Pigment Distributions

Porphyrins

The ten sub-samples indicated above were found to contain low amounts of metalloporphyrins and free base alkyl porphyrins, with the free bases in greater abundance (20-800 μg g^{-1} organic carbon, Keely *et al.*, 1995). Analysis of the free base alkyl porphyrin fractions from samples in cycles III-VII by probe or electrospray MS, in addition to normal phase HPLC, revealed simple distributions dominated by C_{32} (DPEP; **16**) and C_{31} CAP species as well as C_{33} BiCAP components with varying relative abundances in each sample or sub-sample. Furthermore, the mass spectra failed to denote the presence of any HMW CAP species. However, a C_{34} CAP (*m/z* 504) was detected by liquid chromatography – photodiode array – mass spectrometry (LC-PDA-MS) in three of the marl IV sub-samples (Keely *et al.*, 1995). It is thought that the dominance of the C_{31} and C_{32} CAPS, and the C_{33} BiCAP components in the electrospray and probe spectra masked the presence of the C_{34} CAP, which was tentatively assigned, on carbon number grounds only, an origin from the Bchls of the Chlorobiaceae.

More recently, Turner (1998) confirmed the presence of major C_{31} and C_{32} CAP components plus the C_{33} BiCAP found previously by Keely *et al.* (1995). It was also found that most sub-samples within marl IV (*e.g.* IV-2, IV-4, IV-6 and IV-8) and the entire VdG deposition (*e.g.* II, VI, VIIIa and X) contained CAPs within the carbon number range C_{31} to C_{36}. However, no LC-MS peaks for Bchl *d*-derived CAPs corresponding to available standards with the same carbon skeleton as certain members of the Bchl *d* (**10**) series were found. Instead, a minor C_{35} component eluting within the HMW region (*e.g.* samples IV-4 and IV-6) was detected. However, this component did not seem to be part of any pseudohomologous series as no C_{34} or C_{36} CAPs were found. Therefore it was tentatively proposed, on the grounds of carbon number only, that the HMW components (*i.e.* $>C_{33}$) might have originated from the Bchls *c* (**12**) or *e* (**13**).

Carotenoids

The presence of the intact diaromatic carotenoid, isorenieratene (**15**) and a geometrical isomer (*cis*-isorenieratene) was revealed using reversed phase HPLC, UV/Vis and LC-MS (Keely *et al.*, 1995). Isorenieratane (**34**), in addition to several other diaryl isoprenoids (*e.g.* C_{32}, C_{33} and C_{40}), was detected in the products after sulfide cleavage of the kerogens with $Li/EtNH_2$ (Schaeffer *et al.*, 1995) and also in the polar and asphaltene fractions of the extract after treatment with nickel boride (Kenig *et al.* 1995). Furthermore, $\delta^{13}C$ data show that the aforementioned isoprenoid compounds were enriched in ^{13}C; for example the major diaryl C_{40} component (isorenieratane, **34**) was found to have a $\delta^{13}C$ value of -13.7 ± 0.5 ‰ (Schaeffer *et al.*, 1995), thus providing further evidence of Chlorobiaceae-derived isorenieratene (**15**). Hence, the structural and isotopic data from the marls clearly suggest that the brown strains of Chlorobiaceae once existed in the water column and that PZA was indeed recurrent throughout the deposition of the entire VdG sequence (Keely *et al.*, 1995; Schaeffer *et al.*, 1995; Kenig *et al.* 1995; Sinninghe Damsté *et al.*, 1995). In contrast, chlorobactene (**3**) or expected products were not found (Keely *et al.*, 1995; Schaeffer *et al.*, 1995; Kenig *et al.* 1995; Sinninghe Damsté *et al.*, 1995). Thus, there is no evidence to suggest that the green strains of Chlorobiaceae existed in the palaeo water column during deposition of the VdG marls.

THIS STUDY

As mentioned previously, the aim was to further substantiate the work of the above authors and demonstrate the relative ease with which maleimides can be used as indicators of PZA compared with the isoprenoid compounds. A sequence of ten sub-samples (IV-1 base, IV-10 top) was taken from marl IV (total thickness 1.3m, each sub-sample approx. 13cm), along with a second sequence of three sub-samples (VIII-a base, VIII-c top) from marl VIII (total thickness 50cm, each sub-sample approx. 17cm); both sets of samples (Fig. 3.2) correspond to those studied previously by Keely *et al.* (1995). The free maleimide distributions and concentrations throughout both marls have been determined and minor nickel porphyrin fractions throughout marl IV were quantified using UV/Vis spectrophotometry. Furthermore, free base alkyl porphyrins from samples IV-1 and IV-5, in addition to nickel porphyrins from

samples IV-4, IV-5, IV-6, IV-7, IV-8 and IV-10, were isolated and photo-oxidised to maleimides whose distributions were determined; $\delta^{13}C$ values for Me,*n*-Pr (**36c**) and Me,*i*-Bu (**36f**) maleimides were obtained for samples IV-1 and IV-3 and finally, $\delta^{13}C$ values for Me,Et maleimide (**36a**) were monitored over the ten sub-samples of marl IV.

RESULTS

VENA DEL GESSO – (MARL IV)

Extractable (Free) Maleimides

Maleimides in the polar fraction (F4.2) show a simple distribution throughout the ten sub-samples. Components observed by GC-MS include: Me,H (**36b**), Me,Me (**36d**), Me,Et (**36a**), Et,Et (**41c**), Me,*n*-Pr (**36c**) and Me,*i*-Bu (**36f**) maleimide, of which Me,Et maleimide (**36a**) is the most dominant (*e.g.* Fig. 3.3). The Me,Et (**36a**) and Et,Et (**41c**) components were confirmed by comparison with standards obtained by the oxidation of aetioporphyrin III (**17**) and octaethylporphyrin (**48**) respectively. The mass spectra and relative retention times of the other components agree with those observed by Quirke *et al.* (1980). The different maleimides are distinguished from one another by a few characteristic ions, primarily the molecular ion (Figs. 3.4 and 3.5). For Me,Et (**36a**) and Et,Et (**41c**) maleimides there are additional ions at *m/z* 124 and *m/z* 138 respectively that result from loss of a methyl radical due to β cleavage of the ethyl group. Furthermore, 3-methyl-1*H*-pyrrole-2,5-diones with chains ($\geq C_3$) at C-4 have an additional ion at *m/z* 125 which results from a McLafferty type rearrangement (*cf.* Grassel *et al.*, 1963) involving the C=C bond. The concentrations were also obtained (Figs. 3.6 and 3.7). Phthalimide (**45**) was added as an internal standard to samples IV-1 to IV-9 at the TOE stage. Quantification for sample IV-10 was achieved by co-injection with phthalimide (**45**) as an external standard.

Porphyrins

Nickel porphyrins were detected in relatively minor amounts (*ca.* 100-240 ng/g sed.) throughout. The isolated fractions were quantified using UV-Vis spectrophotometry

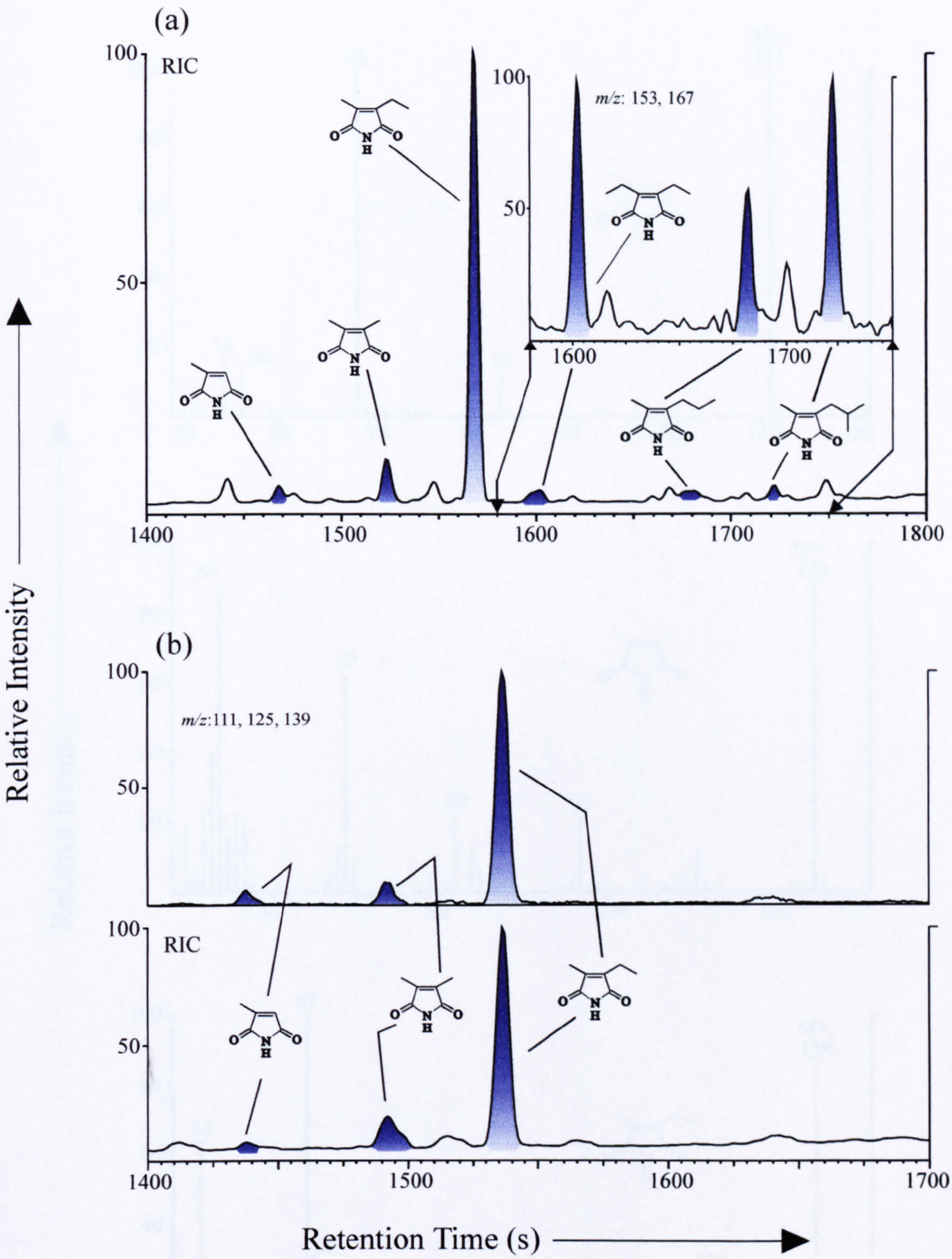

Fig. 3.3 Partial RIC and Mass Chromatograms of Solvent Extractable Maleimides from (a) VdG IV-5 and (b) VdG IV-10 using CP-WAX 52 CB Stationary Phase

Fig. 3.4 Mass Spectra of Free Maleimides Obtained from Sample VdG IV-10

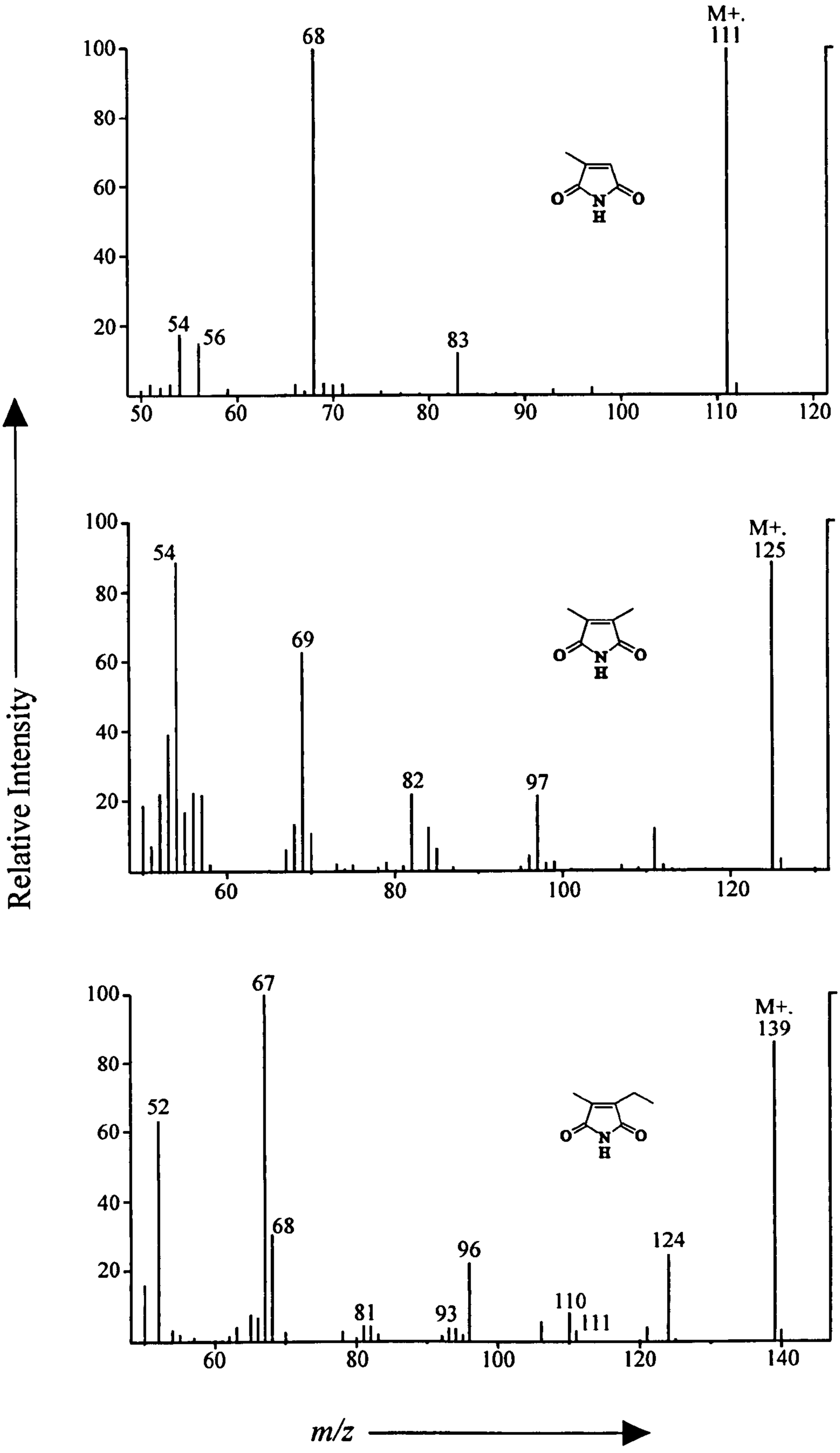

Fig. 3.5 Mass Spectra of Free Maleimides Obtained from Sample VdG IV-5

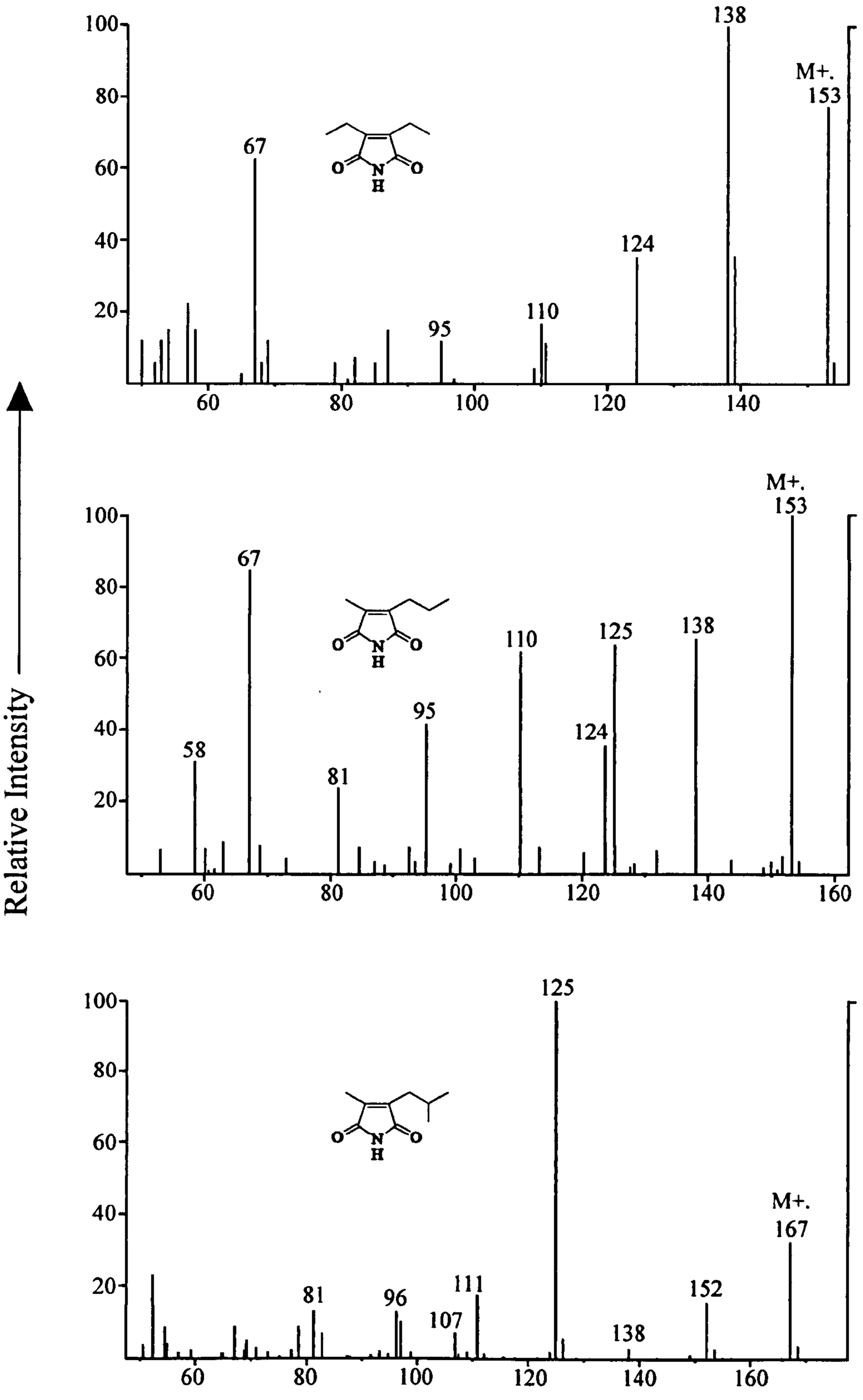

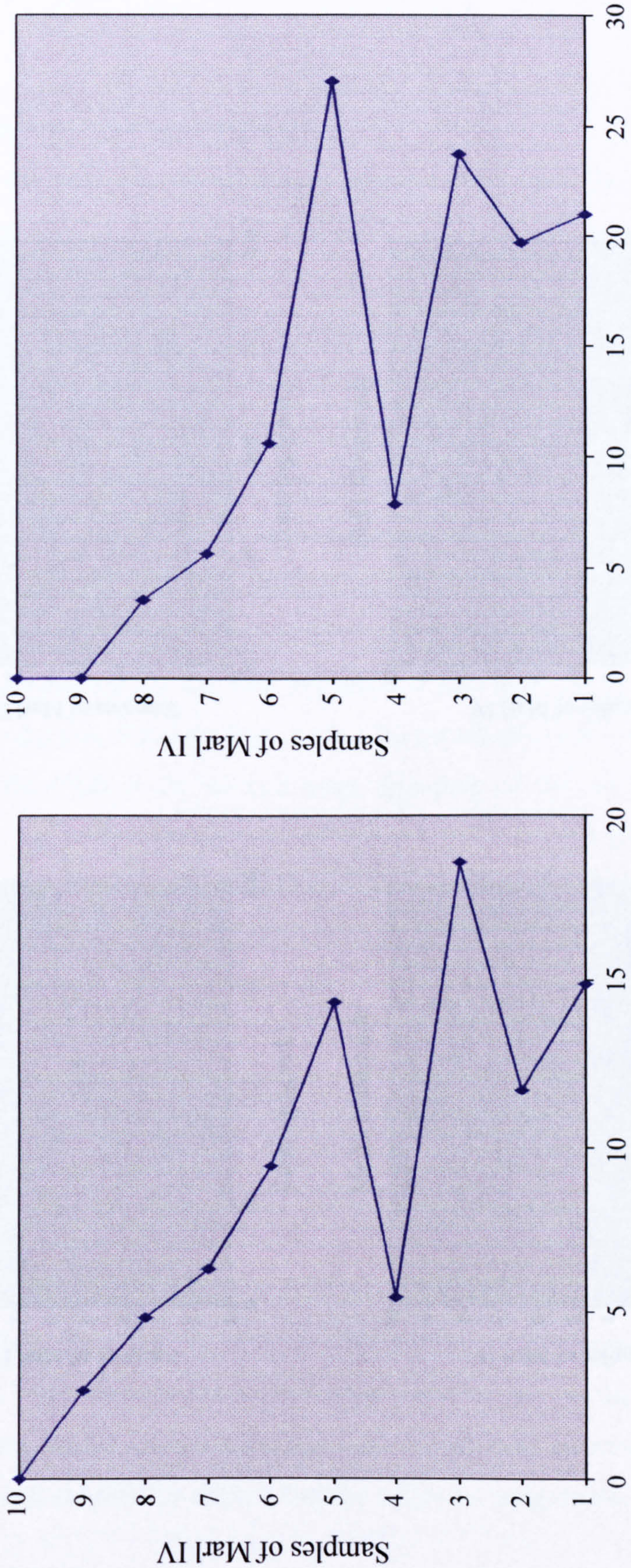

Fig. 3.6 Concentration Depth Profiles for Minor Maleimides

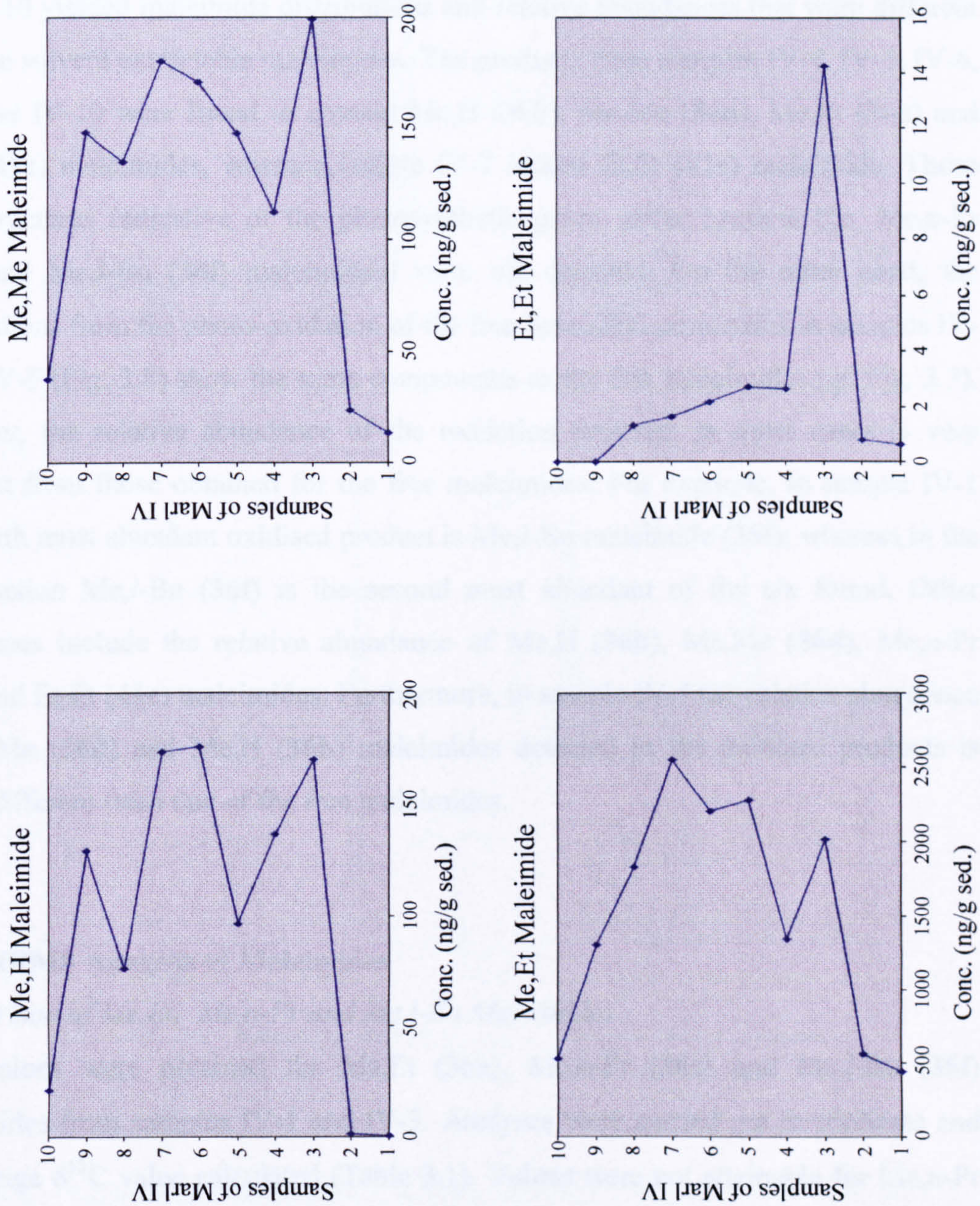

Fig. 3.7 Concentration Depth Profiles for Maleimides through Marl IV

and the concentrations show a similar distribution to the free base alkyl porphyrins obtained by Keely *et al.* (1995).

Maleimides from Porphyrin Photo-Oxidation

Photo-oxidation of the nickel porphyrins from samples IV-4, IV-5, IV-6, IV-7, IV-8 and IV-10 yielded maleimide distributions and relative abundances that were different from the solvent extractable maleimides. The products from samples IV-4, IV-5, IV-6, IV-8 and IV-10 were found to contain Me,H (**36b**), Me,Me (**36d**), Me,Et (**36a**) and Et,Et (**41c**) maleimides, whereas sample IV-7 lacked Et,Et (**41c**) maleimide. Those with structures indicative of the photosynthetic green sulfur bacteria (*i.e.* Me,*n*-Pr (**36c**) and Me,*i*-Bu (**36f**) maleimides) were not detected. On the other hand, the distributions from the photo-oxidation of the free base alkyl porphyrins in samples IV-1 and IV-5 (Fig. 3.8) show the same components as the free maleimides (*cf.* Fig. 3.3). However, the relative abundance of the oxidation products in some cases is very different from those obtained for the free maleimides. For example, in sample IV-1 the fourth most abundant oxidised product is Me,*i*-Bu maleimide (**36f**); whereas in the free fraction Me,*i*-Bu (**36f**) is the second most abundant of the six found. Other differences include the relative abundance of Me,H (**36b**), Me,Me (**36d**), Me,*n*-Pr (**36c**) and Et,Et (**41c**) maleimides. Furthermore, in sample IV-5 the relative abundance of Me,Me (**36d**) and Me,H (**36b**) maleimides detected in the oxidised products is subtly different from that of the free maleimides.

GC-C-IRMS Analysis of Maleimides

Comparison of Me,Et, Me,n-Pr and Me,i-Bu Maleimides

$\delta^{13}C$ values were obtained for Me,Et (**36a**), Me,*n*-Pr (**36c**) and Me,*i*-Bu (**36f**) maleimides from samples IV-1 and IV-3. Analyses were carried out in triplicate and an average $\delta^{13}C$ value calculated (Table 3.1). Values were not attainable for Me,*n*-Pr (**36c**) and Me,*i*-Bu (**36f**) maleimides in the other samples due to the low relative abundance of the key minor components and also, in the case of sample IV-2, the mass spectrum showed possible co-elution with an unknown component.

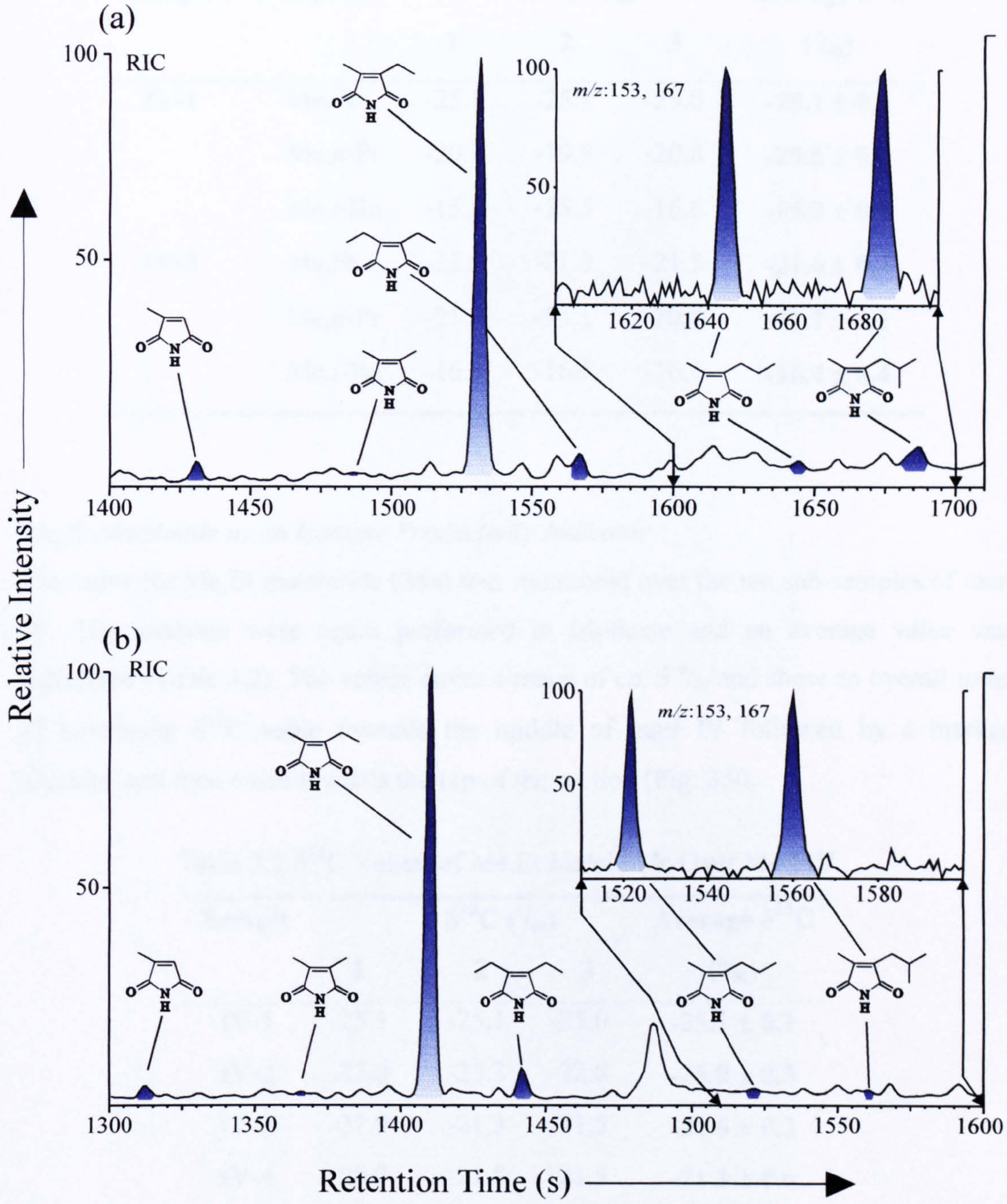

Fig. 3.8 Partial RIC and Mass Chromatograms of Maleimides Obtained from Photo-oxidation of Free Base Porphyrins from

(a) VdG IV-1
and (b) VdG IV-5

using CP-WAX 52 CB Stationary Phase

Table 3.1 $\delta^{13}C$ values of selected maleimides in samples IV-1 and IV-3

Sample	Component	$\delta^{13}C$ (‰)			Average $\delta^{13}C$ (‰)
		1	2	3	
IV-1	Me,Et	-25.1	-25.1	-25.0	**-25.1 ± 0.1**
	Me,*n*-Pr	-20.7	-19.9	-20.8	**-20.5 ± 0.5**
	Me,*i*-Bu	-15.5	-15.5	-16.6	**-15.9 ± 0.6**
IV-3	Me,Et	-21.9	-21.3	-21.5	**-21.6 ± 0.3**
	Me,*n*-Pr	-21.2	-23.1	-20.8	**-21.7 ± 1.2**
	Me,*i*-Bu	-16.3	-16.9	-16.1	**-16.4 ± 0.4**

Me,Et Maleimide as an Isotopic Productivity Indicator

The value for Me,Et maleimide (**36a**) was monitored over the ten sub-samples of marl IV. The analyses were again performed in triplicate and an average value was calculated (Table 3.2). The values cover a range of *ca.* 5 ‰ and show an overall trend of increasing $\delta^{13}C$ value towards the middle of marl IV followed by a marked decrease and then a rise towards the top of the section (Fig. 3.9).

Table 3.2 $\delta^{13}C$ Values of Me,Et Maleimide Over Marl IV

Sample	$\delta^{13}C$ (‰)			Average $\delta^{13}C$ (‰)
	1	2	3	
IV-1	-25.1	-25.1	-25.0	**-25.1 ± 0.1**
IV-2	-23.0	-23.3	-22.8	**-23.0 ± 0.3**
IV-3	-21.9	-21.3	-21.5	**-21.6 ± 0.3**
IV-4	-20.7	-21.8	-21.5	**-21.3 ± 0.6**
IV-5	-23.9	-23.3	-23.6	**-23.6 ± 0.3**
IV-6	-22.1	-22.0	-22.6	**-22.2 ± 0.3**
IV-7	-22.5	-22.8	-22.5	**-22.6 ± 0.2**
IV-8	-24.5	-24.4	-23.8	**-24.2 ± 0.4**
IV-9	-21.8	-21.3	-21.6	**-21.6 ± 0.3**
IV-10	-20.9	-20.5	-20.1	**-20.5 ± 0.4**

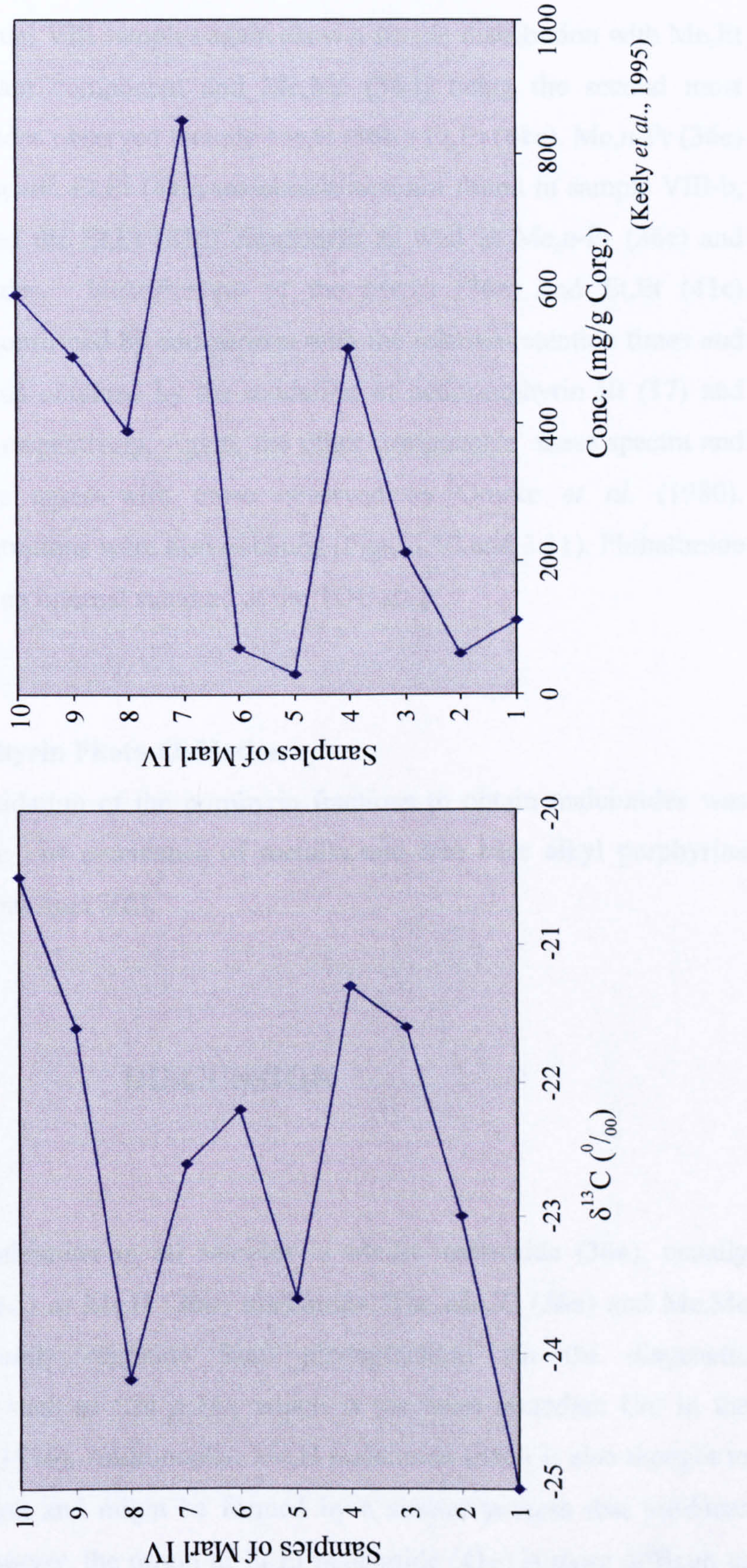

Fig. 3.9 $\delta^{13}C$ Me,Et Maleimide *vs.* Porphyrin Concentration

VENA DEL GESSO – (MARL VIII)

Extractable (Free) Maleimides

The maleimides of the marl VIII samples again show a simple distribution with Me,Et (**36a**) being the dominant component and Me,Me (**36d**) being the second most abundant. Other maleimides observed include Me,H (**36b**), Et,Et (**41c**), Me,*n*-Pr (**36c**) and Me,*i*-Bu (**36f**). However, Et,Et (**41c**) maleimide was not found in sample VIII-b, and sample VIII-c lacked the Et,Et (**41c**) component as well as Me,*n*-Pr (**36c**) and Me,*i*-Bu (**36f**) maleimides. Identification of the Me,Et (**36a**) and Et,Et (**41c**) components was again confirmed by comparison with the relative retention times and mass spectra of standards obtained by the oxidation of aetioporphyrin III (**17**) and octaethylporphyrin (**48**) respectively. Again, the other components' mass spectra and relative retention times agree with those observed by Quirke *et al.* (1980). Furthermore, the concentrations were also obtained (Figs. 3.10 and 3.11). Phthalimide (**45**) was again added as an internal standard at the TOE stage.

Maleimides from Porphyrin Photo-Oxidation

Unfortunately, photo-oxidation of the porphyrin fractions to obtain maleimides was not possible, due to the low abundance of metallo and free base alkyl porphyrins found in sub-samples from marl VIII.

DISCUSSION

FREE MALEIMIDES

The most dominant maleimide in all samples is Me,Et maleimide (**36a**), usually followed by Me,Me (**36d**) or Me,H (**36b**) maleimide. The Me,Et (**36a**) and Me,Me (**36d**) components mainly originate from phytoplankton *via* the diagenetic transformation of Chls such as Chl *a* (**1**), which is the most abundant Chl in the biosphere (Grice *et al.*, 1996). Additionally, Me,H maleimide (**36b**) is also thought to be derived from plankton and might be formed by a similar process that produces CAPs (such as **49**). However, the origin of Et,Et maleimide (**41c**) is more difficult to

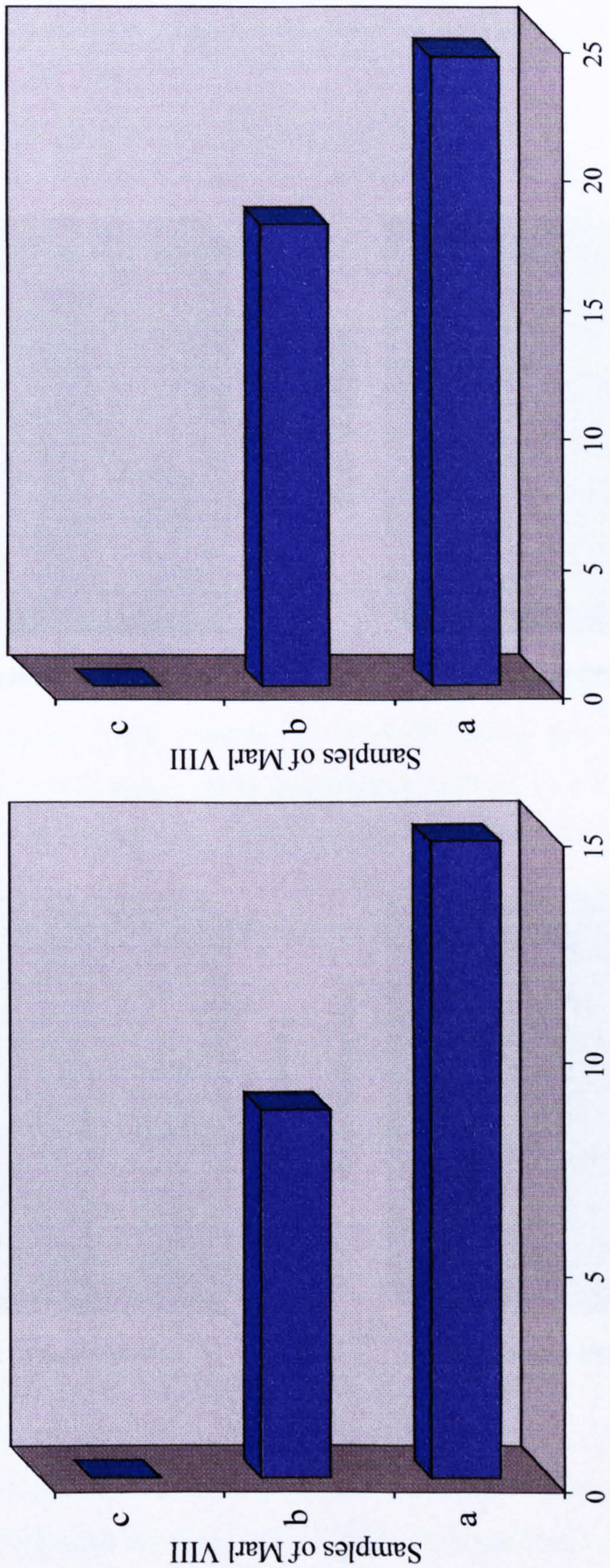

Fig. 3.10 Concentration Depth Profiles for Minor Maleimides

Fig. 3.11 Concentration Depth Profiles for Maleimides through Marl VIII

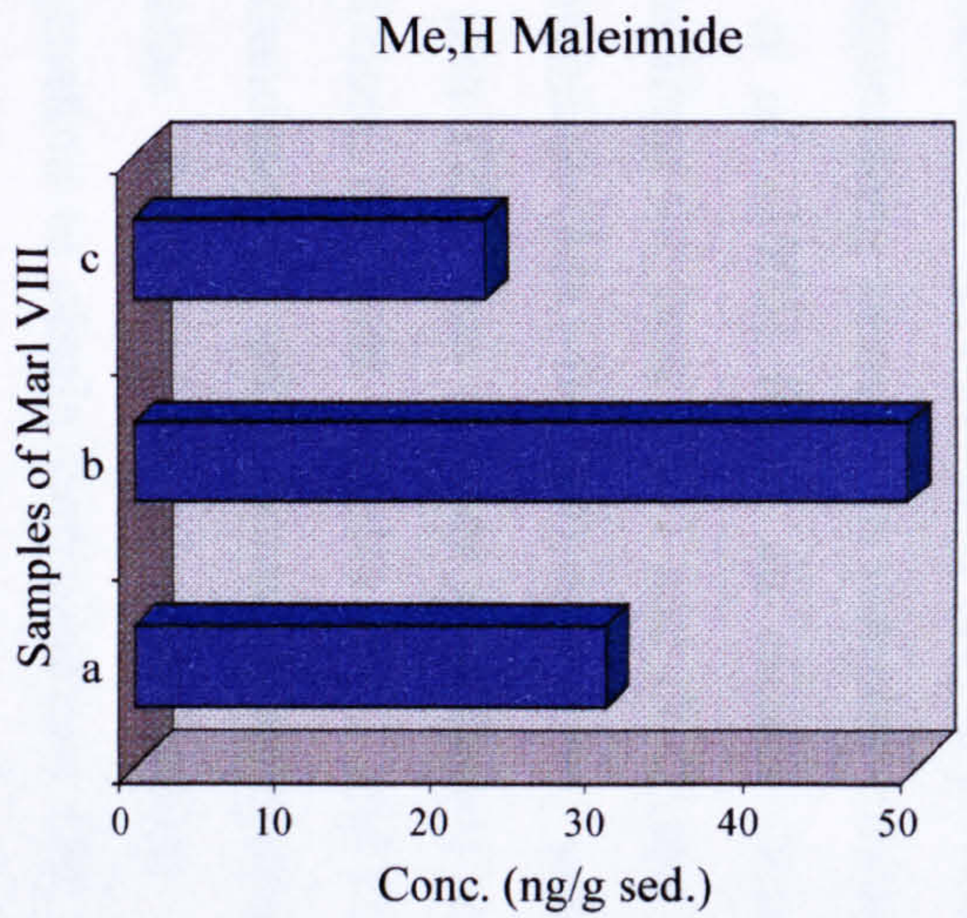

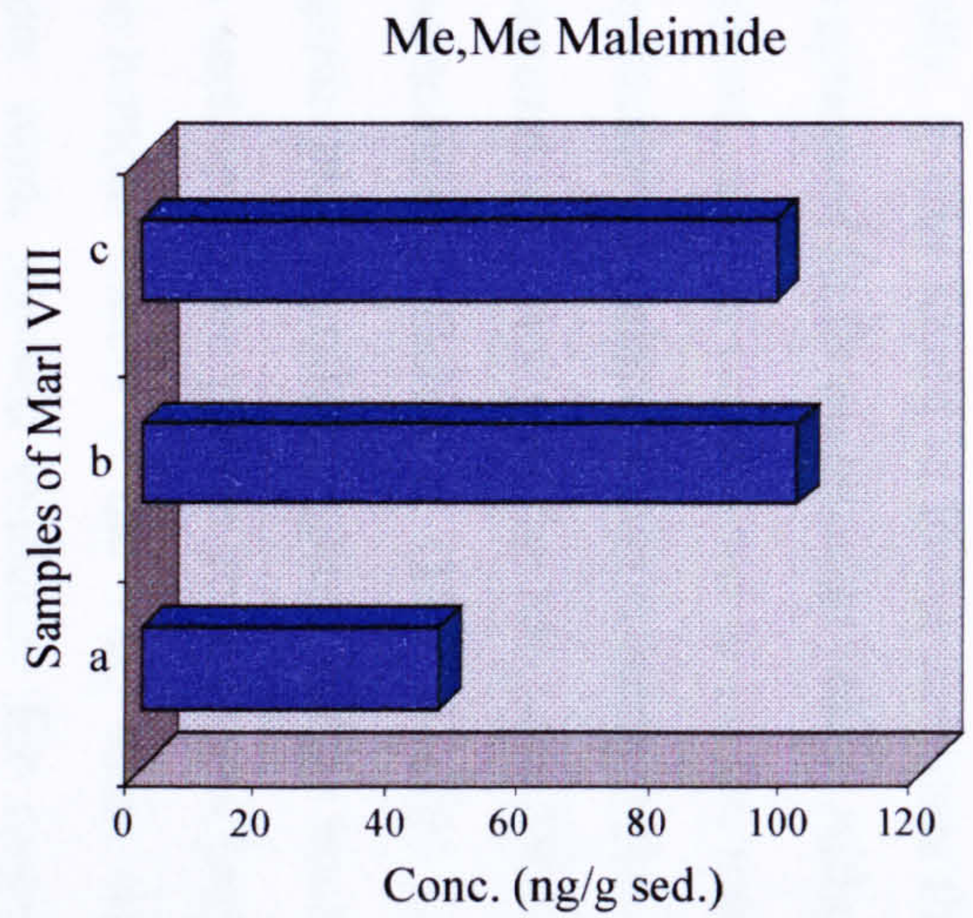

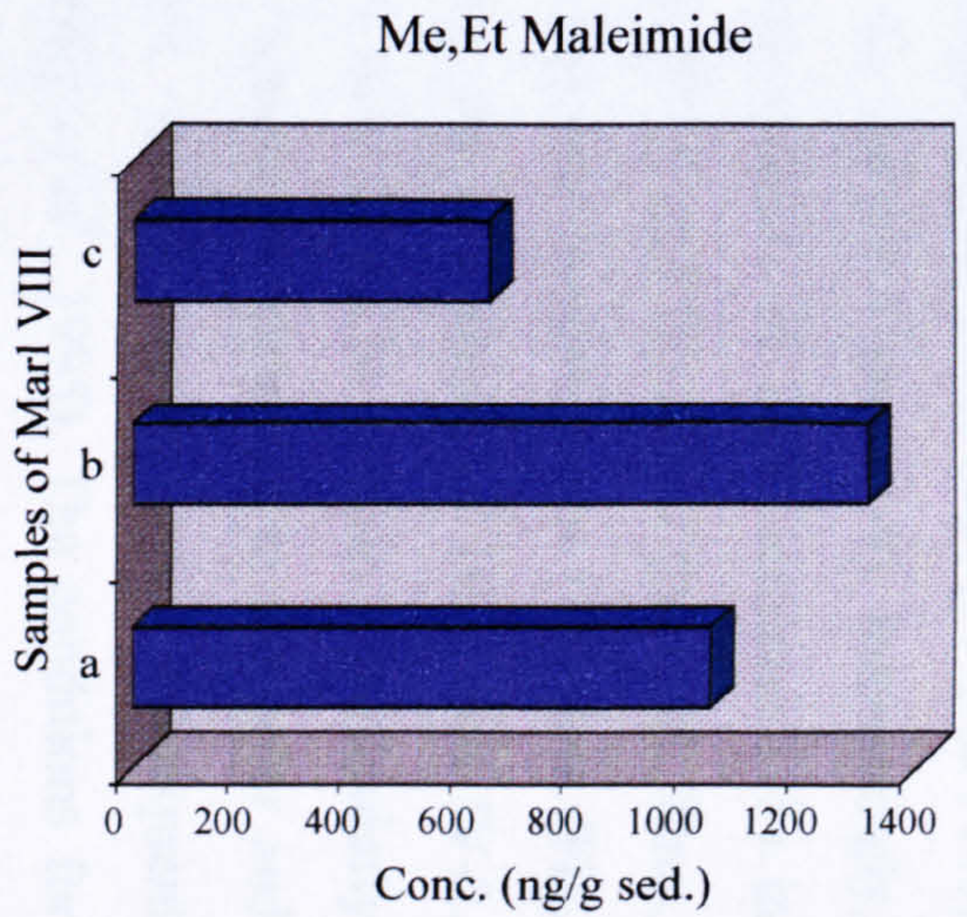

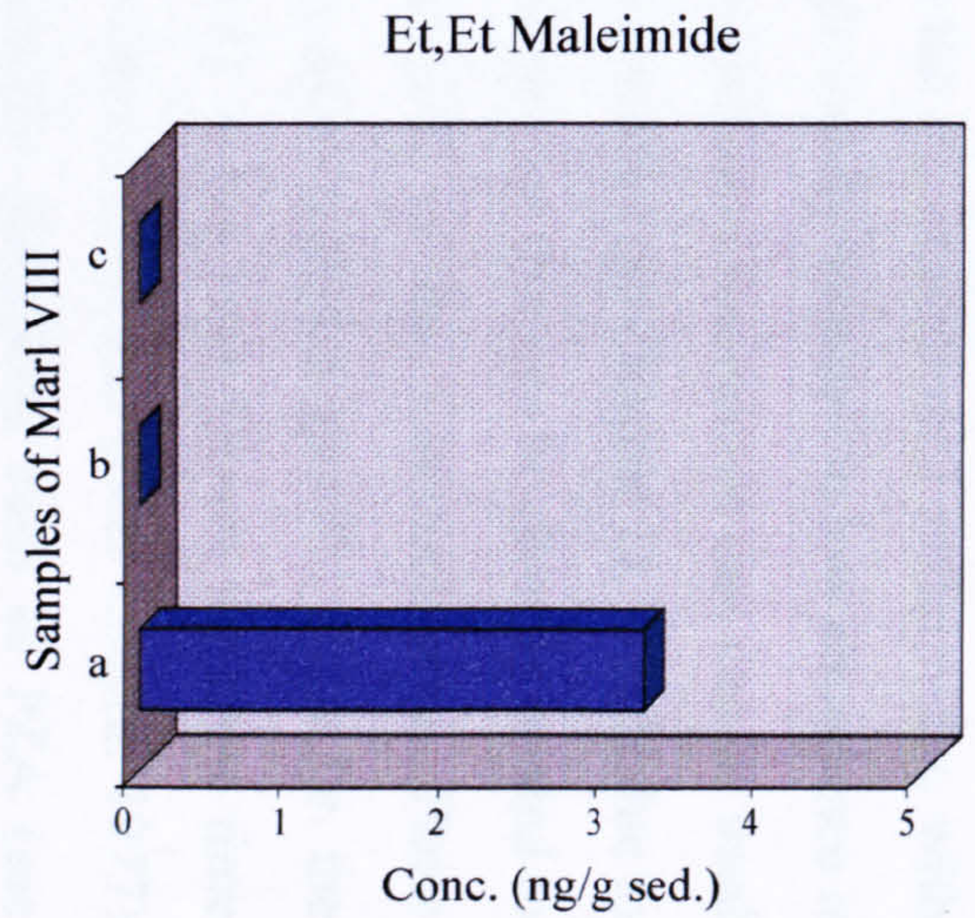

explain; although detected in very low abundance it has been observed in a number of other sediments (*e.g.* Kupferschiefer, Grice *et al.*, 1996; Crawford, 1998). It is assumed that it is of tetrapyrrole origin (see Chapter 2), but there are no known Chls with the Et,Et substituent.

Me,*i*-Bu maleimide (**36f**) was detected in the lower eight of the ten marl IV samples and again in the lower two of the three marl VIII samples (Figs. 3.6 and 3.10). Generally, it was found in lower amounts than the aforementioned maleimides, with the exception of Et,Et maleimide (**41c**). Although usually detected in low abundance it is important, as it is considered to be the most significant maleimide that can be used as an indicator of palaeo water column redox conditions (see Chapter 1). This is due to the structural specificity of the Me,*i*-Bu (**36f**) component that can be directly related to the characteristic Bchls *c* (**12**), *d* (**10**) or *e* (**13**) of the Chlorobiaceae. These anoxygenic photosynthetic green sulfur bacteria exist within a specific niche *i.e.* the anoxic section of the photic zone (see Chapter 1). It has been known for some time that the bottom waters of the VdG basin were anoxic (Vai and Ricci Lucchi, 1977) and later work showed evidence for more specific conditions such as PZA (see Chapter 1). For example, depth profiles of isorenieratene (Chlorobiaceae) were calculated for samples covering the entire sequence as well as for sub-samples from marls IV and VIII (Keely *et al.*, 1995). In marl IV (Fig. 3.12) the greatest concentration of isorenieratene (**15**) is present in the middle of the marl (IV-3 to IV-6) with diminishing amounts in samples towards the top (IV-7 and IV-8). Interestingly, Keely *et al.* (1995) found an almost complete absence of isorenieratene (**15**) in samples from the base (IV-1 and IV-2) and top (IV-9 and IV-10) of the marl. Thus, the maleimide (Me,*i*-Bu **36f**) data show, unlike the free isorenieratene (**15**) data (Fig. 3.12), that PZA was already established during the deposition of IV-1 and IV-2. Furthermore, the base samples (IV-1 and IV-2) were found to contain a particularly high abundance of sulfur-bound isorenieratene which was detected in the polar and asphaltene fractions by desulfurisation with nickel boride and subsequent hydrogenation to obtain isorenieratane (**34**; Kenig *et al.*, 1995). The conditions for sulfurisation were thought to be most favourable during the deposition of these samples, but became gradually less so towards the top of the marl. The most likely theory proposed by Kenig *et al.* (1995) is that in the presence of a high chemocline organic compounds will reach the anoxic zone faster, where reduced sulfur species are available for sulfurisation. To support this, they found a high concentration of

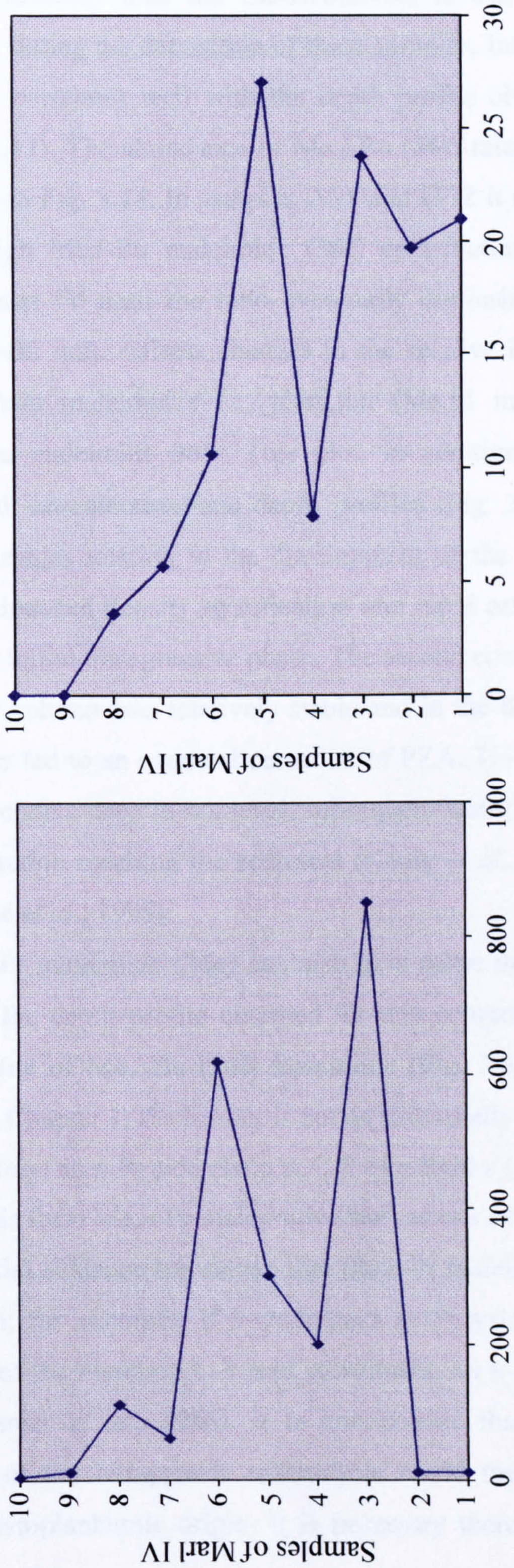

Fig. 3.12 Isorenieratene *vs.* Me,*i*-Bu Maleimide (Keely *et al.*, 1995)

Chromaticeae-derived lipids in samples IV-1 and IV-2, suggesting the presence of a relatively high chemocline in the palaeo water column and, since these bacteria require a higher light intensity than the Chlorobiaceae, it was proposed that the chemocline was highest during the deposition of these samples. Interestingly, the total isorenieratane/-ene plot correlates well with the depth profile obtained for Me,*i*-Bu maleimide (**36f**) (Fig. 3.13). The abundance of Me,*i*-Bu (**36f**) relative to Me,Et (**36a**) maleimide is illustrated in Fig. 3.14. In samples IV-1 and IV-2 it is clear that there is initially a relatively high Me,*i*-Bu maleimide (**36f**) contribution, which gradually decreases throughout marl IV until the ratio eventually diminshes in sample IV-9. Hence, the Me,Et/Me,*i*-Bu ratio reflects changes in the relative inputs of organisms contributing to these two maleimides *i.e.* plankton (Me,Et maleimide **36a**) and Chlorobiaceae (Me,*i*-Bu maleimide **36f**). This plot, in addition to the maleimide (Me,*i*-Bu **36f**) and total isorenieratene/ane depth profiles (Fig. 3.13), indicates that there were three main stages relating to the development of the water column. The first stage was salinity-induced density stratification and rapid establishment of PZA during or soon after the initial transgressive phase. The second corresponds to a period during which the water column was relatively stable and in the third and final stage, the evaporation of water led to an eventual cessation of PZA. This is thought to have occurred because of a relative drop in sea level, subsequent water column mixing and the zone of light penetration reaching the sediment (Kenig *et al.*, 1995; Keely *et al.*, 1995; Sinninghe Damsté *et al.*, 1995).

The presence of Me,*n*-Pr maleimide (**36c**) can also give some indication of the past existence of PZA and the depth profile obtained for this component almost exactly matches the depth profile of Me,*i*-Bu (**36f**) maleimide (Fig. 3.6). Unfortunately, as described previously in Chapter 1, the former is not as structurally-specific as Me,*i*-Bu maleimide (**36f**). Certainly, an *n*-Pr side chain at C-8 of a Bchl *c* (**12**), *d* (**10**) or *e* (**13**) would, during diagenesis form Me,*n*-Pr maleimide (**36c**) as one of its products. On the other hand, circumstantial evidence has shown that Me,*n*-Pr maleimide (**36c**) may also be of Chl *a* (**1**) origin; for example, if it undergoes hydrolysis of the C-17 ester, followed by reduction of the resulting C-3 acid substituent, an *n*-Pr side chain would be formed (Verne-Mismer *et al.*, 1986). It is conceivable that during diagenesis oxidative degradation of the tetrapyrrole macrocycle could then produce Me,*n*-Pr maleimide (**36c**) of phytoplanktonic origin. It is necessary therefore, in the case of

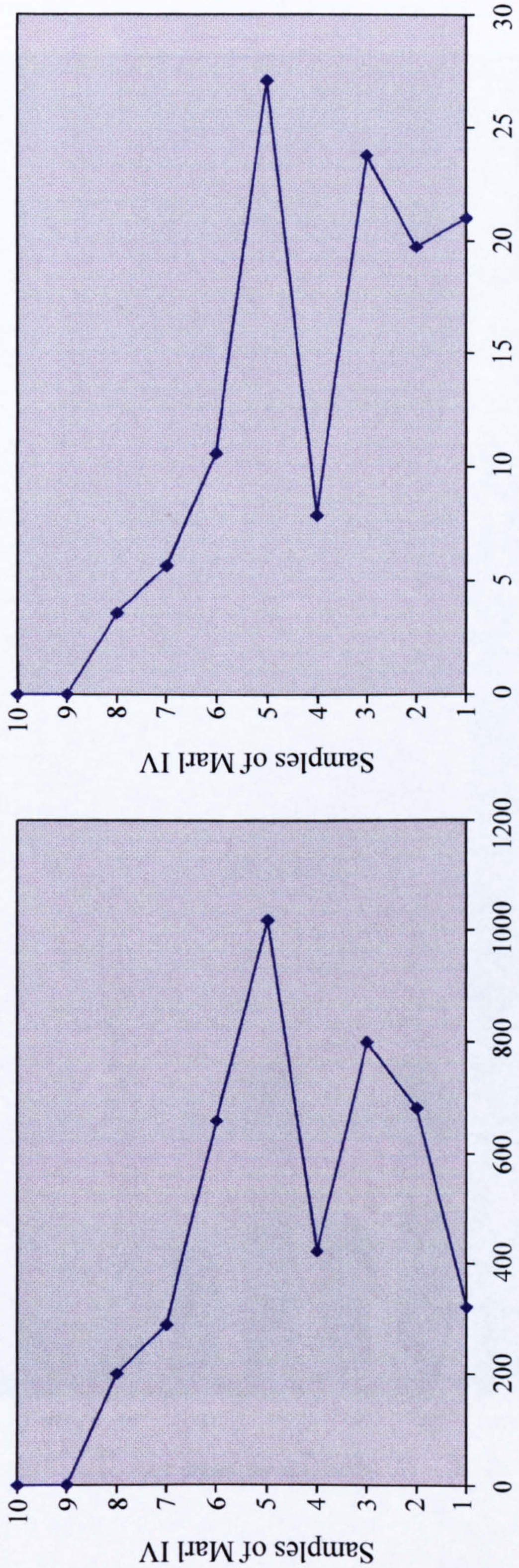

Fig. 3.13 Isoprenoid *vs.* Me,*i*-Bu Maleimide

(Kenig *et al.*, 1995)

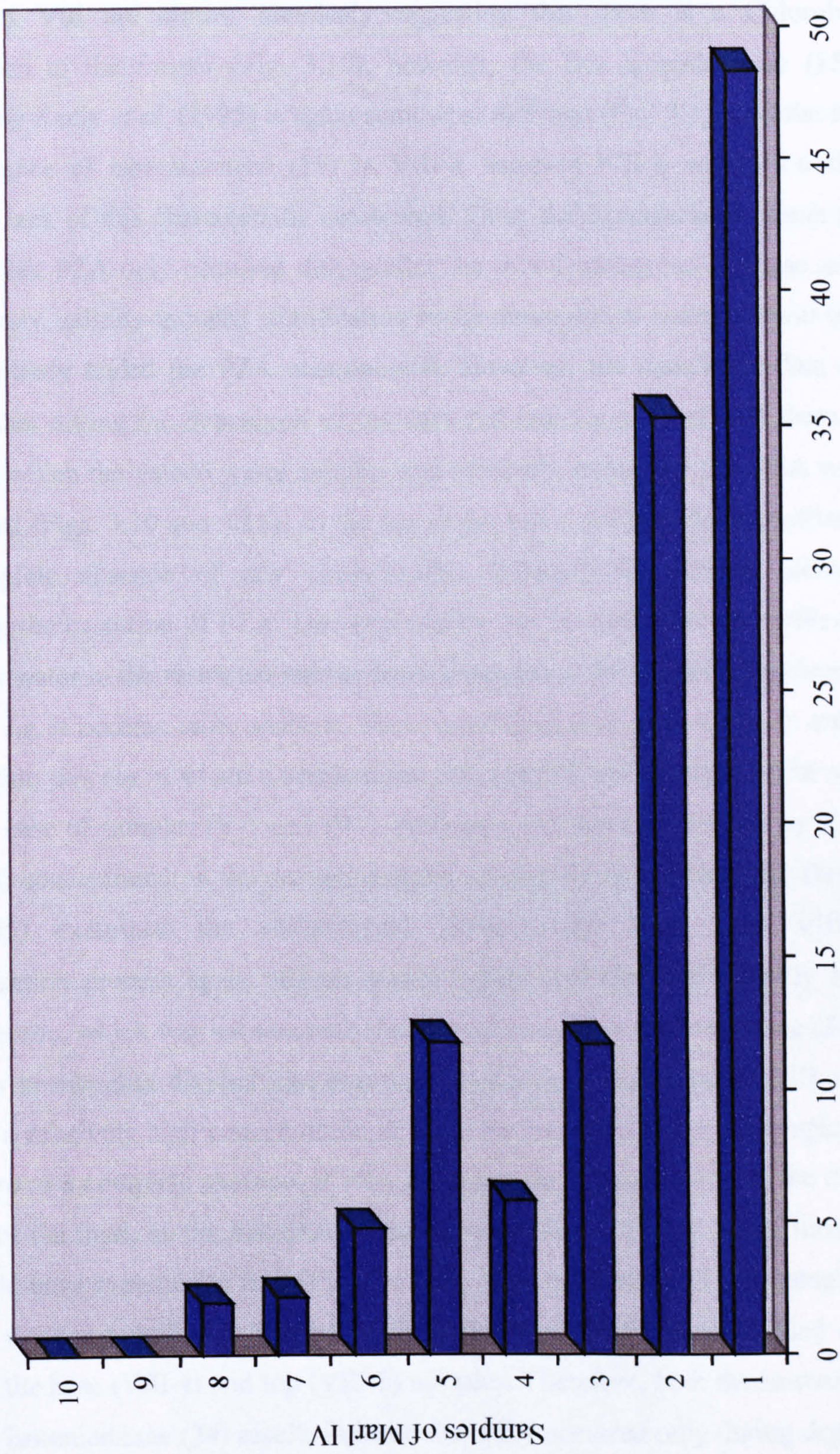

Fig. 3.14 Plot of Me,*i*-Bu/Me,Et Maleimide

Me,*n*-Pr maleimide (**36c**) to obtain stable isotope measurements in order to confirm its source (see later).

The concentration depth profiles for Me,*n*-Pr (**36c**) and Me,*i*-Bu (**36f**) maleimides from marl VIII are almost identical, suggesting that there is a Chlorobiaceae contribution to the former (Fig. 3.10); however, the free isorenieratene (**15**) plot obtained by Keely *et al.* (1995) is again somewhat different (Fig. 3.15). Whilst there is an abundance of isorenieratene (**15**) in VIII-a, samples VIII-b and VIII-c show a complete lack of this characteristic carotenoid. Thus, the isorenieratene depth profile suggests that PZA only occurred during/after the initial transgressive phase and that subsequently, salinity-induced stratification broke down due to water column mixing, which abruptly ended the PZA phenomenon. However, the maleimide data clearly indicate that during the deposition of the dark red interval of marl VIII there was a period in which the palaeo water column was relatively stable and that PZA was still established (Figs. 3.10 and 3.15). At the top of the marl, all three depth profiles show the complete absence of any characteristic Chlorobiaceae-derived biomarkers, indicating the cessation of PZA. One explanation for the difference in profiles could be that as water in the restricted marine basin evaporated, the depth of the chemocline changed, *i.e.* it became more shallow. These conditions may have led to an enhanced sulfurisation process in which isorenieratene (**15**) reacted with reduced sulfur species, as in the case of samples IV-1 and IV-2. Although, the study carried out by Kenig *et al.* (1995) concentrated on the ten sub-samples of marl IV only, Sinninghe Damsté *et al.* (1995) examined the sulfur-bound isorenieratene from marl VIII. The desulfurisation process again utilised nickel boride and liberated partially reduced isorenieratene, which was subsequently fully hydrogenated to isorenieratane (**34**). The marl was presumably divided into two equal sub-samples and sample VIII-a (base) revealed a relatively high concentration of isorenieratane (**34**), whereas sample VIII-b (top) showed a complete absence. If PZA did occur during deposition of the dark red interval of the marl, as the maleimide data suggest (Figs. 3.10 and 3.15), then surely one would have expected to find at least a trace of isorenieratane (**34**) in sample VIII-b (top), since the dark red interval of the marl would have been divided equally amongst the base (VIII-a) and top (VIII-b) samples. Therefore, both the isorenieratene (**15**) and isorenieratane (**34**) results indicate that PZA occurred only during deposition of the base of marl VIII, whereas the maleimide data (Me,*i*-Bu) clearly suggest the continuing presence of PZA during deposition of the dark red interval of the marl. A

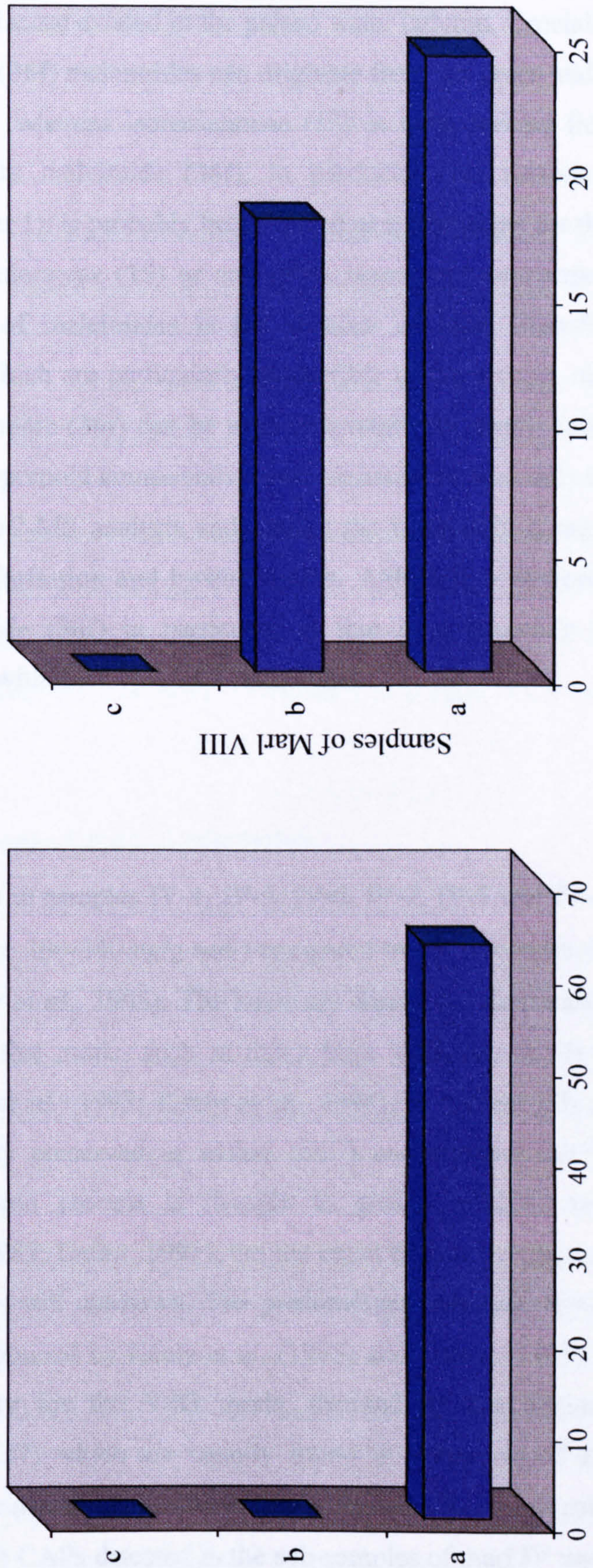

Fig. 3.15 Isorenieratene *vs.* Me,*i*-Bu Maleimide

(Keely *et al.*, 1995)

possible explanation for the difference between the isorenieratene/ane and maleimide profiles is that during deposition of the dark red interval of marl VIII only the green strains of the Chlorobiaceae existed in the palaeo water column. Crucially, both Me,*n*-Pr (**36c**) and Me,*i*-Bu (**36f**) maleimides can originate from the green and brown strains of the Chlorobiaceae, whereas isorenieratene (**15**) is only derived from the brown strains. Thus, Me,*i*-Bu maleimide (**36f**), in particular (for reasons of structural specificity, see Chapter 1), is probably better suited as a biomarker for the green sulfur bacteria than is isorenieratene (**15**) or any of its isoprenoid counterparts. A further structural advantage of maleimides is the absence of long aliphatic unsaturated hydrocarbon chains which are particularly susceptible to the process of sulfurisation; hence, Me,*i*-Bu maleimide (**36f**) can be used as a relatively simple indicator of PZA compared with the isoprenoid compounds, since maleimides need only to be extracted and purified before GC-MS analysis and, unlike the isoprenoid compounds, do not require lengthy desulfurisation and hydrogenation. Although, a distinct disadvantage for Me,*i*-Bu maleimide (**36f**) in particular, is that it is generally found in low abundance compared with the isoprenoid compounds.

PORPHYRINS

The nickel porphyrins in samples IV-4, IV-5, IV-6, IV-7, IV-8 and IV-10 are present in low abundances (*ca.* 100-240 ng/g sed.) compared to the free bases (20-800 $\mu g\ g^{-1}$ organic carbon, Keely *et al.*, 1995). The latter are clearly the dominant tetrapyrroles, which often indicate that marls, such as those from VdG, are relatively young and immature (Schaeffer *et al.*, 1993; Keely *et al.*, 1994). In ancient oils and sediments porphyrins are usually preserved as nickel (Ni^{2+}) and vanadyl (VO^{2+}) complexes because the metallation process is thought to greatly enhance the stability of porphyrins (Quirke, 1987; Callot, 1991), but the exact diagenetic stage at which metal ion insertion occurs is still unknown. The predominant porphyrin distributions (C_{31}, C_{32} and C_{33} CAPs) obtained by Keely *et al.* (1995) and Turner (1998) also suggest a low level of maturity for the VdG marls, denoted by the distinct absence of aetioporphyrins (*e.g.* **17**) which are usually found in sediments of greater thermal maturity (*e.g.* Barwise and Roberts, 1984). Unfortunately, the C_{34} (Keely *et al.*, 1995) and C_{35} (Turner, 1998) CAPs detected in the sub-samples of marl IV were assigned on

carbon number grounds only and although this confirms the occurrence of HMW CAPs (*i.e.* $>C_{32}$) it must be remembered that their presence alone is not sufficient evidence for PZA (see Chapter 1).

MALEIMIDES FROM PORPHYRIN OXIDATION

The photo-oxidised free base alkyl porphyrins from samples IV-1 and IV-5 provide additional structural evidence for the past existence of Chlorobiaceae and in turn PZA, since Me,*n*-Pr (**36c**) and Me,*i*-Bu (**36f**) maleimides were present in both cases. Interestingly, although the distribution for the oxidised products was the same as that obtained for the free maleimides, the relative abundance particularly in the case of sample IV-1 was very different. Furthermore, photo-oxidation of nickel porphyrins from samples IV-4, IV-5, IV-6, IV-7, IV-8 and IV-10 yielded maleimides that also had subtly different relative abundances compared to the free maleimides and what's more, show a different distribution. Hence, these results provide yet further evidence to suggest that maleimides are not oxidative artefacts of storage (see Chapter 2).

GC-C-IRMS ANALYSIS OF MALEIMIDES

Comparison of Me,Et, Me,*n*-Pr and Me,*i*-Bu Maleimides

Me,*n*-Pr (**36c**) and Me,*i*-Bu (**36f**) maleimides were present, albeit in low relative abundance, in all sub-samples except those at the top of marl IV and VIII, and are considered on purely structural grounds to be derived from the Bchls *c* (**12**), *d* (**10**), or *e* (**13**) of the anoxygenic green sulfur bacteria (Chlorobiaceae). However, in some cases further evidence may be required from stable carbon isotope measurements, since some maleimides have a phytoplanktonic origin and others a bacterial origin. For example, in the Permian Kupferschiefer Me,*n*-Pr (**36c**) and Me,*i*-Bu (**36f**) maleimides were significantly enriched in ^{13}C over Me,Et maleimide (**36a**) of phytoplanktonic Chl origin by approximately 10 and 11 ‰ respectively, in keeping with a Chlorobiaceae origin (Grice *et al.*, 1996). On the other hand, the Me,*n*-Pr maleimide (**36c**) in a C/T black shale had a similar $\delta^{13}C$ value to Me,Et maleimide (**36a**), indicating a phytoplanktonic origin (Crawford, 1998). These studies emphasise the importance of obtaining $\delta^{13}C$ values to confirm the origin of certain maleimides,

especially Me,*n*-Pr maleimide (**36c**). Me,*i*-Bu maleimide (**36f**) appears to be a highly specific marker for a bacterial origin, whereas Me,*n*-Pr maleimide (**36c**) can have a bacterial, phytoplanktonic (*cf.* Verne Mismer *et al.*, 1986; also see Chapter 2) or mixed origin. The $\delta^{13}C$ values of Me,Et (**36a**), Me,*n*-Pr (**36c**) and Me,*i*-Bu (**36f**) maleimides from samples IV-1 and IV-3 (Table 3.1) show Me,*i*-Bu maleimide (**36f**) to be enriched in ^{13}C relative to Me,Et maleimide (**36a**) by approximately 9 and 5 ‰ respectively. The lighter isotopic values for the Me,*n*-Pr (**36c**) component in the two sub-samples ($\delta^{13}C$ -20.5 and -21.7 ‰ respectively) *vs* the Me,*i*-Bu (**36f**) component ($\delta^{13}C$ -15.9 and -16.4 ‰ respectively) indicate however a mainly phytoplanktonic origin for the former component *via* reduction of either the C_3-acid substituent at C-17 of phytoplanktonic Chl *a* (**1**) or of free hematinic acid (**44**) after degradation of the tetrapyrrole macrocycle (see Chapter 2). Indeed, for sample IV-3 the similarity in $\delta^{13}C$ values of Me,*n*-Pr maleimide (**36c**) and Me,Et (**36a**) maleimide (-21.6 ‰) indicates that in this sample the Me,*n*-Pr (**36c**) component is entirely of phytoplanktonic origin, whereas the $\delta^{13}C$ value of Me,*n*-Pr (**36c**) maleimide for sample IV-1, suggests a 50:50 mix. These results emphasise the necessity of carrying out stable isotope measurements in conjunction with structural determination when using maleimides (especially Me,*n*-Pr maleimide) as palaeoenvironmental indicators.

Me,Et Maleimide as an Isotopic Productivity Indicator

The concentration and isotopic composition of dissolved CO_2, often referred to as the ultimate carbon source, play an essential role in controlling the variation in isotopic signals. It is thought that high concentrations of dissolved CO_2 cause ^{13}C-depletion, whilst increased growth rates cause ^{13}C-enrichment (Laws *et al.*, 1995; Bidigare *et al.*, 1997; Bidigare *et al.*, 1999). An increase in local productivity, possibly combined with enhanced growth rate of phytoplankton in surface waters could lead to an increase in the rate of burial (local) of organic carbon. Subsequently, these conditions may lead to a decrease in the concentration of dissolved CO_2 in surface waters. At the same time, because phytoplankton utilise the C3 pathway for carbon fixation and preferentially assimilate ^{12}C as opposed to ^{13}C, ^{13}C-enrichment of local surface waters may occur and should be detected in both the $\delta^{13}C$ values of organic matter and of $CaCO_3$. In the case of VdG, Kenig *et al.* (1995) obtained almost constant $\delta^{13}C$ values for the free C_{29}

and C_{31} *n*-alkanes, which are thought to originate mainly from terrigenous plant waxes; this indicates that the isotopic composition of atmospheric CO_2 was for the most part constant during the deposition of marl IV. Such evidence is not that surprising since it has been estimated that the entire deposition of marl IV occurred over a period of less than 100 ka (Sinninghe Damsté *et al.*, 1995) and that during the Messinian time the isotopic composition of marine carbonate only varied by *ca.* 0.4 ‰ / 100 ka. If these trends also reflect dissolved inorganic carbon (DIC) $\delta^{13}C$ values in local surface waters, then algal productivity changes in the VdG palaeo water column might account for the 3.5 ‰ difference observed in $\delta^{13}C$ values for Me,Et maleimide (**36a**) from samples IV-1 and IV-3 (-25.1 and –21.6 ‰ respectively), since it mainly originates from phytoplanktonic Chl. This could be caused by either decreased CO_2 concentrations in surface waters and/or higher growth rates due to enhanced productivity during deposition of IV-3.

Therefore, the $\delta^{13}C$ values of Me,Et maleimide (**36a**) were determined in the remaining eight samples of marl IV (Table 3.2.; Fig. 3.9). Interestingly, the highest concentrations of porphyrins were found in marl IV (Keely *et al.*, 1995), and since porphyrins predominantly reflect a phytoplanktonic input, a comparison of the $\delta^{13}C$ values obtained for Me,Et maleimide (**36a**) was made with the abundance of the free base alkyl porphyrins (Keely *et al.*, 1995; Fig. 3.9). However, the correlation between the plots was poor (Fig. 3.9). Despite these results, one would expect the isotopic shifts to relate to changes in CO_2 demand since high porphyrin abundances, suggesting high productivity, should correlate with heavy $\delta^{13}C$ values of Me,Et maleimide (**36a**). However, in addition to productivity, other factors such as temperature and salinity may also exert a control on the concentration of dissolved CO_2 in local surface waters. For example, very warm highly saline surface waters should have a lower concentration of dissolved CO_2 than their cold less saline counterparts. In consequence, all of the above factors may affect the isotopic fractionation associated with the fixation of carbon by autotrophs, as well as the identities and metabolic characteristics of organisms found within the community (Kenig *et al.*, 1995).

CONCLUSIONS

- Me,*i*-Bu maleimide (**36f**) was detected in the lower eight of the ten marl IV samples and again in the lower two of the three marl VIII samples (Figs. 3.6 and 3.10); strongly indicating that PZA occurred during the deposition of marls IV and VIII.

- The photo-oxidised free base alkyl porphyrins from samples IV-1 and IV-5 provide additional structural evidence for the past existence of Chlorobiaceae and in turn PZA, since Me,*i*-Bu (**36f**) maleimide was present in both cases.

- The $\delta^{13}C$ values of Me,Et (**36a**) and Me,*i*-Bu (**36f**) maleimides from samples IV-1 and IV-3 (Table 3.1) show Me,*i*-Bu maleimide (**36f**) to be enriched in ^{13}C relative to Me,Et maleimide (**36a**) by approximately 9 and 5 $^{0}/_{00}$ respectively, again confirming a Chlorobiaceae origin.

- Overall, both the Me,*i*-Bu maleimide (**36f**) and diaromatic isoprenoid (Keely *et al.*, 1995; Kenig *et al.* 1995; Sinninghe Damsté *et al.*, 1995) data indicate that the VdG lagoonal basin was stratified and that PZA occurred during the early and middle stages of marl deposition.

CHAPTER 4:

CENOMANIAN/TURONIAN OCEANIC ANOXIC EVENT

INTRODUCTION

OCEANIC ANOXIC EVENTS

General

During the Deep Sea Drilling Project (DSDP) of the 1970s, it became apparent that organic-rich black shales were deposited within certain Cretaceous time intervals (*e.g.* Schlanger and Jenkyns, 1976; Fischer and Arthur, 1977; Ryan and Cita, 1977), which indicated that the global ocean system was probably oxygen-deficient throughout most of the Cretaceous period [*i.e.* from the Hauterivian (131 Ma) to Santonian (87.5)]. Furthermore, the almost-simultaneous widespread deposition of such shales during certain ages [*e.g.* late Barremian (125 Ma) through Albian (113 Ma), and late Cenomanian through early Turonian] of the Cretaceous period led Schlanger and Jenkyns (1976) to term the phrase "Oceanic Anoxic Events" (OAEs). Such important relatively brief events likely reflect specific global factors that influenced the production, deposition and preservation of OM.

Black Shales

Black or bituminous shales are essentially rich in organic matter (OM) and their potential as hydrocarbon source rocks has long been recognised. Their occurrence is a worldwide phenomenon and they are typically deposited under inferred oxygen-depleted conditions. Generally, TOC values are in the range of 4 to 10%, but occasionally some may reach 50%, with others being as low as 1% (*e.g.* Stein *et al.*, 1986; Weissert, 1981; Arthur *et al.*, 1990). As the name suggests, black shales are often dark in colour and the presence of fine laminations indicates an absence of benthic organisms and suboxic/anoxic conditions. Other characteristic features include enhanced levels of certain trace elements (*e.g.* Cd, Cu, Ni, U and V) and phosphates, combined with a high abundance of iron sulfides (*e.g.* pyrite) and low carbonate content. The exact colour depends on many factors; thermal maturity, TOC level and even the type of OM can significantly alter the colour. Oxygen-depleted conditions help to preserve fine laminations, which may also arise due to changes in productivity (*e.g.* seasonal phytoplanktonic blooms), re-deposited turbidite sediments (*e.g.* Stow and Dean, 1984) and the existence of sulfide-oxidising bacterial mats located at the

sediment/water interface (Arthur and Sagemen, 1994). Black shales are often found interbedded amongst rocks of other lithologies such as marls, limestones or lighter coloured mudstones and shales. It is thought that the lighter coloured interbeds were deposited under oxygenated conditions, since they contain low amounts of OM and show evidence of bioturbation (Demaison and Moore, 1980; Arthur *et al.*, 1984). Furthermore, as a result of the DSDP, which commenced in 1968, black shales have now been recovered from ocean basins all over the world (Weissert, 1981) in addition to widespread continental margin settings (Jenkyns, 1980). The Cretaceous and Jurassic shales are probably the world's most important source of petroleum and consequently, are of huge economic value, since it has been estimated that approximately 70-85% of generated oil is produced from such source rocks (Irving *et al.*, 1974; Tissot, 1979).

Productivity and Preservation of Organic Matter

Primary productivity in the marine environment is essentially controlled by a few key factors such as: levels of light, water temperature (influencing concentrations of dissolved O_2 and CO_2) and nutrient availability (Jahnke, 1990; Meyers, 1997). Phytoplanktonic productivity exclusively occurs in the photic zone and may penetrate to depths of up to 150m in clear water. Essential nutrients such as nitrates, silicates and phosphates are readily consumed by phytoplankton and in order to maintain productivity must be replaced by vertical or horizontal supply. Nutrients may be replenished from the land *via* fresh water sources and during times of increased sea level. Upwelling is a phenomenon controlled by a combination of both prevailing wind action and Coriolis forces, in which the horizontal movement of surface waters is replaced by the vertical movement of deeper nutrient-rich water (Ekman transport). Nutrients are returned to deeper waters *via* bacterial degradation of OM as it sinks through the water column; appropriate bacterial communities will use nitrates, followed by sulfates as oxidants to continue the degradation of OM long after the depletion of oxygen from the water column and shallow sediments. Consequently, areas of high productivity are generally found on the west coasts of the continents and at equatorial divergence zones as a result of upwelling, and it has been estimated that about half of the organic-rich sediments formed in the world were deposited in upwelling regions (Parrish, 1987). Photic zones in areas of low productivity, such as

those found in the mid-latitude centres of oceans, are also predominantly fertilised by wind-driven mixing across the thermocline, *i.e.* upwelling. In the past, the occurrence and extent of primary productivity has not been considered to play a significant part in the formation of black shales and it is generally assumed that OM is preserved to a greater extent in suboxic/anoxic environments (*e.g.* Demaison and Moore, 1980) leading to the formation of organic rich sediments. Yet, almost all OM currently being incorporated in marine sediments is deposited under oxygenated waters along continental margins (Hedges and Keil, 1995). Although correlative information suggests that productivity, sediment accumulation rate, bottom water oxicity and source of OM are key variables, the exact mechanisms controlling the preservation of sedimentary OM remain unclear. Despite this, the wide held belief is that anoxic conditions will lead to considerable preservation of OM (*e.g.* Demaison and Moore, 1980).

Mechanisms for Oxygen-Poor Conditions

Oxygen minimum zone

Upwelling at coastal regions (California, Namibia and Peru; *e.g.* Thiede and Suess, 1983) or divergence in the open ocean (Demaison and Moore, 1980) often brings an influx of nutrients to the surface waters, leading to high phytoplankton productivity in the photic zone; as detritus slowly falls through the water column it is bacterially degraded causing a high demand for dissolved oxygen, which may in turn lead to the development of an oxygen minimum zone (OMZ) at mid depths. The OMZ model as a mechanism for black shale deposition has been suggested by various authors (Schlanger and Jenkyns, 1976; Arthur *et al.*, 1987; Schlanger *et al.*, 1987; Farrimond *et al.*, 1990); it is thought that where this zone encroaches on sediments OM will be preserved by anoxic or suboxic conditions, leading to the formation of organic-rich sediments (Demaison and Moore, 1980; Farrimond *et al.*, 1990). For example, in the present day Gulf of California, deep-water inflow and horizontal movement of surface waters by offshore winds results in seasonal upwelling and high phytoplankton productivity (Lisitzin, 1971). The ensuing OMZ (ranging from 300-1200m) often impinges on a slope, resulting in the formation of laminated organic rich facies, although alternating clay-rich facies are also found and are thought to arise from the seasonal contribution of terrigenous minerals from Mexican rivers. Expanded OMZs

may also form at mid-depths in the open ocean, such as the northern Indian Ocean (Didyk *et al.*, 1978).

Restricted Basin Model

Alternatively, oxygen poor conditions can occur in restricted basins. The prerequisite for such a model involves the presence of a sill or ridge, which partially isolates a large body of water from the open sea or ocean. A ridge or barrier of this kind would prevent both water circulation in the basin and the influx of deeper, colder, oxygenated water from the sea or ocean. Consequently, stratification may occur either through a temperature or a salinity-induced mechanism. Initially, a high concentration of nutrients in the surface waters would ensure an elevated level of phytoplanktonic productivity. However, it is important to note that during periods of intense stratification, nutrients may be confined to the bottom waters and as a result the overall level of productivity will be lower (*e.g.* Hollander *et al.*, 1993). After stratification, anoxic bottom waters would soon develop from the microbial oxidation of detritus as it fell through the water column, since the oxygen demand at the bottom of the basin would ultimately exceed the supply. Such anoxic conditions are thought to strongly enhance the preservation of OM (Rhoads and Morse, 1971) and would continue to ascend the water-column until levels at which oxygen demand equalled oxygen supply, leading in some instances to PZA (see Chapter 1). Interestingly, the contemporary Black Sea and some fjords are the only modern marine locations in which PZA still occurs (Repeta *et al.*, 1989).

Turbiditic Redeposition

A further model has been proposed (Dean and Gardner, 1982; Thurow and Kuhnt, 1986; Degens *et al.*, 1986; Meyers *et al.*, 1986) for the appearance of deep-sea black shales. It is possible that such shales were formed from the turbiditic redeposition of organic-rich sediments from continental shelves, which may have originally been formed in an OMZ. Preservation of the newly deposited OM is likely to occur as a result of further oxidative degradation, eventually leading to the development of anoxic conditions and subsequent absence of benthic fauna.

The Cenomanian/Turonian OAE

The C/T OAE took place *ca.* 91Ma and estimates for its duration range from 200,000 to 700,000 years (Arthur and Premoli-Silva, 1982; Arthur *et al.*, 1987). The C/T event involved the widespread almost-synchronous deposition of organic-rich black shales (TOC typically from *ca.* 1 to >40%). There are a number of marine environments in which black shales have been deposited and these include: continental slopes and shelves, epicontinental seas, submarine plateaus and deep abyssal ocean basins (Farrimond *et al.*, 1990 and references therein). The event is thought to have initially occurred in regions with high productivity, such as the NW coast of Africa (Arthur *et al.*, 1987), but then later progressed to the Tethyan domain and eventually throughout most of the Cretaceous ocean system.

It has been suggested that during the Cretaceous there was an elevated amount of oceanic volcanism, producing atmospheric levels of CO_2 that were three to twelve times higher than at present (Berner, 1992). As a result the Cretaceous interval spanning the Barremian to Turonian (*ca.* 125-88 Ma) is often referred to as the mid-Cretaceous "greenhouse" world (Barron, 1983). This warm, equable climate, in the absence of ice-caps, likely resulted in reduced bottom water circulation due to the absence of oxygenated sinking cold water (Schlanger and Jenkyns, 1976; Jenkyns, 1980). In addition, elevated temperatures and thus lowered solubilities of oxygen at sites of bottom-water formation, favoured anoxia (Berger, 1979).

In the mid-Cretaceous there was a eustatic (global) rise in sea level mainly attributed to a pulse of rapid sea floor spreading (Haq *et al.*, 1987), which was accompanied by an increase in the volume of the mid-ocean ridge system. This in turn led to a major transgression of the sea over low-lying coastal plains (Hays and Pittman, 1973; Schlanger and Jenkyns, 1976). Furthermore, reef-building molluscs experienced widespread extinction near the C/T boundary (*e.g.* Johnson *et al.*, 1996), in addition to planktonic foraminifera (Jenkyns, 1985; Kuhnt *et al.*, 1986; Jarvis *et al.*, 1988; Erbacher *et al.*, 1996). It is thought that an increase in OM supply, probably resulting from a change in oceanic circulation (Schlanger and Jenkyns, 1976; Jenkyns, 1980) associated with a substantial rise in sea level (Haq *et al.*, 1987), placed an increased oxygen demand upon oceanic waters, which were probably already oxygen deficient due to the warm equable Cretaceous climate (Berger, 1979). These effects may have resulted in the formation of an expanded and intensified OMZ at mid-water depths (Farrimond *et al.*, 1990). Previous studies of the North Atlantic, western Tethys and

northern Italy indicate that the formation and expansion of an OMZ may have caused plankton extinctions at the C/T boundary (Erbacher *et al.*, 1996 and references therein). Furthermore, it is thought that where this zone encroached on sediments OM was preserved by anoxic conditions, which led to the formation of organic-rich sediments (Demaison and Moore, 1980; Farrimond *et al.*, 1990).

One of the most noteworthy events that occurred during the well-documented C/T OAE (*e.g.* Schlanger and Jenkyns, 1976) was the rapid world wide positive excursion of *ca.* 2 ‰ in the carbon isotope composition of carbonate ($\delta^{13}C_{carb}$), which occurred between *ca.* 91.5 and 90.3 Ma (Scholle and Arthur, 1980). It is thought that the excursion occurred as a result of a change in the isotopic composition of the ocean-atmosphere carbon reservoir, which was brought about by an increase in the rate of burial of isotopically light (^{12}C) organic carbon. It is generally assumed that the $\delta^{13}C$ value of the total dissolved carbon reservoir has a primary effect on the $\delta^{13}C$ value of marine OM; therefore there should be a good correlation between both the $\delta^{13}C_{carb}$ and $\delta^{13}C_{org}$ excursions. However, the amplitude of the $\delta^{13}C_{org}$ excursion (*ca.* 3 - 4 ‰; *e.g.* Arthur *et al.*, 1988; Kuypers *et al.*, 1999) is almost twice that observed for the $\delta^{13}C_{carb}$ excursion (*ca.* 1.5 - 2 ‰; Scholle and Arthur, 1980). To account for this difference, Arthur *et al.* (1988) proposed that a high level of marine productivity probably led to a decline in both atmospheric and oceanic CO_2 levels. Consequently, they claim that the temporary reduction of CO_2 availability was the major cause for the difference between the two excursions, since both lower CO_2 concentrations and higher growth rates will result in ^{13}C enrichment of marine OM (Laws *et al.*, 1995; Bidigare *et al.*, 1997; Bidigare *et al.*, 1999). After these major events in the marine ecosystem, the mid-Cretaceous warming trend came to an end and was followed by a period of global cooling, which lasted until at least the Maastrichtian (73 Ma; Jenkyns *et al.*, 1994). This deterioration in global temperature is evidenced indirectly by coral reef extinctions (Johnson *et al.*, 1996) and oxygen isotope data, which suggest a cooling of 8-13°C at high latitudes during the early Turonian (Jenkyns *et al.*, 1994). There are two basic models that have been used to explain the significant increase in the burial rate of organic carbon:

The Preservational Model

The preservational model is the first of these and is essentially based on decreased OM remineralisation resulting from a decreased oxygen flux. In the contemporary world, oxygen is supplied to the deep ocean by cold dense bottom waters of polar origin (*e.g.* Jenkyns, 1980). However, it is thought that in the mid-Cretaceous anoxic water column conditions were more prevalent due to the minimal equator-to-pole thermal gradients (Barron, 1983). These warm saline oxygen-deficient bottom waters may have led to anoxic conditions, which occurred only in the deepest parts of tectonically isolated basins such as the Cretaceous South and North Atlantic (de Graciansky *et al.*, 1984; Zimmerman *et al.*, 1987). Furthermore, a recent study of abyssal and shelf sites in the southern North Atlantic indicates that anoxic conditions may have even periodically extended into the photic zone during the C/T OAE (Sinninghe Damsté and Köster, 1998).

The Productivity Model

Alternatively, the productivity model is predominantly based on a significant increase in marine primary productivity, resulting from an increase of nutrient delivery to the surface waters by enhanced upwelling on continental margins or at equatorial divergence zones in the open ocean or during transgressive periods. Other sources of nutrients may include terrestrial run-off (Erbacher *et al.*, 1996) or enhanced volcanism (Sinton and Duncan, 1997). As detritus falls through the water column it is bacterially degraded using dissolved oxygen in the process, leading to the formation of an intensified and expanded OMZ (Schlanger and Jenkyns, 1976; Arthur *et al.*, 1987; Schlanger *et al.*, 1987; Farrimond *et al.*, 1990*)*. Deposition of OM would be particularly enhanced where the OMZ impinged on the continental margin or other prominent regions of the sea floor (*e.g.* submarine plateaus). Thus, the deep abyssal basins may have remained oxic and Schlanger and Jenkyns (1976) have used this model to account for the black shale deposition in the Cretaceous Pacific Ocean.

However, organic-rich sediments have not been discovered in every C/T sequence and the almost-synchronous formation of black shales can probably be attributed to a combination of the previously discussed depositional models: *i.e.* expanded and intensified OMZs, often associated with upwelling (*e.g.* Schlanger and Jenkyns, 1976;

Schlanger *et al.*, 1987; Farrimond *et al.*, 1990), marine water stagnation in restricted/deep basins (*e.g.* de Graciansky *et al.*, 1984; Zimmerman *et al.*, 1987), turbiditic redeposition of organic-rich sediments from continental shelves (Dean and Gardner, 1982; Thurow and Kuhnt, 1986; Degens *et al.*, 1986; Meyers *et al.*, 1986) and high input of OM from allochthonous sources (*e.g.* terrestrial run-off).

This Study

The study on Vena del Gesso (Chapter 3) involved the possibility of PZA occurring in a restricted marine basin as a result of salinity-induced stratification; however, previous work on black shales from the Northern Tethys (Italy) of the Cretaceous C/T OAE suggests the possible occurrence of PZA in a more open ocean setting (Crawford, 1998; Turner, 1998). Here, six black shale deposits (M3, M5, M7, M9, M12 and M13) of the Moria sequence from the Umbrian region of central Italy (Fig. 4.1) were investigated with respect to the distribution and concentration of the solvent-extractable maleimides. Furthermore, the nickel and vanadyl porphyrin fractions in samples M3, M5, M7 and M9 were quantified using UV/Vis spectrophotometry and the former were photo-oxidised to maleimides whose distributions were also determined. In addition, $\delta^{13}C$ values for Me,Et maleimide (**36a**) were monitored over eight samples (MP0-MP7) from the MP sequence (Fig. 4.1). Finally, the maleimide concentrations were determined for samples throughout this sequence, as Crawford (1998) had only determined the distributions (except MP2) in a previous study. In theory, one would expect the isotopic shifts of Me,Et maleimide (**36a**) to relate to changes in CO_2 demand since high Me,Et maleimide (**36a**) abundances, suggesting high productivity, should correlate with heavy $\delta^{13}C$ values of Me,Et maleimide (**36a**).

Livello Bonarelli, Central Italy

The Livello Bonarelli (Bonarelli horizon) was deposited in the Umbrian Apennines of central Italy (Fig. 4.1) and ranges in thickness from 65 cm to just over 1m. Deposition is thought to have occurred on the Tethyan continental margin at roughly 1000m water depth or less (Arthur and Premoli-Silva, 1982; Farrimond *et al.*, 1990). It is comprised of pelagic grey/brown, radiolarian organic-poor siltstones and interbedded

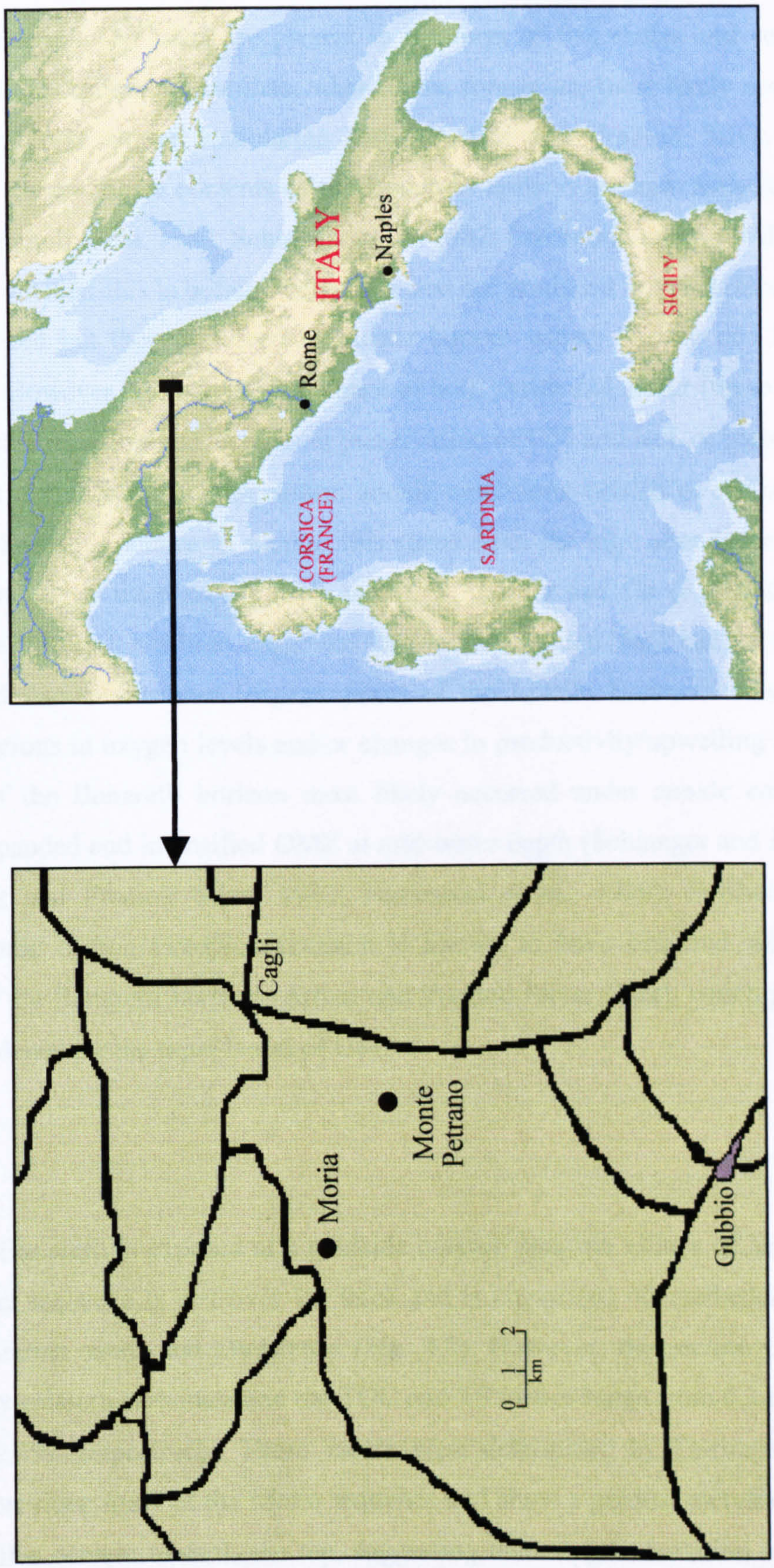

Fig. 4.1 Location of Moria and Monte Petrano sites

mudstone that is highly enriched in organic carbon (up to 31% TOC; Farrimond *et al.*, 1990). The OM consists of non-bioturbated very thinly laminated shales that are dark brown/black in colour. Also present, are fine laminae composed of siliceous and phosphatic material. The latter are present in the form of fish scales and vertebrae, often seen on the surfaces of laminae, whereas the former are most likely comprised of compressed and altered radiolarian tests (Arthur and Premoli Silva, 1982). Furthermore, the carbonate contents of the Bonarelli horizon are extremely low (*e.g.* Arthur and Premoli Silva, 1982; Schlanger *et al.*, 1987; Farrimond *et al.*, 1990), and it is not known whether this is because carbonate was not produced in the surface waters or was produced but then dissolved in caustic bottom waters (Arthur and Premoli Silva, 1982). However, there is an abundance of both pyrite and sulfur (up to 1.84%) in organic-rich shales, and the significant preservation of OM and lack of bioturbation indicates that during sediment deposition anoxic conditions existed at and/or above the sea bed. Further evidence to support this stems from the high abundance of iron (as Fe_2O_3) and other trace metals such as Cu, V, Zn, Cr and Co (*e.g.* Arthur and Premoli Silva, 1982). It has been suggested that the interbedded black shales (organic-rich) and radiolarian siltstones (organic-poor) of the Livello Bonarelli result from cyclical variations in oxygen levels and/or changes in productivity/upwelling and that deposition of the Bonarelli horizon most likely occurred under anoxic conditions during an expanded and intensified OMZ at mid-water depth (Schlanger and Jenkyns, 1976; Arthur and Premoli Silva, 1982; Farrimond *et al.*, 1990). Furthermore, a positive organic carbon isotopic excursion is known to have occurred within the formation of the Bonarelli horizon (Arthur and Premoli Silva, 1982), which provides excellent evidence for the rapid burial of OM.

Moria

The Livello Bonarelli is exposed at a roadside outcrop near the village of Moria (M; Fig. 4.1). The sequence is just over 1m thick and is comprised of interbedded black shales, radiolarian sands and mudstones (Fig. 4.2). However, the section is almost devoid of any calcium carbonate and the TOC and TS values range from 0.3 to 17.6% and 0.3 to 2.4%, respectively. These values were determined by Farrimond *et al.* (1990) in a previous study of the Moria sequence and show a gradual increase in both TOC and sulfur content towards the top, suggesting that oxygen depletion was more

Fig. 4.2 Lithological sequence of C/T Livello Bonarelli at Moria

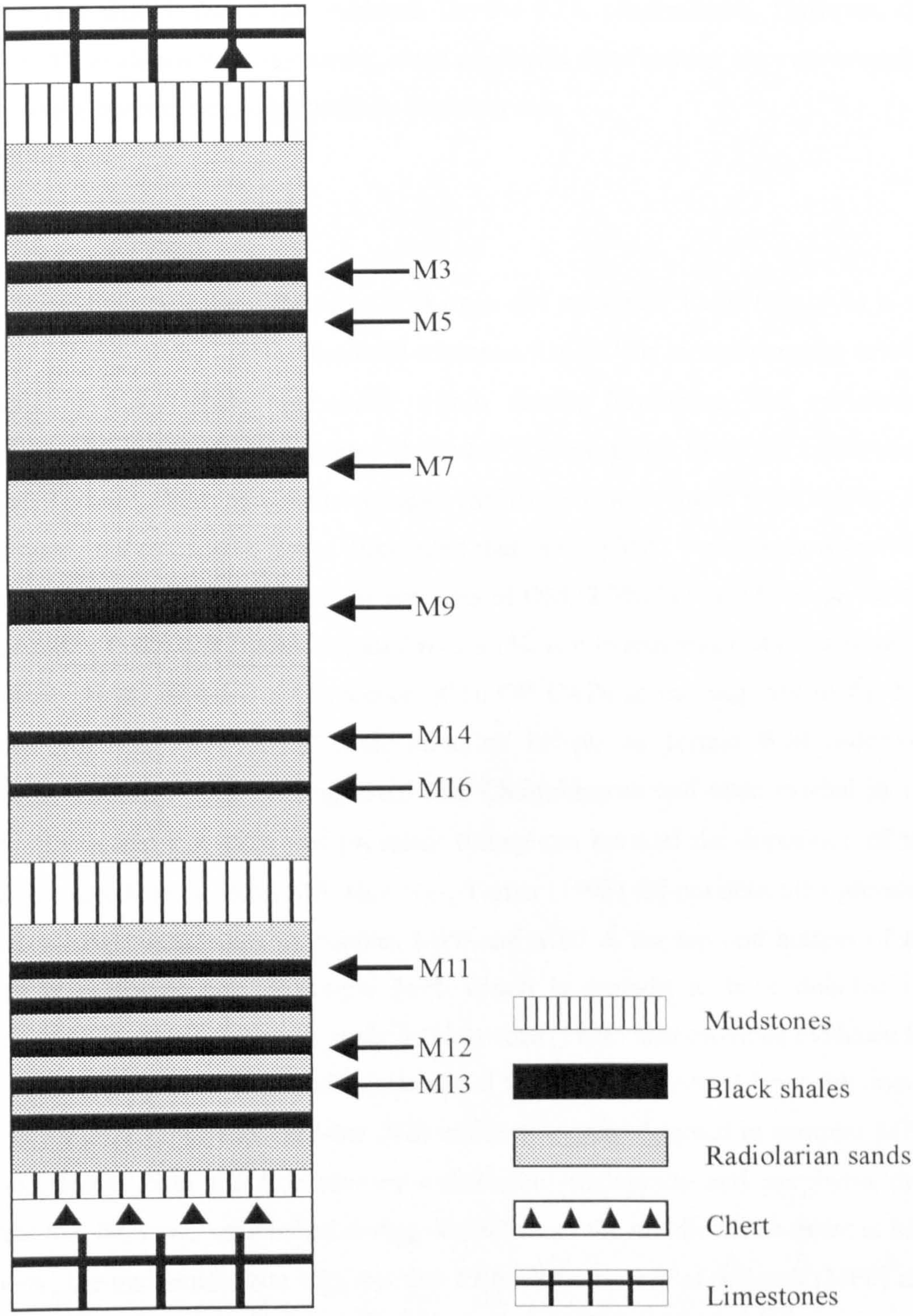

(After Arthur and Premoli Silva, 1982)

prevalent during the deposition of the final part of the Livello Bonarelli section. Interestingly, a comparatively recent study of the porphyrin distributions throughout the Moria sequence (Turner, 1998) suggests that the specific redox conditions of PZA occurred during the deposition of the Livello Bonarelli near Moria, and that such conditions were more prevalent in the middle of the event. Therefore, the maleimide distributions should also show evidence for the PZA phenomenon. However, the HMW CAP evidence is inconclusive, since porphyrin distributions are very complex and the mass spectra are not particularly characteristic.

Monte Petrano, Cagli

Near the summit of Monte Petrano (MP) on a dirt road near Cagli (Fig. 4.1) is an exposed outcrop of the Livello Bonarelli sequence. This 97cm section contains several intervals of black shales imbedded within cherts, limestones and radiolarian sandstones (Fig. 4.3). Eight samples (MP0-MP7) were taken from the black shale intervals (Turner, 1998) and, whilst samples (MP0-MP6) were found to be rich in OM (TOC from 10.9 to 21.9%), it was discovered that sample MP7 was mostly comprised of radiolarian-type material, with low amounts of OM (2.3% TOC). TS values for the eight samples (MP0-MP7) varied from 0.6 to 3.1%. A previous study of these samples by Turner (1998) revealed the presence of HMW CAPs in the majority of the MP samples (MP1-MP5), with the same retention indices as certain Bchl *d*-derived standards. The data therefore suggested that Chlorobiaceae had once existed in the water column and that PZA was prevalent throughout most of the deposition of the Livello Bonarelli sequence at MP. However, Turner (1998) did not detect the presence of such HMW components in samples MP0 and MP7 at the top and bottom of the section respectively, nor in sample MP6 which is thought to have denoted the beginning of the event. A further study by Crawford (1998) also provided evidence for PZA occurring within the Bonarelli sequence at MP. The presence of key components such as Me,*n*-Pr (**36c**) and Me,*i*-Bu (**36f**) maleimide were detected in samples MP0, MP3-6. Hence, both the free (solvent-extractable) maleimide and porphyrin data indicate that PZA was established during deposition of the middle of the event at MP. However, the maleimide data suggests that PZA also occurred at the start (MP6) and end (MP0) of the event, whereas the porphyrin data do not corroborate this.

Fig. 4.3 Lithological sequence of C/T Livello Bonarelli at Monte Petrano

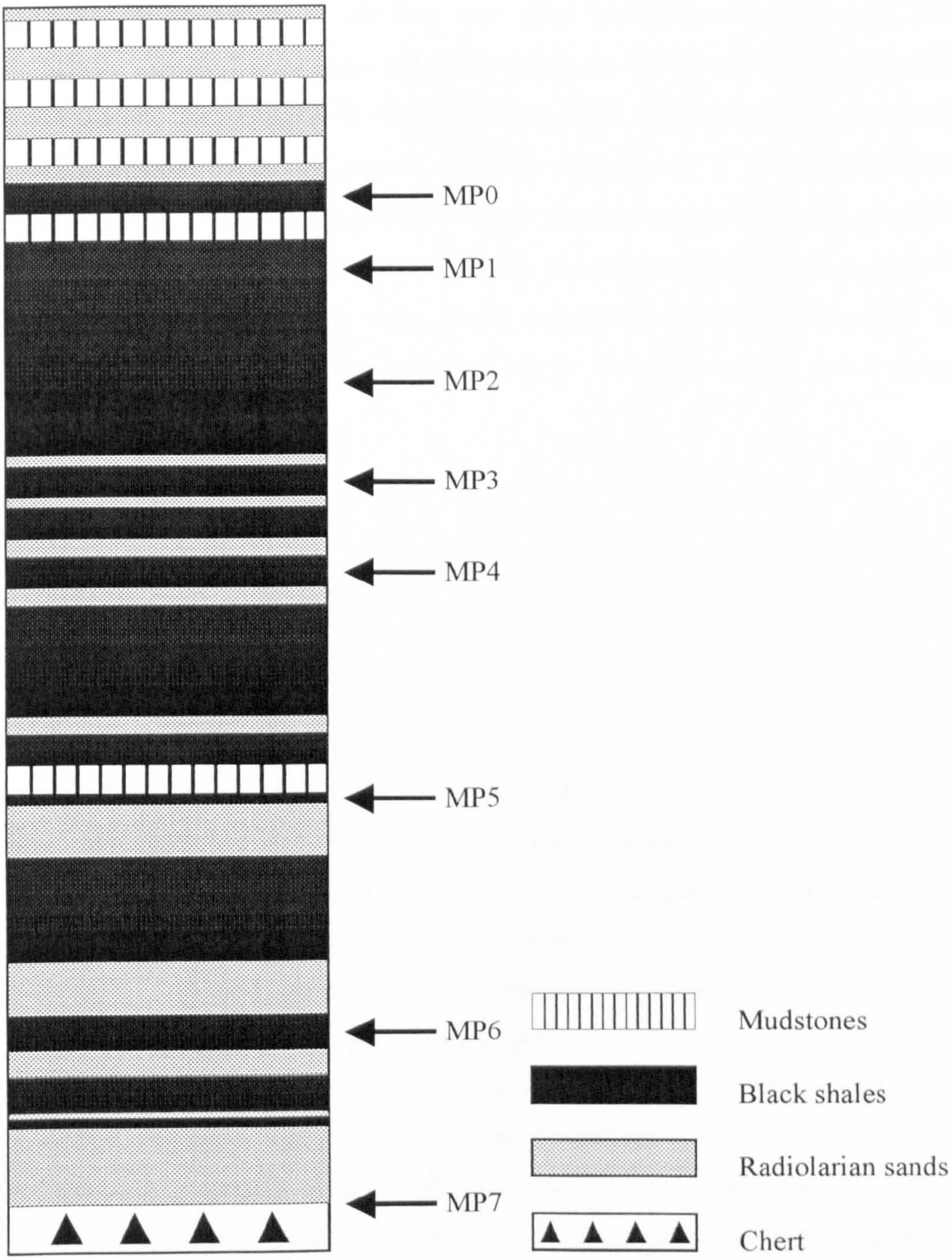

(After Arthur and Premoli Silva, 1982)

In the previous chapter, the $\delta^{13}C$ values of Me,Et maleimide (**36a**) were monitored over the ten sub-samples of marl IV from Vena del Gesso, Italy. Me,Et maleimide (**36a**) was chosen since it is essentially of phytoplanktonic origin, and thus can be ultimately related to the level of productivity in the surface waters during sediment deposition (see previous Chapters). Porphyrins also reflect a mainly phytoplanktonic input and a comparison of the $\delta^{13}C$ values obtained for Me,Et maleimide (**36a**) was made with the abundance of the free base alkyl porphyrins (Keely *et al.*, 1995). Although the correlation between the plots was poor, one would expect the isotopic shifts to relate to changes in CO_2 demand since high porphyrin abundances, suggesting high productivity, should correlate with heavy $\delta^{13}C$ values of Me,Et maleimide (**36a**). Therefore, the positive organic carbon isotopic excursion of *ca.* 4 ‰ (*e.g.* Arthur *et al.*, 1988; Kuypers *et al.*, 1999), should be highlighted throughout the MP Livello Bonarelli sequence using Me,Et maleimide (**36a**) as a biomarker. This work will help to ascertain the utility of Me,Et maleimide (**36a**) as an isotopic productivity indicator.

RESULTS

MORIA

Extractable (Free) Maleimides

The maleimides revealed by GC-MS in the polar fraction (F4.2) of the six Moria samples (M3, M5, M7, M9, M12 and M13) show a simple distribution with Me,Et (**36a**) as usual being the dominant maleimide and Me,Me (**36d**) being the second most abundant (Fig. 4.4). Other maleimides observed included Me,H (**36b**) and Et,Et (**41c**). However, Et,Et maleimide was not found in samples M12 and M13. Furthermore, the key Me,*n*-Pr (**36c**) and Me,*i*-Bu (**36f**) components, indicative of the green sulfur bacteria, were not detected in any of the samples. The Me,Et (**36a**) and Et,Et (**41c**) components were again confirmed by comparison with the relative retention times and mass spectra of standards obtained by the oxidation of aetioporphyrin III (**17**) and octaethylporphyrin (**48**) respectively; the mass spectra and relative retention times of the other components agree with those observed by Quirke *et al.* (1980). The

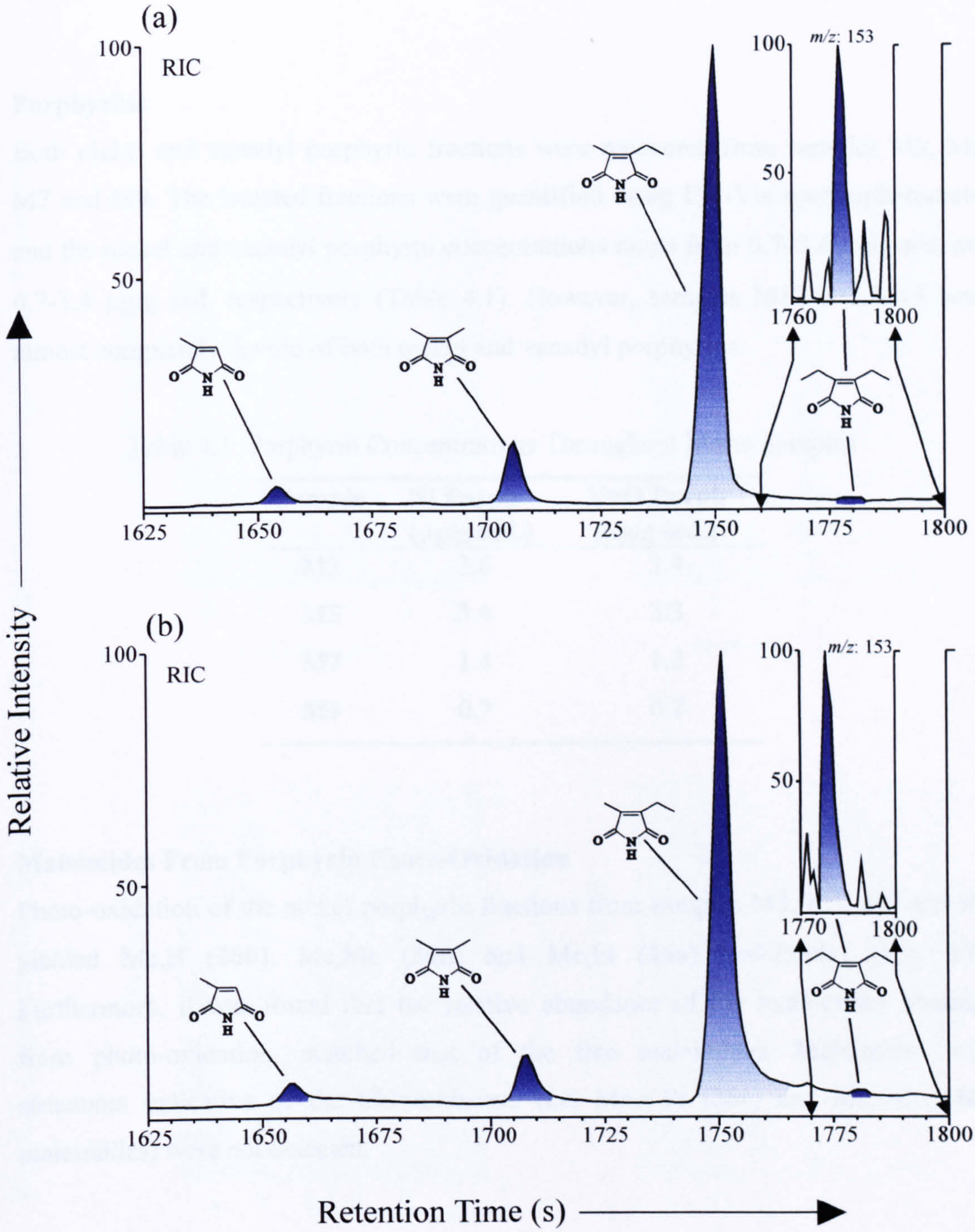

Fig. 4.4 Partial RIC and Mass Chromatograms of Solvent Extractable Maleimides from Moria (a) M3 and (b) M5 using CP-WAX 52 CB Stationary Phase

concentrations were also obtained (Fig. 4.5), using phthalimide (**45**) added as an internal standard at the TOE stage.

Porphyrins

Both nickel and vanadyl porphyrin fractions were recovered from samples M3, M5, M7 and M9. The isolated fractions were quantified using UV-Vis spectrophotometry and the nickel and vanadyl porphyrin concentrations range from 0.7–3.6 μg/g sed. and 0.7-3.4 μg/g sed. respectively (Table 4.1). However, samples M12 and M13 were almost completely devoid of both nickel and vanadyl porphyrins.

Table 4.1 Porphyrin Concentrations Throughout Moria Samples

Sample	Ni Porph (μg/g sed.)	V=O Porph (μg/g sed.)
M3	3.6	3.4
M5	3.4	3.3
M7	1.4	1.2
M9	0.7	0.7

Maleimides From Porphyrin Photo-Oxidation

Photo-oxidation of the nickel porphyrin fractions from samples M3, M5, M7 and M9 yielded Me,H (**36b**), Me,Me (**36d**) and Me,Et (**36a**) maleimides (Fig. 4.6). Furthermore, it was found that the relative abundance of the maleimides obtained from photo-oxidation, matched that of the free maleimides. Maleimides with structures indicative of the Chlorobiaceae (*i.e.* Me,*n*-Pr (**36c**) and Me,*i*-Bu (**36f**) maleimides) were not detected.

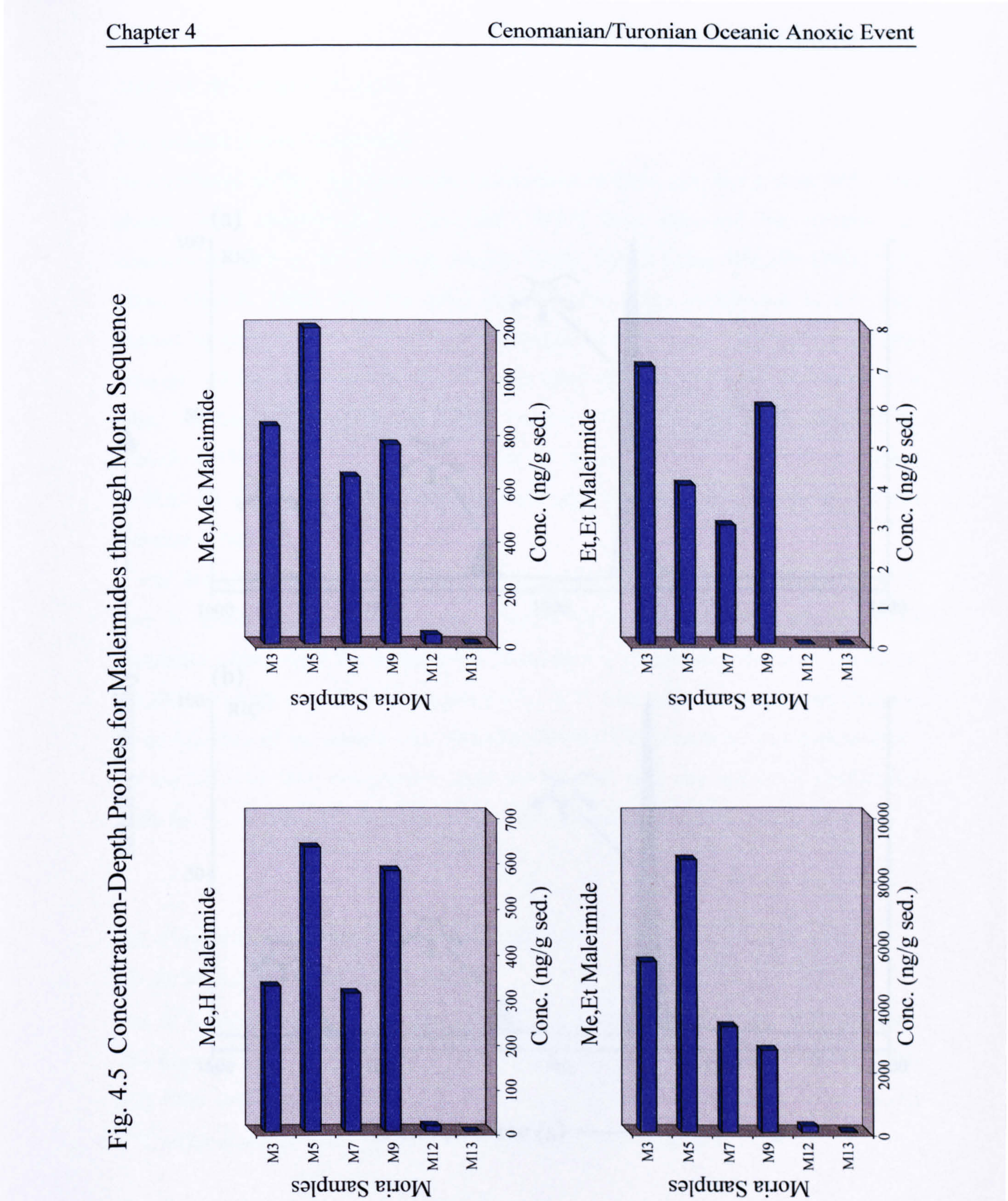

Fig. 4.5 Concentration-Depth Profiles for Maleimides through Moria Sequence

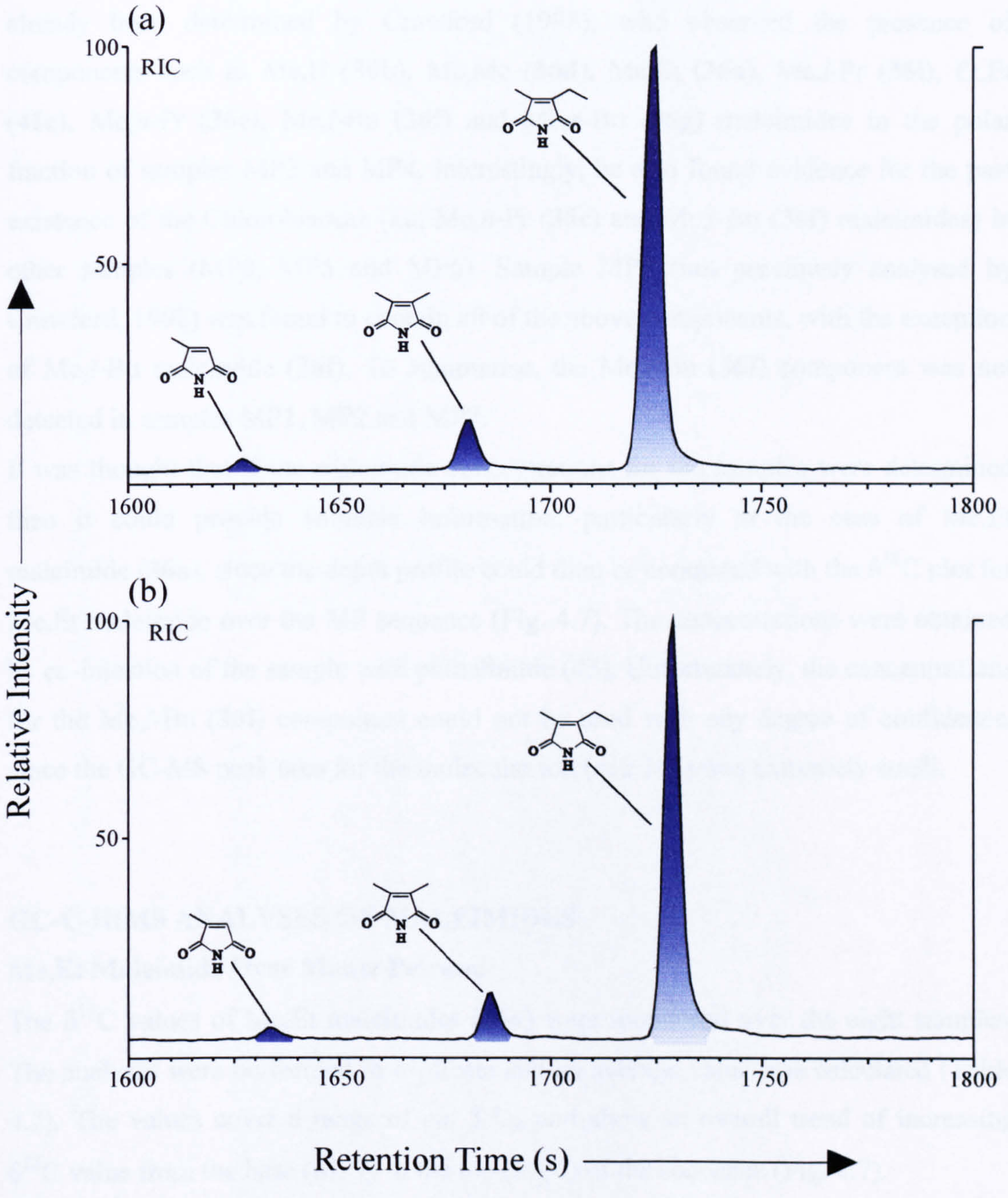

Fig. 4.6 Partial RIC of Maleimides Obtained from Photo-oxidation of nickel porphyrin fractions from Moria (a) M3 and (b) M5 using CP-WAX 52 CB Stationary Phase

MONTE PETRANO, CAGLI

Extractable (Free) Maleimides

As mentioned earlier, the maleimide distributions in these samples (except MP2) had already been determined by Crawford (1998), who observed the presence of components such as Me,H (**36b**), Me,Me (**36d**), Me,Et (**36a**), Me,*i*-Pr (**36i**), Et,Et (**41c**), Me,*n*-Pr (**36c**), Me,*i*-Bu (**36f**) and Me,*n*-Bu (**36g**) maleimides in the polar fraction of samples MP3 and MP4. Interestingly, he also found evidence for the past existence of the Chlorobiaceae (*i.e.* Me,*n*-Pr (**36c**) and Me,*i*-Bu (**36f**) maleimides) in other samples (MP0, MP5 and MP6). Sample MP2 (not previously analysed by Crawford, 1998) was found to contain all of the above components, with the exception of Me,*i*-Bu maleimide (**36f**). To summarise, the Me,*i*-Bu (**36f**) component was not detected in samples MP1, MP2 and MP7.

It was thought that if the maleimide concentrations for the samples were determined then it could provide valuable information, particularly in the case of Me,Et maleimide (**36a**), since the depth profile could then be compared with the $\delta^{13}C$ plot for Me,Et maleimide over the MP sequence (Fig. 4.7). The concentrations were obtained by co-injection of the sample with phthalimide (**45**). Unfortunately, the concentrations for the Me,*i*-Bu (**36f**) component could not be used with any degree of confidence, since the GC-MS peak area for the molecular ion (*m/z* 167) was extremely small.

GC-C-IRMS ANALYSES OF MALEIMIDES

Me,Et Maleimide Over Monte Petrano

The $\delta^{13}C$ values of Me,Et maleimides (**36a**) were monitored over the eight samples. The analyses were performed in triplicate and an average value was calculated (Table 4.2). The values cover a range of *ca.* 3 ‰ and show an overall trend of increasing $\delta^{13}C$ value from the base (MP7) to the top (MP0) of the sequence (Fig. 4.7).

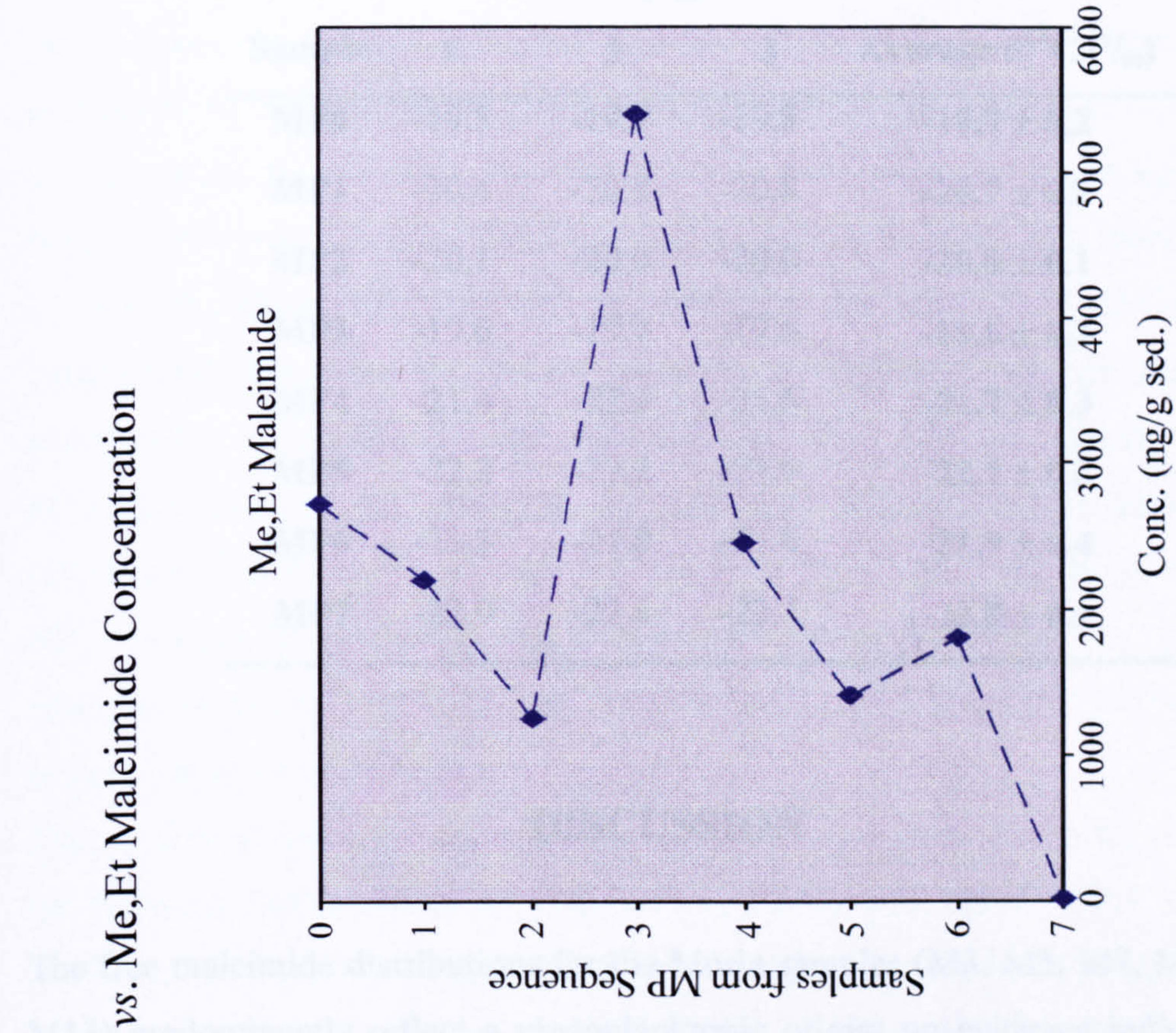

Fig. 4.7 $\delta^{13}C$ Me,Et Maleimide

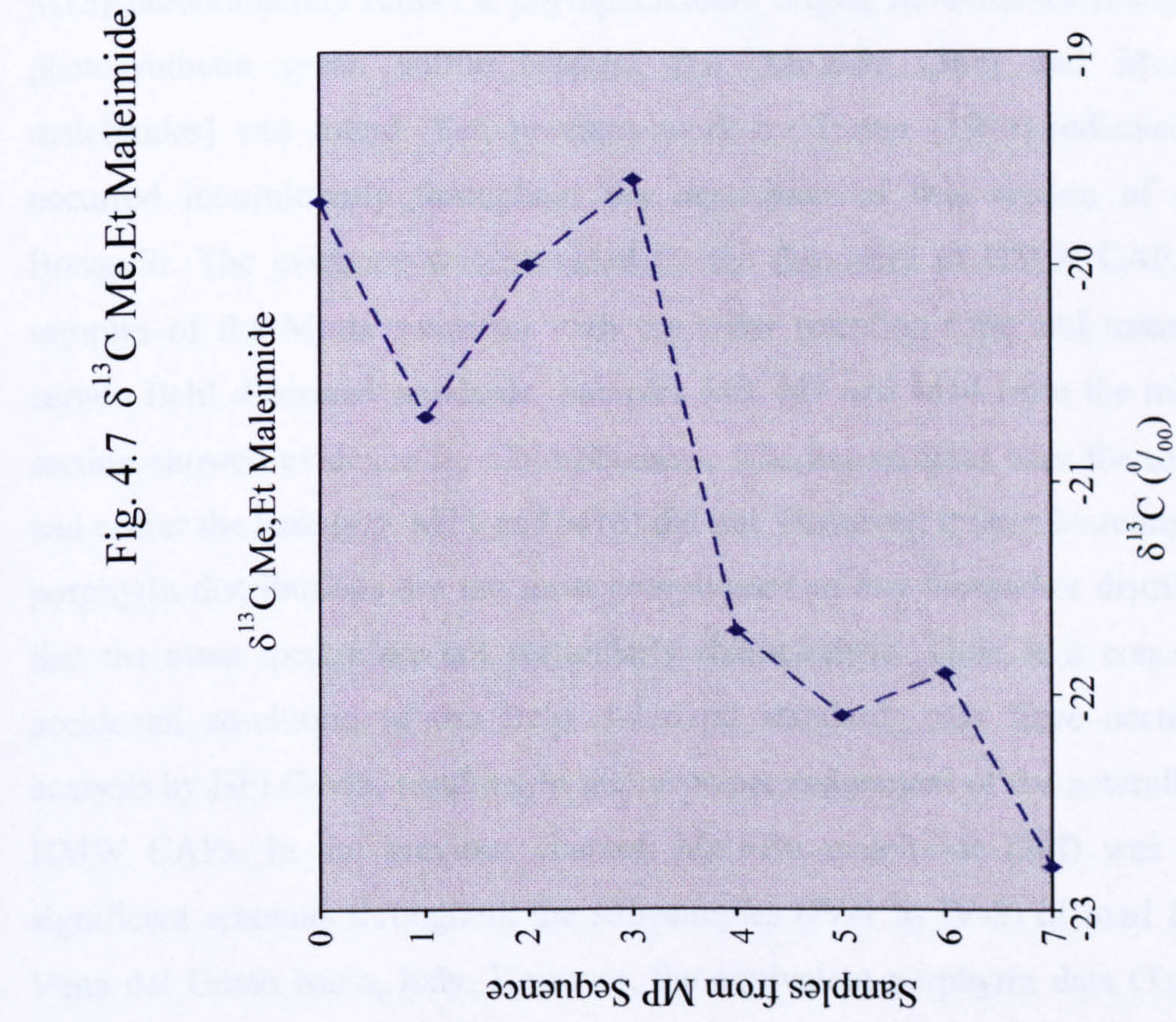

Table 4.2 $\delta^{13}C$ Values of Me,Et Maleimide Over the MP Sequence

	$\delta^{13}C$ (‰)			
Sample	**1**	**2**	**3**	**Average $\delta^{13}C$ (‰)**
MP0	-19.5	-19.7	-19.8	**-19.7 ± 0.2**
MP1	-20.4	-20.8	-20.8	**-20.7 ± 0.2**
MP2	-20.1	-20.0	-20.0	**-20.0 ± 0.1**
MP3	-19.6	-19.7	-19.6	**-19.6 ± 0.1**
MP4	-21.4	-22.0	-21.6	**-21.7 ± 0.3**
MP5	-22.2	-22.2	-21.9	**-22.1 ± 0.2**
MP6	-22.3	-21.8	-21.6	**-21.9 ± 0.4**
MP7	-22.9	-22.8	-22.7	**-22.8 ± 0.1**

DISCUSSION

The free maleimide distributions for the Moria samples (M3, M5, M7, M9, M12 and M13) predominantly reflect a phytoplanktonic origin; no evidence indicative of the photosynthetic green sulfur bacteria [*i.e.* Me,*n*-Pr **(36c)** and Me,*i*-Bu **(36f)** maleimides] was found. Yet, previous work by Turner (1998) indicated that PZA occurred intermittently throughout the deposition of this section of the Livello Bonarelli. The evidence was provided by the discovery of HMW CAPs in certain samples of the Moria sequence with the same retention time and mass spectra as certain Bchl *d*-derived standards. Samples M5, M7 and M14 from the middle of the section showed evidence for Chlorobiaceae, whereas samples near the top (*e.g.* M3) and nearer the base (*e.g.* M11 and M16) did not. However, it must be remembered that porphyrin distributions are the most complicated of any biomarker distributions and that the mass spectra are not particularly characteristic. Thus, it is conceivable that accidental co-elution of the Bchl *d*-derived standards may have occurred during analysis by HPLC-MS, resulting in the incorrect assignment of the naturally occurring HMW CAPs. In the previous chapter, Me,*i*-Bu maleimide **(36f)** was detected in significant amounts throughout the sub-samples (IV-1 to IV-8) of marl IV from the Vena del Gesso basin, Italy. However, the equivalent porphyrin data (Turner, 1998) failed to provide convincing evidence for HMW CAPs derived from the

Chlorobiaceae. Therefore, the balance of evidence would seem to suggest that Me,*i*-Bu maleimide (**36f**) is perhaps a more robust and reliable biomarker for detecting the past existence of the Chlorobiaceae than are HMW CAPs, thus indicating that PZA may not have occurred during the deposition of the Moria sequence. Further evidence to support the lack of PZA was provided with the maleimide distributions obtained from the photo-oxidation of nickel porphyrin fractions isolated from samples M3, M5, M7 and M9, which also failed to yield maleimides characteristic of the Chlorobiaceae. Interestingly, this is not the first occasion where maleimide and porphyrin data seem to contradict one another. Disagreements as to whether PZA has occurred or not, have been highlighted on several occasions in previous analyses carried out by Crawford (1998) and Turner (1998) of other Livello Bonarelli black shale samples (*e.g.* Fosto, MP, Contessa Gorge Quarry and Bottaccione Gorge). However, this usually occurs when the appropriate HMW porphyrin components or Me,*i*-Bu maleimide (**36f**) are at or near the limits of detection.

Despite this, maleimide evidence does exist for the occurrence of episodes of PZA in the Northern Tethys during the C/T OAE in the form of Me,*i*-Bu (**36f**) maleimide in the MP sequence (Crawford, 1998). Crucially, Me,*i*-Bu maleimide (**36f**) has only one known origin, and that is from the Bchls *c* (**12**), *d* (**10**) or *e* (**13**) of the Chlorobiaceae. On the other hand, Me,*n*-Pr maleimide (**36c**) although detected in all of the Bonarelli samples that Crawford (1998) examined, cannot be used as a Chlorobiaceae-biomarker on structural grounds alone, since Crawford (1998) discovered that the $\delta^{13}C$ values of Me,*n*-Pr maleimide (**36c**) found in samples from the Contessa Gorge Quarry were similar to those of Me,Et maleimide (**36a**), which is of phytoplanktonic origin (see previous Chapters).

Sinninghe Damsté and Köster (1998) also investigated the possible occurrence of PZA in a euxinic southern North Atlantic Ocean during the C/T OAE by attempting to find isorenieratane (**34**) and/or related diaryl isoprenoid hydrocarbons. However, their study only included one sample from the Livello Bonarelli horizon, which was obtained from the Gubbio region (Fig. 4.1), and they found no evidence for PZA. On the other hand, LMW monoaromatic aryl isoprenoids were detected in the same sample, but a Chlorobiaceae origin could not be substantiated since the $\delta^{13}C$ values for these compounds were not reported. This is essential, since Koopmans *et al.* (1996) found for a North Sea oil that the $\delta^{13}C$ values of certain monoaromatic aryl

isoprenoids were intermediate between those of β-isorenieratane (from the β-carotene of algae) and isorenieratane (from the isorenieratene of Chlorobiaceae), suggesting a mixed source. This shows that the presence of monoaromatic aryl isoprenoids in sedimentary OM on its own does not necessarily indicate the past existence of the Chlorobiaceae and occurrence of PZA, unless they are considerably enriched in ^{13}C compared to phytoplanktonic components.

To date, most measurements on the C/T $\delta^{13}C_{org}$ excursion have been determined using bulk $\delta^{13}C_{org}$ analyses (*e.g.* Arthur *et al.*, 1988), with the exception of some compound specific studies, *e.g.* sedimentary porphyrins (Popp *et al.*, 1989); Ni-geoporphyrins (Hayes *et al.*, 1989); *n*-alkanes, pristane and phytane (Pancost *et al.*, 1998); terrestrial leaf wax *n*-alkanes, sulfur-bound phytane and steranes (Kuypers *et al.*, 1999). In this study, Me,Et maleimide (**36a**) was used as a simple marine phytoplanktonic isotopic biomarker and a $\delta^{13}C_{org}$ positive excursion of *ca.* 3.2 ‰ was observed over the MP sequence (Fig. 4.7). As mentioned earlier, Me,Et maleimide (**36a**) was chosen since it is essentially of phytoplanktonic origin, and thus can be ultimately related to the level of productivity in the surface waters during sediment deposition (see previous Chapters). Furthermore, the concentration of Me,Et maleimide (**36a**) throughout the MP sequence was obtained and the depth-profile compared with the $\delta^{13}C_{org}$ excursion plot (Fig 4.7). From the plots it can be seen that there is a moderately good correlation for samples MP7 to MP4. The main controls on the carbon-isotopic composition of primary OM are the $\delta^{13}C$ values of dissolved CO_2. It is thought that high concentrations of dissolved CO_2 cause ^{13}C-depletion, whilst increased growth rates cause ^{13}C-enrichment (Laws *et al.*, 1995; Bidigare *et al.*, 1997; Bidigare *et al.*, 1999). Consequently, a high nutrient influx (*e.g.* during periods of upwelling) could increase productivity and remove CO_2 from surface waters; both lower CO_2 concentrations and higher growth rates will result in enrichment of ^{13}C in marine OM. However, in this case the concentration depth-profile for Me,Et maleimide (**36a**) might just coincidentally coincide with the positive carbon isotopic excursion; since the excursion could ultimately reflect either a local or global increase in phytoplankton productivity in surface waters. It has been suggested that during the Cretaceous the partial pressure of CO_2 (pCO_2) was *ca.* 4x higher than at present (Freeman and Hayes, 1992). This estimate compares well to other approximations of Cretaceous atmospheric CO_2 concentration. For example, Berner (1991) proposed that pCO_2,

based on models of global geochemical cycles, was between 2-6x higher than present. However, Arthur *et al.* (1991) suggested that pCO_2 values were even higher (4-12x). In the latter period of the C/T OAE there was a substantial decrease in pCO_2, which can probably be attributed to a high level of productivity in oceanic surface waters.

A recent study by Kuypers *et al.* (1999) estimates that the reduction in atmospheric CO_2 concentration during the C/T OAE may be up to 40-80% greater than that calculated earlier by Freeman and Hayes (1992). Kuypers *et al.* (1999) examined isotope shifts in terrestrial leaf-wax components extracted from abyssal sediments in the northeastern tropical Atlantic Ocean (DSDP site 367). The leaves were wind-transported to the site and the results indicate an abrupt change in the plant communities of the north African continent which was interpreted as a result of the reduction in atmospheric CO_2 concentration during the C/T OAE. $\delta^{13}C$ measurements of the terrestrial *n*-alkanes show a shift coincident with the positive isotope ratio excursion observed for bulk $\delta^{13}C_{org}$ also at DSDP site 367 (Kuypers *et al.*, 1999) and for marine carbonates (Scholle and Arthur, 1980; Arthur *et al.*, 1988; Jenkyns *et al.*, 1994). The *n*-alkane isotope data suggests that C_3 plants were succeeded by C_4 plants during the C/T OAE since C_4 plants exhibit a CO_2-concentrating mechanism and can thus out compete C_3 plants, but only at atmospheric CO_2 concentrations below 500 p.p.m.v. (Cerling *et al.*, 1997). Finally, assuming a 1:1 photosynthetic ratio for CO_2 and O_2, Arthur *et al.* (1988) have suggested that an equal quantity of O_2 would have been returned to the atmosphere during the C/T OAE, which would have increased the oxidising capability of deep marine waters by up to 50%, assuming a constant consumption rate for O_2. This is perhaps evidenced by the deposition of oxidised, reddish pelagic carbonates in the Tethys and also multicoloured, oxidised pelagic clay on the deeper Atlantic ocean floor after the C/T event (Arthur *et al.*, 1988).

It would appear that there are two sides to the argument regarding the exact mechanism behind the formation of the C/T black shales in the southern North Atlantic Ocean: was it enhanced preservation *via* a continuous euxinic water column (Sinninghe Damsté and Köster, 1998) or simply high levels of productivity and the subsequent formation of OMZs at mid-water depth (*e.g.* Farrimond *et al.*, 1990)? Sinninghe Damsté and Köster (1998) after finding isorenieratene derivatives in other samples from the Northern Tethys, in addition to evidence of reducing conditions in sediments, proposed that deposition of the C/T black shales in the southern North Atlantic Ocean probably occurred in a continuously euxinic water column. They

suggested that oxygen-deficient warm saline bottom waters were the driving force behind oceanic circulation during the C/T OAE, and that a substantial flux of sulfide, probably released during episodes of submarine volcanism and from hydrothermal activity was responsible for the upward expansion of euxinic conditions throughout the C/T event. Evidence to support their theory stems from the seawater strontium isotope record (Ingram *et al.*, 1994), which indicates enhanced seafloor spreading and also the sequential extinction of benthic and intermediate-water foraminifera (Jarvis *et al.*, 1988). In essence, Sinninghe Damsté and Köster (1998) calculated that the overall productivity was low during the C/T OAE, and that a high degree of preservation of organic carbon enhanced by a euxinic water column was the key to the formation of the black shales. However, the occurrence of alternate black shales (organic-rich) and radiolarian sands (organic-poor) found in many of the Livello Bonarelli black shale sequences (*e.g.* Moria, Fig. 4.2) suggests that there was a repeating cycle of oxygen-deficient conditions, followed by a return to more oxidising conditions. Indeed, the more widely held theory is that deposition of the black shales occurred under anoxic conditions during an expanded and intensified OMZ at mid-water depth, due to high levels of productivity in surface waters (Fig. 4.8; Schlanger and Jenkyns, 1976; Arthur and Premoli Silva, 1982; Farrimond *et al.*, 1990). Evidence to support this theory arises from the fact that the majority of C/T organic-rich sediments come from exposed horizons on land (*e.g.* the Livello Bonarelli sequence), which show clear evidence of deposition on slopes. Furthermore, there is evidence to suggest that during deposition of the black shales of the Livello Bonarelli an intensified OMZ might have intermittently expanded into the photic zone at certain sites, but not at others. For example, maleimide evidence for the past occurrence of PZA was found at MP (MP0 and MP3-6), but not at Moria. What makes this finding even more intriguing is that these sites are only separated by a distance of a few kilometres, which makes this observation difficult to explain, especially since Me,*i*-Bu maleimide (**36f**) was also detected at other sites in the Umbrian region of central Italy by Crawford (1998): Gorgo A Cerbara, Fosto (F5), Contessa Gorge Quarry (CGQ1), Bottaccione Gorge (BG1 and BG2). Furthermore, isorenieratane (**34**) and/or related diaryl isoprenoid hydrocarbons also indicative of the past occurrence of PZA were not detected in a sample from the Gubbio area (Sinninghe Damsté and Köster, 1998). The fact that evidence for PZA is not found in all the samples at each site indicates an intermittent occurrence of the PZA phenomenon, and thus a temporal variation of appropriate

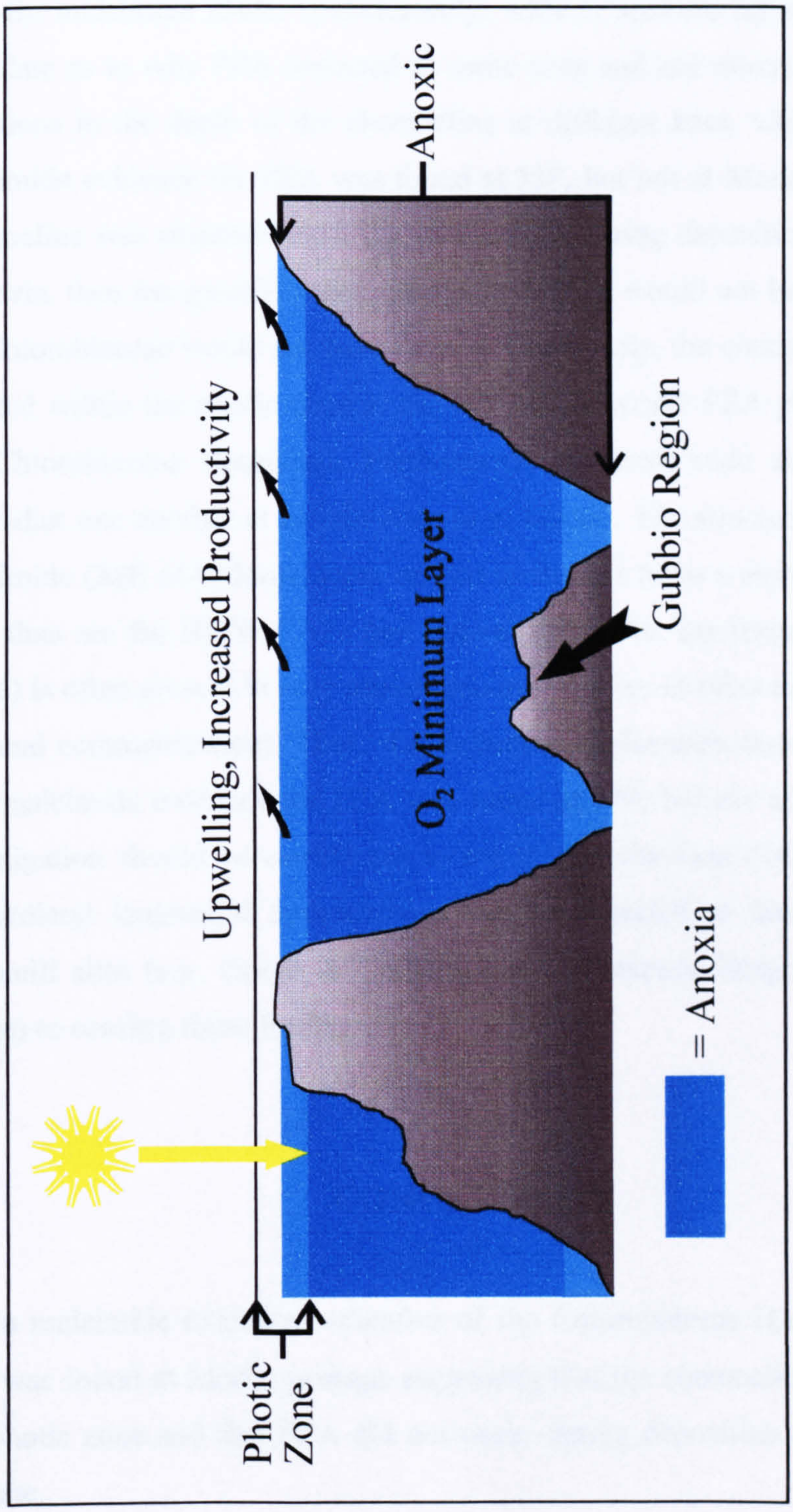

Fig. 4.8 Illustration of possible explanation to account for the occurrence of PZA in an OMZ that may have formed black shales in the Gubbio region of the northern Tethys (modified from Farrimond *et al.*, 1990)

biomarkers in samples (Jenkyns, personal communication). This explanation would seem plausible if only one or two samples were examined from each site. However, six samples were investigated in the case of Moria and not one was found to contain Me,*i*-Bu maleimide (**36f**). Unfortunately, without specific information one can only speculate as to why PZA occurred at some sites and not others. Perhaps, there were variations in the depth of the chemocline at different sites, which may explain why maleimide evidence for PZA was found at MP, but not at Moria. For instance, if the chemocline was situated below the photic zone during deposition of the black shales at Moria, then the specific redox condition of PZA would not have been possible and the Chlorobiaceae would not have existed. Conversely, the chemocline may have been situated within the photic zone at the MP site, whereby PZA probably occurred and the Chlorobiaceae flourished. Furthermore, the maleimide and HMW CAP data contradict one another at certain sites (*e.g.* Moria). The structurally specific Me,*i*-Bu maleimide (**36f**; of Chlorobiaceae origin) is thought to be a more reliable indicator of PZA than are the HMW CAPs (see above). However, the former component (where found) is often present in very minor amounts relative to other maleimides (Crawford, personal communication). Thus, if a definitive explanation cannot ultimately explain why maleimide evidence for PZA was found at MP, but not at Moria then a further investigation should be carried out to see if isorenieratane (**34**) and/or other related mono/diaryl isoprenoid hydrocarbons can be detected at these and other Livello Bonarelli sites (*e.g.* Gorgo A Cerbara, Fosto, Contessa Gorge Quarry, Bottaccione Gorge) to confirm these findings.

CONCLUSIONS

- No maleimide evidence indicative of the Chlorobiaceae (*i.e.* Me,*i*-Bu maleimide **36f**) was found at Moria; perhaps suggesting that the chemocline was situated below the photic zone and that PZA did not occur during deposition of the black shales at this site.

- The $\delta^{13}C_{org}$ values of Me,Et maleimide (**36a**) over the MP sequence show a positive excursion of *ca.* 3.2 ‰ (Fig. 4.7). This plot correlates reasonably well with the

concentration depth-profile obtained for Me,Et maleimide (**36a**) over the same sequence, thus indicating that its use as an isotopic productivity indicator should be explored further in future studies.

CHAPTER 5:

ATTEMPTED $\delta^{15}N$ MEASUREMENT OF MALEIMIDES

INTRODUCTION

GENERAL

Nitrogen Isotopes

Nitrogen exists naturally as two stable isotopes, ^{14}N and ^{15}N. In 1950, Nier successfully determined the composition of atmospheric N_2 as:

^{14}N: 99.634 %

^{15}N: 0.366 %

It also exists in the form of several radioactive isotopes, ^{12}N, ^{13}N, ^{16}N and ^{17}N with respective half-lives of 0.0125s, 603s, 7.38s and 4.14s. However, these are difficult to produce and have minimal use in biogeochemical studies due to their short half-lives. Only ^{13}N has proved to be of experimental value (*e.g.* Krohn and Mathis, 1981; Root and Krohn, 1981 and Cooper *et al.*, 1985), but its use is restricted due to its short half-life. On the other hand, the stable isotope ^{15}N may either be used as a tracer to monitor reactions utilising nitrogen after its addition in an appropriate chemical form, or to investigate the $^{15}N/^{14}N$ ratios in natural materials. Nitrogen is an essential element in the biosphere and less than 1% of it exists in the non-elemental form. Furthermore, it exists in gaseous, dissolved and solid forms as well as numerous oxidation states (NO_3^-, NO_2^-, NO, N_2O, N_2, NH_3, NH_4^+), thus making it an ideal element for exploring the natural variations in its isotopic composition. Schoenheimer and Rittenburg (1939) were the first to report isotopic variations in biological materials and described appropriate MS methods for the determination of $^{15}N/^{14}N$ ratios in amino acids. Since then $\delta^{15}N$ values ranging from *ca.* -50 ‰ (*e.g.* freshwater epibenthic algae; Wada *et al.*, 1981) to +50 ‰ (*e.g.* suspended marine particulate matter; *e.g.* Mariotti *et al.*, 1984; Altabet and McCarthy, 1985) have been recorded, but normally lie within the range of -10 ‰ to +20 ‰. Generally, the average $\delta^{15}N$ values for each environment appear to increase in the order atmosphere < terrestrial < freshwater < estuarine < marine. Atmospheric N_2 has a constant $^{15}N/^{14}N$ ratio (Nier, 1950; Dole *et al.*, 1954; Junk and Svec, 1958; Mariotti, 1983) and is thus used as the standard for $^{15}N/^{14}N$ ratio measurements.

Biological Nitrogen Cycle

A fundamental understanding of the biological nitrogen cycle (Fig. 5.1) is essential if one is to fully comprehend the processes leading to the nitrogen isotope distribution in the geosphere.

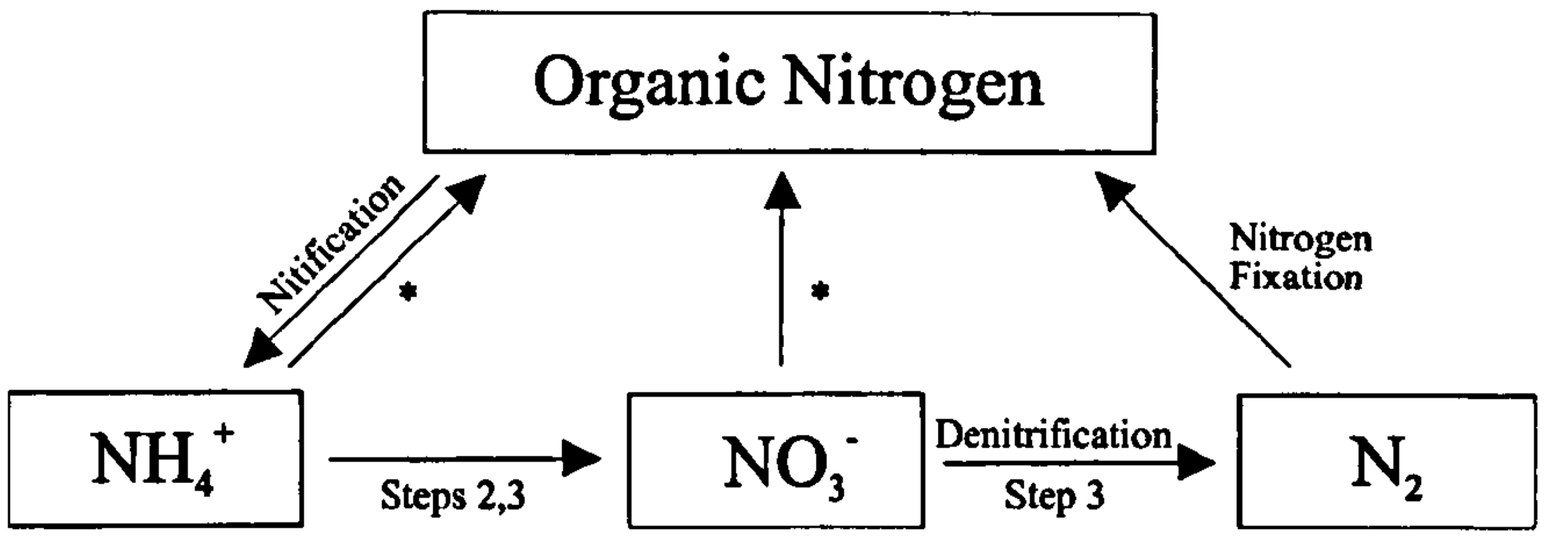

* N is incorporated into plants by assimilation of NH_4^+ or NO_3^-

Fig. 5.1 Main components and interactions in the nitrogen cycle

Nitrogen Fixation

Certain algae and/or bacteria are responsible for the conversion of atmospheric N_2 to organic nitrogen. The nitrogen-fixing bacteria may be either aerobic or anaerobic and either heterotrophic or autotrophic (*i.e.* phototrophic or chemotrophic). However, the enzymes responsible for N_2 fixation are oxygen-sensitive and as a result the fixation process is, in essence, anaerobic. Fixation may be described by the reaction:

$$N_2 + 3H_2O \rightarrow 2NH_3 + 1^1/_2O_2$$

Not surprisingly, the process requires a large amount of energy due to the strength of the molecular nitrogen bond (*ca.* 945 kJ mol^{-1}). Overall, it is extremely inefficient, and many studies have shown that the nitrogen isotopic fractionation effect for this process is miniscule (*i.e.* product differs from substrate by *ca.* –3 to +1 ‰; *e.g.* Fogel and Cifuentes, 1993). Thus, organic nitrogen derived from atmospheric N_2 fixation should have $\delta^{15}N$ values close to atmospheric values and this has been confirmed in numerous studies (*e.g.* Delwiche *et al.*, 1979; Virginia and Delwiche, 1982).

Nitrification

Nitrification occurs under oxic conditions and is essentially the production of nitrate from organic nitrogen. The process is outlined below:

$$\text{Organic N} \xrightarrow{1} NH_4^+ \xrightarrow{2} NO_2^- \xrightarrow{3} NO_3^-$$

NH_3/NH_4^+ is released when OM (containing organic nitrogen) is degraded. Autotrophic aerobic bacteria such as *Nitrosomonas* and *Nitrobacter* are mainly responsible for the conversion of organic nitrogen to simple inorganic nitrogen compounds. *Nitrosomonas* oxidises ammonium (NH_4^+) to nitrite (NO_2^-) and the oxidation to nitrate (NO_3^-) is concluded by *Nitrobacter* (Focht and Verstraete, 1977). In this process, the total nitrogen isotope fractionation depends on which of the above steps are rate limiting. For example, if there is an abundance of NH_4^+ then step 2 or even steps 2 and 3 can become rate limiting, and it has been shown that the resulting nitrate will be depleted in ^{15}N by 20-35 ‰ (Mariotti *et al.*, 1981). However, in reality NH_4^+ is gradually produced from organic nitrogen and so step 1 becomes the rate-determining step, which is not thought to be associated with an isotope effect and the resulting nitrate should have a comparable isotopic composition to that of its organic nitrogen source (Hoefs, 1996).

Denitrification

Denitrification is essentially the conversion of NO_3^- to N_2. It is thought that the process must be in equilibrium with the natural fixation of N_2. If it were not, then the nitrification process would slowly but surely, exhaust the atmospheric N_2 supply. According to Mariotti *et al.* (1982) denitrification probably involves two main steps, the first being the uptake of substrate into the cell. It is thought that this step is not associated with an isotope effect. In the second step the substrate is reduced and the N-O bonds are broken. The N-O bond is remarkably strong and Urey (1947) calculated an isotope fractionation factor (α) of 1.0659 for its cleavage. Thus, it was of no surprise to find a substantial amount of nitrogen isotopic fractionation associated with nitrate reduction. However, Mariotti *et al.* (1982) believe that Urey's single fractionation factor for denitrification is too simplistic and that in fact the process

comprises several consecutive reaction steps ($2NO_3^- \rightarrow 2NO_2^- \rightarrow 2(NO) \rightarrow N_2O \rightarrow N_2$). However, there is still some uncertainty as to whether the NO intermediate is genuine, as Goretski and Hollocher (1988) claim, or is in fact a by-product since earlier work by Aerssens *et al.* (1986) indicated that a specific enzyme is responsible for the reduction of NO_2^- to N_2O and that the formation of NO results from the degeneration of NO^+. Furthermore, denitrification occurs in poorly aerated soil and in stratified anaerobic water bodies because the action of the reductive enzymes (*nitrate*, *nitrite* and *nitrous oxide reductase*) is often repressed in the presence of O_2. However, some of the reductive enzymes are more sensitive to O_2 than others. For example, *nitrous oxide reductase* is apparently more sensitive to the presence of O_2 than *nitrate* or *nitrite reductase* (Mosier and Schimel, 1993). Thus, it is conceivable that the formation of N_2 is greatest in those environments that contain little or no oxygen.

Isotopic Fractionation

The natural variation in ^{15}N would not exist if it was not for isotope fractionation. Fractionation may be simply defined as the unequal partition of isotopes between the substrate of a reaction and the products formed during the reaction (Hayes, 1982). Essentially, fractionation occurs as a result of two different effects:

1. Physical isotope effects.
2. Chemical isotope effects.

Physical Isotope Effects

Physical isotope effects often involve incomplete and unidirectional processes/reactions. For example, some of these may include evaporation, diffusion, dissociation reactions and certain biological reactions. Generally, physical isotopic fractionation arises due to the rapid movement of the lighter isotope compared with that of the heavier isotope. For example, using Graham's law of diffusion, it is possible to calculate the extent of gaseous isotopic fractionation since it is inversely proportional to the square root of the masses of the isotopes. However, calculations such as these are often restricted for use with ideal gases, since they assume that collisions between molecules rarely occur and that intermolecular forces are insignificant. Consequently, isotopic fractionations in the geosphere are often found to

be notably smaller than theory would predict. Nevertheless, a sound knowledge of physical isotope effects plays a crucial role in helping to explain reaction pathways in detail (see Owens, 1987 and references therein for a more in-depth discussion about the theory of physical isotope fractionation).

Chemical Isotope Effects

Essentially, chemical isotope effects comprise equilibrium and irreversible chemical reactions. Isotopic fractionation arises during a chemical reaction because it is more likely that a bond containing ^{14}N will break, than an equivalent bond containing ^{15}N. This is simply because a bond involving a heavy isotope has a lower vibrational frequency than a bond involving a lighter isotope. In other words, bonds containing ^{15}N are stronger than equivalent bonds containing ^{14}N. For example, irreversible chemical reactions usually involve the conversion of a substrate to a product. At the start of the chemical reaction (*e.g.* a Rayleigh distillation), the $\delta^{15}N$ value of the substrate gradually increases (*i.e.* becomes enriched) relative to the newly formed product, since the lighter isotope is reacting at a faster rate. Consequently, as the reaction proceeds, the ^{15}N content of the product slowly increases. If the reaction is allowed to go to completion in a closed system, then the product will have the same $\delta^{15}N$ value as the initial substrate. Thus, even though there is no observed overall ^{15}N enrichment or depletion, it is important to note that isotopic fractionation still occurred during the reaction (Owens, 1987 and references therein).

$\delta^{15}N$ – Applications

Generally, the stable isotopes of nitrogen have been used to a much lesser extent than those of carbon. This can be mainly attributed to analytical problems associated with the lower fractional abundance of ^{15}N than ^{13}C in the biosphere, the low ratio of nitrogen to carbon atoms in most organic molecules and the greater complexity of the nitrogen cycle compared to that of carbon. Furthermore, the study of carbon isotopes largely derives from that of carbonates and crucially the equivalent nitrogen analogue is not readily preserved. Despite these problems, advances in the design of IRMS systems now allow precise analysis of stable isotopes. In recent years, there has been a

substantial increase in the use of such instruments to trace biological, chemical and physical processes in a variety of scientific disciplines.

Biochemistry

GC-C-IRMS is becoming increasingly important in metabolic and nutritional research especially in paediatrics, since stable isotope labelled tracers are now recognised as feasible alternatives to radioactive tracers (Meier-Augenstein, 1999; Koletzko *et al.*, 1998). Heavy stable isotopes such as ^{15}N do not induce adverse effects and are safe even at high enrichments (Koletzko *et al.*, 1998). Thus, it is hoped that compound-specific isotope analysis of nitrogenous compounds such as amino acids can greatly enhance our understanding of the metabolism of organic nitrogen. For example, a study of plasma albumin synthesis using L-[^{13}C-1, ^{15}N] alanine and L-[^{13}C-1, ^{15}N] leucine showed that both amino acids underwent transamination and re-amination with nitrogen from the body's nitrogen pool, before being incorporated into plasma protein (Rennie *et al.*, 1996). More recently, Metges and Petzke (1997) have described a high-precision methodology for the "on-line" determination for the natural abundance of $^{15}N/^{14}N$ isotopic composition of amino acids in human adults and claim that their method offers new possibilities for the investigation of amino acid metabolism *in vivo*.

Trophic Studies

Animal physiologists and ecologists are only just starting to realise and utilise the full potential of stable isotope measurements in their fields (Gannes *et al.*, 1997 and 1998). The importance of such work can be shown in an earlier study by Ambrose *et al.* (1986), who used a combination of $\delta^{13}C$ and $\delta^{15}N$ values from bone collagen to characterise the distinctive feeding strategies of forty-three species of African mammals. The carbon isotopes allowed differentiation between grazers and browsers, and between savanna grassland and forest-floor grazers, whilst the nitrogen isotopes allowed discrimination between carnivores and herbivores.

Interestingly, stable nitrogen isotopes have since been used in many other food web studies. For example, Fantle *et al.* (1999) have recently attempted to determine the dietary habits of commercially important juvenile Atlantic blue crabs in two locations:

Delaware Bay and Delaware Estuary. Nitrogen isotopes used in conjunction with carbon isotopes have helped to elucidate the structure of both the Bay and marsh components of the juvenile blue crab's food web. Fantle *et al.* (1999) inferred from the bulk nitrogen isotope data that juvenile blue crabs living in the marsh habitat fed mostly on primary consumers, such as marsh periwinkles or fiddler crabs, whereas juvenile blue crabs living in the Bay fed predominantly on a plankton-based diet.

Stable nitrogen isotopes have also been employed to aid our understanding of the ecology of migratory animals (see review by Hobson, 1999 and references therein). Such studies attempt to track animal movements (*e.g.* breeding, wintering and intermediate stopover sites) over geographic regions. Again, this work relies on the fact that food web isotopic signatures are reflected in the tissues of organisms. For example, the applications of stable isotopes to trace diets and migration have recently been combined in a study of the effects of salmon spawning on freshwater ecosystems (Bilby *et al.*, 1996; Kline *et al.*, 1994). It is known that large marine carnivores have a greater enrichment of $\delta^{13}C$ and $\delta^{15}N$ because they feed at the top of rather long trophic webs (Minagawa and Wada, 1984; Peterson and Fry, 1987). On the other hand, freshwater food webs are typically shorter and so are characterised by lower carbon and nitrogen isotope values than their marine counterparts (Peterson and Fry, 1987). During the autumn, salmon spawn in the streams in western Washington, and Bilby *et al.* (1996) found that during the winter decomposing salmon carcasses present in the streams increased the $\delta^{13}C$ and $\delta^{15}N$ values by up to 4 and 3 ‰ respectively at all trophic levels. Based on this, they argued that almost one fifth of all nitrogen in riparian vegetation along the streams is in fact marine nitrogen from decomposing salmon carcasses and they attribute 10 to 40% of the carbon and nitrogen in most heterotrophs found in the streams to such marine sources. This study highlights the significance of spawning to primary and secondary production in freshwater systems.

Productivity

The fact that climate influences terrestrial life is readily apparent. At the same time, it is clear that constituents of the biosphere also affect climate. Although many details about the interdependence of climate and the biosphere remain unknown, it is certain that there are relatively fixed supplies of certain elements essential to life (*i.e.* nutrients) that circulate in the environment. These materials are transported by wind or

water and move in biogeochemical cycles (*e.g.* carbon and nitrogen cycles). Climate, through atmospheric circulation, influences life by its effect on the flow of nutrients through these cycles. Many of these materials help to determine the composition of the atmosphere, which in turn affects climate. The impact of climate at the air-ocean interface controls the salinities and temperatures of surface ocean waters. The density of seawater is determined by these parameters and, in turn, controls to which depths in the ocean the water masses flow. Photosynthesis, the fundamental basis for oceanic life, takes place just below the air-water interface, where the necessary ingredients of solar energy, carbon dioxide, and other essential nutrients (*e.g.* nitrates) are available. During periods of coastal upwelling, nutrients may be supplied to surface waters for assimilation by phytoplankton, leading to high phytoplankton productivity in the photic zone; as detritus slowly falls through the water column it is bacterially degraded causing a high demand for dissolved oxygen, which may in turn lead to the development of an OMZ at mid depths (see Chapter 4). Denitrification (*i.e.* conversion of NO_3^- to N_2 or N_2O) is the main mechanism for removal of fixed nitrogen from the biosphere (Altabet *et al.*, 1995). In the oceans, denitrification is mediated by bacteria in suboxic subsurface waters (*i.e.* strong OMZs) and generates significant ^{15}N-enrichment in subsurface nitrate (Altabet *et al.*, 1995 and references therein). In essence, these denitrifying bacteria control the supply of fixed nitrogen (*i.e.* ^{15}N-enriched NO_3^-, transported vertically from subsurface to surface waters) and isotopic fractionation occurring during partial assimilation of this nutrient by phytoplankton (Altabet *et al.*, 1995 and references therein), which is reflected in the isotopic composition of sinking particulate nitrogen (Schafer and Ittekkot, 1993). Hence, it is thought that global climate may be influenced by marine primary production, which in many oceanic systems is restricted by the amount of available nitrogen (Altabet *et al.*, 1995 and references therein). Reconstructions of nitrogen availability in past oceanic environments may allow a link to be established between climate change and productivity. Stable isotopes can be used to study past productivity changes. Indeed, stable nitrogen isotope measurements have already been used to elucidate changes in productivity and nitrogen cycling (Francois and Altabet, 1992; Calvert *et al.*, 1992; Altabet *et al.*, 1995). For example, Altabet *et al.* (1995) examined sediment cores from three sites in the Arabian Sea. At all three sites they found large, near-synchronous downcore variations in $^{15}N/^{14}N$. They attributed these variations to regional changes in the isotopic composition of subsurface nitrate, and

hence denitrification (*i.e.* ^{15}N-enriched sediment indicates intense periods of denitrification, which in turn, is associated with high levels of productivity). Furthermore, the variations were found to be synchronous with Milankovitch cycles, which are cycles in the Earth's orbit that influence the amount of solar radiation striking different parts of the Earth at different times of year. Hence, Altabet *et al.* (1995) were able to use bulk sediment $\delta^{15}N$ values to establish a link between climate and productivity.

However, there are limitations to using bulk sediment $\delta^{15}N$ values, since the extent of nitrogen isotopic fractionation during diagenesis is still unclear. It is thought that the isotopic signature of sedimentary nitrogen is partly controlled by kinetic isotope effects associated with nitrate assimilation and denitrification, in addition to processes linked to bacterial degradation. Evidence to support the isotopic alteration of nitrogen during diagenesis was provided by Altabet *et al.* (1991) who showed that the $\delta^{15}N$ values of suspended and sinking particles changed with water depth. Furthermore, Schafer and Ittekkot (1993) discovered that the $\delta^{15}N$ values of particles caught in near-bottom sediment traps were 2-7 ‰ depleted in ^{15}N compared with those found in surficial sediments.

Of course, whole sediment nitrogen isotopic measurements would be the easiest way of reconstructing the amount of available nitrogen in the past, but first it must be shown that the diagenetic effect on $\delta^{15}N$ is constant in space and time (Sachs *et al.*, 1995). To overcome this problem, Sachs *et al.* (1995) decided to determine the effect of diagenesis on the $\delta^{15}N$ values of marine OM by isolating a nitrogen-containing biomarker with a known source for isotopic analysis. They chose Chl, since its macrocycle is relatively resistant to both biological and chemical attack, and it can also be recovered from marine particles and sediments (Louda and Baker, 1986). What is more, as an algal proxy, its $\delta^{15}N$ values might reveal valuable information regarding the assimilation of inorganic nitrogen and moreover, such values could be used as a baseline against which whole-sediment isotopic values could be compared. To achieve these objectives, Sachs *et al.* (1995) successfully employed a four-step transformation to enhance the volatility of the phorbin (Chl degradation products) components for $\delta^{15}N$ and $\delta^{13}C$ analysis by GC-C-IRMS. Crucially, "on-line" $\delta^{15}N$ measurements for the Chl derivatives were found to match the "off-line" values to within the precision of the method (1SD = 0.3 ‰), and a further advantage of the "on-

line" method was that it reduced sample size requirements by two orders of magnitude compared with "off-line" analyses. Sachs *et al.* (1995) claimed that this work would allow them to study the diagenetic effect on isotopic ratios and also assess whether or not whole-sediment $\delta^{15}N$ values could be used to accurately reconstruct past palaeoenvironmental conditions. Such work had already proved useful; for example, a historical record of sedimentary $\delta^{15}N$ values in the Eastern Mediterranean Sea was originally thought to be evidence for increased nutrient availability during recurring deposition of Late Pleistocene sapropels (Calvert *et al.*, 1992). Yet, later analyses of algal Chl $\delta^{15}N$ proved that the bulk sediment isotopic signal was in fact a result of diagenesis (Sachs, 1999b).

More recently, Sachs *et al.* (1999a) attempted (off-line) to ascertain the relationship between the nitrogen and carbon isotopic ratios of Chl *a* (**1**) and total biomass in cultured marine phytoplankton to assess whether or not Chl could be used as an isotopic proxy for photoautotrophs. Their findings suggest that it can, since they observed a relatively constant nitrogen isotopic depletion of 5.06 ± 1.13 ‰ in Chl *a* (**1**) relative to total nitrogen for eight species of marine phytoplankton. To further substantiate this evidence, similar values were also determined for isotopic differences between Chl *a* (**1**) and marine particles (5.27 ± 1.48 ‰ (1 σ); n = 6), and sediments (5.39 ± 0.67 ‰ (1 σ); n = 4) in a diversity of settings. Hence, they claim that marine phytoplankton $\delta^{15}N$ values can be determined from particulate and sedimentary Chl *a* (**1**) by the simple addition of 5.1 ‰. It has been proposed that this depletion factor most likely occurs during the transamination of glutamic acid (**51** GLU) in 5-aminolevulinic acid (**52** ALA) biosynthesis, which is the first committed precursor to Chl (Sachs *et al.*, 1999a; discussed in more detail below). Furthermore, both minor intraspecies and interspecies nitrogen isotopic fractionations were also observed; the former is thought to have resulted from subtle differences in growth rate, whilst the latter was attributed to small differences in the partitioning of nitrogen between protein and other nitrogenous components (Sachs *et al.*, 1999a). Kennicutt *et al.* (1992) have also observed a depletion in Chl *a* (**1**) relative to total cell nitrogen for a variety of plants. However, a very recent study by Beaumont *et al.* (2000) clearly shows enrichment in ^{15}N for Chl *a* (**1**) relative to total biomass for a cyanobacterium (*Anabaena cylindrica*). Interestingly, Sachs *et al.* (1999a) also examined a cyanobacterium (*Synechococcus* WH7803) in their study but again found the Chl *a* (**1**)

to be depleted in ^{15}N relative to total cell nitrogen. Beaumont *et al.* (2000) attribute this inconsistency to the variety of metabolic mechanisms and products found in microorganisms, which may lead to differences in metabolic flow in reaction networks and the observed wide range in $\delta^{15}N$ values for the end-products of tetrapyrrole synthesis in photosynthetic organisms; consequently, they recommend that environmentally important groups should be assessed on an individual basis. These data highlight the danger of making assumptions based on the analyses of only a few species. Nevertheless, Chl is still an ideal component for compound-specific $\delta^{15}N$ studies, since all photoautotrophs are found to contain it as a photosynthetic pigment and although the functional groups on the macrocycle may undergo various transformation reactions during cell senescence (*e.g.* Spooner *et al.*, 1994b), grazing (*e.g.* Head, 1992) and microbial activity (Sun *et al.*, 1991; Sun *et al.*, 1993) the pyrroline rings containing the nitrogen atoms are unaffected (Macko *et al.*, 1993; Sachs *et al.*, 1999a). Based on this, Sachs (1997) has suggested that Chl degradation products such as pheophytins and pheophorbides (Harris *et al.*, 1995), which are usually found in greater abundance than Chl in sediments, may be used instead of intact Chl for $\delta^{15}N$ studies.

THIS STUDY

The main aim was to develop a method for the determination of $\delta^{15}N$ values of maleimides using GC-C-IRMS in view of the fact that if the $\delta^{15}N$ values for each of the pyrroline rings of Chl *a* (**1**) could be obtained and it was found that all four have the same $\delta^{15}N$ values, then Me,Et maleimide (**36a**) could be used as a simple nitrogen isotopic proxy for photoautotrophs. In order to achieve this objective it was decided to:

(i) Use Me,H maleimide (**36b**) as a standard to develop a method for the reliable and routine determination of maleimide $\delta^{15}N$ values using GC-C-IRMS.

(ii) Attempt to measure and compare the $\delta^{15}N$ values of each of the four pyrroline rings in higher plant Chl *a* (**1**) by oxidation of pyropheophorbide

a (**53**) and determination of the $\delta^{15}N$ values of the oxidation products in order to see if these fitted with the biosynthetic prediction.

(iii) Culture three types of phototrophic organisms, which have different nitrogen sources (an alga, a cyanobacterium and a green sulfur bacterium). Isolate the Chl fraction and oxidise it to maleimides. Determine the $\delta^{15}N$ values of the maleimides by GC-C-IRMS to allow comparison, at the molecular level, of the ^{15}N fractionation effects between photosynthetic nitrogen and nitrogen source. Such studies are important, since there are many different enzymes and reaction networks exhibited among a variety of bacterial groups, which can produce diverse nitrogen isotopic patterns within metabolic end-products (Beaumont *et al.*, 2000). Therefore, it is necessary to accurately determine the isotopic significance of organic biomarkers (*e.g.* geoporphyrins) in both modern and ancient environments by relating environmentally-significant populations of bacteria to specific kinetic isotope effects of individual reactions and/or fractionations associated with reaction networks, in order to obtain a greater knowledge of fossil microenvironments and life on early Earth (Beaumont *et al.*, 2000).

MALEIMIDES AND CHLOROPHYLL $\delta^{15}N$

Biosynthetic Pathway

Below is a simplistic outline of the biosynthetic pathway to Chls, which may allow a greater understanding and/or appreciation for the possible $\delta^{15}N$ isotopic fractionation effects that may occur throughout the biosynthesis of Chl (see later).

Plants, algae and anaerobic bacteria use GLU (**51** Kannangara *et al.*, 1988) derived from 2-oxoglutarate (**54**) to produce ALA (**52** Fig. 5.2), in what is often referred to as the C_5 pathway (Milgrom, 1997 and references therein). It is likely that this form of ALA biosynthesis was primarily employed by organisms which did not utilise complete citric acid (Krebs) cycles in the early anaerobic atmosphere. Interestingly, chloroplasts are thought to have evolved from organisms that had the same origin as ancient anaerobic cyanobacteria. In order for them to survive in an aerobic

environment, it is thought that they formed a symbiotic relationship with aerobic organisms, and eventually became incorporated within plant cells. These reasons may help to explain why plants still use the C_5 route for the production of ALA (**52**) as opposed to the Shemin route used by animals (Milgrom, 1997).

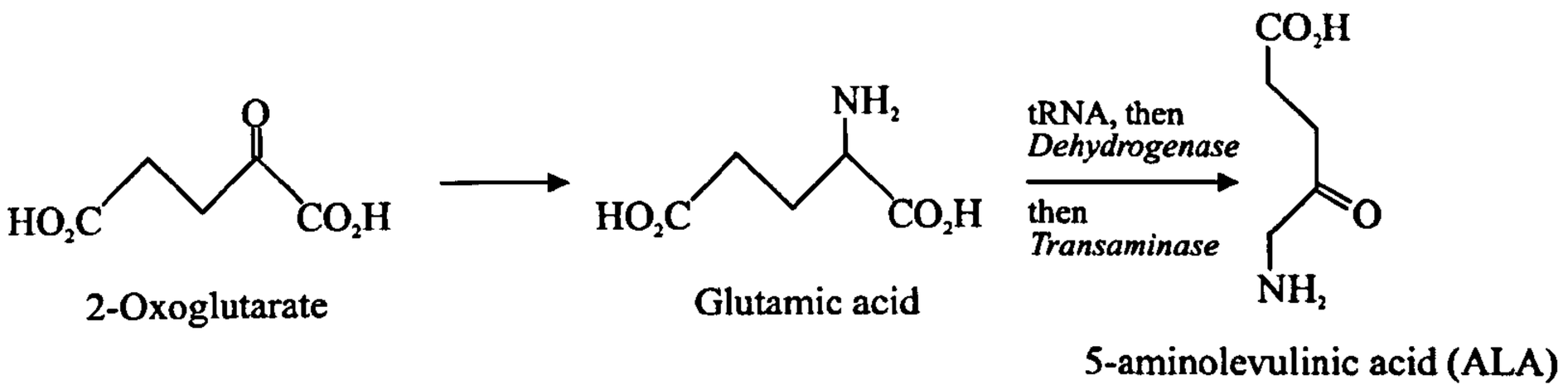

Fig. 5.2 Formation of ALA

The next stage in Chl biosynthesis is a condensation reaction involving two molecules of ALA and the enzyme *ALA dehydratase* to yield the pyrrole known as porphobilinogen (PBG; Fig. 5.3).

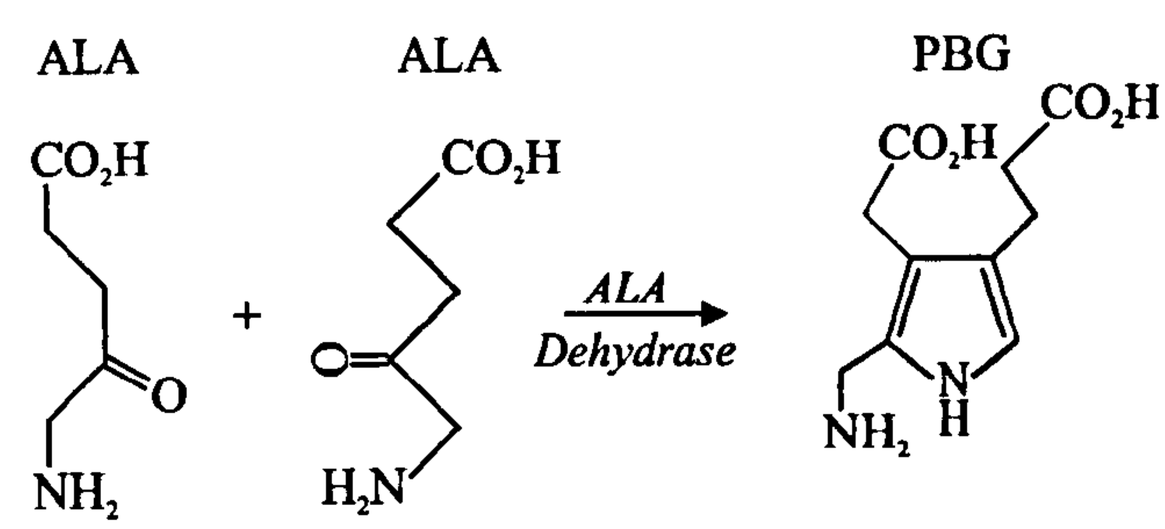

Fig. 5.3 Formation of PBG

This step is followed by the condensation of four PBG molecules to produce uroporphyrinogen III (uro'gen III; Fig. 5.4). Porphyrinogens are reduced porphyrins and this reaction involves the use of two enzymes: *PBG deaminase* and *uro'gen III cosynthetase*. Interestingly, the four identical molecules of PBG are linked in a head-to-tail manner to yield rings A to D; however, in the presence of *uro'gen III cosynthetase* it would appear that ring D flips to yield uro'gen III (Battersby *et al.*, 1980). In the presence of *PBG deaminase* alone, only the type I isomer (uro'gen I; **55**) is produced.

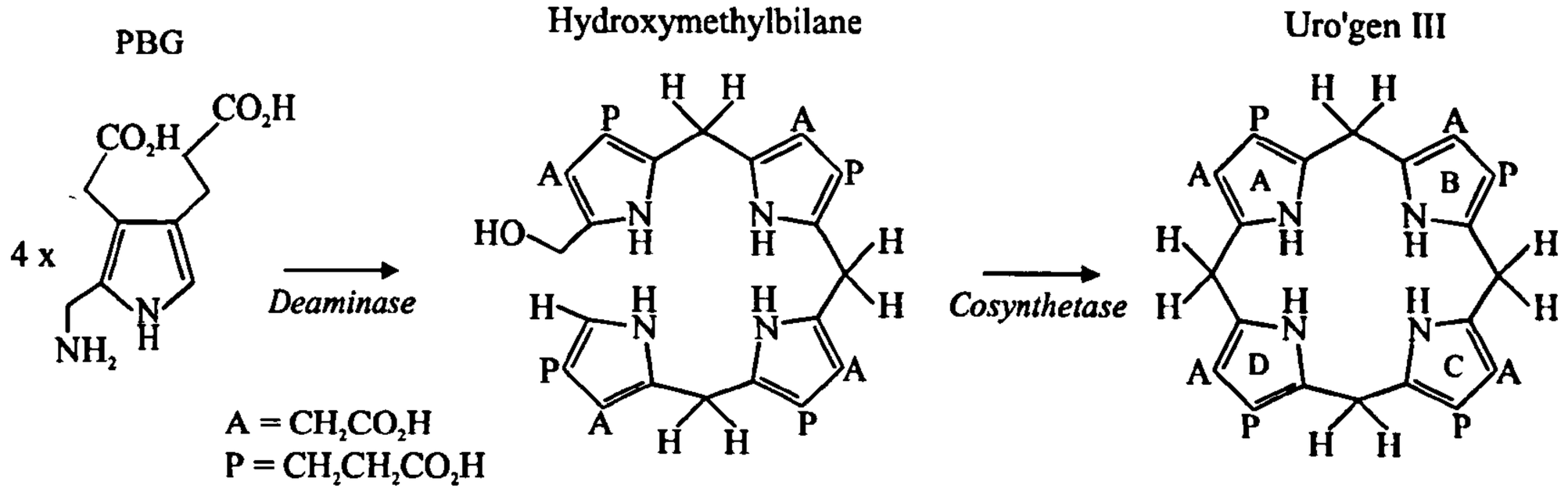

Fig. 5.4 Formation of Uro'gen III

The four acetic side chains are decarboxylated to methyl groups in the presence of *uro'gen decarboxylase* to yield copro'gen III (Fig. 5.5). This is followed by oxidative decarboxylation of the two propionic acid side chains on rings A and B to vinyl groups *via* the enzyme *copro'gen oxidase* to produce proto'gen IX, which is further oxidised by the enzyme *proto'gen oxidase* to form protoporphyrin IX.

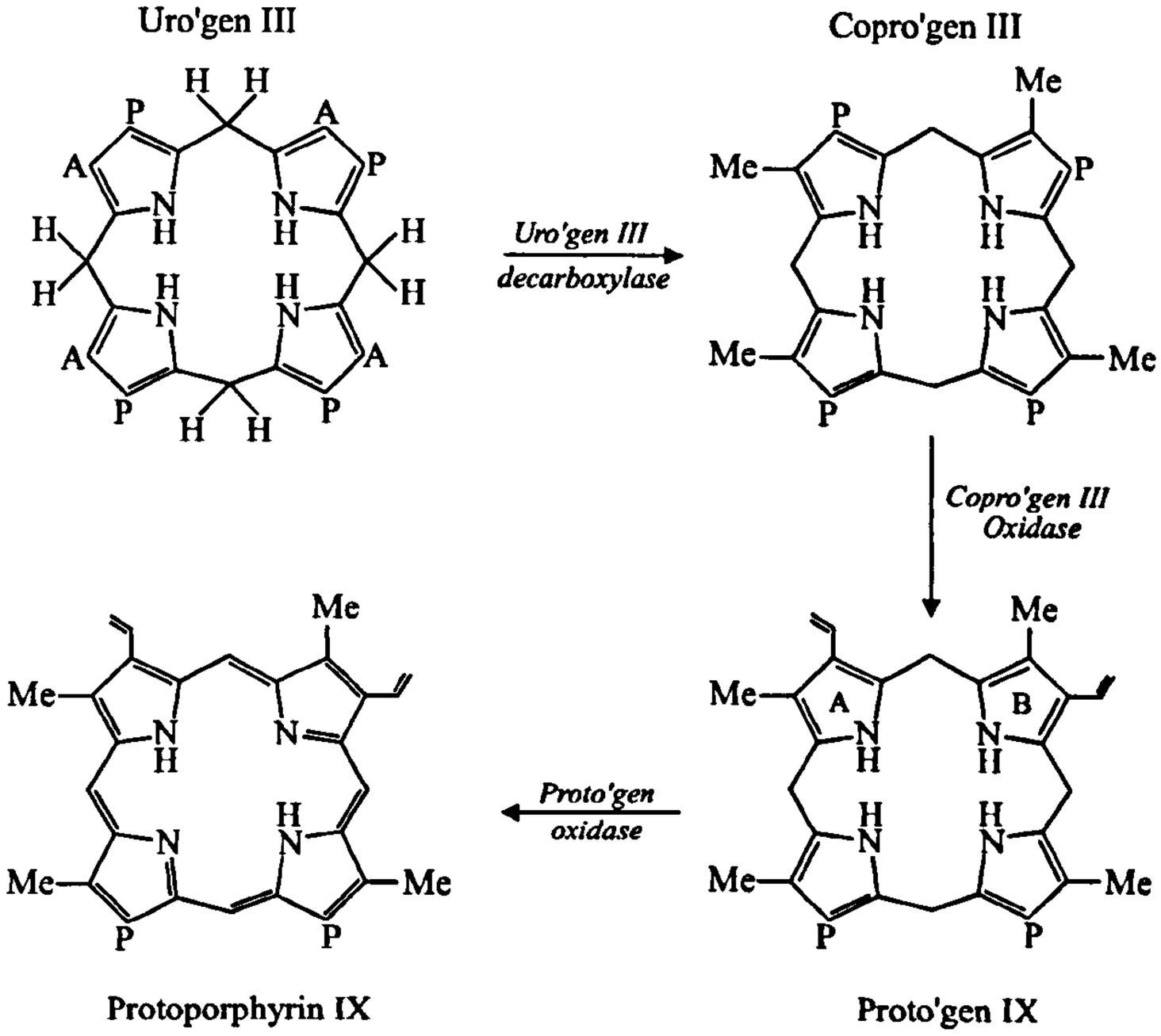

Fig. 5.5 Formation of Protoporphyrin IX

The next stage involves insertion of magnesium in the presence of an enzyme known as *magnesium chelatase* (Fig. 5.6). This step is followed by esterification of the

propionic acid side chain on C-13 by transfer of a methyl group from *S-adenosyl-methionine* (SAM). Also, at this stage the vinyl group at C-8 may be reduced to an ethyl group, but this largely depends on the species of plant.

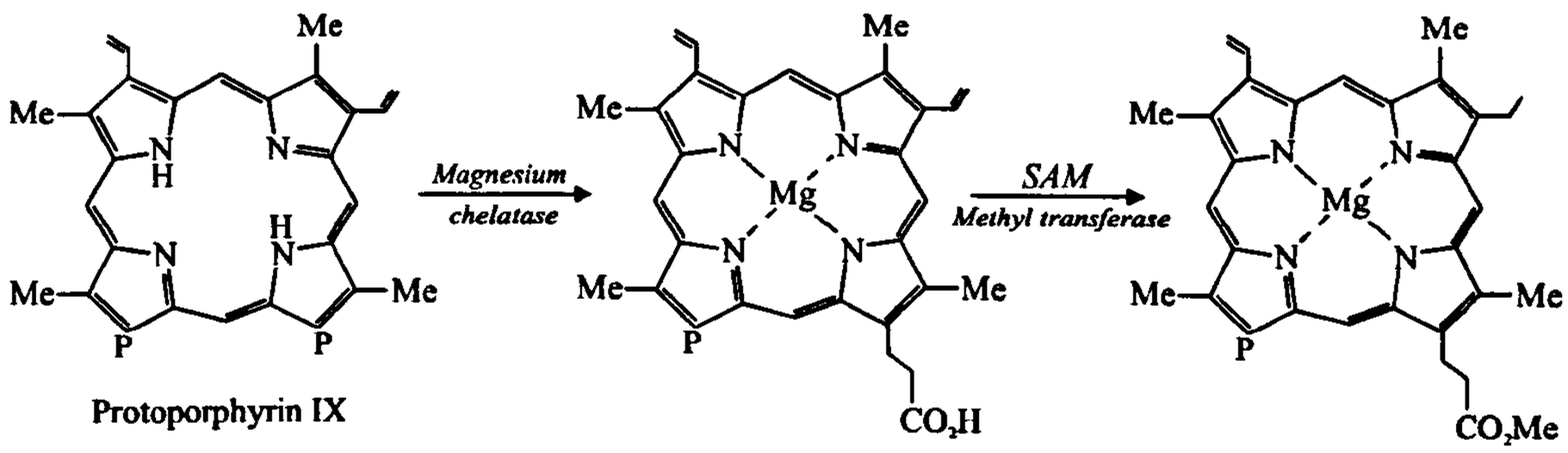

Fig. 5.6 Magnesium Insertion and Methylation

The next step is the conversion of the C-13 propionic acid side chain into a β-keto ester and its subsequent cyclisation to form the exocyclic ring often referred to as ring E (Fig. 5.7). This intermediate is known as protochlorophyllide. The enzyme employed for the cyclisation is an *oxidative cyclase* and requires both oxygen and the reduced form of nicotinamide adenine dinucleotide phosphate (NADPH). The protochlorophyllide is photochemically reduced (ring D) to yield chlorophyllide. *Protochlorophyllide reductase* is required for this reaction, in addition to NADPH.

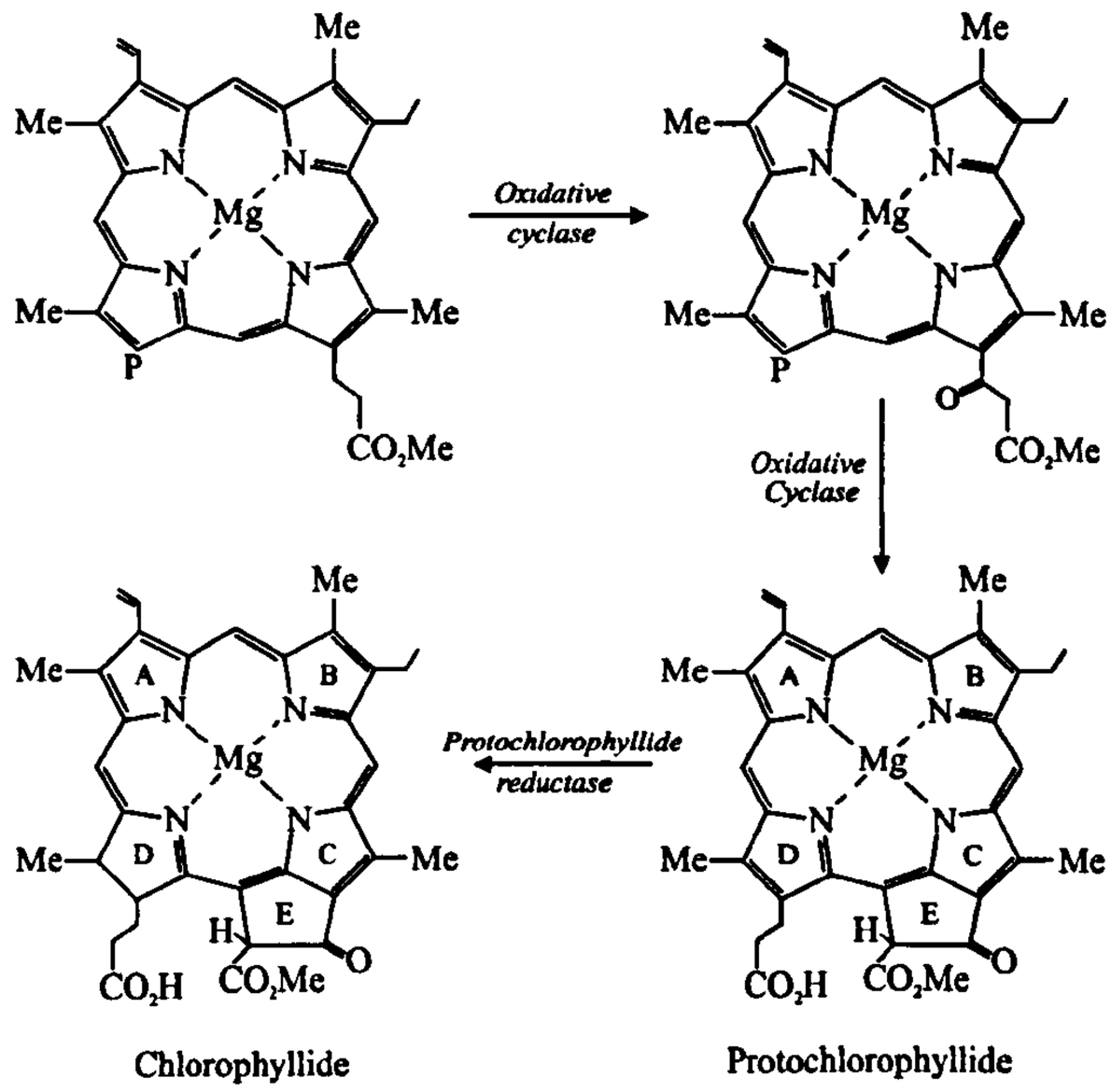

Fig. 5.7 Formation of Chlorophyllide

The final step for the biosynthetic production of Chls is esterification with phytyl diphosphate or geranylgeranyl diphosphate *via* the enzyme *Chl synthetase* (Fig. 5.8).

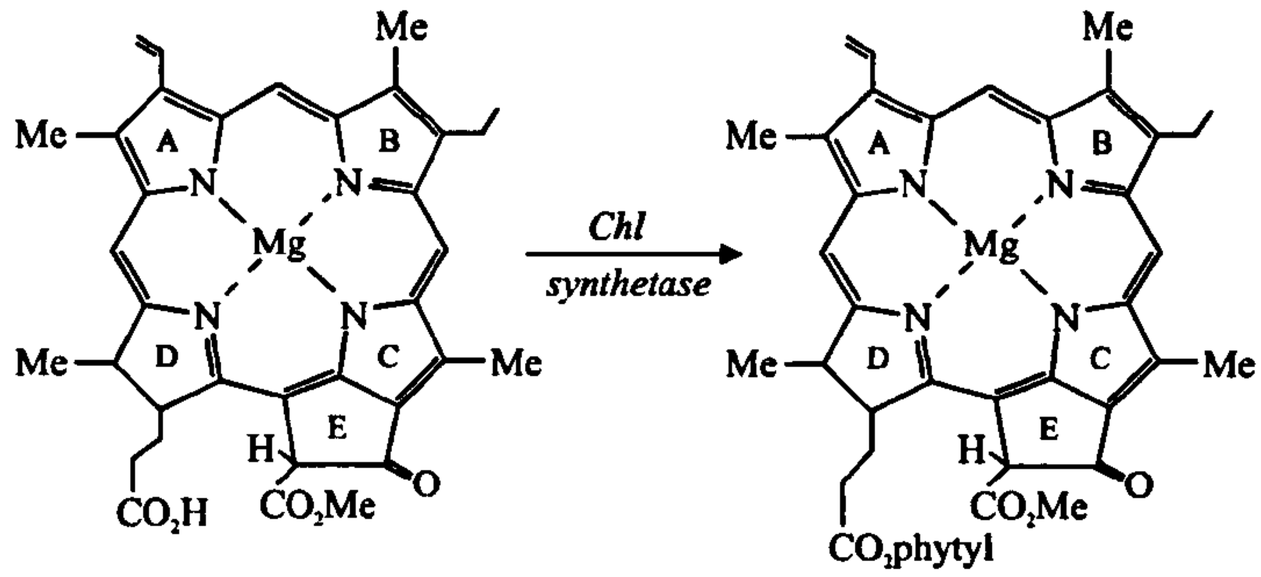

Chlorophyllide Chl *a*

Fig. 5.8 Formation of Chl *a*

Nitrogen Isotopic Fractionation During Chlorophyll Biosynthesis

There are five occasions in the biosynthesis of Chl where bonds to nitrogen are formed or broken and consequently where nitrogen isotopic fractionation may occur (Sachs *et al.*, 1999a). The first two are thought to occur during the transamination of 2-oxoglutarate (**54**) and glutamic acid-1-semialdehyde (**56**) in the formation of GLU (**51**) and ALA (**52**; Fig 5.2; Beale and Weinstein, 1991). Furthermore, Macko *et al.* (1986) have already provided evidence indicating that such isotope effects do indeed occur in their study of the kinetic fractionation of stable nitrogen isotopes during amino acid transamination. They found that significant isotope effects were associated with the reaction of GLU (**51**) and oxaloacetic acid (**57**) to form 2-oxoglutarate (**54**) and aspartic acid (ASP **58**) *via* the enzyme *porcine-heart glutamic oxaloacetic transaminase*. They discovered that the ASP (**58**) produced was depleted in ^{15}N by 8.3 ‰, relative to the GLU (**51**) from which it was synthesised. Thus, the transamination of GLU (**51**) to yield ALA (**52**), which is the first committed precursor in Chl biosynthesis (Beale and Weinstein, 1991), is probably a factor in the nitrogen isotopic depletion of Chl.

The third instance is the formation of PBG from the condensation of two ALAs *via* the enzyme *ALA dehydrase* (Fig. 5.3). Isotope fractionation may occur during this process even if 100% of ALA is converted to PBG because there are two identical amino groups available for reaction (Sachs *et al.*, 1999a). If the enzyme *ALA*

dehydrase favours ^{14}N, then the pyrrole produced should be depleted in ^{15}N and the ^{15}N-enriched terminal amino group would be removed in the next reaction (Sachs *et al.*, 1999a). Evidence to support this stems from an earlier study of a similar reaction by Schimerlik *et al.* (1975) who have shown that *GLU dehydrogenase* exerts a significant nitrogen isotope effect on the dehydration of GLU. The fourth occasion is the deamination of 4 PBGs to yield hydroxymethylbilane. However, this process is not thought to result in isotopic fractionation because bonds are neither formed nor broken to pyrrolic nitrogen (Sachs *et al.*, 1999a). The fifth and final possible source of nitrogen isotopic fractionation is the insertion of magnesium *via* the enzyme *magnesium chelatase* (Fig. 5.6; Sachs *et al.*, 1999a). Protoporphyrin IX may undergo metal insertion reactions with magnesium or iron in the formation of Chls or haemes respectively. Hence, it is conceivable that partial metallation of protoporphyrin IX with magnesium during Chl biosynthesis, followed by a sudden change to haeme production could result in ^{15}N depletion to Chl if the *magnesium chelatase* enzyme exerted an isotope effect. It is not known whether it does or not, but Macko (1981) has demonstrated that equilibrium metal exchange reactions between magnesium-meso-tetraphenylporphin and its demetallated form show an isotopic depletion of 2.2 ‰ for the metallated component.

The five possible incidents of nitrogen isotopic fractionation during the biosynthesis of Chl have now been highlighted and these can explain the observed depletion in ^{15}N Chl relative to total biomass (Sachs *et al.* 1999a). Furthermore, it is important to realise that the $\delta^{15}N$ values of the four pyrrolic nitrogen atoms in the Chl macrocycle should be the same, since four identical PBG units are used to form hydroxymethylbilane (Fig. 5.4). Thus, if the predicted biosynthetic pathway is correct, then sedimentary maleimides, especially the dominant Me,Et **(36a)** component, could be used as a simple nitrogen isotopic proxy for photoautotrophs.

Maleimides as a Proxy for Chlorophyll $\delta^{15}N$ Values

As mentioned earlier, Sachs *et al.* (1995) decided to use $\delta^{15}N$ values of Chl or its degradation products (phorbins) as a baseline against which whole-sediment isotopic values could be compared. They claimed that these measurements would allow them to quantify the effect of diagenesis on nitrogen isotopic ratios. The initial approach used by Sachs *et al.* (1995) involved a four-step transformation to enhance the

volatility of the phorbin components for $\delta^{15}N$ and $\delta^{13}C$ analysis by GC-C-IRMS. They claim that this technique reduced sample size requirements (by *ca.* two orders of magnitude) compared with the conventional "off-line" analysis and also offered enhanced resolution over their previously employed HPLC purification method. However, the four-step transformation to enhance the phorbin volatility is probably both time-consuming and difficult. This may explain why the method was later abandoned in favour of HPLC purification of Chl or its degradation products and conventional "off-line" $\delta^{15}N$ analysis (Sachs *et al.*, 1999a; Sachs *et al.*, 2000). More recently, Sachs *et al.* (1999a) appear to have established a robust relationship between Chl *a* (**1**) and total algal nitrogen. Therefore, they claim that Chl can be used as a nitrogen isotopic surrogate for photoautotrophs. They have shown that two pheophytin (**59**) samples can be prepared in tandem for $\delta^{15}N$ analysis within 8h. However, the purification procedure for this process is both time-consuming and laborious. For example, after a series of solvent-extractions to remove impurities such as carotenoids, the resulting Chl fraction was demetallated to form pheophytin (**59**), which was subsequently purified by reversed (C_{18}) and normal (SiO_2) phase HPLC. However, when using a chromatographic technique such as HPLC, it is essential to ensure that the entire chlorin peak is collected to prevent isotopic alteration of the sample, which may arise from across-peak isotopic variations (Bidigare *et al.*, 1991; Sachs *et al.*, 1999a). Unfortunately, such vigorous purification of the samples was deemed to be necessary, since the $\delta^{15}N$ values were obtained "off-line" and the presence of impurities from other nitrogen-containing compounds could alter the $\delta^{15}N$ signal.

On the other hand, the preparation of maleimide samples for $\delta^{15}N$ analysis is comparatively easy. For example, after the harvesting of an appropriate photosynthetic culture (*e.g.* phytoplanktonic or bacterial), the Chl and/or chlorins may be solvent-extracted from the filters upon which they were collected. The Chl/chlorin fraction may then be chemically oxidised (CrO_3 for *ca.* 15 min) and the resulting maleimides extracted and purified using TLC (*ca.* 1h). Once purified the maleimides are ready for GC-C-IRMS analysis. However, there is a distinct disadvantage in that the oxidation reaction gives rise to very low yields (see later) of maleimides; the most abundant product formed during the reaction is Me,Et maleimide (**36a** see later). A further advantage for the dominant Me,Et maleimide (**36a**), is that it may be solvent-extracted

in its "free" form from oceanic sediment cores and its $\delta^{15}N$ values used to assess the degree of nitrogen availability in past oceanic environments, which may eventually allow a link to be established between climate change and productivity. This of course is assuming that maleimides once formed are stable and that diagenesis will have no effect upon the $\delta^{15}N$ values. Furthermore, it is relatively easy to isolate and purify Me,Et maleimide (**36a**), especially when compared with the method developed for Chl degradation products proposed by Sachs *et al.* (2000). However, before Me,Et maleimide (**36a**) can be used in such studies, it is essential to prove that each of the four pyrrolic nitrogen atoms of the Chl macrocycle has the same $\delta^{15}N$ values as the biosynthetic pathway predicts.

RESULTS AND DISCUSSION

OXIDATION

A large Chl sample, obtained from the British Chlorophyll Co. Ltd., was analysed by HPLC-MS and found to consist mostly of impure pyropheophytin *a* (**60**). A suitable aliquot was hydrolysed to obtain pyropheophorbide *a* (**53**), which was initially oxidised with chromic acid in accordance with the method (CrO_3/H_2SO_4 solution for 4h at –10°C) used by Ellsworth and Aronoff (1968). In addition, bilirubin (**47**) was oxidised using a modified method (*i.e.* CrO_3/H_2SO_4/acetone solution for 4h at –10°C; Ellsworth and Aronoff, 1968; Bonnett and McDonagh, 1969) to obtain authentic Me,vinyl maleimide (**37**) and hematinic acid (**44**; Fig. 5.9).

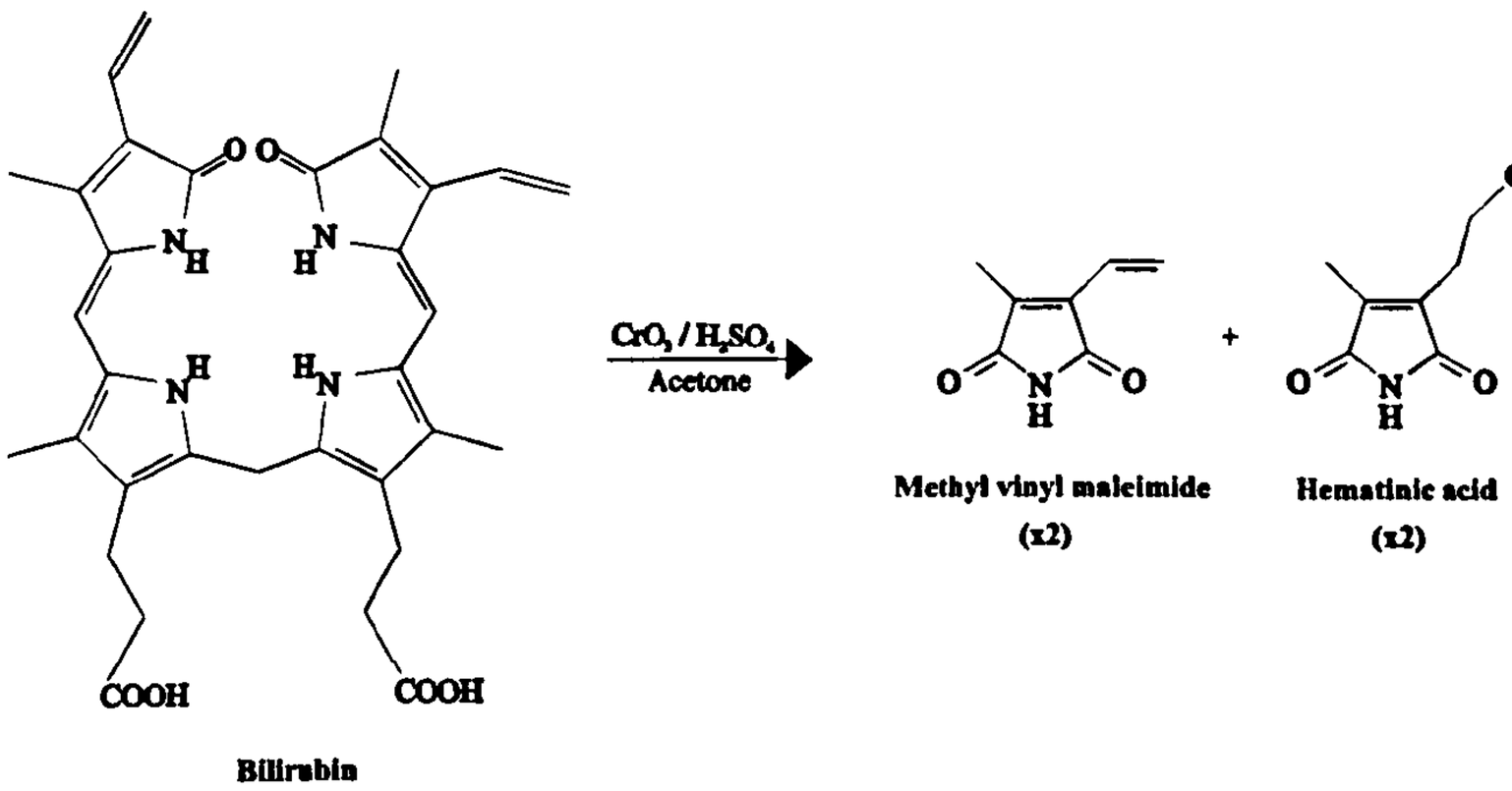

Fig. 5.9 Oxidation products of bilirubin (Bonnett and McDonagh, 1969)

These standards were used to develop suitable methodology (*e.g.* TLC, relative GC retention times and mass spectra) for the isolation, purification and identification of Me,vinyl maleimide (**37**) and hematinic acid (**46** analysed as the methyl ester) obtained in very low abundance from the oxidation of pyropheophorbide *a* (**53**). In order to improve the low yield of the oxidation products from the chlorin it was decided to dissolve the pyropheophorbide *a* (**53**) in acetone prior to oxidation, since pyropheophorbide *a* (**53**) is more soluble in acetone than in aqueous sulphuric acid. Consequently, the slightly modified oxidation (*i.e.* CrO_3/H_2SO_4/acetone solution for 4h at –10°C) of pyropheophorbide *a* (**53**) yielded three pyrrolic products: Me,Et (**36a**) and Me,vinyl (**37**) maleimides in addition to hematinic acid (**46** analysed as the methyl ester). Surprisingly, hematinic (**44**) and not dihydrohematinic (**40**) acid was obtained. It is thought that hematinic acid (**44**) is formed from the over-oxidation of dihydrohematinic acid (**40**; Ellsworth and Aronoff, 1968). However, in order to obtain $\delta^{15}N$ values for all four nitrogen atoms in the chlorin macrocycle a fourth product containing the nitrogen atom in ring C was still required. Crucially, Suzuki *et al.* (1999) had recently used a chromic acid oxidation method to obtain the maleimide derivatives of pyropheophorbide *a* (**53**) to enhance their understanding of the rapid breakdown of Chls in biological systems (Fig. 5.10).

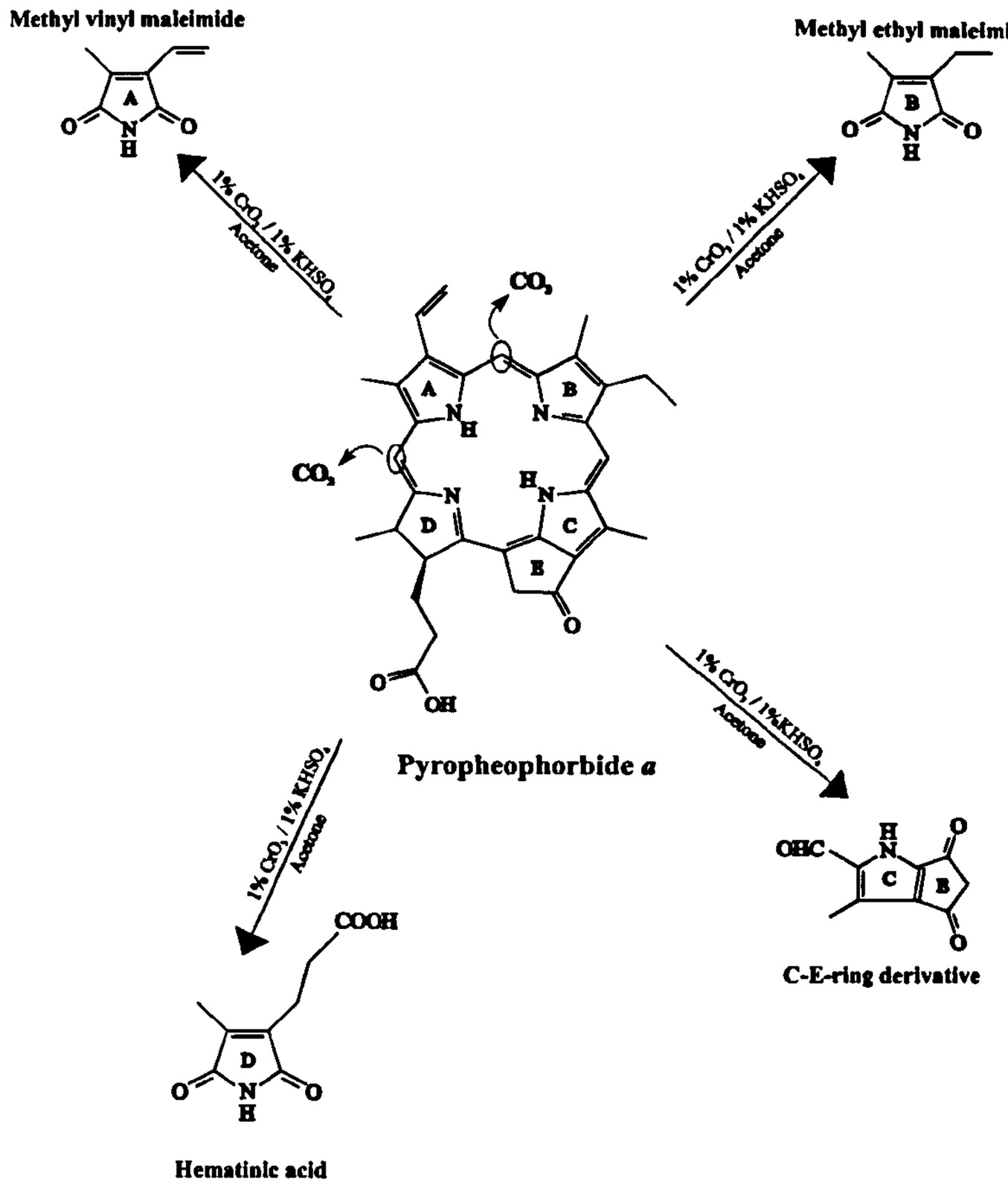

Fig. 5.10 Oxidation products of pyropheophorbide *a*
(Suzuki *et al.*, 1999 and references therein)

The method was slightly modified from that previously used by Shimomura (1980) and references therein. In addition to the products obtained before, Suzuki *et al.* (1999) claim that a C-E ring derivative (**61**) could be isolated as the fourth oxidation product (Fig. 5.10). Thus, oxidation of pyropheophorbide *a* (**53** dissolved in acetone) was carried out under the conditions that they had employed: *i.e.* pH 1.2 at 25°C with 1% (w/v) CrO_3 solution containing 1% $KHSO_4$ for 15 min. Yet again, only three products were obtained (Figs. 5.11 and 5.12): Me,Et (**36a** *ca.* 10% yield) and Me,vinyl (**37** <1% yield) maleimides in addition to hematinic acid (**46** <1% yield, analysed as the methyl ester). The C-E ring derivative (**61**) was difficult to detect, since several orange bands appeared on the TLC plate after spraying with 2,4-dinitrophenylhydrazine, which produces a colour reaction in the presence of pyrrole aldehydes. It is thought that these bands represented several degradation products of the intact C-E ring derivative (**61**). The Rf value for each major band was calculated and the oxidation of pyropheophorbide *a* (**53**) was repeated as above. Each major band

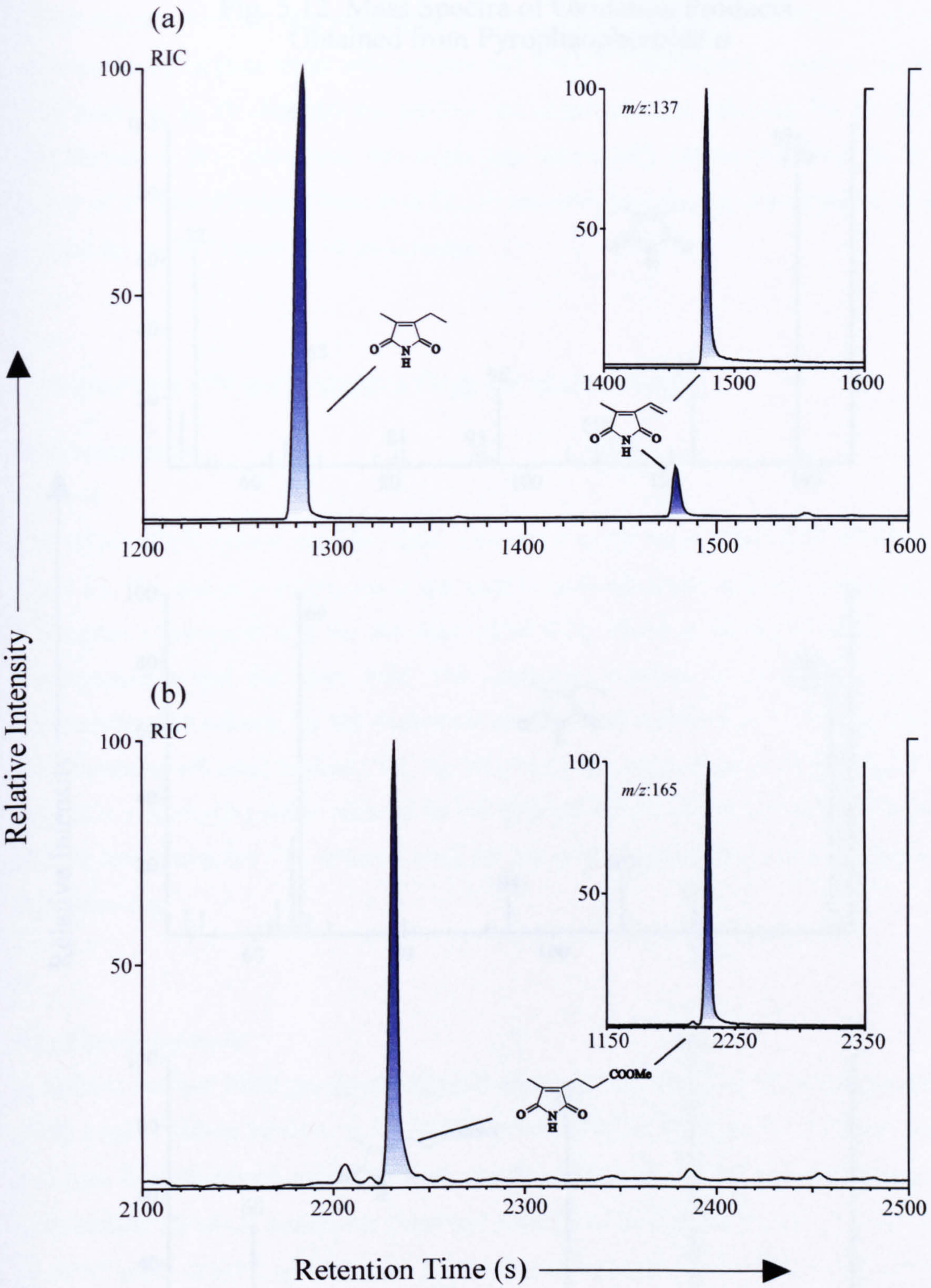

Fig. 5.11 Partial RIC and Mass Chromatograms of Oxidation Products Obtained from Pyropheophorbide *a* using CP-WAX 52 CB Stationary Phase

(a) Me,Et and Me,Vinyl Maleimide and (b) Hematinic Acid Methyl Ester

Fig. 5.12 Mass Spectra of Oxidation Products Obtained from Pyropheophorbide *a*

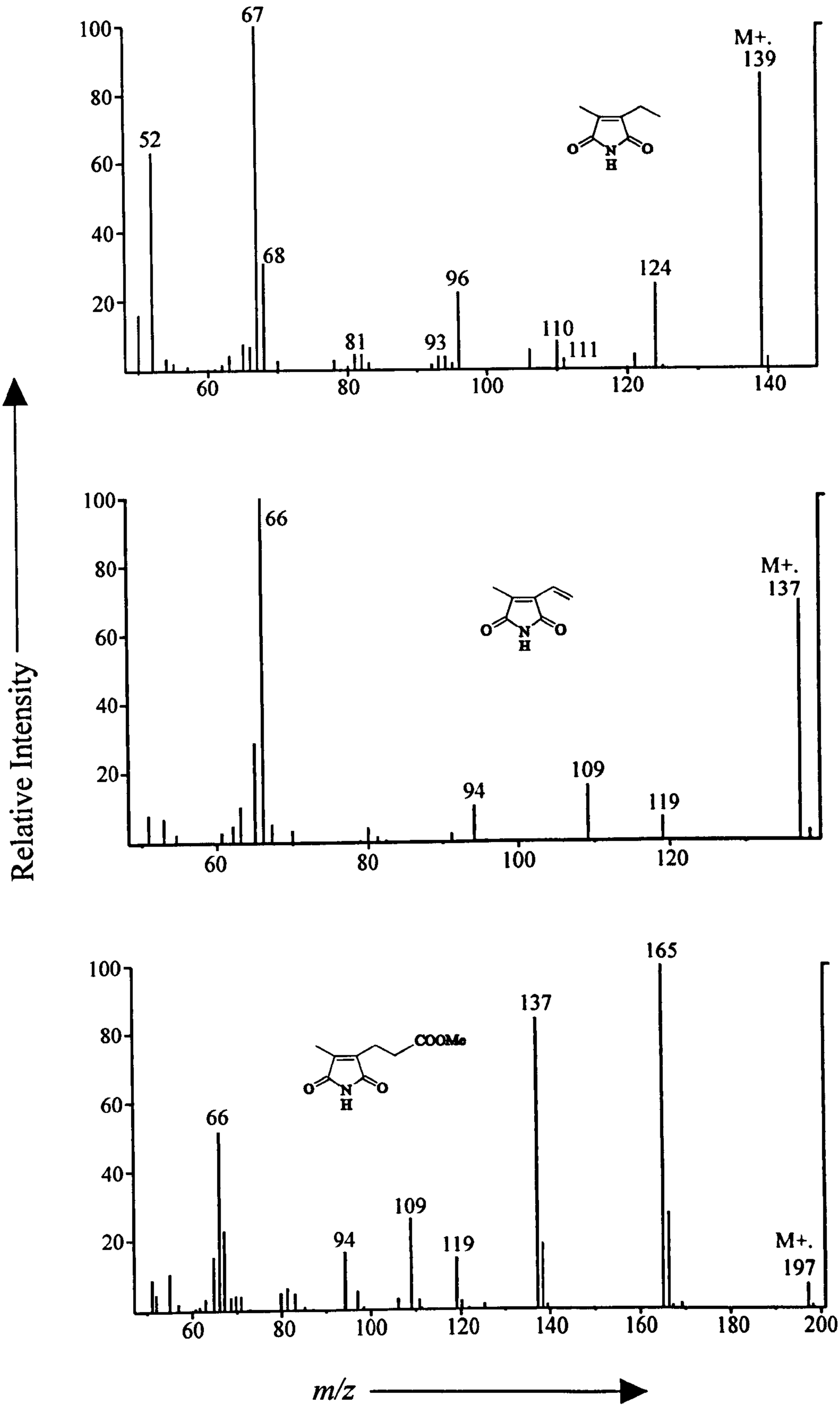

was scraped off the TLC plate using the previously determined Rf values (from the colour reaction with 2,4-dinitrophenylhydrazine) and the silica quickly filtered under vacuum through a glass sinter with acetone and MeOH. Unfortunately, analysis of the band fractions by GC-MS did not produce the expected mass spectrum for the C-E ring derivative (**61**). However, this work was temporarily discontinued due to the arrival of the new Finnigan Delta Plus XL, so attention turned to the development of a method for the $\delta^{15}N$ analysis of maleimides.

ATTEMPTED $\delta^{15}N$ DETERMINATION OF MALEIMIDES

Instrumentation

General

The GC-C-IRMS system used for these nitrogen isotopic measurements is shown in Fig. 5.13. The system is analogous to that used in carbon isotopic analyses, except that it contains a cryogenic trap for the removal of CO_2, which is situated between the water-separator and the open split. The analytical sequence is as follows: (i) a chromatographic column for the separation of individual compounds, (ii) continuous combustion of effluents to yield CO_2, N_2, NO, H_2O, (iii) conversion of NOx to N_2 in a reduction reactor, (iv) water removal as the effluent stream passes through a tubular Nafion membrane, (v) CO_2 removal with the use of a cryogenic trap, (vi) delivery to the ion source.

Gas Chromatography

A Hewlett Packard 6890 gas chromatograph was employed and samples were injected using a split/splitless injector. A ZB WAX column (Phenomenex; 60m x 0.32mm i.d. x 0.2μm film thickness) was employed and the following temperature programmes were utilised for Me,H maleimide (**36b**) and caffeine (**62**) respectively: 80°C - 100°C @ 10°C min^{-1} - 210°C @ 5°C min^{-1} (isothermal 5 min) and 150°C - 240°C @ 10°C min^{-1} (isothermal 10 min).

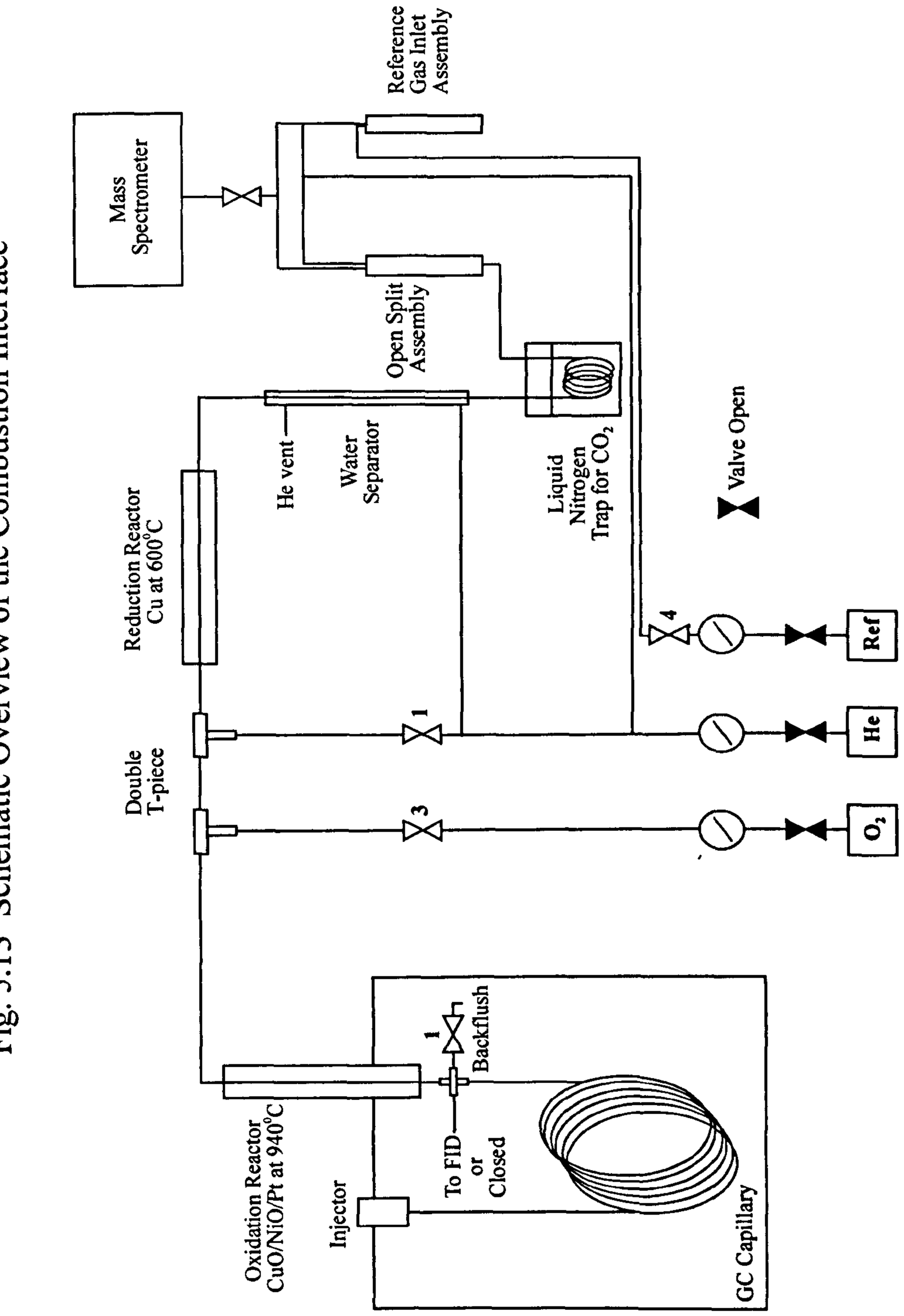

Fig. 5.13 Schematic Overview of the Combustion Interface

Oxidation Reactor

The oxidation reactor is comprised of a non-porous alumina tube (Al_2O_3, 0.5 mm i.d., 1.55 mm o.d., 320 mm length). Inserted into this tube are three twisted wires of approximately equal length (240mm), one Cu, one Ni and one Pt, the diameters of which are 0.1mm, 0.125mm and 0.1mm respectively. The reactor tube is inserted into a resistively-heated Al_2O_3 furnace (1.6 mm i.d., 260 mm length) in which the temperature is regulated to within ± 0.5°C. The usual operating temperature for the reactor is 940°C, although it may occasionally be operated at temperatures as high as 1200°C. O_2 is released by the following chemical reactions:

$$4CuO \leftrightarrows 2Cu_2O + O_2 \quad (1)$$

and

$$2NiO \leftrightarrows 2Ni + O_2 \quad (2)$$

The chemical equilibrium is temperature-dependent and at high temperatures considerably more O_2 will be released from the CuO (reaction **1**), whilst the loss of O_2 is deemed to be insignificant below temperatures of 750°C (Finnigan MAT, 1994). At high temperatures, CuO decomposes rapidly *via* reaction (**1**). In contrast, NiO is stable up to 1900°C and O_2 loss at 1100°C is thought to be minor (Finnigan MAT, 1994). Furthermore, NiO will only release O_2 during the combustion of organic compounds to form CO_2 and H_2O. Thus, it is thought that the combination of Cu/Ni in the reactor maintains a high degree of oxidation, since the O_2 loss of the CuO is compensated for by the formation of NiO. However, the hybrid reactor still requires infrequent re-oxidation (*ca.* once a week for *ca.* 5 min), since NiO only reacts on the surface and its capacity as an O_2 donor is thus limited (Finnigan MAT, 1994).

Reduction Reactor

The reactor material and furnace components are identical to those used in the oxidation reactor except for the reactor packing, which is pure Cu (three twisted Cu wires of 0.1 mm diameter). It is usually maintained at a temperature of 600°C. This reactor is responsible for the reduction of NOx to N_2 and also serves to remove surplus oxygen released from decomposing CuO in the oxidation reactor.

Water Removal

Water produced during combustion is removed from the effluent stream with the use of a Nafion membrane. The Nafion tube (Permapure; 0.6 mm i.d., 0.8 mm o.d., 20 cm length) is mounted coaxially inside a glass tube and the annular volume is continuously purged by a counter-current stream of dry He at a flow rate of 2-3 ml/min.

Removal of CO_2

CO_2 is removed from the effluent stream with the use of a liquid nitrogen trap. The fused silica capillary (0.32mm i.d.) exiting the Nafion tubing is inserted downstream from the water removal unit and upstream from the open split into a dewar containing liquid nitrogen (20-30 cm of silica capillary is immersed in liquid nitrogen). Hence, CO_2 is frozen out of the effluent stream and is prevented from entering the ion source. The significance of this for $\delta^{15}N$ analysis is discussed later.

Mass Spectrometer

Nitrogen enters the ion source *via* a capillary leak connected to the open split. The spectrometer was operated at an accelerating potential of 3 kV and ions were generated by electron ionisation (100 eV). Triple Faraday cups were used to measure ion currents for *m/z* 28, 29 and 30.

Gas Flow Modes

There are two standard modes of the flow of analyte and purge gas:

(i) straight mode

(ii) backflush mode

Straight Mode - This mode allows the analyte gas to travel through the interface to the open split, which forms the connection to the mass spectrometer. The two valves labelled "**1**" are closed (Fig. 5.13).

Backflush Mode - This mode prevents effluent from the GC entering the oxidation reactor. Since both valves labelled "**1**" are open (Fig. 5.13), the flow in the oxidation reactor is reversed. This is important since the preclusion of solvent prevents O_2 depletion occurring in the oxidation reactor. This mode is also utilised when the oxidation reactor is being re-oxidised. Hence valve "**3**" is opened (Fig. 5.13) which allows a stream of oxygen/helium to enter the oxidation reactor. During this process the helium backflush also prevents the stream of O_2 from entering the reduction reactor.

Nitrogen Isotopic Standards

Reference Standard

Atmospheric N_2 is the internationally recognised primary reference material for nitrogen and is assigned an arbitrary δ value of zero. The ^{15}N content of atmospheric N_2 has been found to be constant within the limits of current techniques (Nier, 1950; Dole *et al.*, 1954; Junk and Svec, 1958; Mariotti, 1983); thus its use as a primary reference ensures that all results obtained are comparable (Hayes, 1982).

Calculation of ^{15}N

The conventional method for calculating the natural abundance of ^{15}N is usually given by the expression:

$$\delta^{15}N\ (‰) = \frac{R\ \text{sample} - R\ \text{reference}}{R\ \text{reference}} \times 1000$$

Where R is the ratio of $^{14}N + {}^{15}N$ / $^{14}N + {}^{14}N$ which is equivalent to the *m/z* 29 and *m/z* 28 ion peak heights measured on the MS.

Working Standards

Me,H maleimide (**36b** Sigma-Aldrich) was chosen as the primary $\delta^{15}N$ standard in this study, but other standards that were chosen included phthalimide (**45**; Sigma-Aldrich), aetioporphyrin III (**17**; Porphyrin Products), octaethylporphyrin (**48**; Porphyrin Products) and caffeine (**62**). At the start of this study, the Delta Plus XL had only just been acquired, installed and calibrated and the $\delta^{15}N$ values of the chosen standards were determined "off-line". To ensure that it was functioning at optimum performance, a small quantity (*ca.* 5 – 10mg) of each compound was sent to the Institute of Terrestrial Ecology (ITE Merlewood, Cumbria) and also to Finnigan MAT (Bremen, Germany) for "off-line" $\delta^{15}N$ analysis, since a direct comparison would help to assess the degree of $\delta^{15}N$ inter-variation among the three instruments and would hopefully highlight any problems associated with the newly calibrated Delta Plus XL. The $\delta^{15}N$ measurements for the compounds from each institution are shown in Table 5.1. In addition, a caffeine (**62**) solution was obtained from Finnigan MAT and frequently used to check the accuracy of the Delta Plus XL.

Table 5.1 $\delta^{15}N$ values of standards measured "off-line" at different institutions

	ITE	**Finnigan MAT**	**University of Bristol**
$\delta^{15}N$ Standard	**Av. $\delta^{15}N$ (‰)**	**Av. $\delta^{15}N$ (‰)**	**Av. $\delta^{15}N$ (‰)**
Me,H Maleimide	-3.2 ± 0.1 (n=2)	N/A	-2.7 ± 0.4 (n=5)
Phthalimide	-0.9 ± 0.1 (n=2)	-1.6 ± 0.4 (n=2)	-1.9 ± 0.6 (n=8)
Aetioporphyrin III	0.2 ± 0.1 (n=2)	-0.1 ± 0.2 (n=2)	-0.2 ± 0.4 (n=3)
Octaethylporphyrin	-0.0 ± 0.1 (n=2)	-0.1 ± 0.3 (n=2)	-0.3 ± 0.3 (n=3)
Caffeine	N/A	-29.2 ± 0.2 (n=2)	N/A
Caffeine (on-line)	N/A	-29.9 ± 0.3 (n=3)	-30.4 ± 0.4 (n=3)

N/A – indicates that sample was not analysed

From the data above, it would appear that the three instruments are in reasonable agreement with one another especially given the difficulty with the maleimides (see below). Furthermore, suitable aliquots of aetioporphyrin III (**17**) and octaethylporphyrin (**48**) were chemically oxidised with chromic acid solution to obtain

Me,Et (**36a**) and Et,Et (**41c**) maleimides respectively as standards. Hence, this would eventually allow a check on whether or not the $\delta^{15}N$ value of the maleimide (measured "on-line") would be the same as that of the porphyrin (measured "off-line") from which it was produced.

Initial Approach

The instrument was set-up as described above and checked for leaks since even small amounts of atmospheric gas leaking into the GC-C-IRMS instrument can severely affect $\delta^{15}N$ values (since atmospheric N_2 = 0 ‰). None were found and 1 μl aliquots of the caffeine (**62**) standard were injected. The $\delta^{15}N$ values (*i.e.* –30.4 ± 0.4 ‰ where n = 3) were similar to those obtained at Finnigan MAT (Table 5.1). Thus, an appropriate solution of Me,H maleimide (**36b**) was prepared to produce comparable peak areas with those obtained for caffeine (**62**) and 1 μl aliquots were injected. However, the $\delta^{15}N$ values although consistent, were strongly enriched in ^{15}N (8.1 ± 0.1 ‰, where n = 20) compared with those obtained "off-line" (Table 5.1). Such a large discrepancy between "off-line" and "on-line" values for Me,H maleimide (**36b**) was not to be expected and the caffeine standard was injected again (-29.2 ± 0.3 ‰, where n = 3) indicating that the problem lay with the maleimides.

An inherent advantage for caffeine (**62**) with respect to $\delta^{15}N$ analysis is that each molecule contains four nitrogen atoms compared to the single pyrrolic nitrogen atom found in maleimides. Therefore, at least four mole equivalents of Me,H maleimide (**36b**) are needed to yield the same amount of N_2 as that produced from a single mole of caffeine (**62**). However, differences in the molecular content of nitrogen alone, do not explain why "off-line" and "on-line" values match for caffeine (**62**), but not for Me,H maleimide (**36b**). Most likely, caffeine (**62**) must combust more efficiently and/or yield subtly different oxidation products than does Me,H maleimide (**36b**); this may indicate a problem associated with the "on-line" oxidation or reduction process. The products of combustion for nitrogen-containing organic compounds typically include N_2, NO, CO_2, H_2O, and possibly CO. However, if NO is produced, then a suitable reduction reactor is required to reduce the NO to N_2. This was evidenced with the analysis of nitrobenzene, where N_2 ion currents were barely visible above baseline when combustion reactors were used alone, but were sufficient when a Cu reduction

reactor was used (Merritt and Hayes, 1994). The formation of other nitrogen oxides (*e.g.* NO_2), particularly in CuO reactors is thought to be highly unlikely (Hilkert, personal communication), since the only compounds reported to produce NO_2 when combusted (typically in a Pt furnace below *ca.* 1000 °C with low levels of O_2) are those with nitro groups. In any case, it is thought that NO_2 is also converted to N_2 in CuO furnaces, since it has been shown that all the nitrogen in nitropropane is converted to N_2 during GC-C-IRMS with a CuO furnace (Merritt and Hayes, 1994). There are two possibilities which may adequately account for the significant "on-line" ^{15}N-enrichment of Me,H maleimide (**36b**): the first is the possible generation of NO during combustion coupled with incomplete reduction and the other is the formation of CO due to incomplete combustion of the stable pyrrole ring. Furthermore, neither NO nor CO are effectively removed by cryogenic trapping (see Table 5.2).

Table 5.2 Melting and boiling points of possible combustion products of nitrogen-containing organic compounds (CRC Handbook of Chemistry and Physics 75th edition).

Possible Combustion Products	Melting Point (°C)	Boiling Point (°C)
N_2	- 209.9	-195.8
Nitric Oxide (NO)	-163.6	-151.8
Nitrous Oxide (N_2O)	-90.8	-88.5
Nitrogen Dioxide (NO_2)	-11.2	21.2
CO_2	-78.5	-56.6
CO	-199.0	-191.5

Removal of NO

The formation of NO in the combustion reactor is a potentially serious problem, since its incomplete reduction to N_2 may lead to isotopic fractionation. Additionally, NO will also interfere with the signal at *m/z* 30, which may lead to inaccurate calculations of the *m/z* 29 to *m/z* 28 ratio of N_2. However, it is thought that NO is only likely to be formed from compounds that contain N-O bonds to start with (Merritt and Hayes,

1994); thus, it is perhaps unlikely to be produced in this case, since neither Me,H maleimide (**36b**) nor caffeine (**62**) contain N-O bonds. Yet, it is still conceivable that the complete combustion of certain classes of nitrogen-containing organic compounds at high temperature, especially in the presence of O_2 may well lead to the formation of NO, regardless of whether they contain N-O bonds or not. Indeed, the chemistry in the combustion reactor is very complex and the possibility exists that NO may be produced during the combustion of Me,H maleimide (**36b**). Thus, there are two ways of ensuring that NO does not interfere: the first is to make certain that all NO is reduced to N_2 and the second is to try and prevent its formation in the first place.

Increased Reduction Capacity

Just how efficient are the standard Cu reduction reactors? Merritt and Hayes (1994) claim that a significant improvement in the N_2 ion current was observed after fitting a reduction reactor for the analysis of nitrobenzene, but this does not prove that all the NO was reduced to N_2. One way of improving the reducing power of the standard Cu reduction reactor is to decrease the temperature (400 °C) and replace the elemental Cu with carbonised polyacrylonitrile fibre (Timms, personal communication). Unfortunately, there is a risk of CO being generated under such conditions and a small quantity of CuO was required at the "exit" end of the reduction reactor to ensure that any CO produced was subsequently oxidised to CO_2 and thus cryogenically trapped after leaving the reactor. The experimental reduction reactor was prepared by soaking the carbonised polyacrylonitrile fibre (Courtaulds; *ca.* 0.1 mm diameter; *ca.* 10 cm length) in a saturated solution of copper formaldehyde (10-20 μl). The carbon fibre was inserted into the reactor tube and heated to 400 °C, at which point the copper formaldehyde dissociated to form elemental Cu on the surface of the carbon fibre. Finally a small amount of CuO (*ca.* 0.1mm diameter; *ca.* 5cm) was added to the "exit" end of the reactor. The reactor was maintained at a temperature of 400°C for several hours before a series of injections of Me,H maleimide (**36b**) were made. The results are displayed in Table 5.3.

Table 5.3 Effect of reduction reactor modifications on $\delta^{15}N$ values of Me,H maleimide

	Replicate $\delta^{15}N$ (‰) Analyses										Av.
Modification	**1**	**2**	**3**	**4**	**5**	**6**	**7**	**8**	**9**	**10**	**$\delta^{15}N$ (‰)**
Cu + C	8.5	10.2	11.1	7.5	7.1	8.3	10.5	6.6	6.7	7.0	8.4 ± 1.7
Cu + C + CuO	7.0	8.6	7.7	7.6	6.5	7.1	7.0	6.8	6.4	-	7.2 ± 0.7

These results suggest that the reduction of NO may not be the main or only reason for the observed "on-line" ^{15}N-enrichment of Me,H maleimide (**36b**). Even though the values are slightly less positive (*ca.* 1 ‰) for the Cu + C + CuO reactor, they are still similar to those obtained using the standard Cu reduction reactor at 600°C (8.1 ± 0.1 ‰, where n = 20). Furthermore, the results show that the carbon fibre in the reduction reactor does not generate significant amounts of CO since, although the results obtained using the Cu + C reduction reactor are slightly erratic, they are still similar to the results attained for both the Cu + C + CuO (Table 5.3) and standard Cu reduction reactors (*i.e.* 8.1 ± 0.1 ‰, where n = 20). However, there is a possibility that CO_2 is generated from the carbon fibre, either from a surplus of oxygen released from decomposing CuO in the oxidation reactor, or during the reduction of NO. However, the formation of CO_2 is not a cause for concern as it is later removed in the cryogenic trap. Finally, three repeat injections of the caffeine (**62**) standard were made to study the effect of the modifications upon the $\delta^{15}N$ values (see Table 5.4).

Table 5.4 Effect of reduction reactor modifications on $\delta^{15}N$ values of caffeine

	Replicate $\delta^{15}N$ (‰) Analyses			Av.
Modification	**1**	**2**	**3**	**$\delta^{15}N$ (‰)**
Cu + C	-32.5	-30.2	-31.3	-31.3 ± 1.2
Cu + C + CuO	-30.5	-30.2	-30.3	-30.3 ± 0.2

Interestingly, the results again show a greater variance for the Cu + C modification, whilst the $\delta^{15}N$ values obtained using the Cu + C + CuO are in agreement with those attained using the standard Cu reduction reactor at 600 °C.

Nickel Oxide Combustion Reactor

Merritt and Hayes (1994) claim that a NiO reactor if used at 1100°C and without the addition of gas-phase O_2 has several advantages over a CuO reactor: (i) greater capacity for the oxidation of organic material, (ii) greater retention of oxidising power during successive analyses, (iii) can be used at temperatures exceeding 1100°C continuously without losing oxidation capacity, (iv) the almost-zero bleed of O_2 from the NiO can extend the life of the Cu reduction unit. Based on these claims, it was thought that a NiO/Pt combustion reactor (operated at 1100 °C) would be less likely to produce NO than the hybrid reactor (CuO/NiO/Pt), since NiO does not release O_2 as readily as does CuO. Furthermore, it was hoped that the NiO/Pt oxidation reactor would thermally "crack" the molecules of Me,H maleimide **(36b)** rather than combust them. The results are shown in Table 5.5.

Table 5.5 Effect of NiO/Pt combustion reactor and modified reduction reactor on $\delta^{15}N$ values of Me,H maleimide

	Replicate $\delta^{15}N$ (‰) Analyses										Av.
Modification	**1**	**2**	**3**	**4**	**5**	**6**	**7**	**8**	**9**	**10**	**$\delta^{15}N$ (‰)**
Standard Cu	16.1	15.0	13.9	14.2	12.5	15.3	14.9	13.4	13.2	13.9	14.2 ± 1.1
Cu + C + CuO	8.8	7.5	6.8	7.7	9.1	8.1	9.0	8.8	7.1	9.6	8.3 ± 0.9

The combination of the NiO/Pt combustion reactor and the standard Cu reduction reactor yielded very positive $\delta^{15}N$ values. In contrast, the NiO/Pt reactor used in conjunction with the modified reduction reactor (*i.e.* Cu + C + CuO) gave almost identical $\delta^{15}N$ values to those obtained previously for the CuO/NiO/Pt combustion reactor (*i.e. ca.* 8 ‰). Such a discrepancy (*ca.* 6 ‰) suggested that the low levels of O_2 in the NiO/Pt oxidation reactor were in this case, actually inhibiting the combustion of Me,H maleimide **(36b)**. Consequently, the incomplete combustion of organic compounds may yield CO, which has the potential to severely interfere with the *m/z* 29 to *m/z* 28 ratio of N_2 (see later). Furthermore, it was thought that the CuO at the end of the modified reduction reactor may have been responsible for the oxidiation of the excess CO produced in the NiO/Pt combustion reactor to CO_2, thus lowering the $\delta^{15}N$ values from 14.2 ‰ to 8.3 ‰. Finally, three repeat injections of the caffeine

(62) standard were made to study the effect of the NiO/Pt combustion reactor upon the $\delta^{15}N$ value (Table 5.6).

Table 5.6 Effect of NiO/Pt combustion reactor and Modified reduction reactor on $\delta^{15}N$ values of caffeine

Modification	Replicate $\delta^{15}N$ (‰) Analyses 1	2	3	Av. $\delta^{15}N$ (‰)
Standard Cu	-30.3	-30.2	-30.5	-30.3 ± 0.2
Cu + C + CuO	-29.5	-29.4	-29.7	-29.5 ± 0.2

These results show that the $\delta^{15}N$ values of caffeine **(62)** remain unaffected by the above modifications, since the values are in agreement with those obtained under standard conditions (Table 5.1).

Overall, the results (Tables 5.3 and 5.5) suggest that NO is probably not formed during combustion (as predicted by Merritt and Hayes, 1994), since neither the modified reduction reactor nor the NiO/Pt combustion reactor yielded $\delta^{15}N$ values that matched those obtained "off-line". Instead, the results (Table 5.5) seem to suggest that CO might be a problem, since it is known that certain pyrrole molecules are particularly difficult to combust and they have in the past proved to be especially problematic for the microdetermination of nitrogen (Pietrogrande *et al.*, 1993). If indeed CO is formed during combustion, then the quantities produced must clearly exceed the oxidation capacity of the CuO located at the end of the modified reduction reactor.

Why is CO a Problem?

As previously mentioned, it is unlikely that CO is effectively removed by cryogenic trapping and unfortunately, even if a trace of $^{12}CO^{+\cdot}$ is detected in the signal at *m/z* 28 then it will artificially increase the signal at *m/z* 29, since the natural isotopic ratio of ^{13}C to ^{12}C is proportionately greater than that of ^{15}N to ^{14}N (Table 5.7).

Table 5.7 Natural abundance of stable isotopes of C and N

Ion			
***m/z* 28**	***m/z* 29**	**Isotopic Ratio**	
$^{12}CO^{+\cdot}$	$^{13}CO^{+\cdot}$	^{12}C (98.89 %)	^{13}C (1.11 %)
$^{14+14}N_2^{+\cdot}$	$^{14+15}N_2^{+\cdot}$	^{14}N (99.64 %)	^{15}N (0.36 %)

Furthermore, $CO^{+\cdot}$ has a *m/z* 29 to 28 ratio of 470 ‰ *vs.* N_2 from atmospheric air (Finnigan MAT, 1994).

Attempted Detection of $CO^{+\cdot}$

Unfortunately, the *m/z* 29 to *m/z* 28 ratio cannot be measured directly since it would be impossible to distinguish the signals of CO from N_2. Thus, if CO_2 is not detected, but carbon ($^{12}C^{+\cdot}$) is, then $CO^{+\cdot}$ must be reaching the detector and affecting the authentic *m/z* 29 to *m/z* 28 ratio of N_2.

Detection of CO_2

The Faraday cup detectors were set to measure signals at *m/z* 44, 45 and 46 and 1 µl injections of solutions of Me,H maleimide (**36b**) and caffeine (**62**) were made. However, despite the presence of the cryogenic trap, traces of CO_2 were in fact detected (amplitude of *ca.* 0.0005 V). Thus, it is conceivable that if traces of CO_2 (BP -56.6 °C) were escaping from the cryogenic trap (liquid N_2 BP -195.8°C) and entering the ion source, then CO (BP -191.5°C), if formed, would surely be capable of reaching the detector and contributing to the authentic *m/z* 29 to *m/z* 28 ratio of N_2. Furthermore, $CO^{+\cdot}$ fragments may also be generated from $CO_2^{+\cdot}$ ions *via* unimolecular decomposition in the ion source (*ca.* 10% of the ion current formed from CO_2 is $CO^{+\cdot}$), but in the presence of the cryogenic trap, the amount of $CO_2^{+\cdot}$ and therefore $CO^{+\cdot}$ reaching the detector would be negligible. Hence, the $\delta^{15}N$ values would not be affected.

Attempted Detection of Carbon ($^{12}C^{+\cdot}$)

The Faraday cup detectors were set to measure a signal at *m/z* 12 and 1 µl injections of solutions of Me,H maleimide (**36b**) and caffeine (**62**) were made. However, no signal corresponding to $^{12}C^{+\cdot}$ was observed. Although it could not be proved that $CO^{+\cdot}$ was contributing to the authentic *m/z* 29 to *m/z* 28 ratio of N_2, it was still thought to be the most likely reason for the observed "on-line" ^{15}N-enrichment of Me,H maleimide (**36b**).

Removal of CO

In order to prevent the formation of CO, it was decided to use a freshly oxidised CuO/NiO/Pt combustion reactor at 950°C in conjunction with the modified reduction reactor at 400°C (*i.e.* Cu + C + CuO). It was hoped that under such conditions the molecules of Me,H maleimide (**36b**) would completely combust to yield only N_2, NO, CO_2 and H_2O. Furthermore, it was thought that if the capillary connecting the oxidation and reduction reactors was immersed in a solid CO_2/acetone trap (*ca.* -78°C), that most of the CO_2 generated during combustion would be removed at this point. Unfortunately, H_2O would also be trapped, thus necessitating the removal of the capillary from the solid CO_2/acetone trap after each run. Hence, mostly N_2 and NO (if formed) would actually flow into the modified reduction reactor, whereby any NO would subsequently be reduced to N_2.

In order to prove the effective combustion of the freshly oxidised CuO/NiO/Pt furnace the "off-line" and "on-line" $\delta^{13}C$ values of Me,H maleimide (**36b**) were obtained. The results are shown in Table 5.8.

Table 5.8 Comparison of $\delta^{13}C$ values of Me,H maleimide Obtained both "off-line" and "on-line"

Method of Analysis	Replicate $\delta^{13}C$ (‰) Analyses			Av. $\delta^{13}C$ (‰)
	1	2	3	
Elemental analyser (EA)	-25.3	-25.8	-25.1	-25.4 ± 0.4
GC-C-IRMS	-25.0	-24.3	-24.9	-24.7 ± 0.4

The results for both processes are in good agreement, thus proving the effective combustion of Me,H maleimide (**36b**) in the "on-line" CuO/NiO/Pt oxidation reactor. Hence, the Faraday cup detectors were reset to measure signals for N_2 at *m/z* 28, 29 and 30 and a series of 1 µl injections of Me,H maleimide (**36b**) and caffeine (**62**) were made (Table 5.9).

Table 5.9 Effect of freshly oxidised CuO/NiO/Pt combustion reactor, solid CO_2/acetone trap and modified reduction reactor (Cu + C + CuO) on $\delta^{15}N$ values

Standard	Replicate $\delta^{15}N$ (‰) Analyses										Av. $\delta^{15}N$ (‰)
	1	2	3	4	5	6	7	8	9	10	
Me,H maleimide	-2.9	0.1	-1.4	4.1	3.1	2.1	-5.4	4.3	-2.6	3.2	0.5 ± 3.4
Caffeine	-28.8	-29.8	-29.4	-	-	-	-	-	-	-	-29.3 ± 0.5

These results suggest that CO may have in fact been partly responsible for the observed "on-line" ^{15}N-enrichment of Me,H maleimide (**36b**), since the $\delta^{15}N$ values were significantly lower than those obtained previously. Yet, the results are both imprecise and inaccurate, since the "off-line" $\delta^{15}N$ value of Me,H maleimide (**36b**) was previously determined as -2.7 ± 0.4 (n=5). It is still not certain as to why "off-line" and "on-line" $\delta^{15}N$ values for Me,H maleimide (**36b**) do not agree, especially since the caffeine (**62**) standard analysed under the same conditions, yielded $\delta^{15}N$ values (Table 5.9) that matched those previously obtained "off-line" (*i.e.* -29.2 ± 0.2 where n=2).

"Off-line" *vs.* "On-line"

The oxidation and reduction reactors of the EA clearly have oxidation and reduction capacities that exceed that of the reactors used in GC-C-IRMS. This greater oxidation/reduction power may be required for the $\delta^{15}N$ analysis of maleimides, since it is known that certain pyrrole molecules are highly resistant towards oxidation, even when combusted in an EA (Pietrogrande *et al.*, 1993). This inertness towards oxidation must be linked in some way to their chemical structure. For example, an increase in resistance to oxidation has been observed when pyrrole nitrogen is protected by adjacent methyl groups (Pietrogrande *et al.*, 1993).

The EA

The analyser uses a "flash combustion" method, which instantaneously converts all organic and inorganic substances into combustion products by complete oxidation of the sample. The gaseous combustion products, primarily CO_2, N_2, NOx and H_2O, pass through a reduction reactor comprised of elemental copper at 600°C, whereby any NOx compounds are reduced to N_2. Typically, the samples are packed in tin containers and stored in an autosampler carousel where they are continuously purged with a flow of He. Once the run is initiated they are dropped into a vertical quartz tube (oxidation reactor), which is maintained at temperatures of 1000-1050°C. At this point, the He stream is then enriched with pure oxygen and the sample and its container are completely oxidised in a "flash" combustion reaction at temperatures of up to 1800°C.

Oxidation/Reduction Reactors

These reactors are situated in a single furnace block of the EA. Each furnace is fitted with an alumina ceramic tube heated by an electrical element and insulated with a refractory material. The exact packing of the reactors is illustrated in Fig. 5.14.

Fig. 5.14 Packing of EA Oxidation/Reduction Reactors

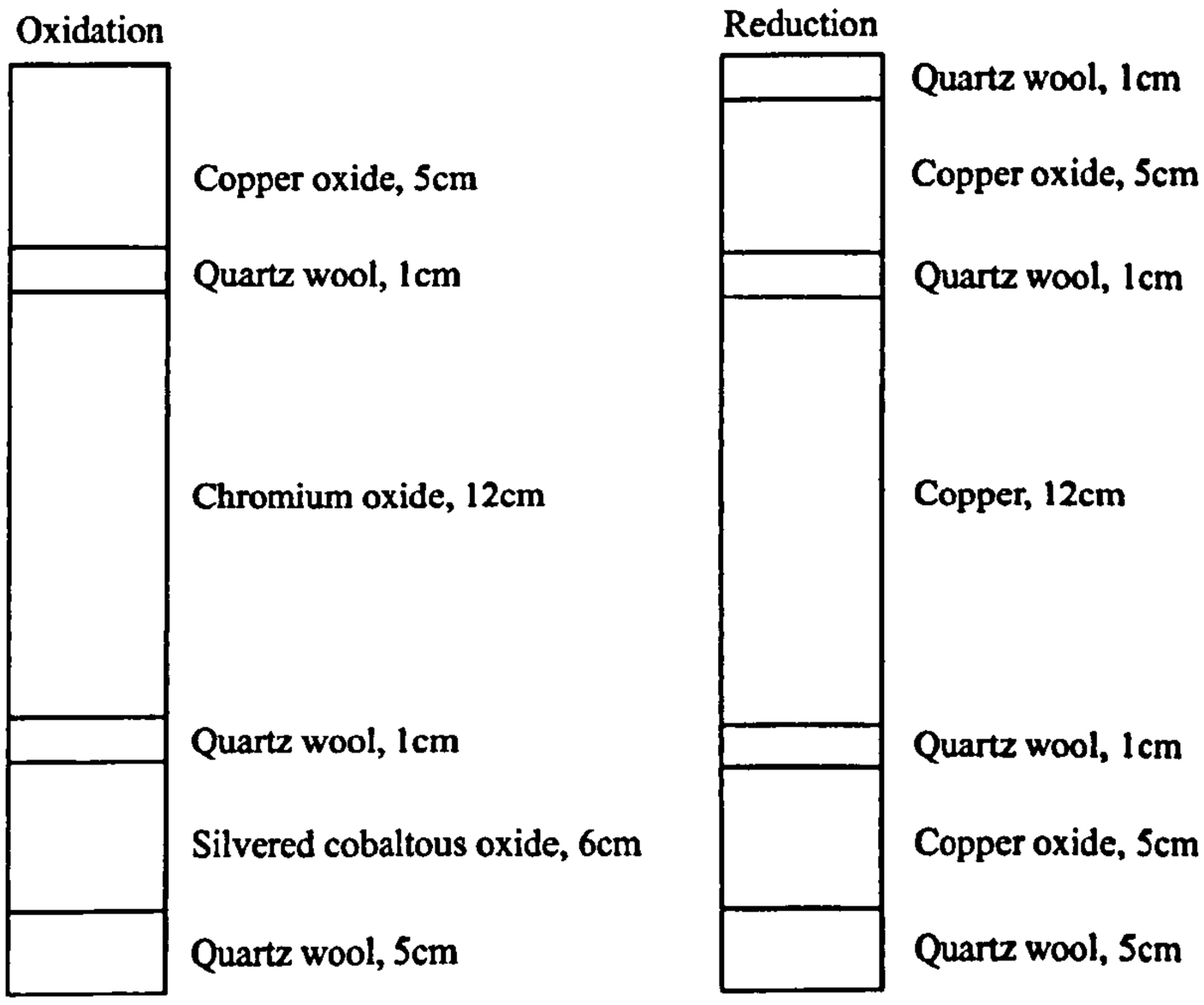

The oxidation and reduction reactors of the EA contain different materials (*e.g.* chromium oxide and silvered cobaltous oxide) to those found in the reactors of the GC-C-IRMS system. In addition, they are also present in much greater quantities as the reactors themselves are considerably larger (18 mm i.d.) compared with the reactors for the GC-C-IRMS system (0.5 mm i.d.). A further advantage for the EA system is the combustion of the tin container in which the sample is stored, since this actually serves to enhance the combustion of the sample. Moreover, combustion of the sample and its container is accompanied by a stream of pure O_2 producing a "flash" combustion reaction with temperatures reaching as high as 1800°C. The EA reduction reactor contains a greater amount of elemental Cu than does the equivalent reactor for the GC-C-IRMS system. Thus, there is a greater chance of the NOx compounds being reduced to N_2 in the EA reactor, since they will be in contact with the elemental Cu for a longer period of time (*ca.* 50s) than in the GC-C-IRMS reduction reactor (*ca.* 1.5s). It is thought that the larger oxidation and reduction capacity of the EA system compared with that of the GC-C-IRMS technique, allows the successful and reproducible determination of $\delta^{15}N$ values for Me,H maleimide (**36b**). Unfortunately, there are limitations to the amount of packing material that can be placed in the reactors on the GC-C-IRMS system. Perhaps combinations of small amounts of other materials (*e.g.* chromium oxide) will eventually lead to the successful oxidation of maleimides and subsequent reduction of the combustion products to yield $\delta^{15}N$ values that match those obtained "off-line".

CONCLUSIONS

In summary, it would appear that NO is not responsible for the observed ^{15}N-enrichment of Me,H maleimide (**36b**). Since neither the modified reduction reactor (Cu + C + CuO) nor the NiO/Pt oxidation reactor produced $\delta^{15}N$ values that matched those obtained "off-line". Instead, it seems likely that there is a problem associated with the "on-line" combustion of Me,H maleimide (**36b**). Although it could not be proved, it is possible that CO is formed during combustion. Even a trace of $CO^{+\cdot}$ in the ion source could artificially increase the $\delta^{15}N$ values, especially since it is reported to have a *m/z* 29 to 28 ratio of 470 ‰ *vs.* N_2 from atmospheric air (Finnigan MAT,

1994). Attempts to prevent the formation of CO were at least partially successful, since the $\delta^{15}N$ values were significantly lower than those obtained previously. Yet, the results were both imprecise and inaccurate compared with those obtained "off-line". It would appear that the greater oxidation and reduction capacities of the EA reactors are required for the successful and reproducible determination of $\delta^{15}N$ values for Me,H maleimide (**36b**). Further work (Chapter 6) and/or experiments involving different packing materials might one day allow the $\delta^{15}N$ of these compounds to be readily determined "on-line".

CHAPTER 6:

OVERVIEW AND FUTURE RECOMMENDATIONS

OVERVIEW AND FUTURE RECOMMENDATIONS

OVERVIEW

Maleimides as Molecular Markers for PZA

Priest Pot/Lake Pollen

The investigations carried out on two Recent sediments: Priest Pot (England) and Lake Pollen (Norway) further supports previous circumstantial evidence (Rontani *et al.*, 1991; Crawford, 1998) that sedimentary maleimides are genuine water column degradation products of tetrapyrrole pigments. An earlier attempt to obtain the maleimide distribution from Priest Pot had been unsuccessful due to the high abundance of chlorins, which were suspected to have masked the presence of maleimides during GC-MS (Crawford, personal communication). To overcome this problem, a GPC method was developed, which enabled separation of maleimides from the vast majority of the chlorins. The distributions and concentrations of the alkyl maleimides were obtained by GC-MS. Both Me,H (**36b**) and Me,Et (**36a**) maleimides were detected in the Priest Pot sediment and Me,Et (**36a**) and Et,Et (**41c**) maleimides were discovered in the Lake Pollen sediment. However, Me,*n*-Pr (**36c**) and Me,*i*-Bu (**36f**) maleimides were not detected. The Me,*i*-Bu (**36f**) component ultimately arises from members of the Bchls *c* (**12**), *d* (**10**) or *e* (**13**), which are characteristic of the photosynthetic green sulfur bacteria (Chlorobiaceae). These obligate anaerobes exist within a specific niche in the environment, specifically, an expanse of anoxic water within a photic zone under conditions commonly referred to as "photic zone anoxia" (PZA). Unfortunately, Me,*n*-Pr maleimide (**36c**) is not as structurally specific as Me,*i*-Bu maleimide (**36f**) and can have a bacterial, phytoplanktonic (*cf.* Verne Mismer *et al.*, 1986; also see Chapter 2) or mixed origin. Therefore, it is essential in the case of Me,*n*-Pr maleimide (**36c**) to obtain stable isotope measurements in order to confirm its source. However, both Me,*n*-Pr (**36c**) and Me,*i*-Bu (**36f**) maleimides should have been detected in the Priest Pot sediment, since the bottom waters and sediments are anoxic during summer (Robinson *et al.*, 1984) and light is able to reach the sediment, as the lake is very shallow (4m). Although maleimides indicative of the Chlorobiaceae were not detected in the Priest Pot sediment they have been discovered in a variety of other sediments; for example, the relatively immature sediments of the VdG basin, Italy (Chapter 3) and also in older sediments of C/T age (Crawford, 1998; see Chapter 4).

Thus, it would appear that the maleimide signal is strengthened during diagenesis by removal of interfering components such as chlorins.

Vena del Gesso

The distribution and concentration of the free maleimides in ten sub-samples of marl IV and three sub-samples of marl VIII from the Vena del Gesso (Italy) Messinian evaporitic sequence were obtained. Both Me,*n*-Pr (**36c**) and Me,*i*-Bu (**36f**) maleimides were discovered in the lower eight samples of marl IV and in the lower two samples of marl VIII. Me,*n*-Pr maleimide (**36c**) was also detected in sample IV-9. $\delta^{13}C$ values were obtained for Me,Et (**36a**), Me,*n*-Pr (**36c**) and Me,*i*-Bu (**36f**) maleimides for certain samples from marl IV. The results for samples IV-1 and IV-3 show Me,*i*-Bu maleimide (**36f**) to be enriched in ^{13}C relative to Me,Et maleimide (**36a** mainly of phytoplanktonic origin) by *ca.* 9 and 5 ‰ respectively, since the Chlorobiaceae uniquely use the reversed TCA cycle for carbon fixation (Evans *et al.*, 1966), which discriminates less against the incorporation of ^{13}C than does the C3 pathway utilised by algae. However, the lighter isotopic values for Me,*n*-Pr maleimide (**36c**) indicate a mixed (50:50) origin in sample IV-1 and an entirely phytoplanktonic origin in sample IV-3. Additionally, the free base alkyl porphyrins isolated from samples IV-1 and IV-5 were photo-oxidised to maleimides. The distributions also show structural evidence for the past existence of Chlorobiaceae, since Me,*i*-Bu maleimide (**36f**) was present in both cases.

Overall, the results strongly indicate that there must have been periods of salinity-induced stratification where anoxic conditions extended into the photic zone of the palaeo-water column during marl deposition. The work is also supported by earlier studies (Keely *et al.*, 1995; Schaeffer *et al.*, 1995; Kenig *et al.* 1995; Sinninghe Damsté *et al.*, 1995) which clearly suggest that the Chlorobiaceae once existed in the water column and that PZA was indeed recurrent throughout the deposition of the entire VdG sequence.

Cenomanian/Turonian Oceanic Anoxic Event

The above study on Vena del Gesso involved the possibility of PZA occurring in a restricted marine basin as a result of salinity-induced stratification, whereas previous

work on black shales from the Northern Tethys (Italy) of the Cretaceous C/T OAE suggested the possible occurrence of PZA in a more open ocean setting (Crawford, 1998; Turner, 1998). It is thought that a eustatic rise in sea level, submarine volcanicity and warm oxygen deficient bottom waters combined with an equable climate and increased local productivity led to the development of an intense and expanded OMZ, which intermittently penetrated the photic zone, producing an environment in which the Chlorobiaceae could flourish. Maleimide distributions and concentrations were determined for a black shale sequence from a site near the village of Moria. However, Me,*n*-Pr (**36c**) and Me,*i*-Bu (**36f**) maleimides were not detected in the samples (M3, M5, M7, M9, M12 and M13) analysed, suggesting that PZA did not occur during the deposition of these sediments. In contrast, a previous study by Turner (1998) suggested that PZA might have occurred intermittently throughout the deposition of this section of the Livello Bonarelli. HMW CAPs were discovered in certain samples (M5, M7 and M14) from the middle of the Moria sequence with the same retention time and mass spectra as certain Bchl *d*-derived standards. However, porphyrin distributions are very complicated and the mass spectra are not particularly characteristic. Further evidence to support the lack of PZA was provided by the maleimide distributions obtained from the photo-oxidation of nickel porphyrin fractions isolated from samples M3, M5, M7 and M9, which also failed to produce maleimides characteristic of the Chlorobiaceae. Thus, PZA does not appear to have occurred during deposition of the black shales at the Moria site.

The structurally specific Me,*i*-Bu maleimide (**36f**) appears to be a much more reliable and robust biomarker for the past existence of the Chlorobiaceae than do the HMW CAPs. This was also evident in the VdG study (Chapter 3), where a strong signal was observed for Me,*i*-Bu maleimide (**36f**) in the lower eight marl IV samples. Yet, the corresponding HMW CAP data (Turner, 1998) proved to be inconclusive. Despite the absence of the Me,*i*-Bu component in black shale samples from the Moria site maleimide evidence does exist for the occurrence of the PZA phenomenon in the Northern Tethys during the C/T OAE. For example, Me,*i*-Bu maleimide (**36f**) was detected in Livello Bonarelli samples from Monte Petrano (MP0 and MP3-6) by Crawford (1998). The Moria and MP sites are only separated by a distance of a few kilometres, and the fact that Me,*i*-Bu maleimide (**36f**) was detected at MP, but not at Moria is intriguing. What makes this finding even more difficult to explain is that Me,*i*-Bu maleimide (**36f**) was also detected at other sites in the Umbrian region of

central Italy (Crawford, 1998). One possible explanation is that the depth of the chemocline varied during deposition of the Livello Bonarelli sequence at different sites. Indeed, the Chlorobiaceae could not have existed if the chemocline was situated beneath the photic zone during black shale deposition at the Moria site, which would account for the complete absence of Me,*i*-Bu maleimide **(36f)** in these shales.

Me,Et Maleimide as a $\delta^{13}C$ Isotopic Productivity Indicator

Vena del Gesso

Me,Et maleimide **(36a)** is mainly of phytoplanktonic origin and should ultimately relate to the level of marine productivity in the surface waters at the time of deposition of organic rich sediments. This work was carried out to assess the utility of Me,Et maleimide **(36a)** as an isotopic productivity indicator. $\delta^{13}C$ values for Me,Et maleimide **(36a)** were monitored over the ten sub-samples from marl IV. These cover a range of *ca.* 5 ‰ and show a trend of increasing $\delta^{13}C$ values towards the middle of the marl followed by a marked decrease and then a rise towards the top of the section. The results were compared with the abundance of the free base alkyl porphyrins (Keely *et al.*, 1995), but the correlation between the plots was poor. In theory the isotopic shifts should relate to changes in CO_2 demand since high porphyrin abundances, suggesting high productivity, should correlate with heavy $\delta^{13}C$ values of Me,Et maleimide **(36a)**. Unfortunately, the isotopic shifts did not correlate well with the concentration depth-profile for Me,Et maleimide **(36a)** either. Again, one would expect higher concentrations of Me,Et maleimide **(36a)** to coincide with heavy $\delta^{13}C$ values.

Cenomanian/Turonian Oceanic Anoxic Event

One of the most significant events in the Cretaceous geological record was the rapid world wide positive excursion of both carbonate (*ca.* 2 ‰ ^{13}C enrichment; Scholle and Arthur, 1980) and organic carbon (*ca.* 4 ‰ ^{13}C enrichment; *e.g.* Arthur *et al.*, 1988; Kuypers *et al.*, 1999), which occurred at the C/T boundary. This isotopic shift resulted from an increase in the rate of sedimentary burial of immense quantities of isotopically light OM (*i.e.* depleted in ^{13}C) in response to the well-documented C/T

OAE (*e.g.* Schlanger and Jenkyns, 1976). Me,Et maleimide (**36a**) was again used as a simple isotopic productivity indicator and a $\delta^{13}C$ positive excursion of *ca.* 3.2 ‰ was observed over the MP sequence. An advantage of using a compound-specific isotopic biomarker (*e.g.* Me,Et maleimide **36a**) is that it is unlikely to be contaminated with carbon from terrestrial sources and as such, is probably more accurate than bulk $\delta^{13}C_{org}$ measurements. Maleimide concentrations were also determined for samples MP0-MP7 inclusive, as Crawford (1998) had only determined the distributions (except MP2) in a previous study. The concentration-depth profile for Me,Et maleimide (**36a**) was compared with the $\delta^{13}C$ Me,Et maleimide (**36a**) excursion plot. On this occasion the plots showed a moderately good correlation for samples MP7 to MP4. This work showed the effectiveness of Me,Et maleimide (**36a**) as a carbon isotopic productivity indicator. However, in this case the concentration depth-profile for Me,Et maleimide (**36a**) might just coincidentally coincide with the positive carbon isotopic excursion; since the excursion could ultimately reflect either a local or global increase in phytoplankton productivity in surface waters.

Nitrogen Isotope Work

It is thought that global climate is influenced by marine primary production, which in many oceanic systems is restricted by the amount of available nitrogen. Therefore, reconstructions of nitrogen availability in past oceanic environments may allow a link to be established between climate change and productivity. However, there is a substantial amount of evidence to suggest that nitrogen isotopic fractionation occurs during diagenesis (Altabet *et al.*, 1991; Schafer and Ittekkot, 1993). To overcome this problem, Sachs *et al.* (1995) decided to determine the effect of diagenesis on the $\delta^{15}N$ of marine OM by isolating a nitrogen-containing biomarker with a known source for isotopic analysis. They chose Chl claiming that $\delta^{15}N$ analysis of Chl transformation products would allow them to study the diagenetic effect on isotopic ratios and also assess whether or not whole-sediment $\delta^{15}N$ values could be used to accurately reconstruct past palaeoenvironmental conditions. Furthermore, Sachs *et al.* (1999a) have recently explored the relationship between the nitrogen and carbon isotopic ratios of Chl *a* (**1**), and total biomass in cultured marine phytoplankton to assess the utility of Chl as an isotopic proxy for photoautotrophs; their findings suggest that a 5.1

‰ isotopic depletion of Chl *a* (**1**) relative to total algal nitrogen is a robust relationship that justifies the use of Chl as a nitrogen isotopic surrogate for photoautotrophs. The main aim of the work in Chapter 5 was to develop a method for the determination of $\delta^{15}N$ values in maleimides using GC-C-IRMS in view of the fact that if the $\delta^{15}N$ values for each of the pyrroline rings of Chl *a* (**1**) could be obtained and it was found that all four have the same $\delta^{15}N$ values (as the biosynthetic pathway predicts), then Me,Et maleimide (**36a**) could be used as a nitrogen isotopic proxy for photoautotrophs. Once this is established, a further use for Me,Et maleimide (**36a**), is that it could be solvent-extracted in its "free" form from oceanic sediment cores and its $\delta^{15}N$ values used to assess the degree of nitrogen availability in past oceanic environments, which may elucidate a link between climate change and productivity. This of course, is based on the assumption that maleimides once formed are stable and that diagenesis will have no effect on their $\delta^{15}N$ values. Furthermore, nitrogen isotopic productivity indicators are thought to be better than their carbon counterparts. Carbon isotopic excursions may reflect either a local or global change in productivity, whereas nitrogen isotopic excursions are thought to represent local changes only. CO_2 has a relatively low natural abundance in the atmosphere compared to N_2. Thus, pCO_2 could be affected during either local or global productivity changes, since an increase in productivity in surface waters could lead to an increase in the rate of burial of OM, which may lead to a decrease in the concentration of dissolved CO_2 in surface waters. In order to maintain equilibrium, CO_2 from the atmosphere would dissolve in the surface waters, causing a decrease in pCO_2. Algae preferentially assimilate $^{12}CO_2$ compared to $^{13}CO_2$ and consequently ^{13}C-enrichment of the surface waters may occur, which should be detected in both the $\delta^{13}C$ values of OM and of $CaCO_3$. Hence, the resulting carbon isotopic excursion may reflect either a local or global change in productivity. On the other hand, fluctuations in the nitrogen cycle have little effect on the high relative abundance of N_2 in the atmosphere. Indeed, ^{15}N-enrichment of marine OM is brought about by denitrification (conversion of NO_3^- to N_2 or N_2O), which results in considerable ^{15}N-enrichment of subsurface nitrate (Altabet *et al.*, 1995 and references therein) and subsequently OM. Denitrification occurs within strong OMZs, which are formed during periods of increased productivity. Nitrogen availability (*i.e.* nitrates) exerts a fundamental control on local marine productivity therefore nitrogen isotopic excursions should reflect this.

However, the accurate and precise determination of $\delta^{15}N$ values for maleimides proved to be more difficult than was first thought. There appeared to be a problem associated with the "on-line" combustion of Me,H maleimide (**36b**). Most likely, CO was produced during combustion and was consequently responsible for the artificial positive increase in $\delta^{15}N$ values of Me,H maleimide (**36b**). Attempts to prevent the formation of CO were at least partially successful, but the $\delta^{15}N$ values were both inaccurate and imprecise compared with those obtained "off-line". Further work is clearly required and the ideas outlined below should help to at least identify the source of the problem.

FUTURE RECOMMENDATIONS

Maleimide Studies

1. If the "on-line" $\delta^{15}N$ values of Me,Et maleimide (**36a**) could be readily obtained, then they could be used to reconstruct the degree of nitrogen availability in past oceanic environments, which may allow a link to be established between climate change and productivity. Furthermore, they could be used to determine, at the molecular level, the ^{15}N fractionation effects between photosynthetic nitrogen and nitrogen source. However, before Me,Et maleimide (**36a**) can be used in such investigations, it is essential to prove that the four oxidation products of Chl (Chapter 5) have the same $\delta^{15}N$ values, as the biosynthestic pathway predicts; unfortunately there is still a number of problems to resolve.

The first problem is associated with the "on-line" combustion process during $\delta^{15}N$ analysis of maleimides, as indicated by the results (Chapter 5). One way to resolve this problem is to set up a GC-C-MS system, fitted only with an oxidation reactor. Such a set-up should allow the "true" combustion products of Me,H maleimide (**36b**) to be determined. This investigation could also be extended to include a variety of other organic N-containing compounds in an attempt to identify certain "problematic" classes of compound. Once these are identified work could be carried out to determine the optimum conditions under which they will combust, which may involve the addition of certain non-standard packing materials to the oxidation reactor. Furthermore, the addition of a reduction reactor to the GC-C-MS system could be used to check that any NOx compounds produced during combustion were completely

reduced to N_2. The combustion efficiency of each compound would be evaluated by comparison of its "on-line" and "off-line" $\delta^{15}N$ values.

The second problem, is associated with the chemical oxidation of a bulk sample of pyropheophorbide *a* (**53**), since only three of the four potential N-containing oxidation products have been obtained: Me,Et (**36a**) and Me,vinyl (**37**) maleimides, in addition to hematinic acid (**46** analysed as the methyl ester). The oxidation procedure (Suzuki *et al.*, 1999 and references therein) needs to be perfected and/or slightly modified in order to obtain the fourth oxidation product (**61** C-E ring derivative). However, there is a further problem in that Me,Et (**36a**) and Me,vinyl (**37**) maleimide co-elute during TLC purification and as a result are injected on to the GC column as a mixture. Both compounds are well resolved from one another, but Me,Et maleimide (**36a**) has a far greater relative abundance than Me,vinyl (**37**) maleimide (*e.g.* Fig 5.11; Chapter 5). This is to be expected, since the yield for Me,vinyl maleimide (**37**) is lower than that for Me,Et maleimide (**36a**) by a factor of *ca.* 10. If the problem associated with the "on-line" combustion of maleimides was resolved, then the $\delta^{15}N$ values of Me,Et maleimide (**36a**) could be readily obtained, however, a much greater concentration of Me,vinyl maleimide (**37**) would have to be injected in order to obtain a suitable peak area (corresponding to an amplitude of at least 0.5V). This of course, would result in overloading of the column by Me,Et maleimide (**36a**) and therefore, it may be necessary to use preparative GC to separate the two components before analysis by GC-C-IRMS.

Once these problems have been resolved then further work, in a preliminary study, could involve the culturing of three types of phototrophic organisms, which would have different nitrogen sources (an alga, a cyanobacterium and a green sulfur bacterium). The Chl fraction could then be isolated and oxidised to maleimides. Subsequent determination of the $\delta^{15}N$ values of Me,Et maleimide (**36a**) by GC-C-IRMS would allow comparison, at the molecular level, of the ^{15}N fractionation effects between photosynthetic nitrogen and nitrogen source. Such studies are important, since there are many different enzymes and reaction networks exhibited among a variety of bacterial groups, which can produce diverse nitrogen isotopic patterns within metabolic end-products (Beaumont *et al.*, 2000). Furthermore, Me,Et maleimide (**36a**) could also be extracted in its "free" form from oceanic sediment cores and the $\delta^{15}N$ values could be used to reconstruct the degree of nitrogen

availability in past oceanic environments, which may allow a link to be established between climate change and productivity.

2. The present balance of evidence strongly indicates that maleimides are formed naturally in the water column and that they are not simply artefacts formed from the oxidation of tetrapyrrole compounds during sample storage (Chapter 2). However, the exact origin of certain maleimides (*e.g.* Et,Et maleimide, **41c**; discussed in Chapter 2) is still unclear. It is thought that Et,Et maleimide (**41c**) must derive from early diagenetic product tetrapyrroles that contain the appropriate alkyl side chains. One possibility is that it could arise through opening of the exocyclic E ring of certain of the Bchls *c*, *d* or *e* (**12**, **10** or **13**; Grice, 1995). A further possibility is that the Et,Et (**41c**) component could arise from the rearrangement of Chls and/or their early transformation products (Grice *et al.*, 1996). Comparison of the $\delta^{13}C$ values of this component with those obtained for Me,Et (**36a**; mainly of phytoplanktonic origin) and Me,*i*-Bu (**36f**; ultimately derived from Chlorobiaceae) maleimides might reveal that it has a phytoplanktonic, bacterial or mixed origin, as does Me,*n*-Pr maleimide (**36c**; *cf.* Verne Mismer *et al.*, 1986; also see Chapter 2). Similarly, this approach could be extended to obtain the $\delta^{13}C$ values of other components [*e.g.* Et,*n*-Pr (**41b**), Me,*i*-Pr (**36i**), Me,*sec*-Bu (**36e**) and Me,*n*-pentyl (**36j**)] whose origins are also uncertain. However, these relatively minor components, in addition to Et,Et maleimide (**41c**), may require preparative GC as the last step to GC-C-IRMS analysis. Such work has already proved useful, for example, Grice *et al.* (1996) found that the $\delta^{13}C$ value of Me,*n*-Bu maleimide (**36g**) extracted from Kupferschiefer sediment (Lower Rhine Basin, Germany) was depleted in ^{13}C relative to other maleimides and concluded that it must derive from an organism utilising a source depleted in ^{13}C.

Sample Studies

This study (Chapter 4) and others (Crawford, 1998; Turner, 1998; Sinninghe Damsté and Köster, 1998) have attempted to ascertain whether or not the specific redox condition of PZA occurred during deposition of the Livello Bonarelli during the C/T OAE. Yet, at certain sites (*e.g.* Moria; Chapter 4) the maleimide and HMW CAP data appear to contradict one another. The structurally specific Me,*i*-Bu maleimide (**36f**; of Chlorobiaceae origin) is thought to be a more reliable indicator of PZA than are the

HMW CAPs (Chapter 4). However, the former component (where found) is often present in very minor amounts relative to other maleimides (Crawford, personal communication). Thus, it would be interesting to see if isorenieratane (**34**) and/or other related mono/diaryl isoprenoid hydrocarbons could be detected at both Moria and MP in addition to other Livello Bonarelli sites (*e.g.* Gorgo A Cerbara, Fosto, Contessa Gorge Quarry, Bottaccione Gorge) to confirm these findings. Of course, $\delta^{13}C$ values for some of these compounds (*e.g.* **35**) would have to be obtained in order to substantiate the findings, since certain diagenetic products of isorenieratene (**15**) can originate from β-carotene of non-bacterial origin (*i.e.* algae). Furthermore, maleimide studies of samples from other areas should include, for example, black shales from the Pacific Ocean where deposition is also thought to have occurred under anoxic conditions (Jenkyns, 1980).

In a previous study, Crawford (1998) only investigated the possible occurrence of PZA in association with black shale deposition at one site (Valdorbia, Italy) during the Toarcian and Aptian OAEs. Therefore, further investigations should be carried out at other sites (*e.g.* German and Paris Basins) to substantiate these findings. Indeed, aryl isoprenoids have already been detected in a suite of Toarcian samples from the SW German Basin (van Kaam-Peters, 1997b), so detection of the structurally specific Me,*i*-Bu maleimide (**36f**; of Chlorobiaceae origin) may provide further information about the extent of PZA in these relatively shallow epicontinental seas.

Furthermore, Hoefs *et al.* (1995) discovered the presence of low amounts of isorenieratane (**34**) in the bottom sediments of the Arabian Sea. The area in which it was detected is characterised by a present day OMZ and the evidence tentatively suggests the occurrence of PZA. It would be interesting to carry out maleimide studies for these sediments in an attempt to confirm these findings, especially since it may help to establish the possible occurrence of PZA, in sediments that have been deposited within an OMZ.

Finally, the presence of HMW CAPs corresponding to Bchl *d* CAPs (from a bulk Kupferschiefer sample, due to low amounts of available standard) were detected in samples from the Mulhouse Basin (Alsace, France; Turner, 1998). Therefore, it would be interesting to see if the maleimide data corroborate these findings.

CHAPTER 7:

EXPERIMENTAL

EXPERIMENTAL

GENERAL

Glassware

All glassware was soaked in a *ca.* 5% Micro solution for several hours and then rinsed with tap water and distilled water before drying in an oven. Prior to use glassware was rinsed with either acetone or dichloromethane (DCM).

Solvents

All solvents used were glass distilled or HPLC grade (Rathburn). Water was double-distilled prior to use.

Sample Storage

All samples were stored without solvent in a freezer.

SAMPLE EXTRACTION

Prior to extraction, the sediment was crushed and pulverised using a laboratory disc mill (Tema). The powder was homogenised before weighing and appropriate aliquots (10-485g) were extracted (x3 or x4) ultrasonically (20 min; Dawe Instruments Ltd.) with DCM/MeOH (9:1, v/v). After centrifugation (12 min; 3000 rpm; Sorvall Instruments RC5C) the supernatant was decanted off and the solvent removed by rotary evaporation. Combined extracts were transferred to a round bottom flask (250 or 500 ml) and the remaining solvent carefully removed by rotary evaporation. Once dry, the combined extract (TOE) was immediately wrapped in foil and stored in a freezer.

FRACTIONATION

Column Chromatography

The TOE was fractionated by flash column chromatography (Still *et al.*, 1978) using clean, dry columns (3 cm i.d., *ca.* 30cm length) typically packed with DCM-extracted,

dry, activated silica gel 60 (150°C, 24h). The columns were pre-eluted with hexane (*ca.* 2 or 3 column volumes). Extracts were pre-adsorbed on to the minimum amount of silica (*ca.* 0.5g) before being applied to the top of the column. The crude fractions were eluted with solvents of increasing polarity (*ca.* 2 column volumes each; Fig 7.1). Four fractions were initially obtained (Fig. 7.1); a hydrocarbon fraction (F1), a crude nickel porphyrin and aromatic fraction (F2), a crude vanadyl porphyrin fraction (F3), and a polar fraction possibly containing free 1*H*-pyrrole-2,5-diones (maleimides), in addition to vanadyl, iron and free base alkyl porphyrins (F4). Fractions F2 and F4 were fractionated further by another stage of flash column chromatography on a smaller scale. Firstly, aromatics were separated from the nickel porphyrins using hexane:dichloromethane (9:1) and a crude maleimide fraction was isolated from the polar fraction (F4) using dichloromethane:acetone [95:5 (Fig. 7.1)]. If small amounts of vanadyl porphyrins were present in fraction F4 (Fig. 7.1) they were combined with fraction F3.

Thin Layer Chromatography (TLC)

Free Maleimides

Free maleimides obtained in fraction F4.2 were purified using TLC. A suitable aliquot was applied in acetone to a pre-eluted (ethyl acetate) pre-activated (150 °C, 24h) plate (Merck 20x20 cm silica gel, 60g). A mixture of hexane/acetone (80/20 v/v) was used to elute the plate using Me,H (**36b** R_f = *ca.* 0.1; Sigma-Aldrich) and Et,Et (**41c** R_f = *ca.* 0.3; obtained from chemical oxidation of octaethylporphyrin **48**; Porphyrin Products) maleimides as retention standards. After examination under UV light (254 nm) the appropriate components were scraped off in the region between and parallel with that outlined by the two retention standards. The removed silica was quickly filtered under vacuum through a glass sinter funnel using acetone (x2) followed by MeOH (x2) to recover the maleimides.

Free Base Alkyl Porphyrins

Free base alkyl porphyrins were separated from the free maleimides using the TLC method described above. The free base alkyl porphyrins (red band R_f = *ca.* 0.7) were

Fig. 7.1 Analytical Scheme I

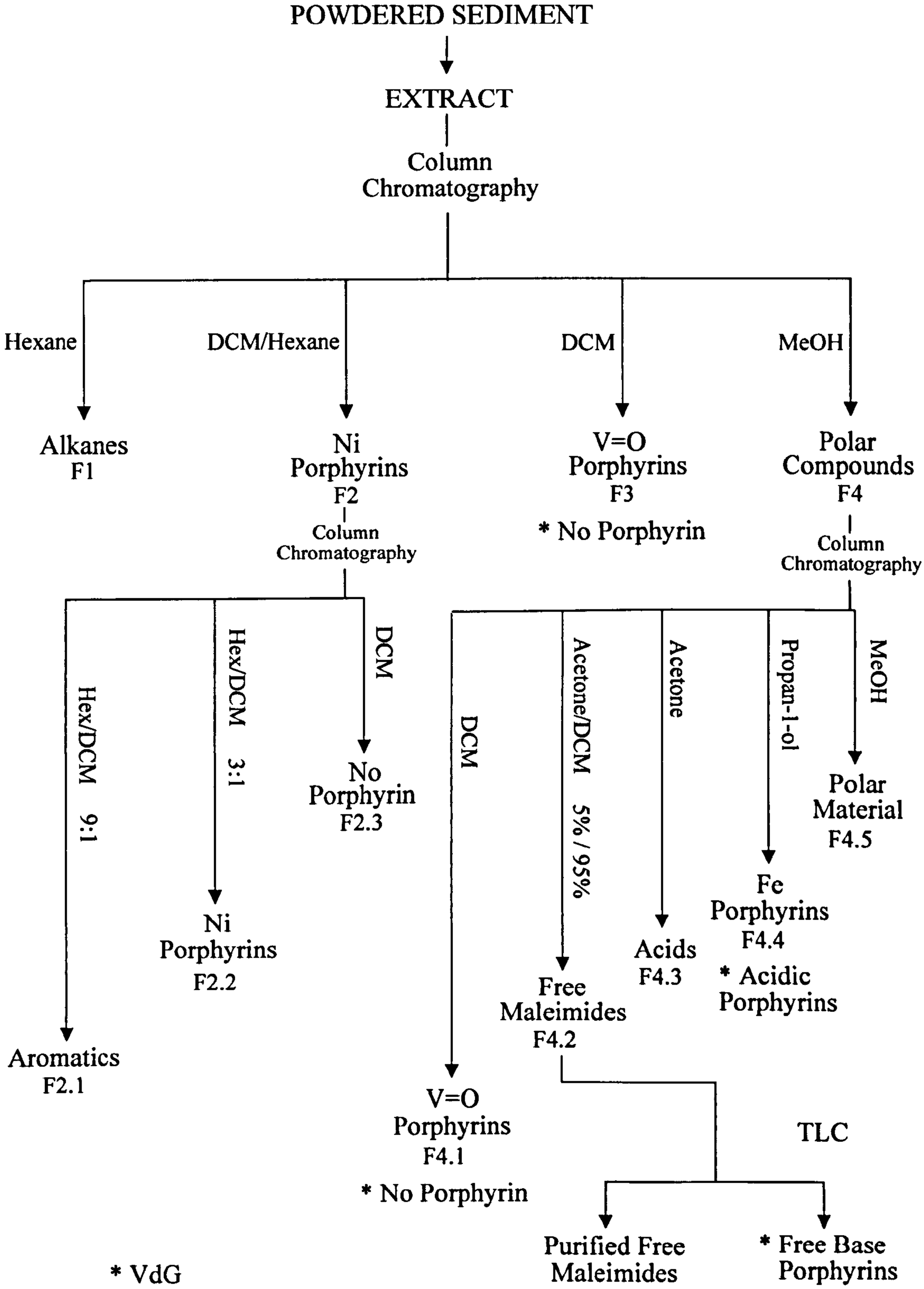

scraped off and the silica quickly filtered under vacuum through a glass sinter funnel using acetone (x2) and MeOH (x2).

Oxidation Products of Pyropheophorbide a

Me,Et (**36a** $R_f = 0.2$) and Me,vinyl (**37** $R_f = 0.2$) maleimides in addition to hematinic acid methyl ester (**46** $R_f = 0.1$) were purified (Fig. 7.2) using the same TLC method as that used above. Authentic Me,vinyl maleimide (**37**) and hematinic acid methyl ester (**46**) obtained from the chemical oxidation (see later) of bilirubin (**47**), were used as retention standards. Unfortunately, Me,Et (**36a**) and Me,vinyl (**37**) maleimides were found to co-elute, but the band was easily identified, as Me,vinyl maleimide (**37**) gave a bright white fluorescence under UV light (366 nm). The appropriate band was scraped off and the silica quickly filtered under vacuum through a glass sinter with acetone (x2) and MeOH (x2).

Gel Permeation Chromatography (GPC)

The "usual" extraction and purification procedure for maleimides (*i.e.* flash columns and TLC) was insufficient to deal with the high chlorin content found in Recent sediments such as Priest Pot (Chapter 2). Thus, a GPC method was employed to separate the maleimides from the vast majority of the chlorins. Fractionation was performed using a Polymer Laboratories (Shropshire, UK) PL-GEL, 10 μl, 50 Å, (600 x 7.5 mm) column and a Waters 600-MS HPLC system fitted with a Rheodyne 7125 injection valve and a 100 μl injection loop. An isocratic solvent program using DCM (51%) and MeOH (49%) was passed through the column at a flow rate of 1.5 ml min^{-1} and into a Waters 991 photodiode array (PDA) detector (400 nm), although no specific peaks were observed. Maleimides were obtained by collecting the eluant from 8 to 13 min. The free maleimide fraction was further purified using TLC (as above).

Aminopropyl Cartridges

An aminopropyl cartridge (500mg) was used to separate the neutral and acid fractions obtained from the oxidation of pyropheophorbide *a* (**53**; Fig. 7.2). The cartridge was pre-eluted (DCM/*i*-propanol; 2:1 v/v) and the sample applied to the top of the column.

Fig. 7.2 Analytical Scheme II

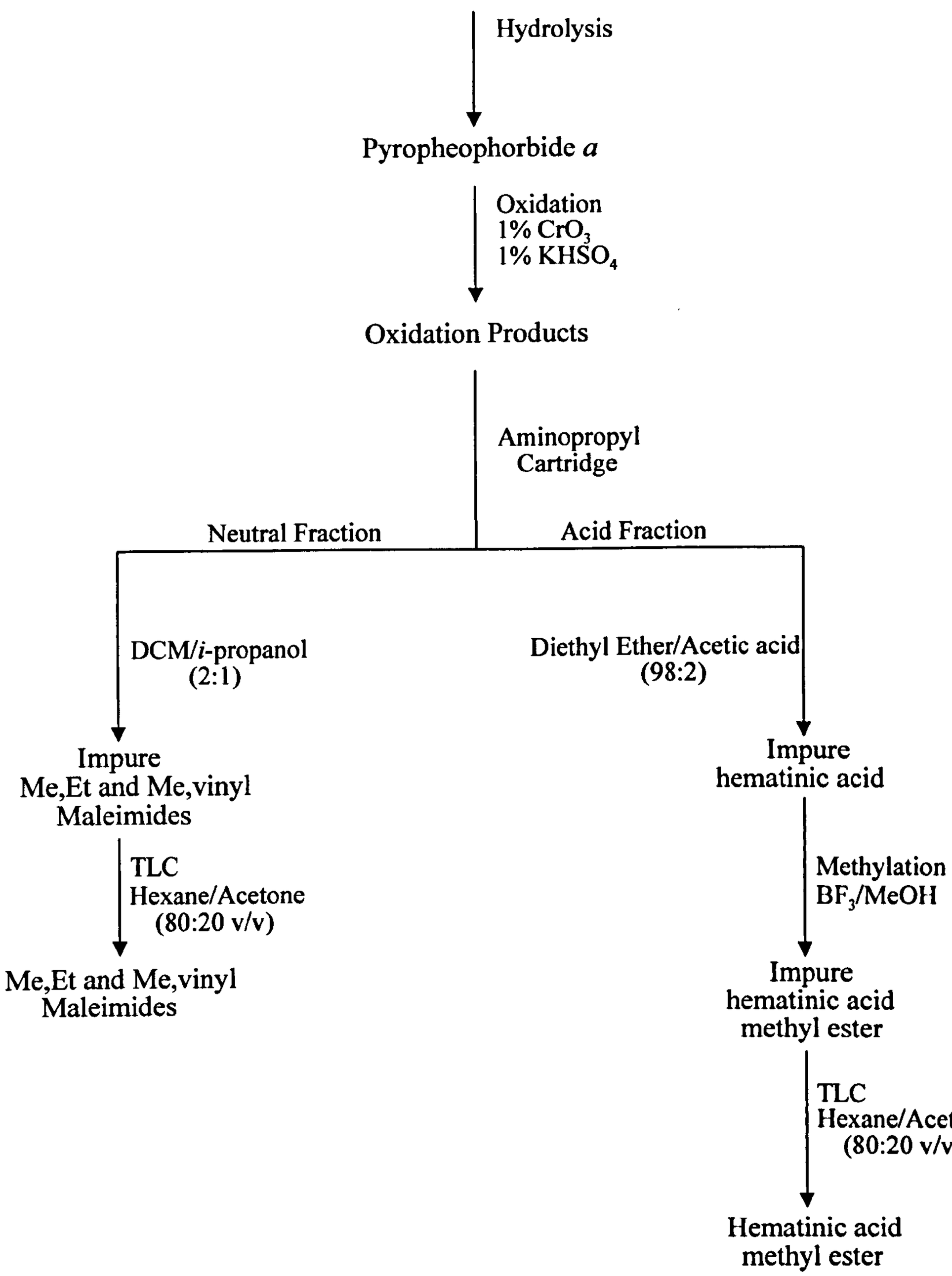

The neutral fraction was eluted with DCM/*i*-propanol (2:1 v/v). The acid fraction was eluted with diethyl ether:acetic acid (98:2 v/v). Solvent was carefully removed with a stream of nitrogen and the fractions stored in the freezer.

HYDROLYSIS

Pyropheophytin *a* to Pyropheophorbide *a*

Pyropheophytin *a* (**60** *ca.* 70mg) was dissolved in cold (0 °C) aqueous trifluoroacetic acid (TFA; *ca.* 15 ml) in accordance with Waseilewski and Svec (1980). Nitrogen was bubbled through the TFA for 10 min. to remove air. The resulting solution was excluded from light and stirred under a nitrogen atmosphere for 4h at 0°C. The reaction mixture was poured into water and subsequently extracted (x3) with DCM. The solvent was carefully removed using a rotary evaporator to yield a dark green oily product, pyropheophorbide *a* (**53** *ca.* 50 mg; UV/Vis, acetone solvent; *ca.* 85%).

OXIDATION

Chemical Oxidation of Porphyrin Standards

Me,Et (**36a**), Et,Et (**41c**) and Me,vinyl (**37**) maleimides, in addition to hematinic acid (**44**) were produced from the chromic acid oxidation of aetioporphyrin III (**17** Porphyrin Products), octaethylporphyrin (**48** Porphyrin Products) and bilirubin (**47** Sigma-Aldrich). A slightly modified Ellsworth and Aronoff (1968) method was employed using chromic acid. The chromic acid solution consisted of 1 g of CrO_3 dissolved in 3.8 ml of H_2SO_4 acid per 50 mg of porphyrin. The porphyrin was dissolved in the minimum amount of acetone (Bonnett and McDonagh, 1969) and the chromic acid solution added slowly dropwise. The mixture was placed in an ice bath (2h) and left at room temperature (2h). The maleimides were extracted with diethyl ether (5 x 20 ml). Soxhlet-extracted (DCM) magnesium sulfate was used to dry the extract, which was then decanted off and the solvent carefully evaporated to dryness (rotary evaporator). The maleimides were purified using TLC (as above).

Chemical Oxidation of Pyropheophorbide *a*

The oxidation of pyropheophorbide *a* (**53** dissolved in acetone; Fig. 7.2) was carried out under the conditions employed by Suzuki *et al.* (1999) and references therein: *i.e.* pH 1.2 at 25°C with 1% (w/v) CrO_3 solution containing 1% $KHSO_4$ for 15 min. The products [Me,Et (**36a**), Me,vinyl (**37**) maleimides and hematinic acid (**44**)] were extracted with diethyl ether (5 x 20 ml) and the extract dried with Soxhlet-extracted (DCM) magnesium sulfate, which was later decanted off and the solvent carefully evaporated to dryness (rotary evaporator). The products were divided into neutral and acid fractions using an aminopropyl cartridge (see above). The acid fraction was methylated (see later). The products were then purified using TLC (as above).

Photo-Oxidation of Porphyrin Samples

This is an alternative to the chromic acid oxidation method (Crawford, 1998). The nickel and free base porphyrin fractions (*ca.* 0.5-1 mg) were dissolved in acetone (*ca.* 40 ml) in a 100 ml round bottom flask attached to a condenser and the solution (pink-red in colour) was irradiated with UV light (365 nm) from a Gallenkamp bulb (125 W) until bleached. The period of irradiation was typically for 10-20h depending on amount of starting material. Solvent was carefully removed by rotary evaporation and the maleimides purified by TLC (as above).

METHYLATION

1ml BF_3/MeOH was added to the sample, which was heated (60°C; 1h); 1ml of water was added to the sample to destroy the BF_3/MeOH. The methylated components were subsequently extracted (x3) with DCM:hexane (4:1 v/v) and the solvent carefully removed under a stream of nitrogen.

QUANTIFICATION

Phthalimide (**45**) was added as an internal standard (typically 80μg) to the TOE. The concentrations (typically ng g^{-1} dry wt. sediment) of maleimides in the samples were calculated from GC-MS peak areas.

INSTRUMENTATION

Ultraviolet/visible (UV/vis) Spectrophotometry

Nickel, vanadyl or free base alkyl porphyrin fractions obtained by flash column chromatography were identified as such by UV/vis spectrophotometry (ATI Unicam UV2 spectrophotometer; slit width 2.0 nm; scan speed 120 nm min^{-1}; absorbance range typically 450-700 nm). Samples were analysed as DCM solutions in quartz cells of 1cm path length. The concentrations were calculated using the Beer-Lambert formula:

$$A = \varepsilon.c.\,l$$

Where A = absorbance, ε = extinction coefficient ($mol^{-1}cm^{-1}$), c = concentration (mol l^{-1}) and l = path length (cm). The extinction coefficients (ε) used were: nickel = 22000, vanadyl = 17600 and free base alkyl porphyrins = 15600 (Chicarelli, 1985).

Gas Chromatography (GC)

GC analyses were carried out using a Carlo Erba 5300 Mega series gas chromatograph equipped with an on-column injector. An FID was used to detect the components and the data were recorded using an Xchrom data system. Hydrogen was used as the carrier gas. Maleimides were analysed using a CP WAX 52 CB column (Chrompack; 50m x 0.32mm i.d. and 0.2μm film thickness) with the following temperature programme: 40°C - 100°C @ 10°C min^{-1} - 240°C @ 4°C min^{-1} (isothermal 25 min).

Gas Chromatography-Mass Spectrometry (GC-MS)

A Finnigan MAT 4500 quadrupole MS directly coupled to a Carlo Erba 5160 GC fitted with an on-column injection port (electron ionisation 70 eV, 300 μA; source

temperature 170°C; 1 scan s^{-1}) was used; helium was used as the carrier gas. Maleimide analyses were performed with the CP WAX 52 CB column using the following temperature programme: 40°C - 100°C @ 10°C min^{-1} - 240°C @ 4°C min^{-1} (isothermal 25 min).

Gas Chromatography-Combustion-Isotope Ratio Mass Spectrometry (GC-C-IRMS)

Delta S

A Finnigan MAT Delta-S stable isotope MS coupled to a Varian 3400 GC fitted with a SPI injector (electron ionisation 100eV, 1mA; triple Faraday cup collectors for *m/z* 44, 45 and 46; CuO/Pt combustion reactor set at 850°C) was used. All samples were analysed in triplicate using helium as carrier gas and a ZB WAX column (Phenomenex; 60m x 0.32mm i.d. 0.2µm film thickness) with the following temperature programme 40°C - 100°C at 10°C min^{-1} - 240°C at 4°C min^{-1} (isothermal 25 min).

Delta Plus XL

A Finnigan MAT Delta Plus XL stable isotope MS linked to a Hewlett Packard 6890 GC equipped with a split/splitless injector (electron ionisation 100eV, 1mA; triple Faraday cup collectors for *m/z* 28, 29 and 30; CuO/NiO/Pt combustion reactor set at 940°C; Cu reduction reactor set at 600°C) was used. Samples were analysed using the ZB WAX column and helium as carrier gas with the following temperature programmes for Me,H maleimide (**36b**) and caffeine (**62**) respectively: 80°C - 100°C @ 10°C min^{-1} - 210°C @ 5°C min^{-1} (isothermal for 5 min) and 150°C - 240°C @ 10°C min^{-1} (isothermal 10 min).

High Performance Liquid Chromatography-Atmospheric Pressure Chemical Ionisation-Mass Spectrometry (HPLC-APCI-MS)

A Waters 600-MS HPLC system (with Millenium software) was linked to a Finnigan MAT TSQ 700 triple quadrupole MS *via* a Finnigan MAT APCI interface (vaporiser

temperature 450°C; capillary temperature 300°C; corona discharge current 7μA). Nitrogen was used as the sheath gas (50 psi), with the auxillary gas turned off. On-line separation of chlorins was achieved using reversed phase HPLC; Phenomenex ODS3 column (150 mm x 4.6 mm i.d., 1 ml min^{-1}) with a guard column (30 mm x 4.6 mm i.d.) and gradient solvent program (Table 7.1). Separation was also monitored with an on-line Waters 996 PDA detector, which provided electronic spectra of individual components from 350 to 700nm.

Table 7.1 Gradient solvent programme employed for chlorin analysis

Time (min)	Acetone (%)	MeOH (%)	H_2O (%)
0	0	80	20
5	0	80	20
15	30	60	10
25	30	60	10
35	60	30	10
50	90	5	5
80	90	5	5
85	0	80	20

STRUCTURES

1

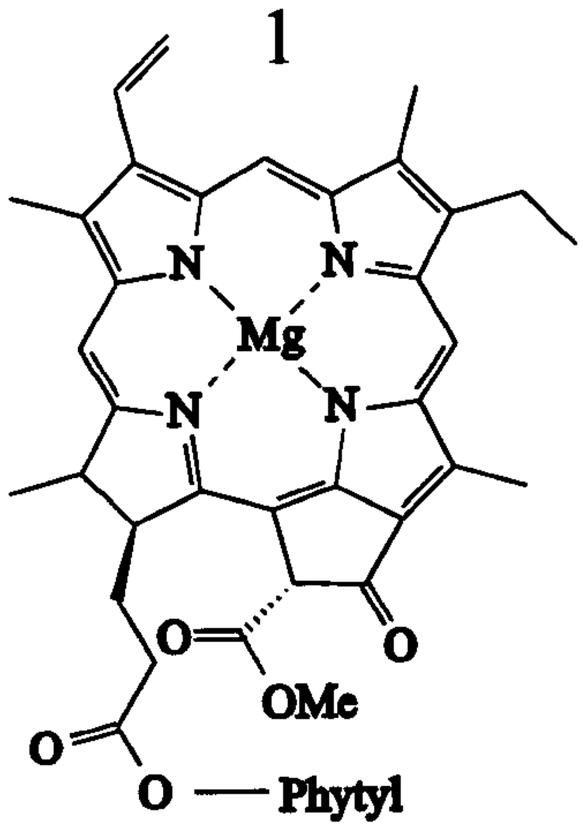

Chlorophyll *a*

2

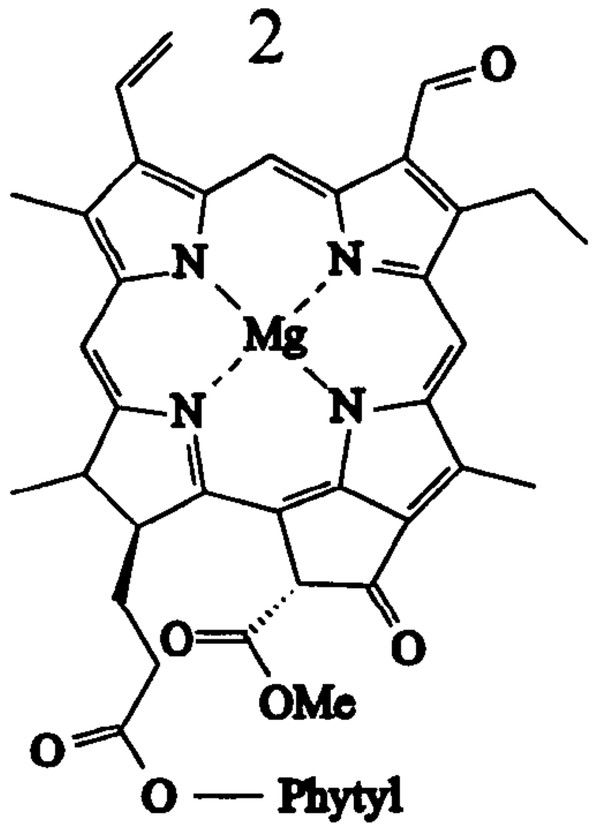

Chlorophyll *b*

4

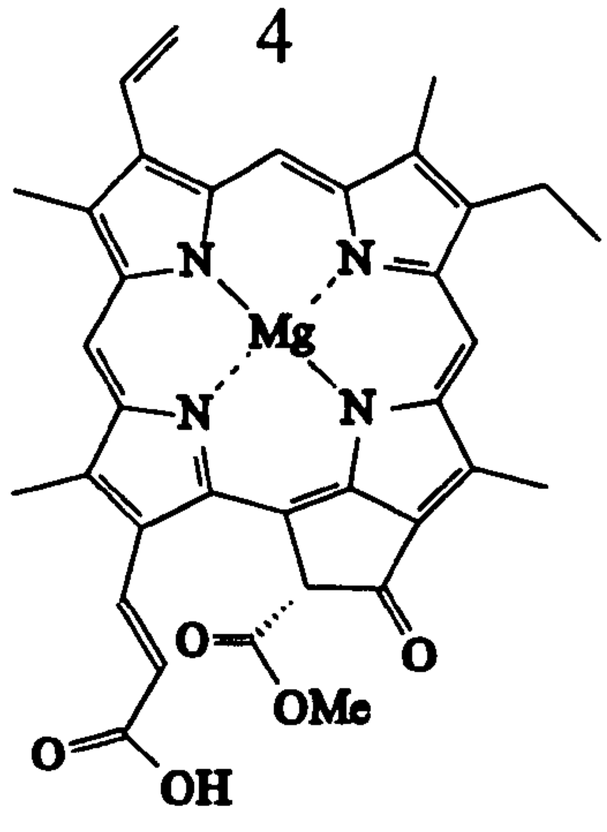

Chlorophyll *c* 1

3

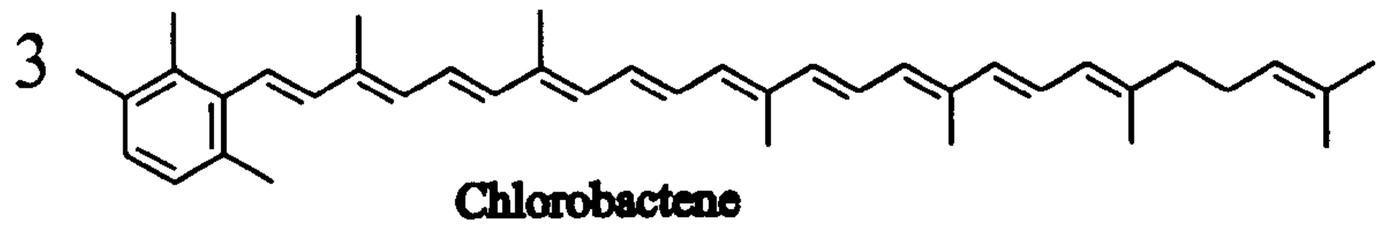

Chlorobactene

5

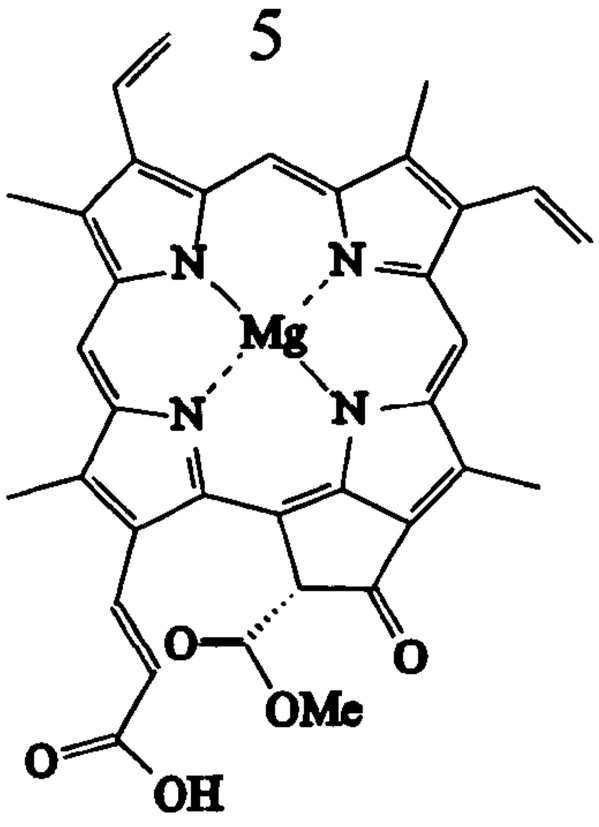

Chlorophyll *c* 2

6

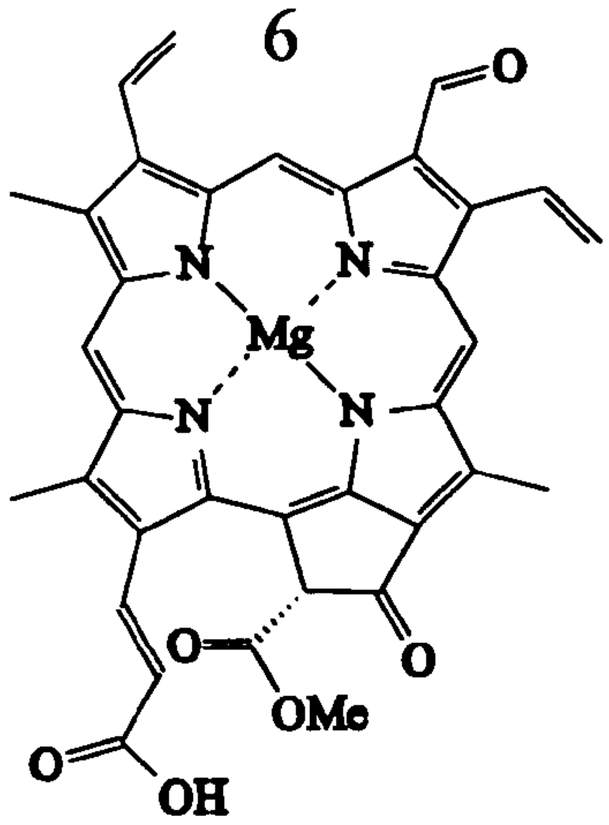

Chlorophyll *c* 3

7

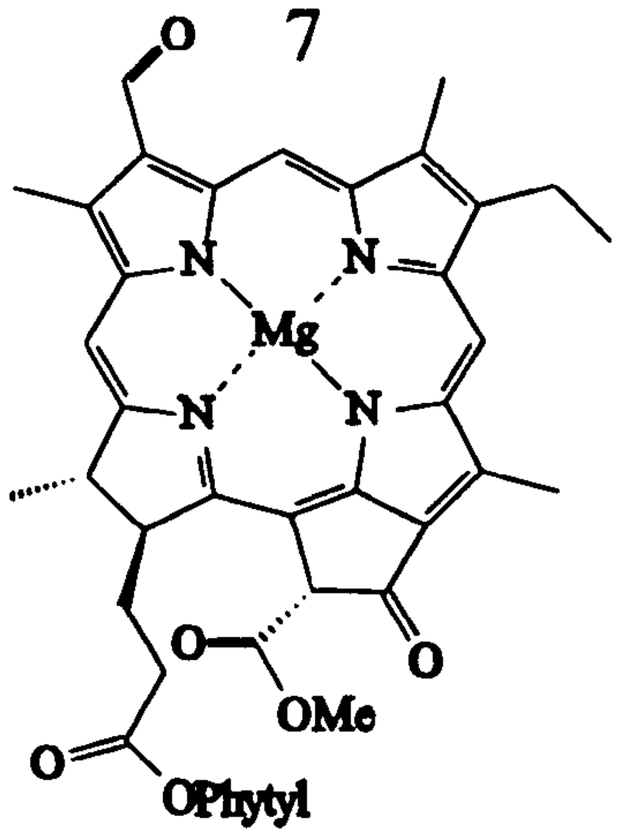

Chlorophyll *d*

8

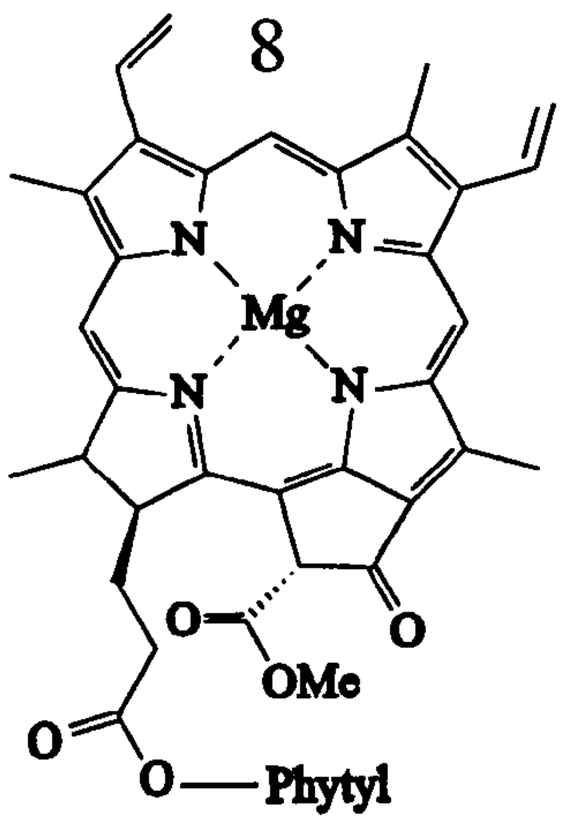

[8-Vinyl]-Chl *a*

9

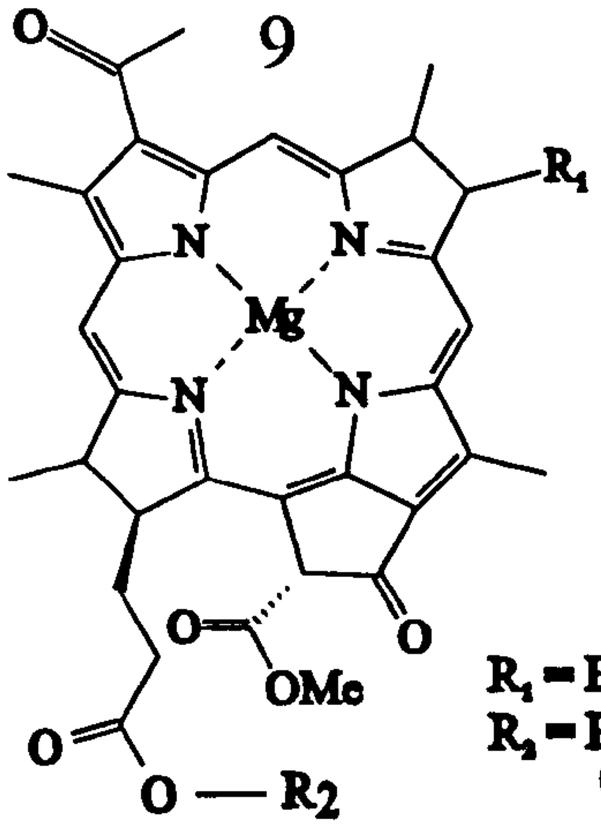

Bacteriochlorophylls *a*

10

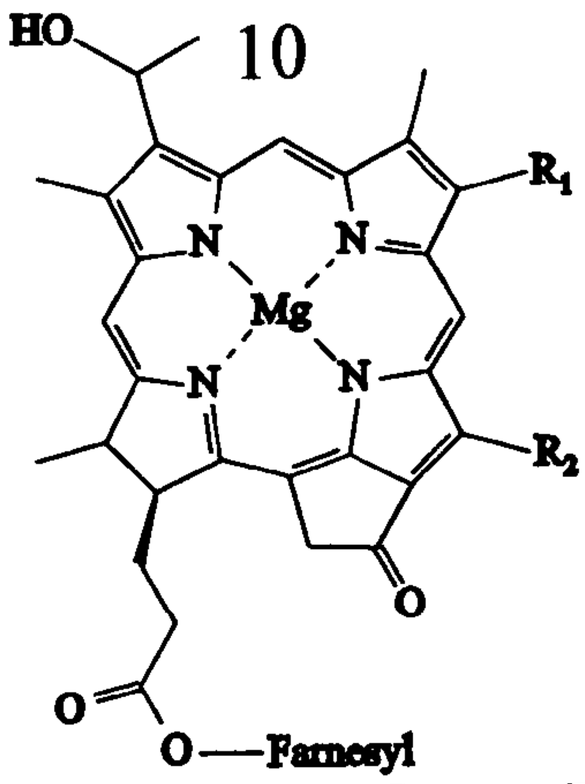

R_1 = Et, *n*-Pr, *i*-Bu, neo-Pent
R_2 = Me, Et

Bacteriochlorophylls *d*

11

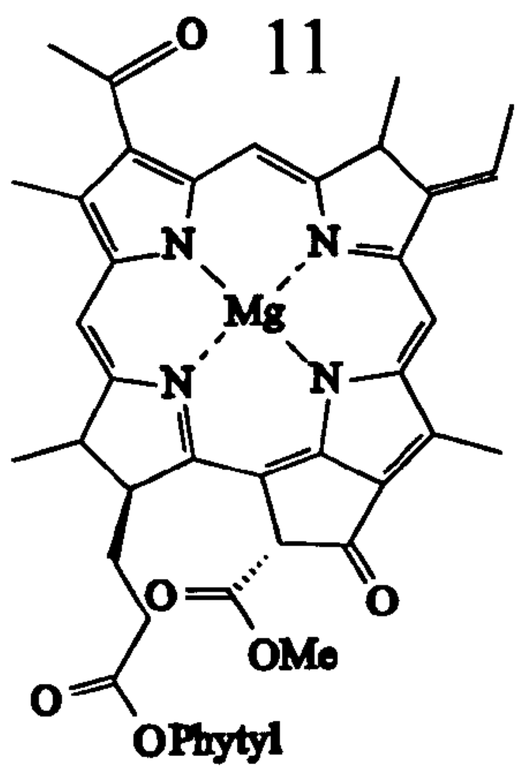

Bacteriochlorophylls *b*

12

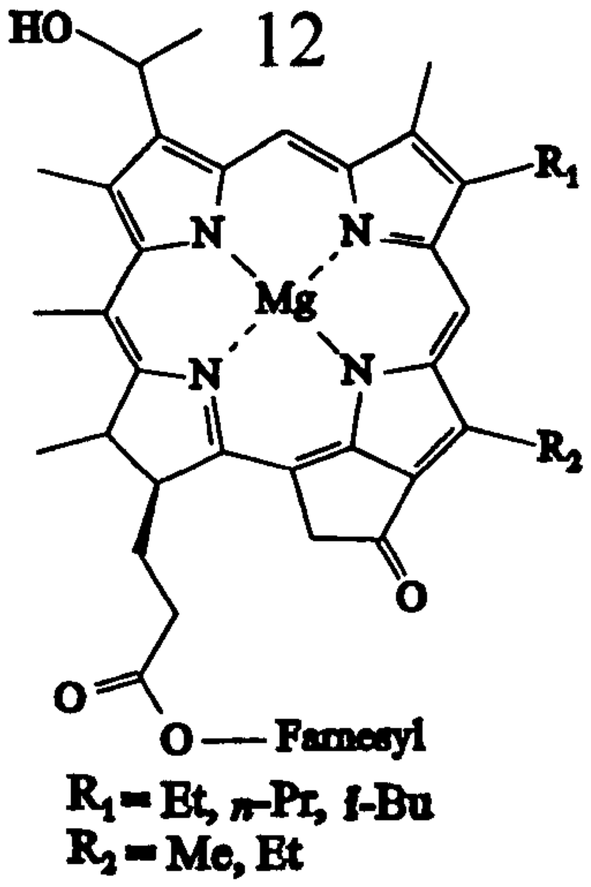

R_1 = Et, *n*-Pr, *i*-Bu
R_2 = Me, Et

Bacteriochlorophylls *c*

13

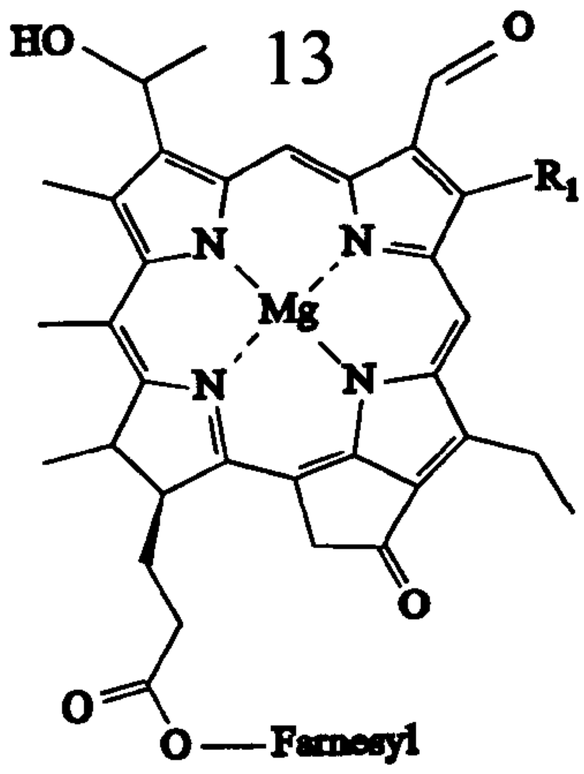

R_1 = Et, *n*-Pr, *i*-Bu

Bacteriochlorophylls *e*

14

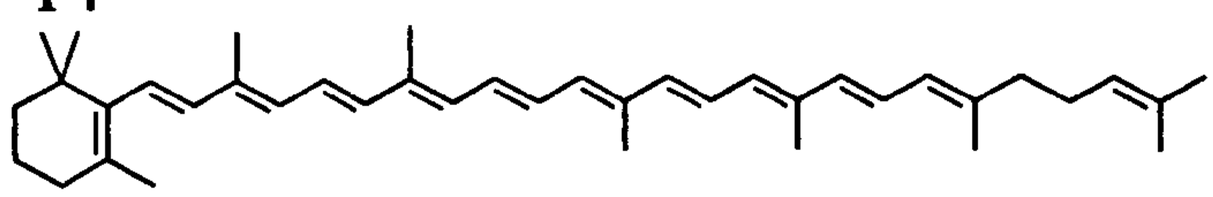

γ-carotene

15

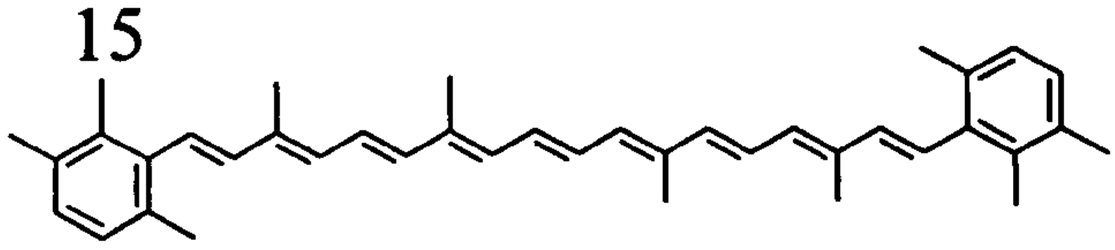

Isorenieratene

16

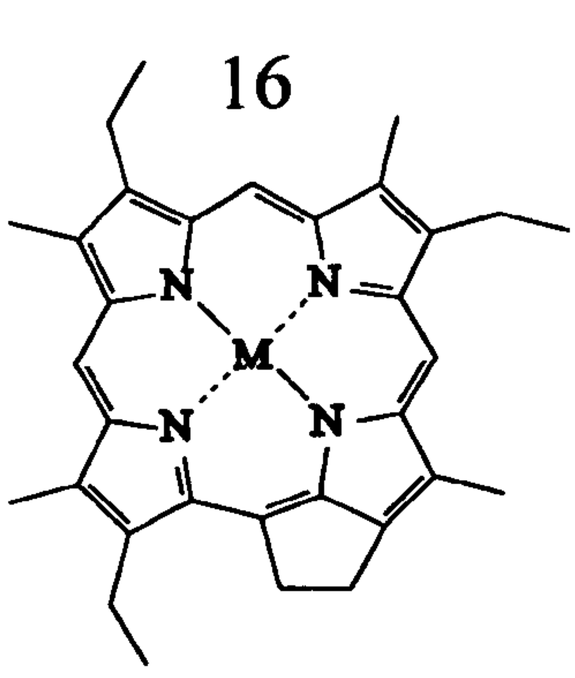

DPEP

17

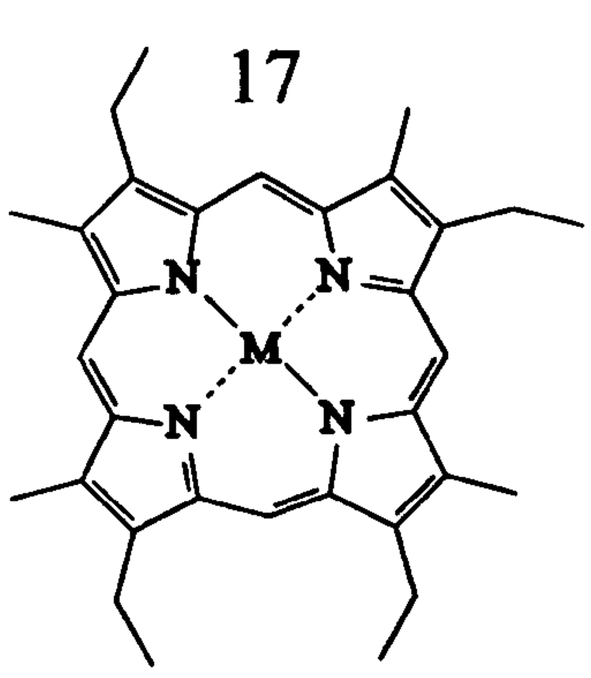

Actioporphyrin III

18 a R = Me
b R = Et

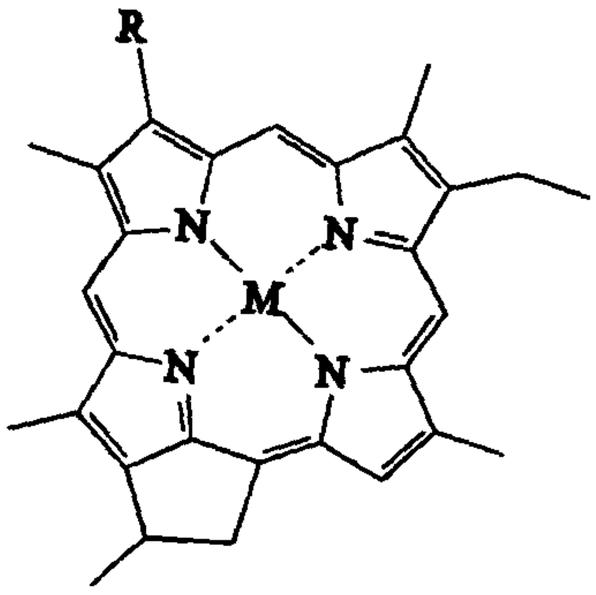

19 a R = Me
b R = Et

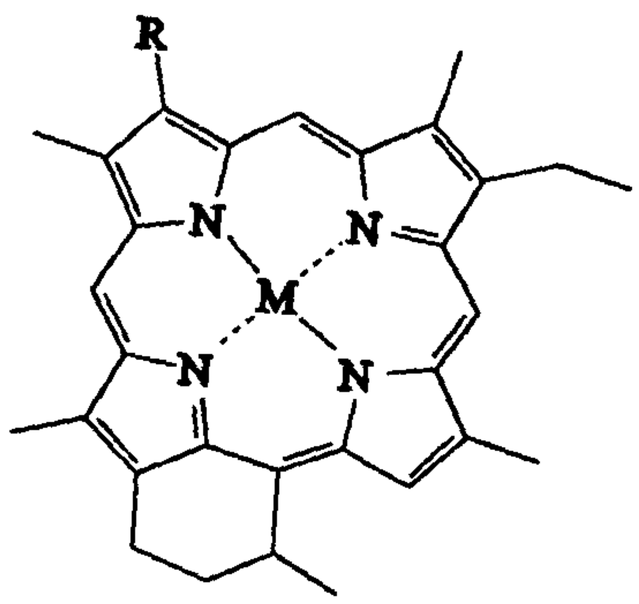

20 a R = Me
b R = Et

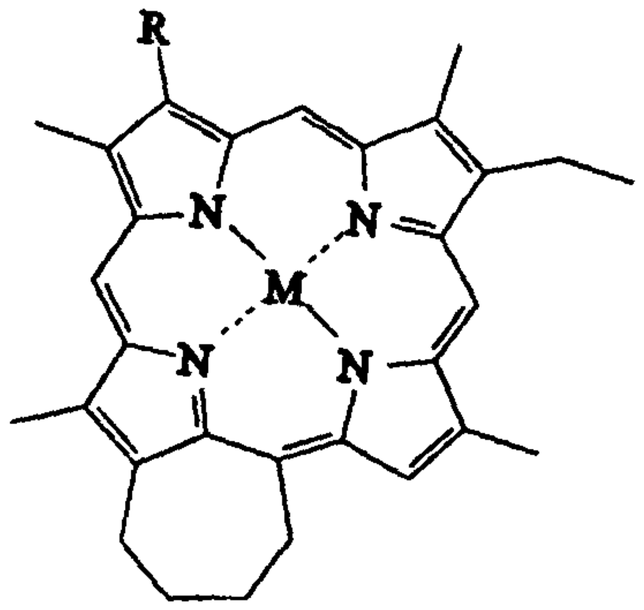

21 a R = Me
b R = Et

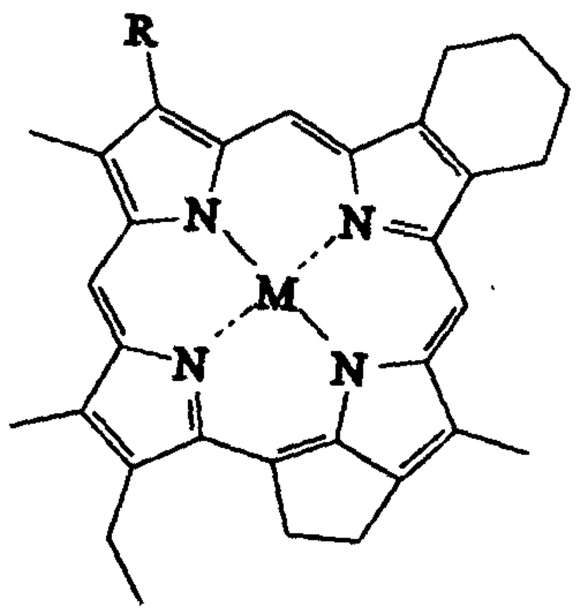

22

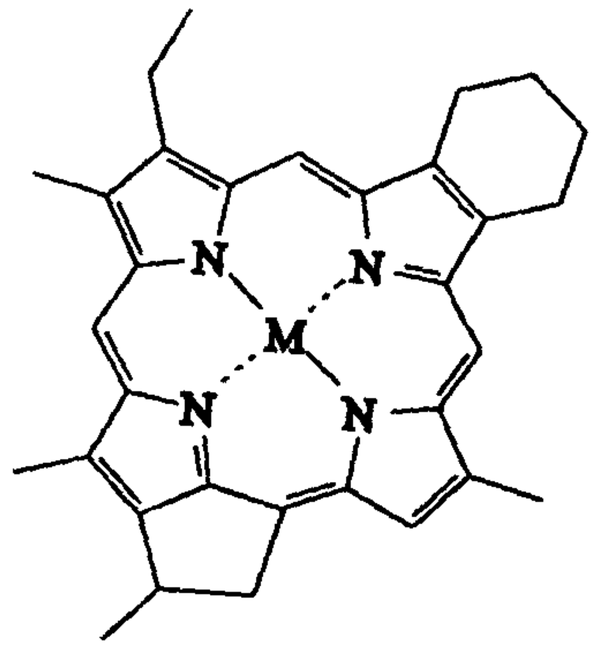

23 a R = Me
b R = Et

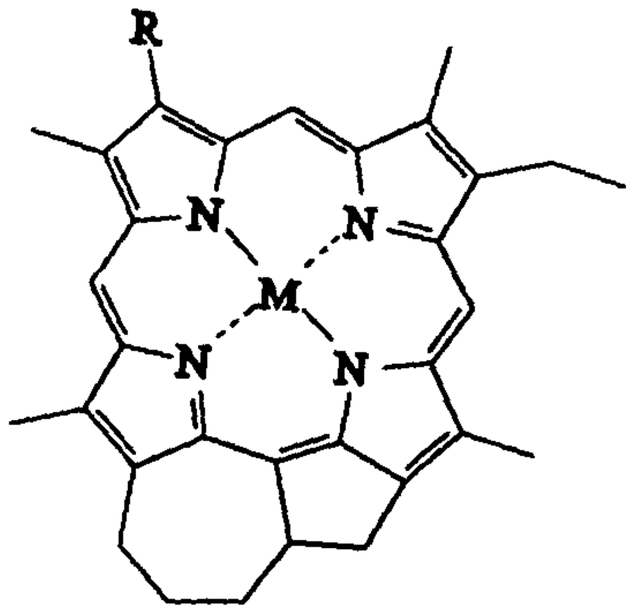

24 a R = Me
b R = Et

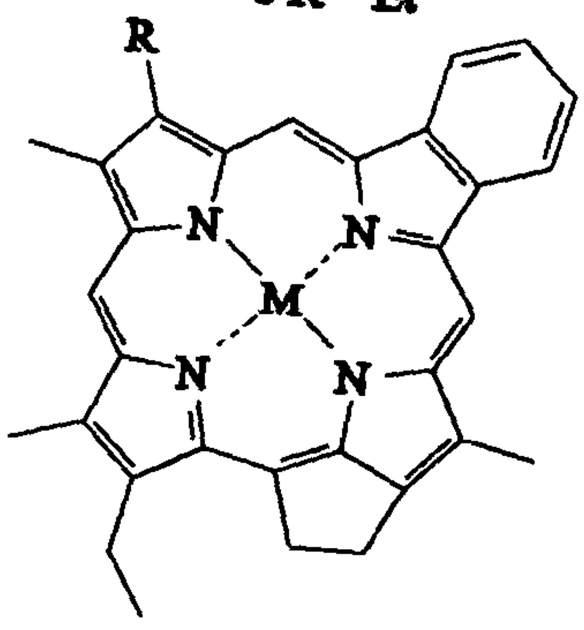

25

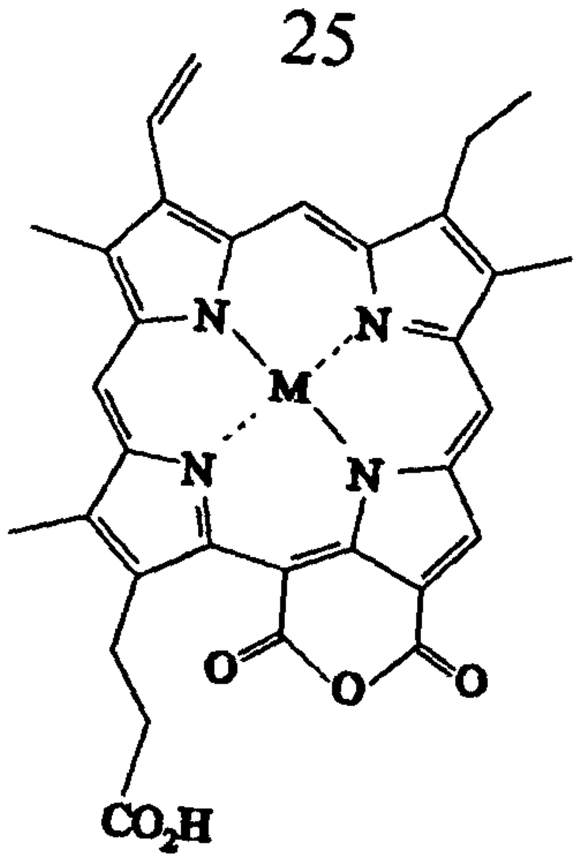

26

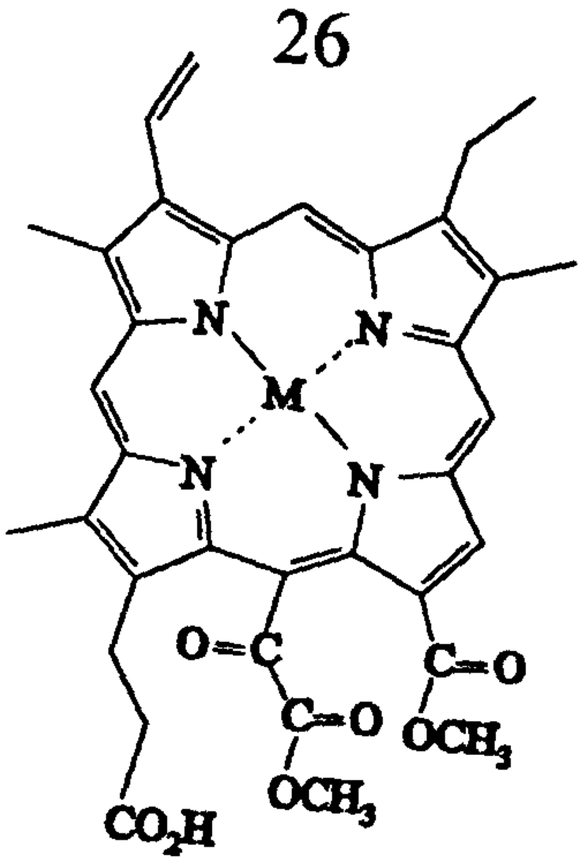

27 a R = H
b R = Et

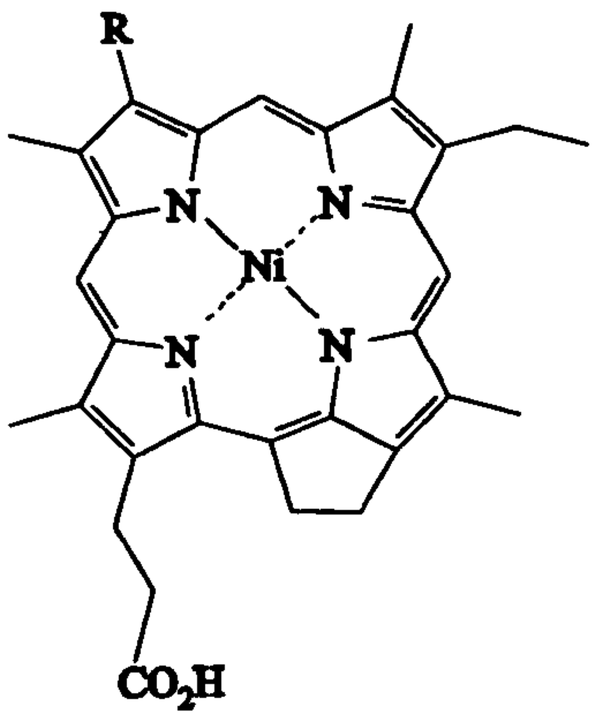

28 a R = Et
b R = *n*-Pr
c R = *i*-Bu

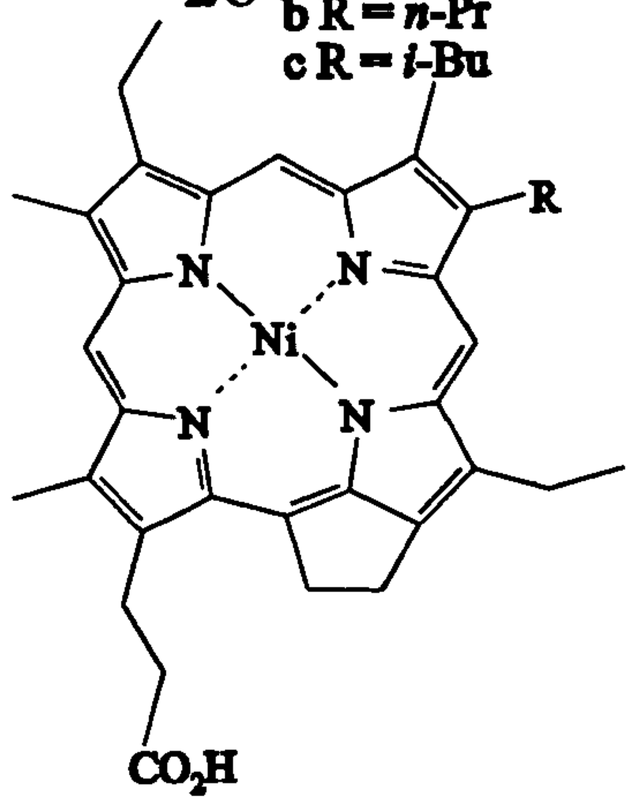

29

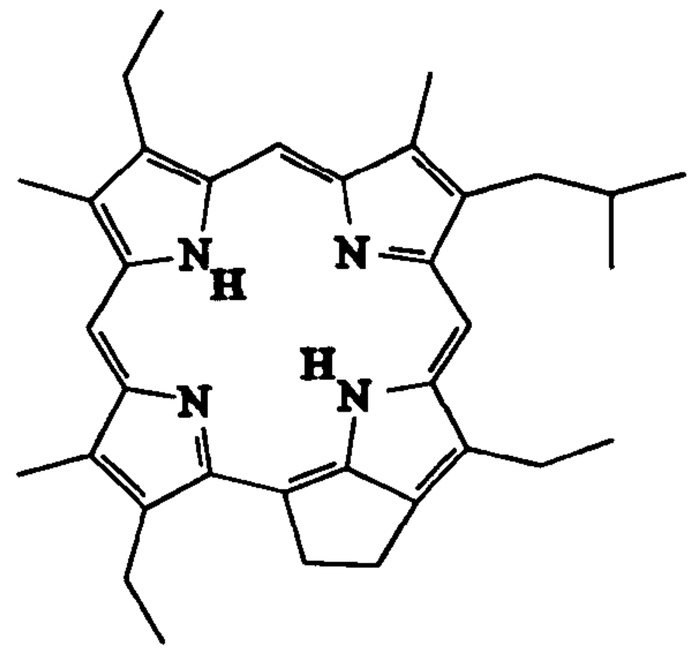

30

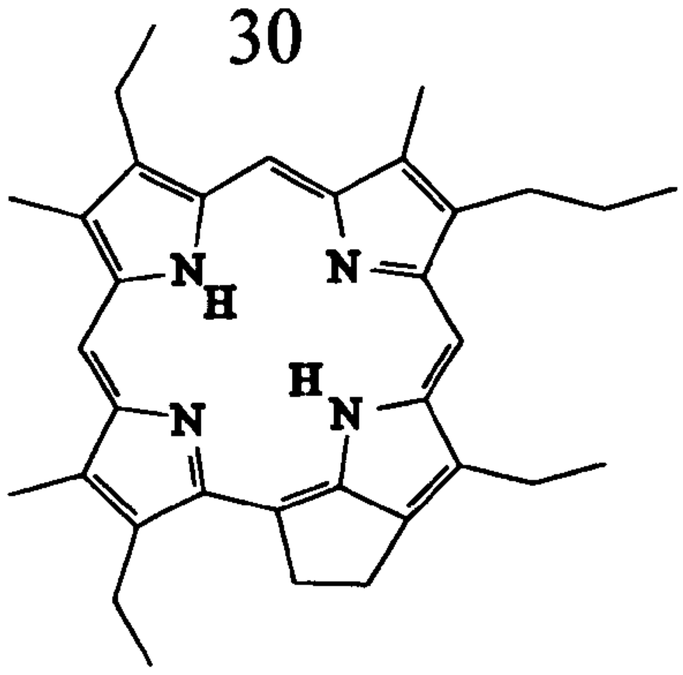

31

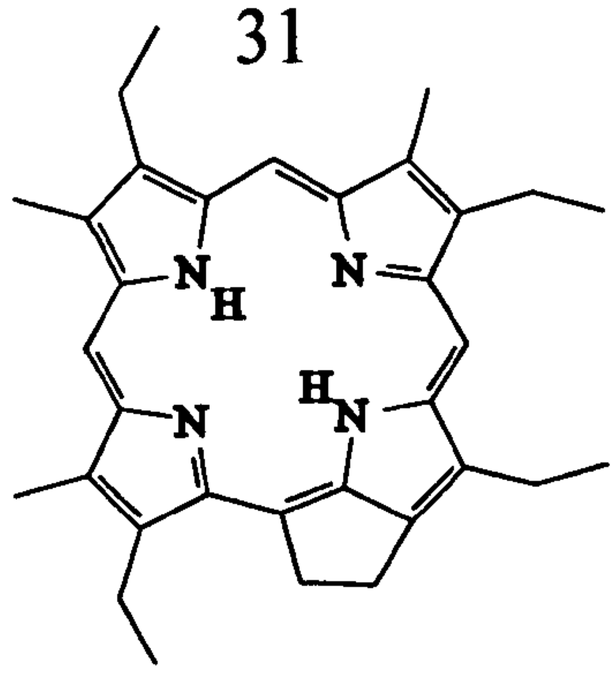

32

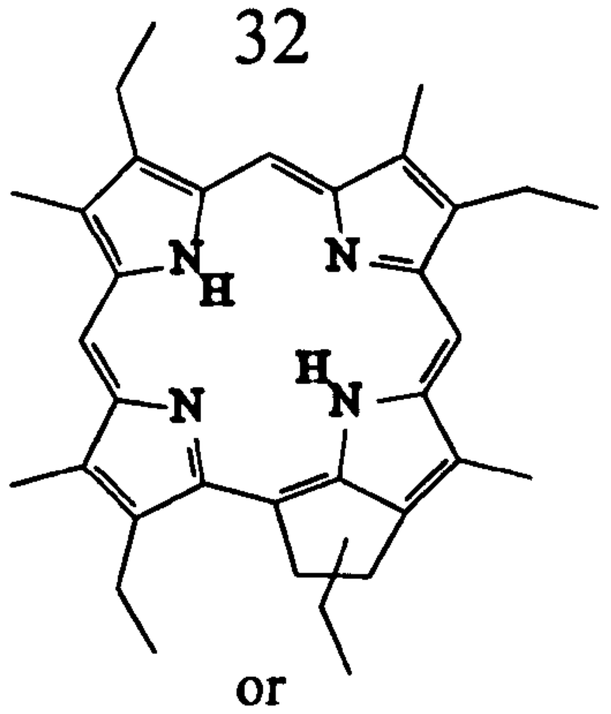

or

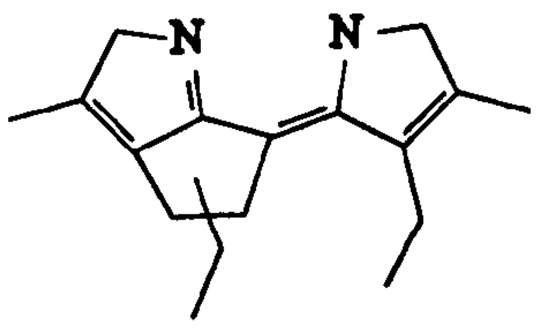

33

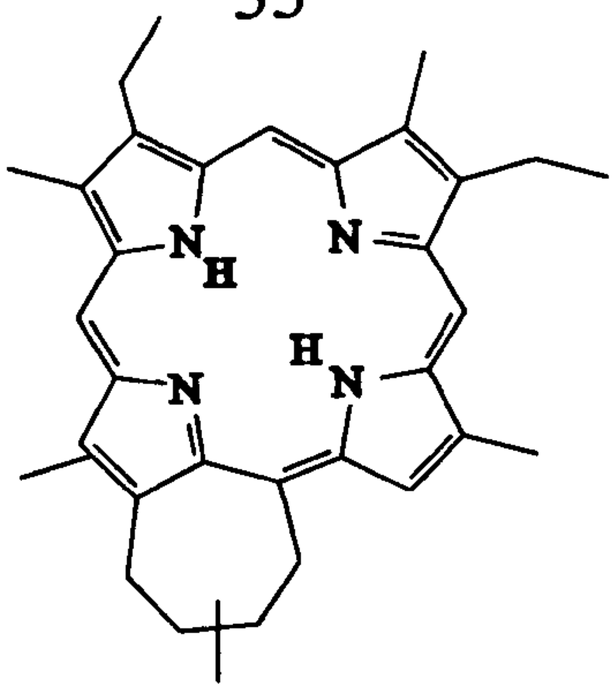

35

34

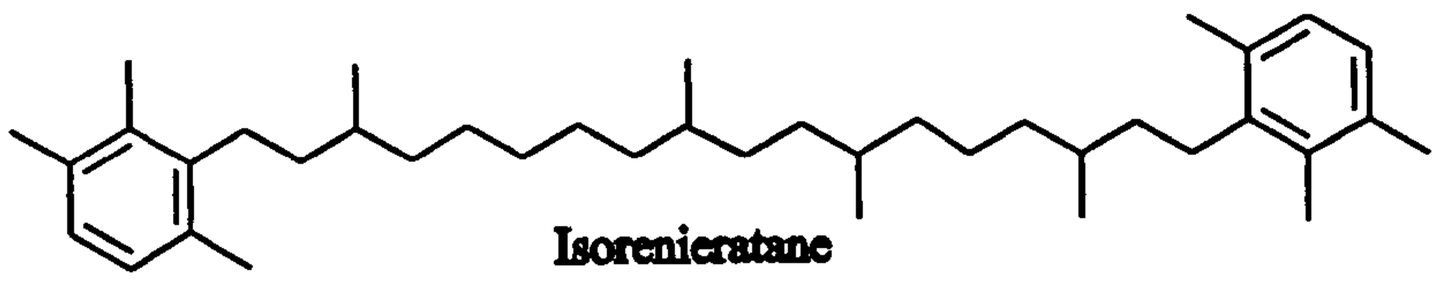

Isorenieratane

36 a R = Et
b R = H
c R = *n*-Pr
d R = Me
e R = *sec*-Bu
f R = *i*-Bu
g R = *n*-Bu
h R = *n*-Hex
i R = *i*-Pr
j R = *n*-Pentyl

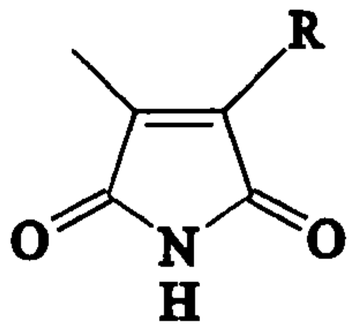

37

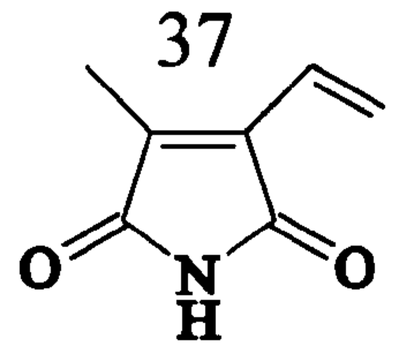

Me,vinyl maleimide

38

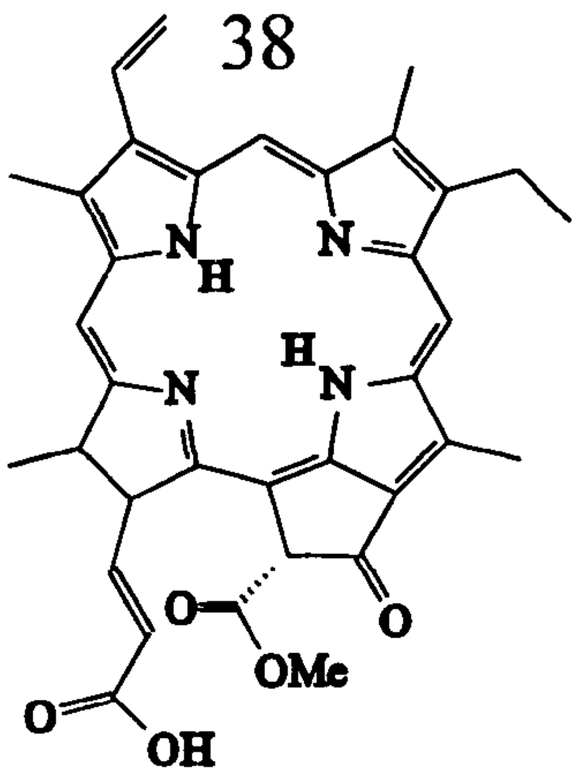

Pheophorbide *a*

39

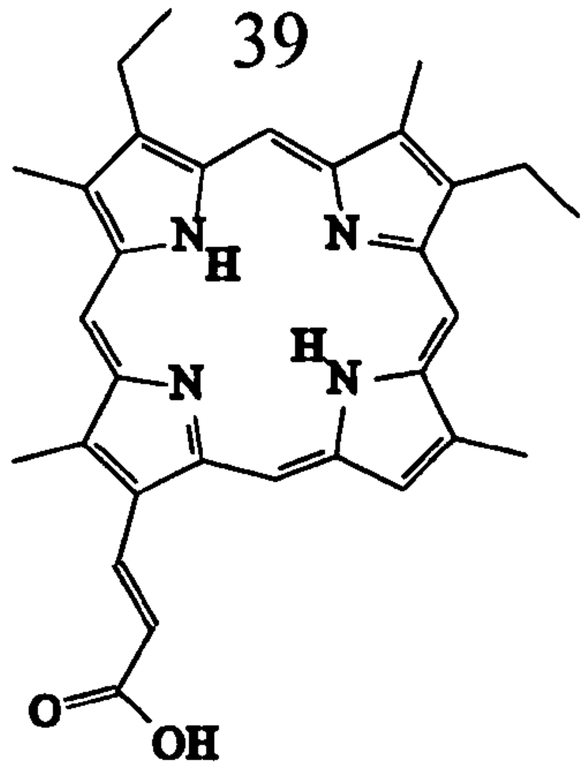

Pyrroporphyrin XV

40

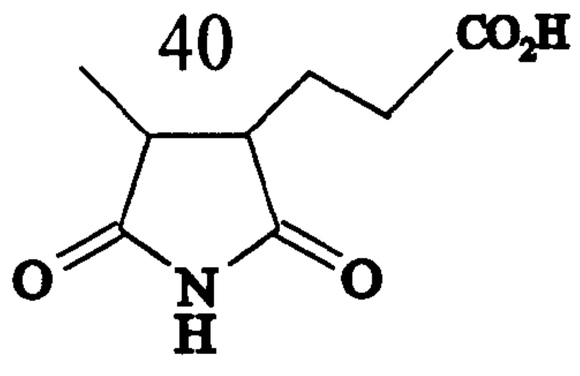

Dihydrohematinic acid

41

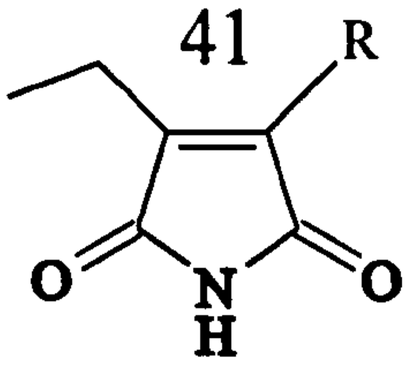

a R = H
b R = *n*-Pr
c R = Et

42

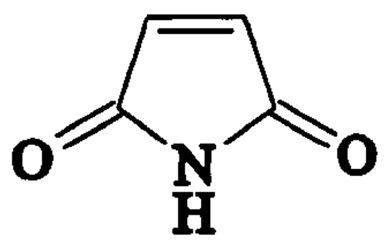

H,H maleimide

43

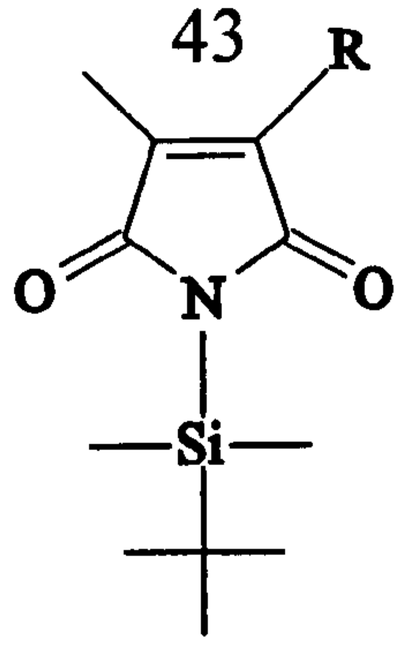

a R = Et
b R = *n*-Pr
c R = *i*-Bu

44

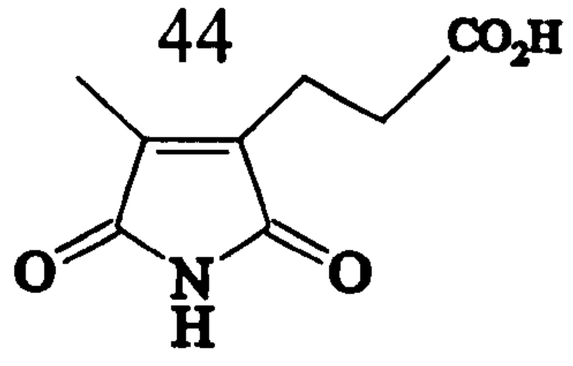

Hematinic acid

45

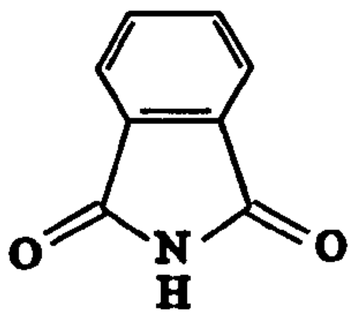

Phthalimide

46

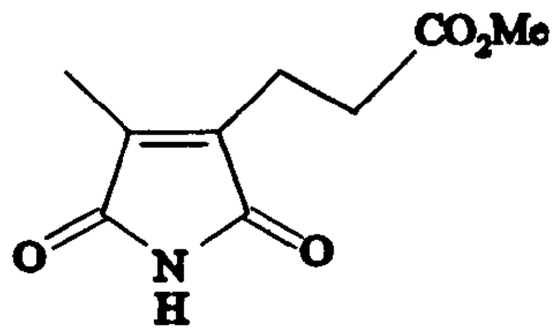

Hematinic acid methyl ester

47

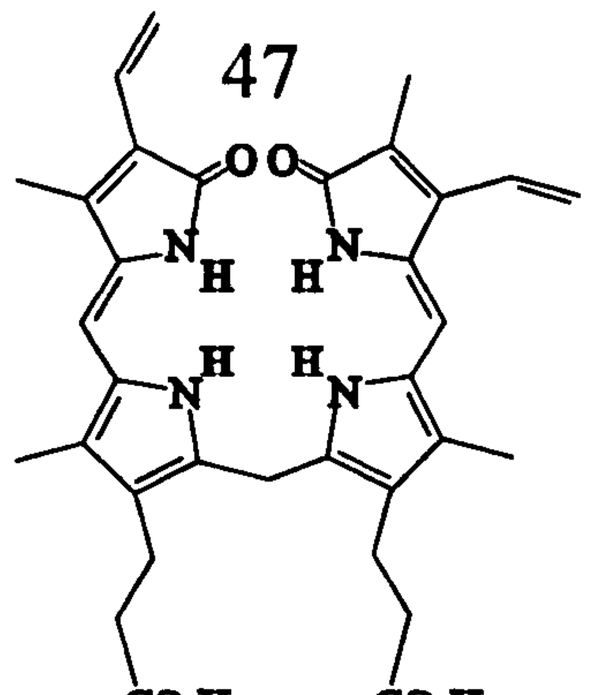

Bilirubin

48

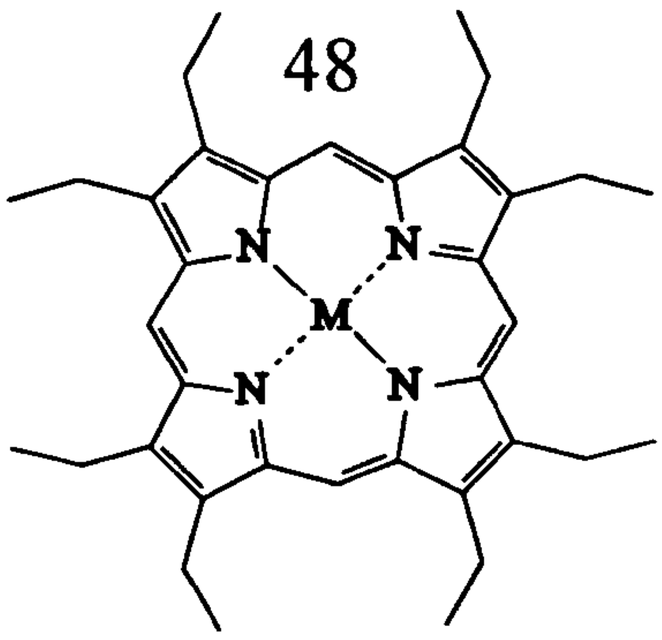

Octaethylporphyrin

49

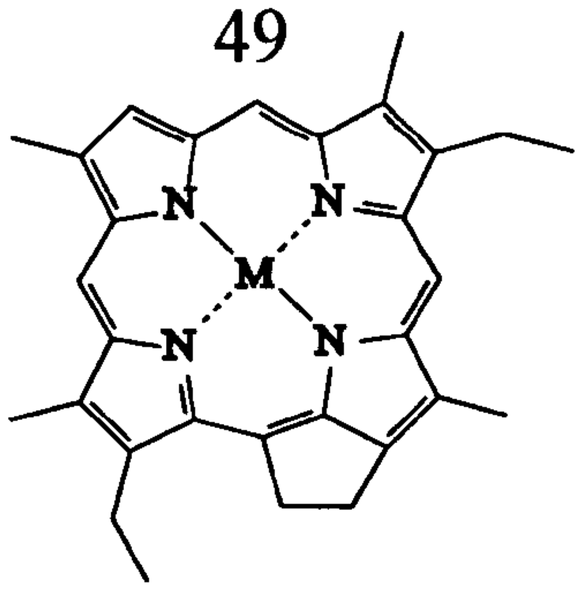

C_{30} DPEP

50

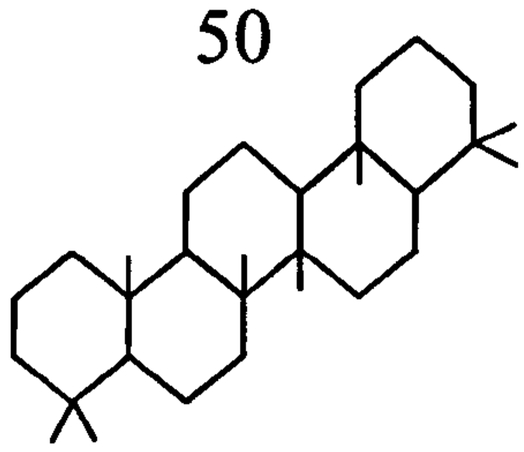

Gammacerane

51

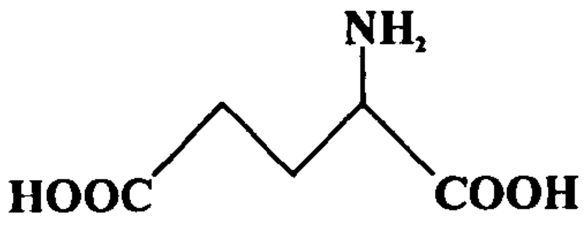

Glutamic acid

52

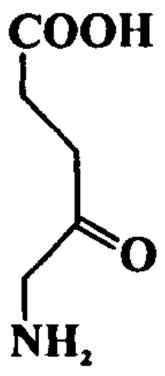

5-aminolevulinic acid

53

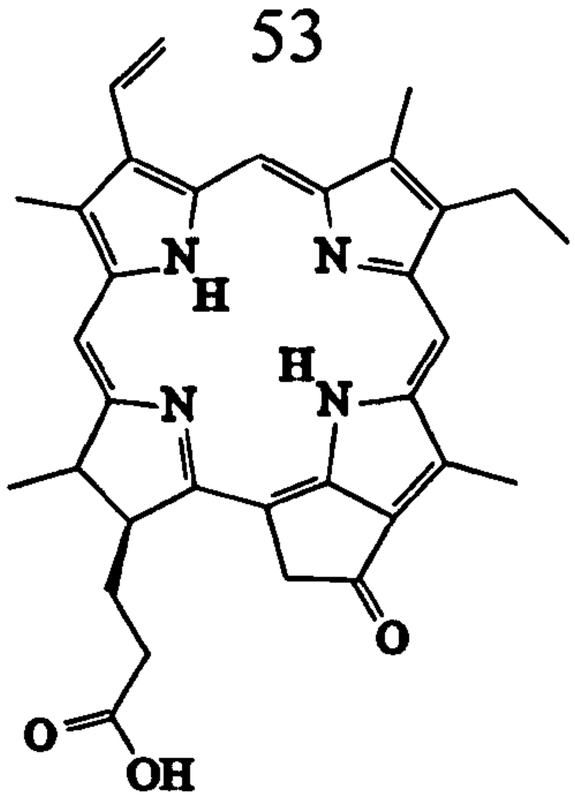

Pyropheophorbide *a*

54

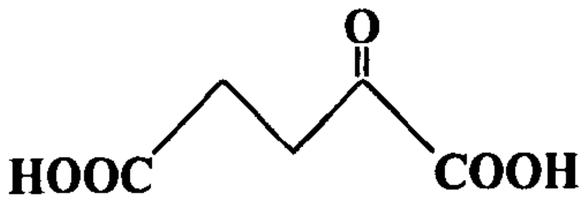

2-Oxoglutarate

55

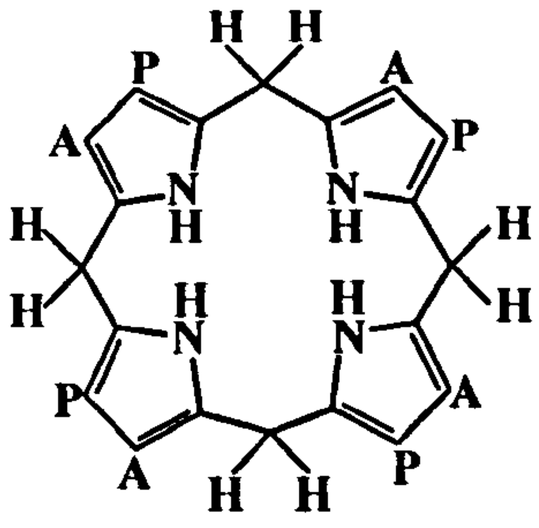

Uroporphyrinogen I

56

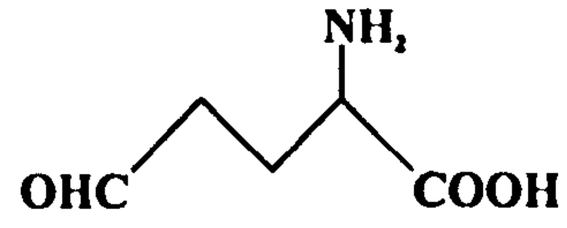

Glutamic acid-1-semialdehyde

57

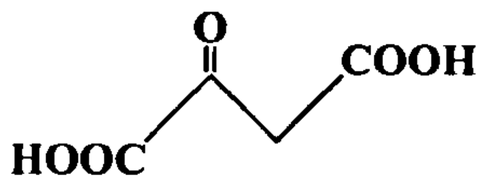

Oxaloacetic acid

58

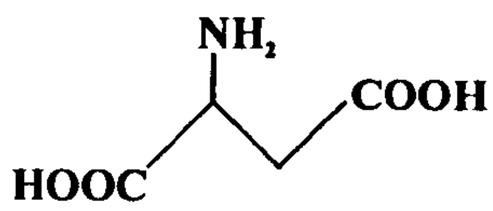

Aspartic acid

59

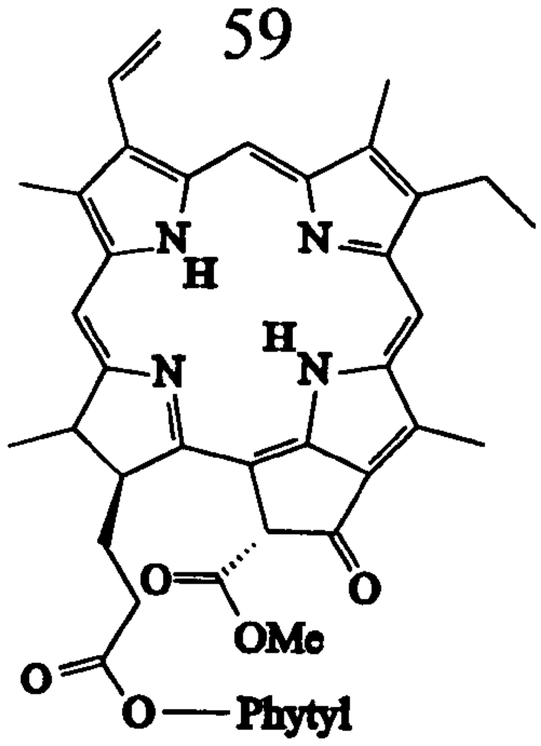

Pheophytin *a*

60

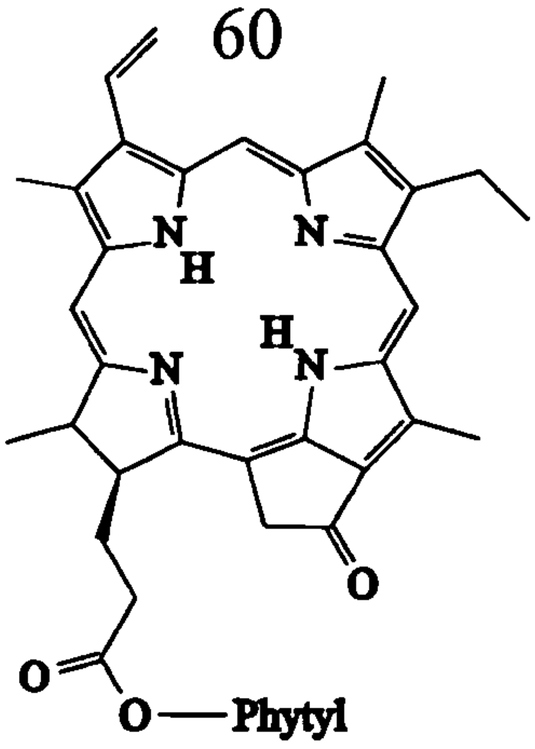

Pyropheophytin *a*

61

C-E-ring derivative

62

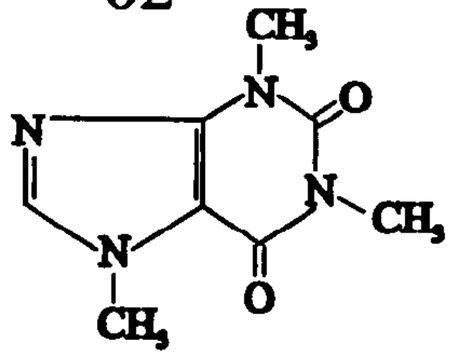

Caffeine

REFERENCES

REFERENCES

Adam P., Schmid J.C., Mycke B., Strazielle C., Connan J., Huc A., Riva A. and Albrecht P. (1993) Structural investigation of nonpolar sulphur cross-linked macromolecules in petroleum. *Geochim. Cosmochim. Acta*, **57**, 3395-3419

Aerssens E. Tiedje J.M. and Averill B.A. (1986) Isotope labelling studies on the mechanism of N-N bond formation in denitrification. *Journal of Biological Chemistry*, **261**, 9652-9656

Altabet M.A., Deuser W.G., Honjo S. and Stienen C. (1991) Seasonal and depth-related changes in the source of sinking particles in the North Atlantic. *Nature*, **354**, 136-139

Altabet M.A., Francois R., Murray D.W. and Prell W.L. (1995) Climatically-linked variations in Arabian Sea denitrification from sediment $^{15}N/^{14}N$. *Nature*, **373**, 506-509

Altabet M.A. and McCarthy J.J. (1985) Temporal and spatial variations in the natural abundance of 15N in PON from a warm-core ring. *Deep-Sea Research*, **32**, 755-772

Ambrose S.H. and DeNiro M.J. (1986) The isotopic ecology of East African mammals. *Oecologia*, **69**, 395-406

Arthur *et al.*, (1984) Rhythmic bedding in Mesozoic-Cenozoic pelagic carbonate sequences: the primary and diagenetic origin of Melankovitch-like cycles. In: *Milankovitch and Climate* (Eds. Berger A., Imbrie J., Hays J., Kukla G. and Saltzman B.), Riedel Publ. Co., Holland, pp. 191-222

Arthur M.A., Dean W.E. and Pratt L.M. (1988) Geochemical and climatic effects of increased marine organic carbon burial at the Cenomanian/Turonian boundary. *Nature*, **335**, 714-717

Arthur M.A., Hinga K.R., Pilson M.E.Q., Whitaker E. and Allard D. (1991) Estimates of pCO_2 for the last 120 Ma based on the $\delta^{13}C$ of marine phytoplanktonic organic matter. *Eos Trans. AGU*, **72**, 166

Arthur M.A., Jenkyns H.C., Brumsack H.J. and Schlanger S.O. (1990) Stratigraphy, geochemistry and palaeoceanography of organic carbon-rich Cretaceous sequences. In: *Cretaceous resources, events and rhythms* (Eds: Ginsburg R.N. and Beaudoin B.), Kluwer Academic Press, Dordrecht, pp. 75-119

Arthur M.A. and Premoli Silva I. (1982) Development of widespread organic-rich strata in the Mediterranean Tethys. In: Nature and origin of Cretaceous carbon-rich facies (Eds: Schlanger S.O. and Cita M.B.), Academic Press, London, pp. 7-54

Arthur M.A. and Sageman B.B. (1994) Marine black shales: Depositional mechanisms and environments of ancient deposits. *Annu. Rev. Earth Planet. Sci.*, **22**, 499-551

Arthur M.A., Schlanger S.O., Jenkyns H.C. (1987) The Cenomanian-Turonian oceanic anoxic event, II. Palaeoceanographic controls on organic matter production and preservation. See Brooks and Fleet 1987, pp. 401-420

Baker E.W., Yen T.F., Dickie J.P., Rhodes R.E. and Clark L.F. (1967) Mass spectrometry of porphyrins. II. Characterisation of petroporphyrins. *J. Am. Chem. Soc.*, **89**, 3631-3639

Barakat A.O. and Rullkötter J. (1998) Product distribution from oxidative degradation of sulphur-rich kerogens from the Nordlinger Ries (southern Germany). *Fuel*, **77**, 85-94

Barron E.J. (1983) A warm, equable Cretaceous: the nature of the problem. *Earth-Science Reviews*, **19**, 305-338

Barwise A.J.G. and Roberts I. (1984) Diagenetic and catagenetic pathways for porphyrins in sediments. *Org. Geochem.*, **6**, 167-176

Battersby A.R., Fookes C.J.R., Matcham G.W.J. and McDonald E. (1980) Biosynthesis of the pigments of life: formation of the macrocycle. *Nature*, **285**, 17-21

Beale S.I and Weinstein J.D. (1991) Biochemistry and regulation of photosynthetic pigment formation in plants and algae. In: *Biosynthesis of Tetrapyrroles* (ed. Jordan P.M.), Elsevier, pp. 155-235

Beaumont V.I., Jahnke L.L. and Des Marais D.J. (2000) Nitrogen isotopic fractionation in the synthesis of photosynthetic pigments in *Rhodobacter capsulatus* and *Anabaena cylindrica*. *Org. Geochem.*, **31**, 1075-1085

Berger W.H. (1979) Impact of deep-sea drilling on paleoceanography. In: *Deep Drilling Results in the Atlantic Ocean: continental margins and paleoenvironment.* (Eds. Talwani M., Hay W. and Ryan W.B.F.). Maurice Ewing Series, **3**, *Am. Geophys. Union*, 297-314

Berger W.H., Smetacek V.S. and Wefer G. (1989) Productivity of the oceans: Present and past. New York: Wiley Interscience, **471**

Berner R.A. (1992) Palaeo-CO_2 and climate. *Nature*, **358**, 114-114

Berner R.A. (1991) A model for atmospheric CO_2 over Phanerozoic time. *Am. J. Sci.*, **291**, 339-376

Bidigare R.R., Fluegge A., Freeman K.H., Hanson K.L., Hayes J.M., Hollander D., Jasper J.P., King L.L., Laws E.A., Milder J., Millero F.J., Pancost R., Popp B.N., Steinberg P.A. and Wakeham S.G. (1997) Consistent fractionation of ^{13}C in nature and in the laboratory: Growth-rate effects in some haptophyte algae. *Global Biogeochemical Cycles*, **11**, 279-292

Bidigare R.R., Hanson K.L., Buesseler K.O., Wakeham S.G., Freeman K.H., Pancost R.D., Millero F.J., Steinburg P., Popp B.N., Latasa M., Landry M.R. and Laws E.A. (1999) Iron-stimulated changes in ^{13}C fractionation and export by

equatorial Pacific phytoplankton: Toward a paleogrowth rate proxy. *Paleoceanography*, **14**, 589-595

Bidigare R.R., Kennicutt M.C., Keeney-Kennicutt W.L. and Macko S.A. (1991) Isolation and purification of chlorophylls *a* and *b* for the determination of stable carbon and nitrogen isotope compositions. *Anal. Chem.*, **63**, 130-133

Bilby R.E., Fransen B.R. and Bisson P.A. (1996) Incorporation of nitrogen and carbon from spawning coho salmon into the trophic system of small streams: Evidence from stable isotopes. *Canadian Journal of Fisheries and Aquatic Sciences*, **53**, 164-177

Bonnett R. and Czechowski F. (1980) Gallium porphyrins in bitumous coal. *Nature*, **283**, 465-466

Bonnett R. and Czechowski F. (1981) Metals and metal complexes in coal. *Phil. Trans. R. Soc. Lond. A*, **300**, 51-63

Bonnett R., Burke P.J. and Reszka A. (1983) Iron porphyrins in coal. *J. Chem. Soc., Chem. Commun.*, 1085-1087

Bonnett R. and McDonagh A.F. (1969) Methylvinylmaleimide (the "nitrite body") from chromic acid oxidation of tetrapyrrolic pigments. *Chemistry and Industry*, **4**, 107-108

Boreham C.J., Fookes J.R., Popp B.N. and Hayes J.M. (1989) Origins of etioporphyrins in sediments: evidence from stable carbon isotopes. *Geochim. Cosmochim. Acta*, **53**, 2451-2455

Brassell S.C. (1993) Applications of biomarkers for delineating marine paleoclimate fluctuations during the Pleistocene. In *Organic Geochemistry*: *Principles and Applications*, ed. M.H. Engel and S.A. Macko, pp. 699-738. Plenum, New York

Brassell S.C., Comet P.A., Eglinton, G., Isaacson P.J., McEvoy J., Maxwell J.R., Thomson I.D., Tibbetts P.J.C. and Volkman J.K. (1980) Preliminary lipid analysis of sections 440A-7-6, 440B-3-5, 440B-8-4, 440B-68-2 and 436-11-4: legs 56 and 57, Deep Sea Drilling Project. *Initial Reports of the Deep Sea Drilling Project*, **56/57**, 1367-1390

Brassell S.C., Eglinton G. and Maxwell J.R. (1983) The geochemistry of terpenoids and steroids. *Biochem. Soc. Trans.*, **11**, 575-586

Bricaud A., Allali K., Morel A., Marie D., Veldhuis M.J.W., Partensky, F. and Vaulot D. (1999) Divinyl chlorophyll *a*-specific absorption coefficients and absorption efficiency factors for *Prochlorococcus marinus*: kinetics of photoacclimation. *Mar. Ecol. Prog. Ser.*, **188**, 21-32

Brown S.B., Smith K.M., Bisset G.M.F. and Troxler R.F. (1980) Mechanism of photo-oxidation of bacteriochlorophyll *c* derivatives. *J. Biol. Chem.*, **225**, 8063-8068

Brumsack H.J. (1980) Geochemistry of Cretaceous black shales from the Atlantic Ocean (DSDP Legs 11, 14, 36 and 41). *Chem. Geol.*, **31**, 1-25

Callot H.J. (1991) Geochemistry of Chlorophylls. *In*: Chlorophylls Scheer H. (*ed*) 339. CRC Press. Florida

Calvert S.E., Nielsen B. and Fontugne M.R. (1992) Evidence from nitrogen isotope ratios for enhanced productivity during formation of Eastern Mediterranean sapropels. *Nature*, **359**, 223-225

Cerling T.E., Harris J.M., MacFadden B.J., Leakey M.G., Quade J., Eisenmann V. and Ehleringer J.R. (1997) Global vegetation change through the Miocene/Pliocene boundary. *Nature*, **389**, 153-158

Chicarelli M.I. (1985) The porphyrins of Serpiano oil shale: structures and significance. Ph.D. Thesis, University of Bristol

Chicarelli M.I., Kaur S. and Maxwell J.R. (1987) Sedimentary porphyrins: Unexpected structures, occurrence and possible origins. In: *Metal complexes in fossil fuels: Characterisation and Processing* (Eds: Filby R.H. and Branthaver J.F.); ACS symposium series **344**, pp. 40-67

Cooper A.J.L., McDonald J.M., Gelbard A.S., Gledhill R.F. and Duffy T.E. (1979) The metabolic fate of ^{13}N-labelled ammonia in rat brain. *Journal of Biological Chemistry*, **254**, 4982-4992

Cranwell P.A. (1985) Long-chain unsaturated ketones in recent lacustrine sediments. *Geochim. Cosmochim. Acta*, **49**, 1545-1551

Cranwell P.A., Eglinton G. and Robinson N. (1987) Lipids of aquatic organisms as potential contributors to lacustrine sediments. II. *Org. Geochem.*, **11**, 513-527

Crawford N. (1998) Maleimides (1*H*-pyrrole-2,5-diones) from ancient sediments as indicators of photic zone anoxia. Ph.D. Thesis, University of Bristol

Dean W.E., Arthur M.A. and Stow D.A.V. (1984) Origin and geochemistry of Cretaceous deep-sea black shales and multicoloured claystones, with emphasis on Deep Sea Drilling Project Site 530, Southern Angola Basin. *Init. Repts. DSDP*, **75** (Eds: Hay W.W. *et al.*), 819-844

Dean W.E. and Gardener J.V. (1982) Origin and geochemistry of redox cycles of Jurassic to Eocene age, Cape Verde Basin (DSDP site 367), continental margin of north-west Africa. See Schlanger and Cita, 1982, pp. 55-75

Degens E.T., Emeis K.C., Mycke B. and Wiesner M.G. (1986) Turbidites, the principal mechanism yielding black shales in the early deep Atlantic Ocean. See Summerhayes and Shackleton (1986) pp. 361-376

de Graciansky P.C., Deroo G., Herbin J.P., Montadert L., Muller C., Schaaf A. and Sigal J. (1984) Ocean-wide stagnation episode in the Late Cretaceous. *Nature*, **308**, 346-349

Delwiche C.C., Zinke P.J., Johnson C.M., and Virginia R.A. (1979) Nitrogen isotope distribution as a presumptive indicator of nitrogen fixation. *Botanical Gazette*, **140**, 65-69

Demaison G.J. and Moore G.T. (1980) Anoxic environments and oil source-bed genesis. *Org. Geochem.*, **2**, 9-31

de Wit R. (1992) Sulphide-containing environments. *In*: Encyclopaedia of Microbiology, **4**, 105-121

de Wit R. and Caumette P. (1995) An overview of the brown-coloured isorenieratene-containiing green sulfur bacteria (Chlorobiaceae). *Org. Geochem.*: *developments and applications to energy, environment and human history*, 908-909

Didyk B.M., Simoneit B.R.T., Brassell S.C. and Eglinton G. (1978) Geochemical indicators of palaeoenvironmental conditions of sedimentation. *Nature*, *272*, 216-222

Dole M., Lane G.A., Rudd D.P. and Zaukelies D.A. (1954) Isotopic composition of atmospheric oxygen and nitrogen. *Geochim. Cosmochim. Acta*, **6**, 65-78

Dougherty R.C., Strain H.H., Svec W.A., Uphaus R.A. and Katz J.J. (1970) The structure, properties and distributions of chlorophyll *c*. *J. Am. Chem. Soc.*, **92**, 2826-2833

Ellsworth R.K. (1970) Gas chromatographic determination of some maleimides produced by the oxidation of heme and chlorophyll *a*. *J. Chromatogr.*, **50**, 131-134

Ellsworth R.K. and Aronoff S. (1968) Purification and mass spectra of maleimides from the oxidation of chlorophyll and related compounds. *Arch. Biochem. Biophys.*, **124**, 358-364

Erbacher J., Thurow J. and Littke R. (1996) Evolution patterns of radiolaria and organic matter variations: A new approach to identify sea-level changes in mid-Cretaceous pelagic environments. *Geology*, **24**, 499-502

Evans M.C.W., Buchanan B.B. and Arnon D.I. (1966) A new ferredoxin-dependent carbon reduction cycle in a photosynthetic bacterium. *Biochemistry*, **55**, 928-934

Fantle M.S., Dittel A.I., Schwalm S.M., Epifanio C.E. and Fogel M.L. (1999) A food web analysis of the juvenile blue crab, *Callinectes sapidus*, using stable isotopes in whole animals and individual amino acids. *Oecologia*, **120**, 416-426

Farrimond P., Eglinton G., Brassell S.C. and Jenkyns H.C. (1990) The Cenomanian/Turonian anoxic event in Europe: an organic geochemical study. *Mar. Pet. Geol.*, **7**, 75-89

Ficken K.J. (1994) Lipid and sulphur geochemistry of Recent sediments from oxic and anoxic environments. Ph.D. thesis, University of Newcastle

Finnigan MAT (1994) Isotope ratio mass spectrometer, Operating manual, section 2, pp. 5-7

Fischer A.G. and Arthur M.A. (1977) Secular variations in the pelagic realm. *Spec. Publ. Soc. Econ. Paleont. Miner.*, **25**, 19-50

Focht D.D. and Verstraete W. (1977) Biochemical ecology of nitrification and denitrification. *Advances in Microbial Ecology*, **1**, 135-214

Fogel M.L. and Cifuentes L.A. (1993) Isotope fractionation during primary production. In: Organic Geochemistry (Eds: Engel M.H. and Macko S.A.), Plenum Press, New York, pp. 73-98

Francois R. and Altabet M.A. (1992) Glacial to interglacial changes in surface nitrate utilization in the Indian sector of the southern ocean as recorded by sediment $\delta^{15}N$. *Paleoceanogr.*, **7**, 589-606

Freeman K.H. and Hayes J.M. (1992) Fractionation of carbon isotopes by phytoplankton and estimates of ancient CO_2 levels. *Global Biogeochemical Cycles*, **6**, 185-198

Gannes L.Z., Martínez del Rio C. and Kock P. (1998) Natural abundance variations in stable isotopes and their potential uses in animal physiological ecology. *Comp. Biochem. Physiol.*, **119**, 725-737

Gannes L.Z., O'Brien D.M. and Martínez del Rio C. (1997) Stable isotopes in animal ecology: Assumptions, caveats and a call for more laboratory experiments. *Ecology*, **78**, 1271-1276

Gibbison R. (1996) Porphyrins and 1*H*-pyrrole-2,5-diones (maleimides) as indicators of anoxygenic photosynthesis in palaeo water columns. Ph.D. Thesis, University of Bristol

Gibbison R., Peakman T.M., Maxwell J.R. (1995) Novel porphyrins as molecular fossils for anoxygenic photosynthesis. *Tetrahedron Lett.*, **36**, 9057-9060

Goretski J. and Hollocher T.C. (1988) Trapping of nitric oxide produced during denitrification by extracellular hemoglobin. *Journal* of *Biological Chemistry*, **263**, 2316-2323

Grassel M., Coy U., Seyffert R. and Lynen F. (1963) Die chemische konstitution des cytohamins. *Biochem. Zeits.*, **338**, 771-795

Grice K. (1995) Distributions and stable isotopic compositions of individual biological markers from the Permian Kupferschiefer (Lower Rhine Basin, N.W. Germany). Ph.D. Thesis, University of Bristol

Grice K., Gibbison R., Atkinson J.E., Schwark L., Eckardt C.B. and Maxwell J.R. (1996) 1*H*-pyrrole-2,5-diones (maleimides) as indicators of anoxygenic photosynthesis in ancient water columns. *Geochim. Cosmochim. Acta*, **60**, 3913-3924

Grice K., Schaeffer P., Schwark L. and Maxwell J.R. (1997) Changes in palaeoenvironmental conditions during deposition of the Permian Kupferschiefer (Lower Rhine Basin, N.W. Germany) from variations in isotopic compositions of biomarker components. *Org. Geochem.*, **26**, 677-690

Haq B.U., Hardenbol J. and Vail P.R. (1987) Chronology of fluctuating sea levels since the Triassic. *Science*, **235**, 1156-1167

Harland W.B., Cox A.V., Llewellyn P.G., Pickton C.A.G., Smith A.G. and Walters R. (1982) *A Geological Time Scale*. Cambridge Univ. Press, Cambridge

Harradine P.J. and Maxwell J.R. (1998) Pyrophaeoporphyrins *c*1 and *c*2: grazing products of chlorophyll *c* in aquatic environments. *Org. Geochem.*, **28**, 111-117

Harris P.G., Carter J.F., Head R.N., Harris R.P., Eglinton G. and Maxwell J.R. (1995) Identification of chlorophyll transformation products in zooplankton faecal pellets and marine sediment extracts by liquid chromatography / mass spectrometry atmospheric pressure chemical ionisation. *Rapid Comm. Mass Spectr.*, **9**, 1177-1183

Hayes J.M. (1982) Fractionation, *et al*: an introduction to isotopic measurements and terminology. *Spectra*, **8**, 3-8

Hayes J.M., Popp B.N., Takigiku R. and Johnson M.W. (1989) An isotopic study of biogeochemical relationships between carbonates and organic carbon in the Greenhorn Formation. *Geochim. Cosmochim. Acta*, **53**, 2961-2972

Hays J.D. and Pitman W.C. (1973) Lithospheric plate motion, sea level changes and climatic and ecological consequences. *Nature*, **246**, 18-22

Head E.J.H. (1992) Gut pigment accumulation and destruction by Arctic copepods *in Vitro and in Situ*. *Mar. Biol.*, **112**, 583-592

Hedges J.I. and Keil R.G. (1995) Sedimentary organic matter preservation: an assessment and speculative synthesis. *Marine Chemistry*, **49**, 81-115

Hobson K.A. (1999) Tracing origins and migration of wildlife using stable isotopes: a review. *Oecologia*, **120**, 314-326

Hodgson G.W., Strosher M. and Casagrande D.J. (1971) Geochemistry of porphyrins: Analytical oxidation to maleimides. In: Advances in Organic Geochemistry (Eds: Gaertner H.R.V. and Wehner H.), Pergamon Press, Oxford, pp. 151-161

Hoefs J. (1996) Stable Isotope Geochemistry (Eds: Fallick T., Harmon R. and Longinelli A.), Springer, pp. 43-47

Hoefs M.J.L., Sinninghe Damsté J.S. and de Leeuw J.W. (1995) Organic geochemistry of Arabian Sea surface sediments: Palaeoenvironmental implications. In: Organic Geochemistry: Developments and Applications to Energy, Climate, Environment and Human History: 17th International Meeting on Organic Geochemistry (Eds. Grimalt J.O. and Dorronsoro C).

Hollander D.J., McKenzie J.A., Hsü K.J. and Huc A.Y. (1993) Application of an eutrophic lake model to the origin of ancient organic-carbon-rich sediments. *Global Biogeochemical Cycles*, **7**, 157-179

Hsü K.J., Cita M.B. and Ryan W.B.F. (1973) The origin of the Mediterranean evaporites. *Initial Rep. D.S.D.P.* **13**, 1203-1231

Huseby B. and Ocampo R. (1995) Study of porphyrins released from the Messel oil shale kerogen by selective chemical degradation. *Organic Geochemistry: developments and applications to energy, climate, environment and human history*, 997-998

Ingram B.L., Coccioni R., Montanari A. and Richter F.M. (1994) Strontium isotopic composition of mid-Cretaceous seawater. *Science*, **264**, 546-550

Innes H.E., Bishop A.N., Fox P.A., Head I.M. and Farrimond P. (1998) Early diagenesis of bacteriohopanoids in Recent sediments of Lake Pollen, Norway. *Org Geochem.*, **29**, 1285-1295

Innes H.E., Bishop A.N., Head I.M. and Farrimond P. (1997) Preservation and diagenesis of hopanoids in Recent lacustrine sediments of Priest Pot, England. *Org. Geochem.*, **26**, 565-576

Irving E., North T.K. and Couillard R. (1974) Oil, climate and tectonics. *Can. J. Earth Sci.*, **11**, 1-15

Jahnke R.A. (1990) Early sediment diagenesis and recycling of biogenic debris in a deep continental basin. *J. Mar. Res.*, **48**, 413-436

Jarvis I., Carson G.A., Cooper K., Hart M.B., Leary P., Tocher B.A., Horne D. and Resenfeld A. (1988) Microfossil assemblages and the Cenomanian-Turonian (Late Cretaceous) oceanic anoxic event. *Cretaceous Res.*, **9**, 3-101

Jen J.J. and MacKinney G. (1970b) On the photodecomposition of chlorophyll in vitro-II Intermediates and breakdown products. *Photochem. and Photobiol.*, **11**, 303-308

Jenkyns H.C. (1980) Cretaceous anoxic events: from continents to oceans. *J. Geol. Soc. Lond.*, **137**, 171-188

Jenkyns H.C. (1985) The Early Toarcian and Cenomanian anoxic events in Europe: comparisons and contrasts. *Geol. Runds.*, **74**, 505-518

Jenkyns H.C., Gale A.S. and Corfield R.M. (1994) Carbon- and oxygen-isotope stratigraphy of the English Chalk and Italian Scaglia and its palaeoclimatic significance. *Geol. Mag.*, **131**, 1-34

Johnson C.C., Barron E.J., Kauffman E.G., Arthur M.A., Fawcett P.J. and Yasuda M.K. (1996) Middle Cretaceous reef collapse linked to ocean heat transport. *Geology*, **24**, 376-380

Junk G. and Svec H.J. (1958) The absolute abundance of the nitrogen isotopes in the atmosphere and compressed gas from various sources. *Geochim. Cosmochim. Acta*, **14**, 234-243

Kannangara C.G., Gough S.P., Bruyant P., Hooker J.K., Kahn A. and von Wettstein D. (1988) Transfer RNA-GLU as a cofactor in *delta-aminolevulinate* biosynthesis – steps that regulate chlorophyll synthesis. *Trends Biochem. Sci.*, **13**, 139-143

Kaur S., Chicarelli M.I. and Maxwell J.R. (1986) Naturally occurring benzoporphyrins: bacterial marker pigments? *J. Am. Chem. Soc.*, **108**, 1347-1348

Keely B.J. (1989) Early diagenesis of chlorophyll and chlorin pigments. Ph.D. Thesis, University of Bristol

Keely B.J., Blake S.R., Schaeffer P. and Maxwell J.R. (1995) Distributions of pigments in the organic matter of marls from the Vena del Gesso evaporitic sequence. *Org. Geochem.*, **23**, 527-539

Keely B.J., Harris P.G., Popp B.N., Hayes J.M., Meischner D. and Maxwell J.R. (1994) Porphyrin and chlorin distributions in a Late Pliocene lacustrine sediment. *Geochim. Cosmochim. Acta*, **58**, 3691-3701

Keely B.J. and Maxwell J.R. (1993) The Mulhouse basin: evidence from porphyrin distributions for water column anoxia during deposition of marls. *Org. Geochem.*, **20**, 1217-1225

Keely B.J., Prowse W.G. and Maxwell J.R. (1990) The Treibs hypothesis: an evaluation based on structural studies. *Energy and fuels*, **4**, 628-634

Kenig F., Sinninghe Damsté J.S., Frewin N.L., Hayes J.M. and de Leeuw J.W. (1995) Molecular indicators for palaeoenvironmental change in a Messinian evaporitic sequence (Vena del Gesso, Italy). II: High-resolution variations in abundances and ^{13}C

contents of free and sulphur-bound carbon skeletons in a single marl bed. *Org. Geochem.*, **23**, 485-526

Kennicutt M.C., Bidigare R.R., Macko S.A. and Keeney-Kennicutt W.L. (1992) The stable isotopic composition of photosynthetic pigments and related biochemicals. *Chem. Geol.*, **101**, 235-245

Kline T.C., Goering J.J., Mathisen O.A., Poe P.H., Parker P.L. and Scanlan R.S. (1994) Recycling of elements transported upstream by runs of Pacific salmon: II. $\delta^{15}N$ and $\delta^{13}C$ evidence in the Kvichak River watershed, Bristol Bay, south-western Alaska. *Canadian Journal of Fishery and Aquatic Sciences*, **50**, 2350-2365

Kohnen M.E.L., Schouten S., Sinninghe Damsté J.S. and de Leeuw J.W. (1991a) Biases from natural sulphurisation in palaeoenvironmental reconstruction based on hydrocarbon biomarker distributions. *Nature*. **349**, 775-778

Kohnen M.E.L., Sinninghe Damsté J.S., Kockvandalen A.C., Tenhaven H.L., Rullkötter J. and Deleeuw J.W. (1990) Origin and diagenetic transformations of C-25 and C-30 highly branched isoprenoid sulfur compounds – further evidence for the formation of organically bound sulfur during early diagenesis. *Geochim. Cosmochim. Acta*, **54**, 3053-3063

Koletzko B., Demmelmair H., Hartl W., Kindermann A., Koletzko S., Sauerwald T. and Szitanyi P. (1998) The use of stable isotope techniques for nutritional and metabolic research in paediatrics. *Early Human Development Suppl.*, **53**, 77-97

Koopmans M.P., Schouten S., Kohnen M.E.L. and Sinninghe Damsté J.S. (1996) Restricted utility of aryl isoprenoids as indicators for photic zone anoxia. *Geochim. Cosmochim. Acta*, **60**, 4873-4876

Krohn K.A. and Mathis C.A. (1981) The use of isotopic nitrogen as a biochemical tracer. In: Advances in Chemistry Series Number 197: Short-Lived Isotopes in Chemistry and Biology (Eds: Root J.W. and Krohn K.A.), *American Chemical Society, Washington, D.C.*, pp. 239-249

Kuhnt W., Thurow J., Wiedmann J. and Herbin J.P. (1986) Oceanic anoxic conditions around the Cenomanian/Turonian boundary and the response of the biota. *Mitt. Geol. Pal. Inst. Univ. Hamburg*, **60**, 205-246

Kuypers M.M.M., Pancost R.D. and Sinninghe Damsté J.S. (1999) A large and abrupt fall in atmospheric CO_2 concentration during Cretaceous times. *Nature*, **399**, 342-345

Laws E.A., Popp B.N., Bidigare R.R., Kennicutt M.C. and Macko S.A. (1995) Dependence of phytoplankton carbon isotopic composition on growth rate and $[CO_2]_{aq}$: Theoretical considerations and experimental results. *Geochim. Cosmochim. Acta*, **59**, 1131-1138

Li J., Philp R.P., Pu F. and Allen J. (1996) Long-chain alkenones in Qinghai Lake sediments. *Geochim. Cosmochim. Acta*, **60**, 235-241

Lisitzin A.P. (1971) Distribution of siliceous microfossils in suspension and in bottom sediments. In: *Micropalaeontology of oceans* (Eds: Funnell B.M. and Riedel W.R.), pp.173-195

Louda J.W. and Baker E.W. (1986) The biogeochemistry of chlorophyll. In: Organic Marine Geochemistry (Ed. Sohn H.L.), *Am. Chem. Soc.*, pp. 107-126

Macko S.A. (1981) Stable nitrogen isotope ratios as tracers of organic geochemical processes. Ph.D. Thesis, University of Texas Austin, p.181

Macko S.A., Engel M.H. and Parker P.L. (1993) Early diagenesis of organic matter in sediments. Assessment of mechanisms and preservation by the use of isotopic molecular approaches. In: (Eds. Engel M.H. and Macko S.A.) Organic Geochemistry, Principles and Applications. Plenum Press, New York, pp. 211-224

Macko S.A., Fogel Estep M.L., Engel M.H. and Hare P.E. (1986) Kinetic fractionation of stable nitrogen isotopes during amino acid transamination. *Geochim. Cosmochim. Acta*, **50**, 2143-2146

Manning, W.M. and Strain, H.H. (1943) Chlorophyll *d*, a green pigment of red algae. *J. Biol. Chem.*, **151**, 1

Mariotti, A. (1983) Atmospheric nitrogen is a reliable standard for natural ^{15}N abundance measurements. *Nature* (*London*), **303**, 685-687

Mariotti A., Germon J.C., Hubert P., Kaiser P., Letolle R. and Tardieux P. (1981) Experimental determination of nitrogen kinetic isotope fractionation: some principles, illustration for the denitrification and nitrification processes. *Plant Soil*, **62**, 413-430

Mariotti A., Germon J.C. and Leclerc A. (1982) Nitrogen isotope fractionation associated with the $NO_2 \rightarrow N_2O$ step of denitrification in soils. *Canadian Journal of Soil Science*, **62**, 227-241

Mariotti A., Lancelot C. and Billen G. (1984) Natural isotopic composition of nitrogen as a tracer of origin for suspended organic matter in the Scheldt estuary. *Geochim. Cosmochim. Acta*, **48**, 549-555

Meier-Augenstein W. (1999) Use of gas chromatography-combustion-isotope ratio mass spectrometry in nutrition and metabolic research. *Curr. Opin. Clin. Nutr. Metab. Care*, **2**, 465-470

Merritt D.A. and Hayes J.M. (1994) Nitrogen isotopic analyses by isotope-ratio-monitoring gas-chromatography mass-spectrometry. *J. Am. Soc. Mass Spectr.*, **5**, 387-397

Metges C.C. and Petzke K.J. (1997) Measurement of $^{15}N/^{14}N$ isotopic composition in individual plasma free amino acids of human adults at natural abundance by gas chromatography combustion isotope ratio mass spectrometry. *Anal. Biochem.*, **247**, 158-164

Meyers P.A. (1997) Organic geochemical proxies of palaeoceanographic, palaeolimnologic, and palaeoclimatic processes. *Org. Geochem.*, **27**, 213-250

Meyers P.A., Dunham K.W. and Dunham P.L. (1986) Organic geochemistry of Cretaceous organic-carbon-rich shales and limestones from the western North Atlantic Ocean. See Summerhayes and Shackleton, 1986. pp. 333-345

Milgrom L.R. (1997) The Colours of Life: An introduction to the chemistry of porphyrins and related compounds. Oxford University Press Inc., New York, pp. 23-41

Minagawa M. and Wada E. (1984) Stepwise enrichment of ^{15}N along food chains: Further evidence and the relationship between $\delta^{15}N$ and animal age. *Geochim. Cosmochim. Acta*, **48**, 1135-1140

Montesinos E., Guerrero R., Abella C. and Esteve I. (1983) Ecology and physicology of the competition for light between *Chlorobium limicola* and *Chlorobium phaeobacteroides* in natural habitats. *Applied and Environmental Microbiology*, **4**, 1007-1016

Moore L.R., Goericke R. and Chisholm S.W. (1995) Comparative physiology of *Synechococcus* and *Prochlorococcus*: influence of light and temperature on growth, pigments, fluorescence and absorptive properties. *Mar. Ecol. Prog. Ser.*, **116**, 259-275

Mosier A.R. and Schimel D.S. (1993) Nitrification and Denitrification. In: Nitrogen Isotope Techniques (Eds: Knowles R. and Henry Blackburn T.), pp. 181-182

Naylor C.C. (1997) Early oxidative transformation products of chlorophyll in contemporary environments. Ph.D. Thesis, University of York

Naylor C.C and Keely B.J. (1997) Oxidative transformation products of chlorophylls: Structures, formation and significance. *Absts, 18th Int. Meet. Org. Geochem.*, 22-26 September, 1997, Maastricht, Netherlands., pp. 91-92

Nier A.O. (1950) A redetermination of the relative abundances of the isotopes of carbon, nitrogen, oxygen, argon and potassium. *Physics Review*, **77**, 789-793

Ocampo R., Callot H.J. and Albrecht P. (1985a) Identification of polar porphyrins in oil shale. *J. Chem. Soc., Chem. Commun.*, 198-200

Ocampo R., Callot H.J. and Albrecht P. (1985b) Occurrence of bacterioporphyrins in oil shale. *J. Chem. Soc., Chem. Commun.*, 200-201

Ocampo R., Callot H.J. and Albrecht P. (1989) Different isotope compositions of C_{32} DPEP and C_{32} etioporphyrin III in oil shale. *Naturwissenschaften*, **76**, 419-421

Ocampo R., Callot H.J. and Albrecht P. (1992) Porphyrins from the Messel oil shale (Eocene, Germany): Structure elucidation, geochemical significance and distribution as a function of depth. *Geochim. Cosmochim. Acta*, **56**, 745-761

Owens N.J.P. (1987) Natural variations in ^{15}N in the marine environment. *Advances in Marine Biology*, **24**, 389-451

Palmer S. and Baker E.W. (1978) Copper porphyrins in deep sea sediments: a possible indicator of oxidised terrestial organic matter. *Science*, **201**, 49-51

Pancost R.D., Freeman K.H. and Arthur M.A. (1998) Organic geochemistry of the Cretaceous Western Interior Seaway: A trans-basinal evaluation. In: Stratigraphy and Paleoenvironments of the Cretaceous Western Interior Seaway, USA (Eds: Dean W.E. and Arthur M.A.), SEPM Concepts in Sedimentology and Paleontology, No. 6, pp. 173-188

Parrish J.T. (1987) Palaeo-upwelling and the distribution of organic-rich rocks. See Brooks and Fleet, 1987. pp. 199-206

Partensky F., Hoepffner N., Li W.K.W., Ulloa O. and Vaulot D. (1993) Photoacclimation of *Prochlorococcus* sp. (Prochlorophyta) strains isolated from the North Atlantic and the Mediterranean Sea. *Plant Physiol.*, **101**, 285-296

Peterson B.J. and Fry B. (1987) Stable isotopes in ecosystems studies. *Annual Review of Ecology and Systematics*, **18**, 293-320

Pietrogrande A., Zancato M., Guerrato A. and Porretta G.C. (1993) Nitrogen microdetermination in combustion-resistant nitrogen-containing organic compounds. *Analusis*, **21**, 353-357

Popp B.N., Takigiku R., Hayes J.M., Louda J.W. and Baker E.W. (1989) The post-Paleozoic chronology and mechanism of ^{13}C depletion in primary marine organic matter. *Am. J. Sci.*, **289**, 436-454

Quirke J.M.E. (1987) In: *Metal Complexes in Fossil Fuels*, (Eds. Filby R.H. and Branthaver J.F.) American Chemical Society, Washington, 1987, p. 308

Quirke J.M.E., Shaw G.J., Soper P.D. and Maxwell J.R. (1980) Petroporphyrins II. The presence of porphyrins with extended alkyl substituents. *Tetrahedron Lett.*, **36**, 3261-3267

Rebeiz, C.A., Belanger, F.C., Freyssinet, G. and Saab, D.S., (1980) Chloroplast biogenesis. XXIX. The occurrence of several novel chlorophyll *a* and *b* chromophores in higher plants. *Biochim. Biophys. Acta*, **590**, 234

Rennie M.J., Meier-Augenstein W., Watt P.W., Patel A., Begley I.S. and Scrimgeour C.M. (1996) Use of continuous-flow combustion MS in studies of human metabolism. *Biochem. Soc. Trans.*, **24**, 927-932

Repeta D.J. (1993) A high resolution historical record of Holocene anoxygenic primary production in the Black Sea. *Geochim. Cosmochim. Acta*, **57**, 4337-4342

Repeta D.J., Simpson D.J., Jørgensen B.B. and Jannasch H.W. (1989) Evidence for anoxygenic photosynthesis from the distribution of bacteriochlorophylls in the Black Sea. *Nature*, **342**, 69-72

Requejo A.G., Allan J., Creaney S., Gray N.R. and Cole K.S. (1992) Aryl isoprenoids and diaromatic carotenoids in Paleozoic source rocks and oils from the Western Canada and Williston Basins. In Advances in Organic Geochemistry 1991

(Eds: Eckardt C.B., Maxwell J.R., Larter S.R. and Manning D.A.C.) *Org. Geochem.*, **19**, 245-264

Resnick S.M. and Madigan M.T. (1989) Isolation and characterisation of a mildly thremophylic nonsulfur purple bacterium containing bacteriochlorophyll *b*. *FEMS Microbiol. Lett.*, **65**, 165

Rhoads D.C. and Morse J.M. (1971) Evolutionary and ecological significance of oxygen-deficient marine basins. *Lethaia.*, **4**, 413-428

Robinson N., Cranwell P.A., Finlay B.J. and Eglinton G. (1984) Lipids of aquatic organisms as potential contributors to lacustrine sediments. *Org. Geochem.*, **6**, 143-152

Rohmer M., Bouvier-Nave P. and Ourisson G. (1984) Distribution of hopanoid triterpenes in prokaryotes. *Journal of General Microbiology*. **130**, 1137-1150

Rontani J.F., Baillet G. and Aubert C. (1991) Production of acyclic isoprenoid compounds during the photodegradation of chlorophyll *a* in sea water. *J. Photochem. Photobiol.*, **59**, 369-377

Root J.W. and Krohn K.A. (1981) Advances in Chemistry Series Number 197: Short-Lived Isotopes in Chemistry and Biology (Eds: Root J.W. and Krohn K.A.), *American Chemical Society, Washington, D.C.*

Ryan W.B.F. and Cita M.B. (1977) Ignorance concerning episodes of ocean-wide stagnation. *Mar. Geol.*, **23**, 197-215

Sachs J.P. (1997) Nitrogen isotopes in chlorophyll and the origin of eastern Mediterranean Sapropels. Ph.D. Thesis, Massachusetts Institute of Technology / Woods Hole Oceanographic Institution

Sachs J.P. and Repeta D.J. (2000) The purification of chlorins from marine particles and sediments for nitrogen and carbon isotopic analysis. *Org. Geochem.*, **31**, 317-329

Sachs J.P. and Repeta D.J. (1999b) Oligotrophy and nitrogen fixation during eastern Mediterranean sapropel events. *Science*, **286**, 2485-2488

Sachs J.P., Repeta D.J. and Goericke R. (1999a) Nitrogen and carbon isotopic ratios of chlorophyll from marine phytoplankton. *Geochim. Cosmochim. Acta*, **63**, 1431-1441

Sachs J.P., Repeta D.J. and Hilkert A. (1995) Measurement and assessment of the carbon nitrogen isotopic composition of chlorophyll derivatives. Organic Geochemistry: Developments and applications to energy, climate, environment and human history. pp. 16-18

Sagromsky, H. (1960) Pigments of red algae. *Ber. Dtsch. Bot. Ges.*, **71**, 3-7 and 358-362

Schaeffer P., Harrison, W.N., Keely B.J. and Maxwell J.R. (1995) Product distributions from chemical degradation of kerogens from a marl from a Miocene evaporitic sequence (Vena del Gesso, N. Italy). *Org. Geochem.*, **23** (6), 541-554

Schaeffer P., Ocampo R., Callot H.J. and Albrecht P. (1993) Extraction of bound porphyrins from sulfur-rich sediments and their use for reconstruction of palaeoenvironments. *Nature*, **364**, 133-136

Schaeflé J., Ludwig B., Albrecht P. and Ourisson G. (1977) Hydrocarbures aromatiques d'origine geologique. II. Noveaux carotenoides aromatiques fossiles. *Tet. Lett.*, **41**, 3673-3676

Schafer P. and Ittekkot V. (1993) Seasonal variability of $\delta^{15}N$ in settling particles in the Arabian Sea and its palaeogeochemical significance. *Naturwissenschaften*, **80**, 511-513

Scheer H. (1991) Geochemistry of Chlorophylls. *In*: Chlorophylls Scheer H. (*ed*) 4-30. CRC Press. Florida.

Schimerlik M.I., Rife J.E. and Cleland W.W. (1975) Equilibrium perturbation by isotope substitution. *Biochemistry*, **14**, 5347-5354

Schlanger S.O., Arthur M.A., Jenkyns H.C. and Scholle P.A. (1987) The Cenomanian-Turonian oceanic anoxic event, I. Stratigraphy and distribution of organic carbon-rich beds and the marine $\delta^{13}C$ excursion. See Brooks and Fleet, 1987. pp. 371-400

Schlanger S.O. and Jenkyns H.C. (1976) Cretaceous anoxic events: causes and consequences. *Geol. Mijn.*, **55**, 179-184

Schoenheimer R. and Rittenburg D. (1939) Studies in protein metabolism: I. General considerations in the application of isotopes to the study of protein metabolism. The normal abundance of nitrogen isotopes in amino acids. *Journal of Biological Chemistry*, **127**, 285-290

Scholle P.A. and Arthur M.A. (1980) Carbon isotopic fluctuations in pelagic limestones: Potential stratigraphic and petroleum exploration tool. *Bull. Am. Assoc. Petrol. Geol.*, **64**, 67-89

Schouten S. and Sinninghe Damsté J.S. (1995) The occurrence and distribution of low molecular weight sulphoxides in polar fractions of sediments and petroleum. *Org. Geochem.*, **23**, 129-138

Selli, R. (1973) An outline of the Italian Messinian. *In*: *Messinian events in the Mediterranean* (Ed. by C.W. Drooger), pp. 150-171. North-Holland, Amsterdam, The Netherlands.

Shimomura O. (1980) Chlorophyll-derived bile pigment in bioluminescent euphausiids. *Febs Letters*, **116**, 203-206

Sinninghe Damsté J.S., Frewin N.L., Kenig F. and de Leeuw J.W. (1995) Molecular indicators for palaeoenvironmental change in a Messinian evaporitic

sequence (Vena del Gesso, Italy). I: Variations in extractable organic matter of ten cyclically deposited marl beds. *Org. Geochem.*, **23**, 471-483

Sinninghe Damsté J.S. and Köster J. (1998) A euxinic southern North Atlantic Ocean during the Cenomanian-Turonian oceanic anoxic event. *Earth and Planetary Science Letters*, **158**, 165-173

Sinninghe Damsté J.S., Wakeham S.G., Kohnen M.E.L., Hayes J.M. and de Leeuw J.W. (1993) A 6,000 year sedimentary record of chemocline excursions in the Black Sea . *Nature*, **362**, 827-829

Sinton C.W. and Duncan R.A. (1997) Potential link between ocean plateau volcanism and global ocean anoxia at the Cenomanian-Turonian boundary. *Economic Geology*, **92**, 838-842

Sirevag R., Buchanan B.B., Berry J.A. and Troughton J.H. (1977) Mechanisms of CO_2 fixations in bacterial photosynthesis studied by the carbon isotope fractionation technique. *Arch. Microbiol.*, **112**, 35-38

Smith K.M. (1975) In: Porphyrins and metalloporphyrins pp.21 (Elsevier: Amsterdam)

Smith K.M. and Bobe F.W. (1987) Light adaptation of bacteriochlorophyll *d* producing bacteria by enzymic methylation of their antenna pigments. *J. Chem. Soc., Chem. Commun.*, 276-277

Spooner N., Keely B.J. and Maxwell J.R. (1994b) Biologically mediated defunctionalisation of chlorophyll in the aquatic environment. Senescence/decay of the diatom *Phaeodactylum tricornutum*. *Org. Geochem.*, **21**, 509-516

Spooner N., Rieley G., Collister J.W., Lander M., Cranwell P.A. and Maxwell J.R. (1994a) Stable carbon isotopic correlation of individual biolipids in aquatic organisms and a lake bottom sediment. *Org. Geochem.*, **21**, 823-827

Stein R., Rullkötter J. and Welte D.H. (1986) Accumulation of organic-carbon-rich sediments in the Late Jurassic and Cretaceous Atlantic Ocean – a synthesis. *Chem. Geol.*, **56**, 1-32

Still W.C., Kahn M. and Mitra A. (1978) Rapid chromatographic technique for preparative separations with moderate resolution. *J.Org. Chem.*, **43**, 2923-2925

Stow D.A.V. and Dean W.E. (1984) Middle Cretaceous black shale at Sites 530 in the southeastern Angola Basin. *Init. Repts. DSDP.*, **75**, 809-817

Summons R.E. and Powell T.G. (1986) Chlorobiaceae in Palaeozoic seas revealed by biological markers, isotopes and geology. *Nature*, **319**, 763-765

Sun M., Aller R.C. and Lee C. (1991) Early diagenesis of chlorophyll *a* in Long Island sound sediments: A measure of carbon flux and particle reworking. *J. Mar. Res.*, **49**, 379-401

Sun M., Lee C. and Aller R.C. (1993) Laboratory studies of oxic and anoxic degradation of chlorophyll *a* in Long Island sound sediments. *Geochim. Cosmochim. Acta*, **57**, 147-157

Suzuki Y., Tanabe K. and Shioi Y. (1999) Determination of chemical oxidation products of chlorophyll and porphyrin by high-performance liquid chromatography. *J. Chromatogr. A.*, **839**, 85-91

Talbot H.M., Head R.N., Harris R.P. and Maxwell J.R. (1999) Distribution and stability of steryl chlorin esters in copepod faecal pellets from diatom grazing. *Org. Geochem.*, **30**, 1163-1174

Thiede J. and Suess E. (1983) Coastal upwelling and its sediment record, part B, Sedimentary records of ancient coastal upwelling. Plenum, New York

Thiel V., Jenisch A., Landmann G., Reimer A. and Michaelis W. (1997) Unusual distributions of long-chain alkenones and tetrahymanol from the highly alkaline Lake Van, Turkey. *Geochim. Cosmochim. Acta*, **61**, 2053-2064

Thurow J. and Kuhnt W. (1986) Mid-Cretaceous of the Gibraltar Arch Area. In: North Atlantic Palaeoceanography (Eds. Summerhayes C.P. and Shackleton N.J.) Special publication, *Geol. Soc. Lon.*, **21**, 423-446

Tissot B. (1979) Effects on prolific petroleum source rocks and major coal deposits caused by sea level changes. *Nature*, **277**, 463-465

Treibs A. (1934) Chlorophyll-und Haminderivate in bitumous Gesteinen, Erdolen, Erdwachsen and Asphalten. *Liebigs Ann.*, **510**, 42-62

Treibs A. (1936) Chlorophyll-und Haminderivative in organischen mineralstoffen. *Angewandte Chemie*, **49**, 682-686

Turner A.D. (1998) Recognition of photic zone anoxia from LC-MS studies of porphyrin distributions in ancient sediments. Ph.D. Thesis, University of Bristol

Urey H.C. (1947) The thermodynamic properties of isotopic substances. *J. Chem. Soc. Lon.*, 562-581

Vai G.B. and Ricci Lucchi F. (1977) Algal crusts, autochthonous and clastic gypsum in a cannibalistic evaporite basin: a case history from the Messinian of Northern Apennines. *Sedimentology*, **24**, 211-244

van Kaam-Peters H.M.E. (1997b) Biomarker and compound-specific stable carbon isotope analysis of the Early Toarcian shales in SW Germany. In: *The depositional environment of Jurassic organic-rich sedimentary rocks in NW Europe. A biomarker approach*. Ph.D. Thesis, University of Utrecht, pp. 191-216

van Kaam-Peters H.M.E., Schouten S., Köster J., de Leeuw J.W. and Sinninghe Damsté J.S. (1997a) A molecular and carbon isotope biogeochemical study of biomarkers and kerogen pyrolysate of the Kimmeridge Clay Formation: Palaeoenvironmental implications. *Org. Geochem.*, **27**, 399-422

van Kaam-Peters H.M.E., Schouten S., Köster J. and Sinninghe Damsté J.S. (1999) Controls on the molecular and carbon isotopic composition of organic matter deposited in a Kimmeridgian euxinic shelf sea: Evidence for preservation of carbohydrates through sulfurisation. *Geochim. Cosmochim. Acta*, **62**, 3259-3283

Verne-Mismer J., Ocampo R., Callot H.J. and Albrecht P. (1986) Identification of a novel C_{33} DPEP petroporphyrin from Boscan crude oil: evidence for geochemical reduction of carboxylic acids. *Tetrahedron Lett.*, **37**, 5257-5260

Verne-Mismer J., Ocampo R., Callot H.J. and Albrecht P. (1987) Isolation of a series of vanadyl-tetrahydrobenzopetroporphyrins from Timhadit oil shale. Structure determination and total synthesis of the major constituent. *J. Chem. Soc., Chem. Commun.*, 1581-1583

Virginia R.A. and Delwiche C.C. (1982) Natural ^{15}N abundance of presumed N_2-fixing and non-N_2-fixing plants from selected ecosystems. *Oecologia*, **54**, 317-325

Volkman J.K., Eglinton G., Corner E.D.S. and Forsberg T.E.V. (1980) Long-chain alkenes and alkenones in the coccolithophoroid *Emiliania huxleyi*. *Phytochemistry*, **19**, 2619-2622

Wada E., Shibata R. and Torrii T. (1981) ^{15}N abundance in Antarctica: origin of soil nitrogen and ecological implications. *Nature*, **292**, 327-329

Waseilewski M.R. and Svec W.A. (1980) Synthesis of covalently linked dimeric derivatives of chlorophyll *a*, pyrochlorophyll *a*, chlorophyll *b* and bacteriochlorophyll *a*. *J. Org. Chem.*, **45**, 1969-1974

Watanabe N., Yamamoto K., Ihshikawa H. and Yagi A. (1993) New chlorophyll *a* related compounds isolated as antioxidants from marine bivalves. *J. Nat. Prod.*, **56**, 305-317

Weissert H. (1981) The environment of deposition of black shales in the Early Cretaceous: an ongoing controversy. In: *Deep Sea Drilling Project: a decade of progress*. (Eds: Warme *et al.*) *Soc. Econ. Palaeontal. Mineral., Spec. Publ.*, **32**, 547-560

Zimmerman H.B., Boersma A. and McCoy F.W. (1987) Carbonaceous sediments and palaeoenvironment of the Cretaceous South Atlantic Ocean. *Geological Society Special Publication*, **26**, 271-286